Revised Modeling Protocol
For the Proposed
Desert Rock Energy Facility

Prepared for:
Steag Power, LLC
Houston, TX

Prepared by:
ENSR Corporation

May 2004
Document No. 09417-360-230R1

CONTENTS

LIST OF TABLES

LIST OF FIGURES

1.0 INTRODUCTION

1.1 Project Overview

Steag Power LLC is proposing a mine-mouth coal fired power plant, to be located in northwestern New Mexico. The location of the power plant is approximately 25 - 30 miles (40 - 60 km) southwest of Farmington New Mexico in the Four Corners Area (see Figure 1-1) where Arizona, Colorado, New Mexico and Utah meet. The project is known as the "Desert Rock Energy Facility" and the location lies within the trust lands of the Navajo Nation. The plant will be located near a coal mine operated by BHP Billiton New Mexico Coal, one of the largest domestic suppliers of low sulfur coal. The plant location will be west of the active mine, but close to the mine boundaries.

Figure 1-1 General View – Farmington Region

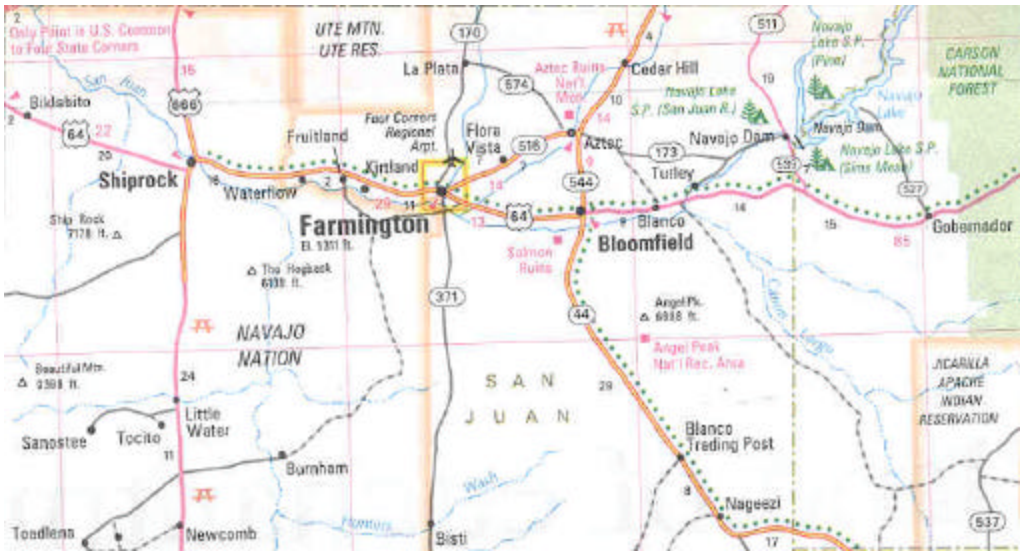

The power plant will be of the supercritical pulverized coal type and will be designed for a total generation capacity of 1500 MW (gross), made up of two separate units, each of which will produce 750 MW gross. Due to the selected location, coal will be delivered via a closed above ground conveyor belt from the crushing facilities at the BHP Billiton mine.

The project will use two dry, natural draft Heller cooling tower systems because water is a critical resource in that region. Part of the design process will be to optimize the use of water, power generation and efficiency.

1.2 Protocol Outline

A description of the proposed project is provided in Section 2, which includes a site description with site drawings, and discusses proposed project emissions. The air quality attainment status and ambient standards are discussed in Section 3.

The meteorology of the Four Corners area is discussed in Section 4, which also documents the complexity of the wind flows that have been extensively studied in this region. Section 5 presents the proposed dispersion modeling approach for this project and for the PSD Class II analysis. Section 6 covers the approach proposed for the PSD Class I analysis. The use of existing monitoring data to characterize current air quality in the area is discussed in Section 7. Section 8 covers additional PSD impact considerations, such as a growth analysis and impacts to soils and vegetation. Section 9 discusses how modeling results will be documented, and Section 10 provides a references section. Appendices to this modeling protocol report include:

- Appendix A: excerpts from the SAI 1982 study, “Air Quality and Meteorology of Northwestern New Mexico”.
- Appendix B: a technical paper that discusses an application of CALPUFF using RUC data in North Dakota.
- Appendix C: RUC40 and RUC20 information from the Forecast Systems Laboratory.
- Appendix D: SCREEN3 Modeling Files for Worst Case Load Determination
- Appendix E: a technical paper that discusses possible refinements to the default FLAG guidance for regional haze assessments.
- Appendix F: a technical paper that discusses the effect of salt particles on extinction.
- Appendix G: a comparison of CALMET (RUC) wind speed and direction to selected surface station wind speed and direction.
- Appendix H: screening documentation for the analysis of acid neutralizing capacity of lakes.

2.0 DESCRIPTION OF PROPOSED PROJECT

2.1 Site Description

The Desert Rock Energy Facility is located on an ~580 acre (2.35 sq. km) site close to the BHP Billiton mine in northwest New Mexico. The site location is ~25 miles (~40 km) Southwest of Farmington, San Juan County, New Mexico in the Navajo Indian Reservation, as shown in Figure 1-1.

The area in the immediate vicinity of the proposed facility is relatively flat, as shown in Figure 2-1. The project site can be characterized as an open flat prairie. The nearby Chaco River is a slow creek with extended wetlands, which may dry out during the summer season.

Figure 2-1 View of Terrain in the Immediate Vicinity of the Proposed Desert Rock Energy Facility

The site can be accessed via highway 249 from Shiprock, New Mexico and further on Indian Service Routes to be improved for transportation purposes by grading, drainage and paving. No transportation is availabile by railway.

2.2 Proposed Facility Design

The boiler plant is of a supercritical pressure design. It consists essentially of a full-load once-through steam generating unit with all necessary heating surfaces and connecting lines, single reheating, direct pulverized bituminous coal firing. Also included are a light oil firing system for ignition and backup, the complete steel supporting structure, the platforms and walkways, the air and flue gas ducts with

forced-draft fan, primary air fan, induced-draft fan, steam air heater and regenerative air heater, ash removal and storage system, lifts and hoists and inspection equipment.

Figure 2-2 shows a side view of the basic elements of one of the boiler units. An air-cooling system in a natural-draft tower is featured on the left side of the figure. Proceeding to the right, we then see the turbine hall and steam generator set of buildings, which becomes the controlling building to establish the Good Engineering Practice stack height (the natural draft cooling tower is too far distant to affect the aerodynamic building downwash at the stack location). Further to the right, the control equipment is located between the turbine hall and the stack.

Figure 2-3 shows a facility plan that includes the property boundary and the generating unit.

2.3 Proposed Project Emissions

Steag Power LLC has elected to design a power generation project that will be truly state-of-the-art, in that the aggregated emission levels proposed will be as stringent as, or in some cases more stringent than, the latest generation of similar coal-fired power plants being permitted in the United States.

Other emission sources at the Desert Rock Energy Facility, including auxiliary boilers, emergency reciprocating engines, and materials handling sources, will also be evaluated for and equipped with BACT. For example, as a mine-mouth power plant, coal will normally be delivered directly to the site via enclosed conveyor without the fugitive emissions associated with on-site rail unloading or management of an active coal pile; transfer towers and silos will be exhausted through bin vent filters, and on-site roadways will be paved. As a result, the Desert Rock Energy Facility is being designed from the very beginning to be among the most modern, lowest emission design facilities of its kind ever constructed in the United States.

The emissions estimates from the proposed Desert Rock facility are provided in more detail in the permit application. This information is based upon current engineering estimates.

The dispersion modeling analysis will use the data from Tables 2-1 through 2-4, to characterize emissions from the main stack and other ancillary combustion sources associated with the plant. There are three start-up and one shut-down emissions scenarios for the facility. All of these scenarios have a duration much less than 24 hours, ranging from 2.6 hours for the “hot start” to 6.5 hours for the “cold start”. Modeling for these cases would consider only pollutants for which there is a regulatory ambient standard with an averaging time of 3 hours or less: SO2 and CO. However, the start-up and shutdown CO and SO2 emissions are all less than all of the normal load operation scenarios, so they need not be separately modeled.

Figure 2-2 Facility Side View of a Boiler Unit at the Proposed Desert Rock Energy Facility

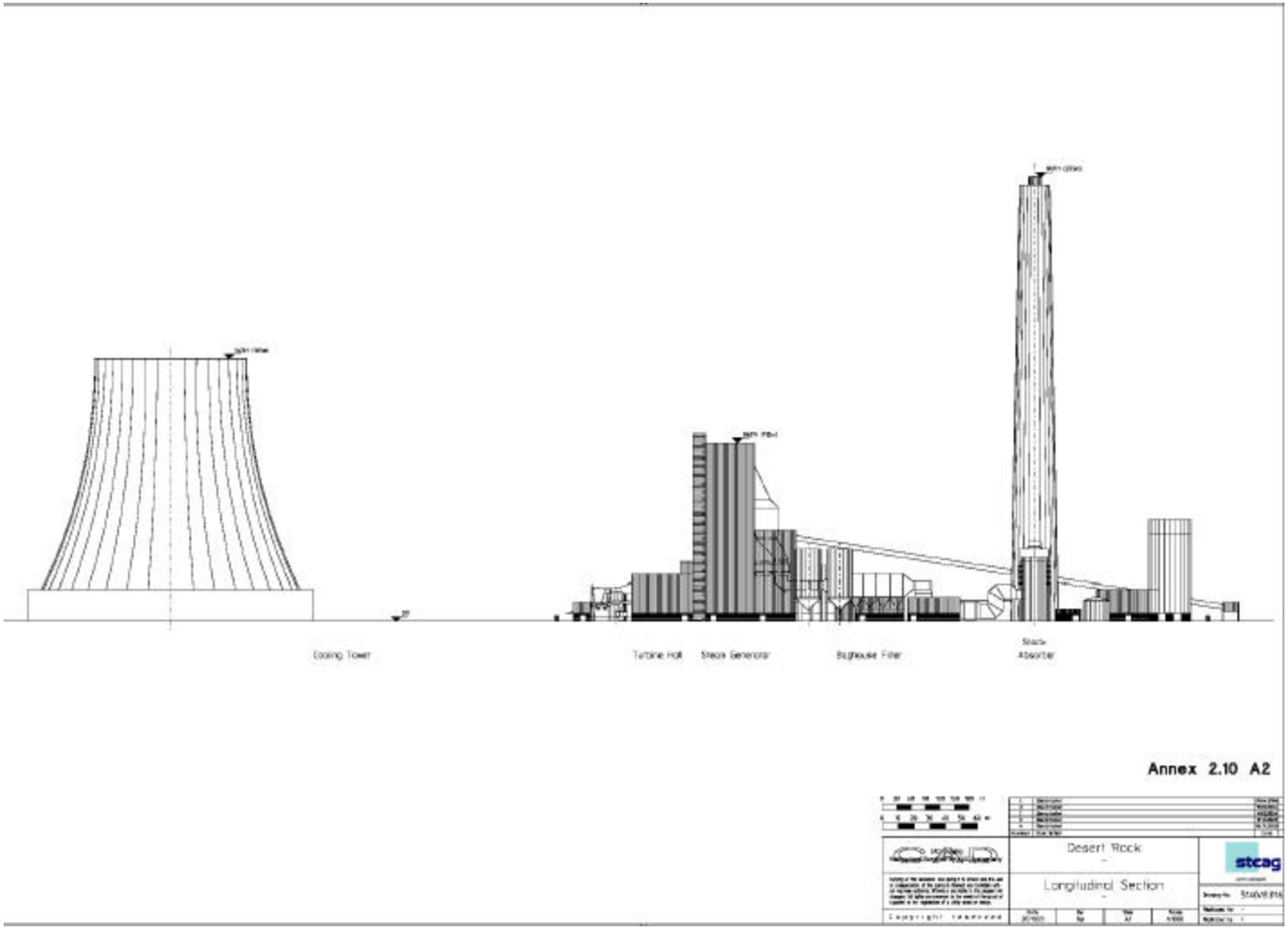

Figure 2-3 Facility Plot

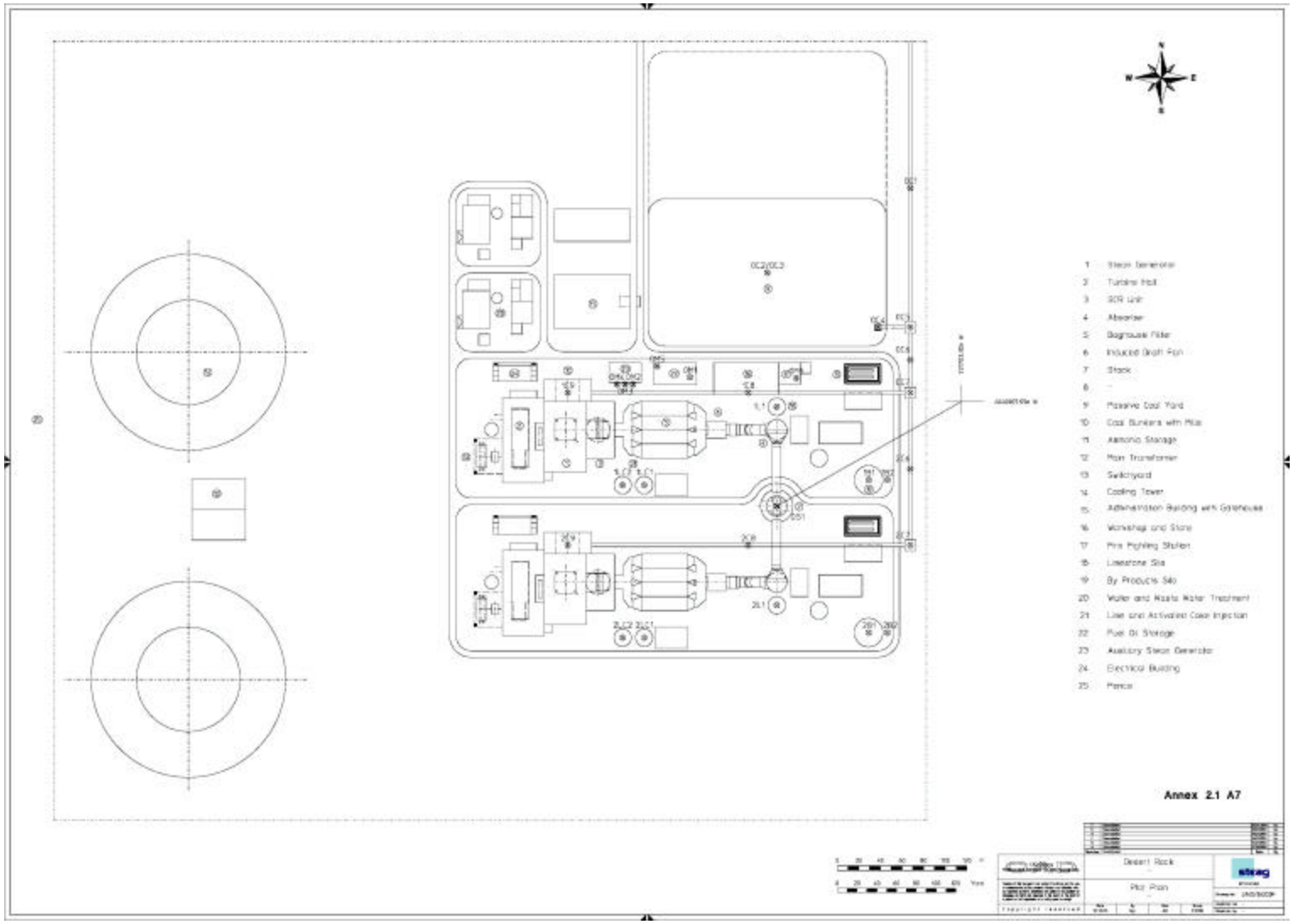

Table 2-1
Design Emissions and Stack Parameters for Each of the Main Boilers at Various Operating Loads

	Units	**100% Load**	**80% Load**	**60% Load**	**40% Load**
Plant Performance					
Full Load Heat Input to Boiler	*MMBtu/hr*	6,810	5,448	4,086	2,724
Emissions per Boiler					
SO_2 (3-hour)	*lb/MMBtu*	0.090	0.090	0.090	0.090
	g/s	77.22	61.87	46.42	30.89
SO_2 (24-hour and Annual)	*lb/MMBtu*	0.060	0.060	0.060	0.060
Hourly Emissions	*g/s*	51.5	41.2	30.9	20.6
Annual Emissions	*ton/yr*	1659.5	not applicable		
NO_X	*lb/MMBtu*	0.060	0.060	0.060	0.060
Hourly Emissions	*g/s*	51.5	41.2	30.9	20.6
Annual Emissions	*ton/yr*	1662.5	not applicable		
PM	*lb/MMBtu*	0.01	0.01	0.01	0.01
Hourly Emissions	*g/s*	8.58	6.87	5.16	3.43
Annual Emissions	*ton/yr*	285	not applicable		
PM_{10} Total	*lb/MMBtu*	0.020	0.020	0.020	0.020
Hourly Emissions	*g/s*	17.16	13.75	10.32	6.86
Annual Emissions	*ton/yr*	560	not applicable		
CO	*lb/MMBtu*	0.100	0.100	0.100	0.100
Hourly Emissions	*g/s*	85.80	68.74	51.58	34.32
Annual Emissions	*ton/yr*	2764.5	not applicable		
H_2SO_4	*lb/MMBtu*	0.0040	0.0040	0.0040	0.0040
Hourly Emissions	*g/s*	3.43	2.75	2.06	1.37
Annual Emissions	*ton/yr*	110.5	116.75	87.56	58.38
Pb	*lb/MMBtu*	0.00020	0.00020	0.00020	0.00020
Hourly Emissions	*g/s*	0.17	0.14	0.10	0.07
Annual Emissions	*ton/yr*	5.55	not applicable		
Stack Parameters					
Stack Gas Exit Temperature	F	122	122	122	122
	K	**323.15**	**323.15**	**323.15**	**323.15**
Stack Gas Exit Velocity	ft/s	79.95	63.96	47.97	31.98
	m/s	24.37	19.50	14.62	9.75
Stack Height	ft	917	917	917	917
	m	279.49	279.49	279.49	279.49
Stack Diameter	ft	36.77	36.77	36.77	36.77
	m	11.21	11.21	11.21	11.21

Table 2-2
Design Emissions and Stack Parameters for the Auxiliary Steam Generators

Maximum Fuel Firing Rate for the Auxiliary	86.4	MMBtu/hr
Heating Value for #2 Fuel Oil:	140,000	Btu/gal
Maximum Fuel Firing Rate:	617	gal/hr
Estimated Maximum Annual Hours of	550	hours/year
Stack Height:	98	feet
Stack Diameter:	2.924	Feet
Average Stack Exit Temperature:	284	F
Stack Exit Velocity:	82	ft/s

Pollutant	Emission Factor	Units	Hourly Emissions			Annual Emissions	
			(lb/hr)	(g/s)	(lb/MMBt	(ton/yr)	(g/s)
CO	5	lb/1,000 gal	3.09	0.39	0.036	0.85	0.024
NO_x	0.1	lb/MMBtu	8.64	1.09	0.1	2.38	0.068
PM_{10} (Total)	3.3	lb/1,000 gal	2.04	0.26	0.024	0.56	0.016
PM	2	lb/1,000 gal	1.23	0.16	0.014	0.34	0.010
VOC	0.34	lb/1,000 gal	0.21	0.026	0.0024	0.06	0.0017
SO_2	7.10	lb/1000 gal	4.38	0.55	0.051	1.20	0.035
H_2SO_4	0.12	lb/1000 gal	0.076	0.010	0.00087	0.021	0.00060
Pb	9	lb/10^{12} Btu	0.00078	0.00010	0.00000	2.14E-04	6.15E-06

SO_2 Emission Factor	
Sulfur Content of Oil	0.05 %

Table 2-3
Design Emissions and Stack Parameters for the Emergency Diesel Generator

Diesel generator output:	1000	KW		
Diesel generator input:	1176	KW	85%	efficiency (Note 1)
Diesel engine output:	1578	Hp	1.341	
Diesel engine output:	4.01	MMBtu/hr	1hp = 2544	Btu/hr
Diesel engine input:	13.38	MMBtu/hr	30%	efficiency (Note 1)
Maximum Annual Hours of Operation:	100	Hours/yea		
Fuel Consumption:	545	Lb/hr		
Stack Height:	45	Feet		
Stack Diameter:	3	Ft		
Stack Flow Rate:	9058	Cfm		
Stack Gas Exit Temperature:	870	Deg F		
Stack Gas Exit Velocity:	21	Ft/s		

Pollutant	Emission Factor	Units	Hourly Emissions			Annual Emissions	
			(lb/hr)	(g/hp-hr)	(g/s)	(ton/yr)	(g/s)
CO	0.13	lb/MMBtu	1.74	0.50	0.22	0.09	2.5E-03
NO_x	1.69	lb/MMBtu	22.61	6.50	2.85	1.13	3.3E-02
PM_{10} Total	0.0573	lb/MMBtu	0.77	0.22	0.10	0.04	1.1E-03
PM	0.1	lb/MMBtu	0.83	0.24	0.11	0.04	1.2E-03
VOC	0.0792	lb/MMBtu	1.06	0.30	0.13	0.05	1.5E-03
SO_2	0.051	lb/MMBtu	0.68	0.19	0.09	0.03	9.7E-04
H_2SO_4	0.0015	lb/MMBtu	0.02	0.01	0.003	0.00	3E-05
Pb	9E-06	lb/MMBtu	1E-04	3E-05	2E-05	6E-06	1.7E-07

Sulfur Content of Fuel	0.05%

NOTES:

1. Efficiencies for the generator and engine are assumed.
2. The emission factor for SO_2 is 1.01 times the sulfur content of the fuel.

Table 2-4
Design Emissions and Stack Parameters for the Diesel Fire Fighting Pump

Diesel engine output:	284	Hp	1.341 hp/kW
Diesel engine output:	0.72	MMBtu/hr	1hp = 2544 Btu/hr
Diesel engine input:	2.41	MMBtu/hr	30% efficiency (Note 1)
Maximum Annual Hours of Operation:	100	hours/year	
Stack Height:	30	feet	
Stack Diameter	0.6	feet	
Stack Flow Rate:	1265	cfm	
Stack Gas Exit Temperature:	900	F	
Stack Gas Exit Velocity:	74	ft/s	

Pollutant	Emission Factor	Units	Hourly Emissions			Annual Emissions	
			(lb/hr)	(g/hp-hr)	(g/s)	(ton/yr)	(g/s)
CO	0.13	lb/MMBtu	0.31	0.50	0.04	1.57E-02	4.50E-04
NO_x	1.69	lb/MMBtu	4.07	6.50	0.51	2.04E-01	5.85E-03
PM_{10} total	0.0573	lb/MMBtu	0.14	0.22	0.02	6.90E-03	1.98E-04
PM	0.062	lb/MMBtu	0.15	0.24	0.02	7.47E-03	2.15E-04
VOC	0.0792	lb/MMBtu	0.19	0.30	0.02	9.54E-03	2.74E-04
SO_2	0.05	lb/MMBtu	0.12	0.19	0.02	6.08E-03	1.75E-04
H_2SO_4	0.002	lb/MMBtu	0.004	0.01	0.0005	1.84E-04	5.30E-06
Pb	9.E-06	lb/MMBtu	2.E-05	3.E-05	3.E-06	1.08E-06	3.12E-08

Sulfur Content of Fuel	0.05%

NOTES:

1. Efficiencies for the generator and engine are assumed.
2. The emission factor for SO_2 is 1.01 times the sulfur content of the fuel.

3.0 AIR QUALITY ATTAINMENT STATUS

This project will be built on land leased from the Navajo Nation. As a federally recognized tribe, the Navajo Reservation is considered sovereign land and is not subject to the regulations of the State of New Mexico. They are subject to the U.S. Environmental Protection Agency (EPA) regulations as are individual States. This project will be under the jurisdiction of EPA Region IX, since the majority of the Navajo Nation is located in Arizona. All local regulations will be administered by the Navajo Nation EPA (NN EPA) which have been adopted for the most part from the New Mexico Environmental Department (NMED) regulations. The Navajo Nation has not been delegated authority under the Clean Air Act to issue a Prevention of Significant Deterioration permit by EPA, so the PSD permit will be issued by EPA Region IX.

New sources of air pollutants are subject to various federal regulations. These regulations and their applicability to the Project are discussed below.

3.1 Area Compliance Status

The facility will be located near Farmington, San Juan County, New Mexico. This area is part of New Mexico Air Quality Control Region (AQCR) 014. AQCR 014 is designated as attaining the National Ambient Air Quality Standards (NAAQS) for all criteria pollutants.

3.2 Federal Regulations

3.2.1 National Ambient Air Quality Standards

As mandated by the Clean Air Act of 1970, EPA has established ambient air quality standards to protect public health (primary standards) and public welfare (secondary standards). Primary standards are based on observable human health responses, and are set at levels that provide an adequate margin of safety for sensitive segments of the population. Secondary standards are intended to protect non-health-based public interests such as structures, vegetation, and livestock. The more stringent of the primary or secondary standards are applicable to the modeling evaluation.

Pollutants for which ambient air quality standards exist are referred to as criteria pollutants. The criteria pollutants are: sulfur dioxide (SO_2), particulate matter with an aerodynamic diameter less than 10 microns (PM_{10}), nitrogen dioxide (NO_2), carbon monoxide (CO), photochemical oxidants as ozone (O_3), and lead (Pb). NO_x and VOC are regulated as precursors to ozone. The PM_{10} NAAQS were promulgated July 1, 1987 at the federal level with the intent of replacing the existing standards limiting Total Suspended Particulates (TSP). EPA, on July 19, 1997, promulgated a new Fine Particulate ($PM_{2.5}$) NAAQS although legal challenges to the new standard have caused EPA to delay implementation until a new health standard review is completed. In the meantime, EPA is in the process of establishing a monitoring network for $PM_{2.5}$. For now, EPA has indicated that PM_{10} should continue to be used as a surrogate (Seitz, 1997).

The NAAQS, listed in Table 3-1, have been developed for various durations of exposure. The short-term (24-hours or less) NAAQS for SO_2 and CO refer to exposure levels not to be exceeded more than once per year. Long-term NAAQS for SO_2, NO_2, and lead refer to limits that cannot be exceeded for exposure averaged over three months (lead) or annually (SO_2 and NO_2). Compliance with the PM_{10} 24-hour and annual standards are statistical, not deterministic. The standards are attained when the expected number of exceedances each year is less than or equal to 1. When modeling with a three-year meteorological data set, compliance with the 24-hour standard is demonstrated when the 4th highest 24-hour concentrations at each receptor, based on the 3-year data set, is predicted to be below the standard. Compliance with the annual standard is demonstrated when the 3-year concentration at each receptor is predicted to be below the standard.

In addition to the ambient air quality standards, the EPA has defined a set of ambient impact levels used to determine whether a new source or modification will "significantly" affect an area. These significant impact levels (SILs), which are also shown in Table 3-1, are interpreted by the EPA and NMED as representing the ambient impact level below which no further analysis of the new source's impacts are required. The primary purpose of comparing a new source's modeled impacts to the SILs is to establish a source's significant impact area (SIA). Major background sources located within the new source's pollutant-specific SIA, as well as other sources which could significantly interact within the proposed source's SIA, are generally modeled as part of the air quality impact analysis. The SILs therefore are merely a regulatory tool to determine the level of analysis required to demonstrate compliance with the applicable air quality standards.

Table 3-1 National Ambient Air Quality Standards and Significant Impact Levels

Pollutant	Averaging Period	Primary NAAQS ($\mu g/m^3$)	Secondary NAAQS ($\mu g/m^3$)	Class II SIL ($\mu g/m^3$)	Class I SIL ($\mu g/m^3$)
NO_2	Annual(1)	100	100	1	0.1
SO_2	Annual(1)	80	None	1	0.1
	24-hour(2)	365	None	5	0.2
	3-hour(2)	None	1,300	25	1
PM_{10}	Annual(4)	50	50	1	0.2
	24-hour(3,5)	150	150	5	0.3
CO	8-hour(2)	10,000	10,000	500	N/A
	1-hour(2)	40,000	40,000	2,000	N/A
O_3(6)	1-hour(3)	0.12	0.12	N/A	N/A
O_3	8-hour(3)	0.08	0.08	N/A	N/A
Pb	3-month(1)	1.5	1.5	N/A	N/A

1. Not to be exceeded.
2. Not to be exceeded more than once per year.
3. Not to be exceeded more than an average of one day per year over three years.
4. Not to be exceeded by the arithmetic average of the annual arithmetic averages from 3 successive years.
5. Compliance with the 24-hour standard is demonstrated when the 4th highest 24-hour concentration at each receptor, based on 3 years of modeling, is predicted below the standard.
6. Units are in ppm.

Source 40 CFR 50

3.2.2 Prevention of Significant Deterioration (PSD) Regulations

PSD review (40 CFR 52.21) is a federally mandated program, which applies to new major sources of regulated pollutants and major modifications to existing sources. PSD review is a pollutant specific review. It applies only to those pollutants for which a project is considered major and the project area is designated as attainment or unclassified. For a new facility to be subject to PSD review, the project's potential to emit (PTE) must exceed the PSD major source thresholds, which are:

- 100 tpy if the source is one of the 28 named source categories, or
- 250 tpy for all other sources

The Project is one of the 28 named categories, specifically a fossil fuel fired steam-generating plant with heat input greater than 250 MMBtu/hr. As such, the applicable PSD threshold is 100 tpy. Table 3-2 compares the preliminary estimated Project annual PTE with the PSD significant emission rates. As shown in the table, the Project's PTE is estimated to be greater than 100 tpy for several criteria pollutants. The Project will therefore require a PSD permit.

Table 3-2
Comparison of Project Annual PTE to the PSD Thresholds

Pollutant	PSD Significant Emission Rate (tpy)	Project PTE (tpy)
Carbon Monoxide (CO)	100	5,529
Nitrogen Oxides (NO_x)	40	3,325
Sulfur Dioxide (SO_2)	40	3,319
Particulate Matter (PM)	25	570
Respirable Particulates (PM_{10})	15	1,120
Ozone (Volatile Organic Compounds)	40	166
Lead	0.6	11.1
Fluorides	3	13.3
Sulfuric Acid Mist	7	221
Hydrogen Sulfide	10	Negligible
Total Reduced Sulfur	10	Negligible
Reduced Sulfur Compounds	10	Negligible

The main technical requirements of the PSD regulations are:

- Demonstrate that the project will incorporate Best Available Control Technology (BACT),

- Evaluate existing ambient air quality,
- Demonstrate that the project will not cause or significantly contribute to a violation of the NAAQS or PSD increments (see Table 3-3),
- Determine the impact of the proposed project on soils, vegetation and visibility at Class I areas, and
- Determine the air quality impacts resulting from indirect growth associated with the project.

Table 3-3
Allowable PSD Increments ($\mu g/m^3$)

Pollutant	Averaging Period	Class I Area	Class II Area	Class III Area
NO_2	Annual(1)	2.5	25	50
SO_2	Annual(1)	2	20	40
	24-hour(2)	5	91	182
	3-hour(2)	25	512	700
PM_{10}	Annual(1)	4	17	34
	24-hour(2)	8	30	60

(1) Not to be exceeded
(2) Not to be exceeded more than once per year

Source 40 CFR 50

3.3 New Mexico Air Regulations

Similar to the NAAQS, New Mexico has established ambient air quality standards (NMAAQS). The Project will be required to demonstrate compliance with both the NAAQS and the NMAAQS for receptors located in New Mexico that extend beyond the Navajo Nation. The NMAAQS are defined in section 20.2.3 NMAC of the New Mexico Air Quality Regulations and are listed in Table 3-4.

The differences between the NAAQS and NMAAQS are:

- annual and 24-hour NMAAQS for SO_2 are more stringent than the NAAQS;
- the NMAAQS includes annual, 30-day, 7-day, and 24-hour standards for Total Suspended Particulate (TSP);
- there are no NMAAQS pertaining to inhalable particulate (PM_{10});

- the 1-hour and 8-hour NMAAQS for CO are more stringent than the NAAQS;
- the annual NMAAQS for NO_2 is more stringent than the NAAQS; the NMAAQS includes a 24-hour standard for NO_2; and
- the NMAAQS include a 1-hour standard for H_2S.

Table 3-4
New Mexico Ambient Air Quality Standards

Pollutant	Averaging Period	Air Quality Standard (ppm)
NO_2	Annual(1)	0.050
	24-hour	0.01
SO_2	Annual(1)	0.02
	24-hour	0.10
	3-hour	-
TSP	Annual(2)	60(3)
	30-day	90(3)
	7-day	110(3)
	24-hour	150(3)
CO	8-hour	8.7
	1-hour	13.1
H_2S	1-hour	0.010(4)
O_3	1-hour	-
Pb	3-month	-

(1) Arithmetic Mean
(2) Geometric mean
(3) $\mu g/m^3$
(4) For the entire State with the exception of Pecos-Permian Basin Intrastate AQCR, no to be exceeded more than once per year.
Source: 20.2.3 NMAC

This page intentionally left blank

4.0 METEOROLOGY OF THE FOUR CORNERS AREA

4.1 Review of Past Studies

During the 1960s and 1970s, two major coal-fired electrical generating stations were built in northwestern New Mexico: the Four Corners Power Plant and the San Juan Generating Station. The locations of these plants are shown in Figure 2-2. These power plants, like the proposed Desert Rock Energy Facility, were commercially viable due to the presence of local coal supplies, adequate water supplies, and electrical transmission infrastructure. The plants were likely built with limited meteorological data and air quality modeling studies. However, concerns about the effects of these two power plants on local air quality led to a number of ambient air monitoring programs that were carried out in northwestern New Mexico.

An excellent collection of ambient air and meteorological monitoring studies is provided in "Air Quality and Meteorology of Northwestern New Mexico", an SAI study conducted in the early 1980s for Arizona Public Service. Excerpts of this report that relate to the wind flows in this area are provided in Appendix A. This report was used, in part, as the basis for the EPA complex terrain field experiment conducted by ERT (now ENSR) in 1982 on the Hogback (see, for example, "EPA Complex Terrain Model Development: Third Milestone Report – 1983). Figure 46 from the EPA Report (also Figure 4-28 of the SAI report) shows the complexity of wind flow for summer morning drainage situations – this is reproduced here as Figure 4-1.

4.2 Available Meteorological Data

The SAI report refers to 61-m data taken at a tower near the Four Corners Power Plant in the 1970s, as well as 10-m winds measured at a tower on the Ute Mountain range to the north, as well as Farmington, NM airport data. The Four Corners tower data is not available to the public, and the SAI report indicates that the data capture over the 5-year period of record was only 75 percent at the top of the tower. Otherwise, there are only single years of 10-m data in the area available from the New Mexico Air Quality Bureau web site (http://www.nmenv.state.nm.us/aqb/modeling/metdata.html) for the Shiprock substation, or several years from the Farmington, New Mexico airport. Because of the 150-m height of the proposed main stack for the Desert Rock Energy Facility, it is likely that 10-m data, especially at locations not close to the proposed plant site, will have questionable representativeness for input to air quality dispersion models.

Due to the lack of available stack-top winds at the proposed plant site, there are two options available for obtaining adequate meteorological data input:

1) Initiate a site-specific 1-year meteorological tower monitoring study, for input to a steady-state Gaussian model such as ISCST3 or AERMOD;

Figure 4-1 Example of Complex Winds in the Four Corners Area[1]

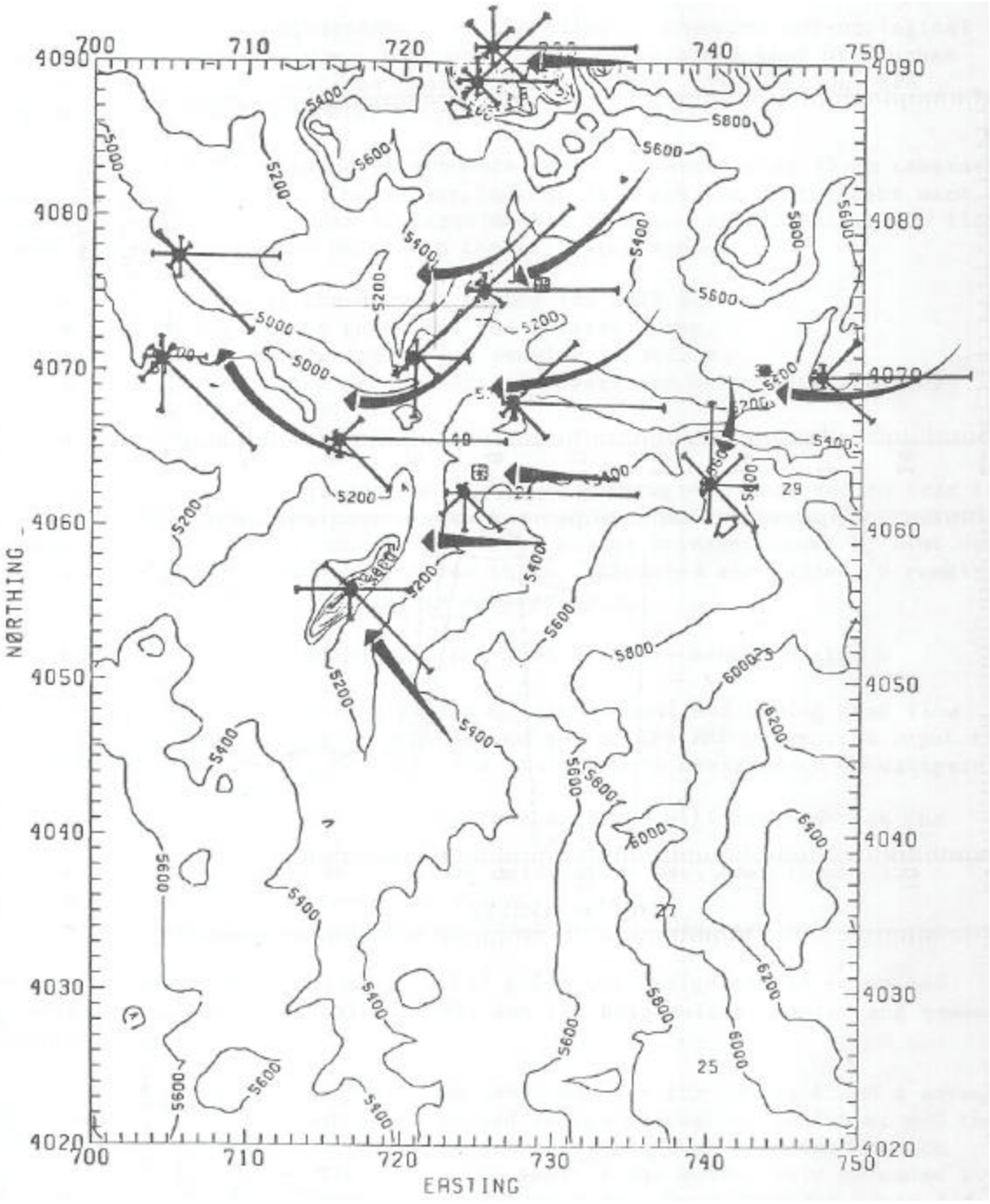

(1) Moore et al., Air Quality and Meteorology of Northwest New Mexico. SAI No. 82014

2) Determine that the area is one with "complex winds" that would be amenable to modeling with CALPUFF for local air quality impacts. The use of three years of recent high quality prognostic mesoscale meteorological data would be proposed as input to CALPUFF.

In the next subsection, we make the argument that the region does feature complex winds, and that there are available meteorological data sets that would support the use of CALPUFF for the local modeling (as well as the long-range modeling needed for determining impacts at PSD Class I areas). This option is better than the use of a single meteorological station that would have a limited area of representative coverage in this area of complex winds.

4.3 Complexity of Local Winds

EPA's Guideline on Air Quality Models (Appendix W to 40 CFR Part 51) has the following discussion of "complex winds" in Section 8.2.8:

> "In many parts of the United States, the ground is neither flat nor is the ground cover (or land use) uniform. These geographical variations can generate local winds and circulations, and modify the prevailing ambient winds and circulations. Geographic effects are most apparent when the ambient winds are light or calm. In general, these geographically induced wind circulation effects are named after the source location of the winds, e.g., lake and sea breezes, and mountain and valley winds. In very rugged hilly or mountainous terrain, along coastlines, or near large land use variations, the characterization of the winds is a balance of various forces, such that the assumptions of steady-state straight-line transport both in time and space are inappropriate. In the special cases described, the CALPUFF modeling system may be applied on a case-by-case basis for air quality estimates in such complex non-steady-state meteorological conditions. The purpose of choosing a modeling system like CALPUFF is to fully treat the time and space variations of meteorology effects on transport and dispersion."

Figure 4-1 (and others in the excerpts from the 1982 SAI report on the meteorology of northwestern New Mexico) clearly shows that the wind flow in the area is not uniform. The mountain range on the eastern side of the Figure 4-1 represents a relief of 1200-1600 feet over 25 kilometers, with both drainage and upslope flows that are not uniform because the terrain slope is not uniform. Therefore, the winds as depicted in the figure show convergence and divergence features due to the non-uniform terrain, and this behavior would be expected in the vicinity of the proposed source as well (at UTM coordinate 721296 UTM E and 4041975 UTM N, zone 12). Therefore, the winds in the area are complex and we propose the use of CALPUFF for both local and long-range transport modeling. This proposed use of CALPUFF is discussed further in Section 6.

This page intentionally left blank

5.0 DISPERSION MODELING APPROACH: PSD CLASS II ANALYSIS

5.1 Review of EPA Modeling Guidance

As noted in Section 5.3, the area in the vicinity of the proposed (Figure 5-1) Desert Rock Energy Facility, and also with the existing Four Corners Power Plant (FCPP) and the San Juan Generating Station (SJGS), features nonuniform winds due to the presence of local terrain influences. The 1982 SAI report indicates that the air mass in the Four Corners area in northwestern New Mexico frequently moves in a "turnaround" day-night cycle, featuring downslope (easterly) flow at night and upslope (westerly) flow during the day. Due to the nonuniform gradient of increasing terrain to the east, the downslope and upslope flows are also not uniform, featuring converging and diverging flows into and out of the San Juan and Chaco Rivers. The drainage flows interact with obstacles such as the Hogback (studied extensively by ERT and EPA as part of the development of the CTDMPLUS model), causing secondary complex wind regimes. Section 8.2.8 of EPA's Guideline on Air Quality Models indicates that CALPUFF (Scire 2000) is suitable for such a complex winds situation.

Another issue regarding the use of CALPUFF is the lineup of the three power plants mentioned above for potential air quality impacts on the elevated terrain to the north, in the Ute Mountain range in far northern New Mexico. The transport distance from the proposed Desert Rock Energy Facility, past the FCPP and SJGS to the Ute Mountains is about 55 kilometers. This long-range transport situation is best handled by CALPUFF, as noted in Section 7.2.3 of the Guideline on Air Quality Models.

For the reasons noted above, Steag proposes the use of CALPUFF for both the PSD Class I and II modeling requirements associated with the proposed project.

5.2 Proposed Use of CALPUFF and RUC Data

ENSR proposes the use of the following versions of the CALPUFF modeling system:

- CALMET version 5.2 (level 000602d),
- CALPUFF version 5.5 (level 010730_1), and
- CALPOST version 5.2 (level 991104d).

These software versions are the ones associated with the latest available user guides. Although EPA has announced the availability of 2003 versions of the CALPUFF modeling system, these are still being debugged and do not have any user's guides available.

Figure 5-1 Proposed Location of the Desert Rock Energy Facility in Relation to Nearby Class II Areas

The meteorological data that will be used as input to CALPUFF will feature three years of prognostic mesoscale meteorological (MM) data, as is recommended by the Guideline on Air Quality Models (Section 9.3.1.2(d)). The most advanced MM data will be used, consisting of 2001-2003 hourly meteorological data archived from the Rapid Update Cycle (RUC) model. Horizontal data resolution for the RUC model is 40 kilometers for 2001 and 2002, and 20 kilometers for 2003. The Rapid Update Cycle data is referred to as "RUC40" for the 40-km resolution data and "RUC20" for the 20-km resolution data. A technical paper on successful use of this type of data in a North Dakota CALPUFF application is provided in Appendix B.

5.3 PSD Class II CALPUFF Modeling Domain

A grid system that extends approximately 105 kilometers in all directions from the proposed source location will be used in this CALPUFF modeling analysis, as shown in Figure 5-2. The total domain size of 210 kilometers was chosen because the distance to the limit of the receptor coverage that includes the high terrain in the Ute Mountains is 55 kilometers from the proposed source location. If a cumulative analysis is needed, additional sources up to 50 kilometers beyond this area may need to be included in the modeling analysis. This design allows a 210 km x 210 km (E-W / N-S) grid with a 1.5-km grid element size. The southwest corner of the grid is located at approximately 35.55°N latitude and 109.75°W longitude.

5.4 CALMET and CALPUFF Processing

CALMET (Scire, 2000), the CALPUFF meteorological pre-processor, will be used to simulate three years (2001, 2002 and 2003) of meteorological conditions. For the hourly wind field initialization, CALMET will use gridded prognostic RUC40 data for 2001 and 2002 and RUC20 data for 2003. This information will be combined with terrain data with a 1.5-km grid resolution to more accurately characterize the wind flow throughout the modeling domain. The Step 2 wind field will be produced with the input of all available National Weather Service hourly surface and upper air twice daily balloon sounding data within and just outside the modeling domain. Data from some second-order hourly surface stations will be used where there are gaps in the coverage of the NWS stations. Other sources of meteorological data may be explored to compensate areas lacking NWS or second order data. RUC20 data was initiated by the National Oceanic and Atmospheric Administration (NOAA) during 2002 as an update to RUC40, and so is available only for 2003. The data providers reformatted the RUC data, without making any enhancements, for input into CALMET. Figure 5-3 shows the location of the RUC40/RUC20 data along with the surface and upper air stations used to produce the 2001, 2002, and 2003 CALMET, CALPUFF-ready, meteorological data.

Except where noted in Table 5-1, the CALMET model parameter settings will follow the recommendations in Appendix A of the IWAQM Phase II report. Due to the size of the modeling domain, a Lambert Conformal coordinate system will be used. The Lambert Conformal grid will be based on the reference coordinates of 36° N latitude and 110° W longitude along with 30° N and 60° N as the two standard parallels. The technical options to be used for the CALPUFF modeling are provided in Table 5-2.

Figure 5-2 Class II CALPUFF Modeling Domain

Figure 5-3 Class II Meteorological Data Used for CALPUFF Modeling

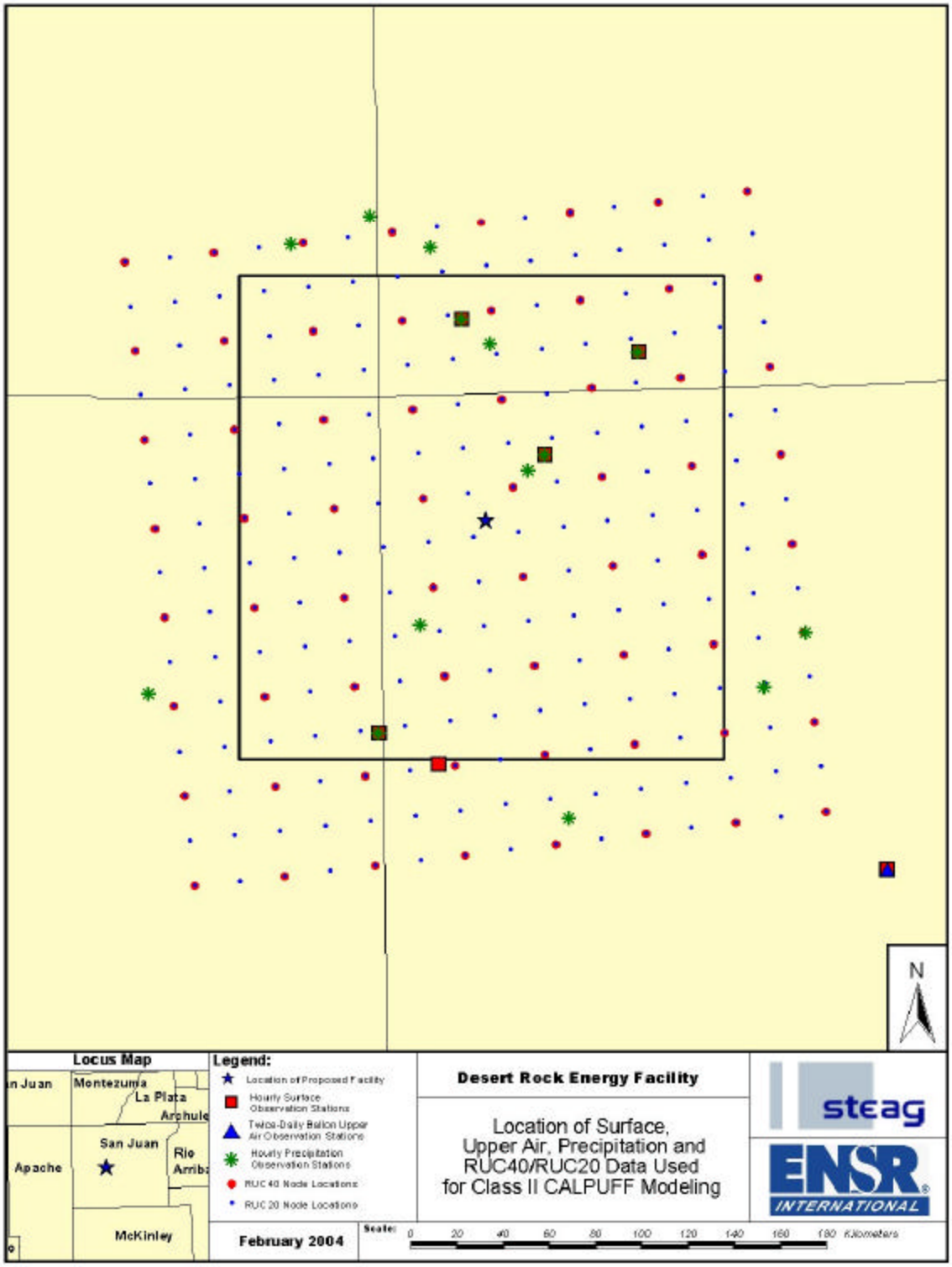

Table 5-1
CALMET User-Defined Fields Not Specified in IWAQM Appendix A (Class II Modeling)

Variable	Description	Value
NX	Number of east-west grid cells	140 (Class II modeling)
NY	Number of north-south grid cells	140 (Class II modeling)
DGRIDKM	Meteorology grid spacing (km)	1.5 km (Class II modeling)
NZ	Number of Vertical layers of input meteorology	12
ZFACE	Vertical cell face heights (m)	0, 20, 40, 80, 120, 180, 260, 400, 600, 800, 1200, 2000, 3000.
IEXTRP	Extrapolation of surface winds to upper layers	-4
RMAX1	Max surface over-land extrapolation radius (km)	10
RMAX2	Max aloft over-land extrapolation radius (km)	20
RMAX3	Maximum over-water extrapolation radius (km)	500
TERRAD	Radius of influence of terrain features (km)	10
R1	Relative weight at surface of Step 1 field and obs	1
R2	Relative weight aloft of Step 1 field and obs	10
ISURFT	Surface station to use for surface temperature	Farmington, NM
IUPT	Station for lapse rates	Albuquerque, NM
IPROG	Gridded initial prognostic wind field – MM5(RUC) data	14
RMIN	Min radius of influence for wind field interpolation	0.1

5.5 Good Engineering Practice Stack Height Analysis

Federal stack height regulations limit the stack height used in performing dispersion modeling to predict the air quality impact of a source. Sources must be modeled at the actual physical stack height unless that height exceeds the Good Engineering Practice (GEP) stack height. If the physical stack height is less than the formula GEP height, the potential for the source's plume to be affected by aerodynamic wakes created by the building(s) must be evaluated in the dispersion modeling analysis.

A GEP stack height analysis will be performed for all point emission sources that are subject to effects of buildings downwash at the proposed facility in accordance with the EPA's "Guideline for Determination of Good Engineering Practice Stack Height" (EPA, 1985). A GEP stack height is defined as the greater of 65 meters (213 feet), measured from the ground elevation of the stack, or the formula height (H_g), as determined from the following equation:

$$H_g = H + 1.5\ L$$

where

H is the height of the nearby structure which maximizes H_g, and

L is the lesser dimension (height or projected width) of the building.

Table 5-2
CALPUFF User-Defined Fields Not Specified in IWAQM Appendix A (Class II Modeling)

Variable	Description	Value
CSPECn	Names of Species	SO_2, NO_x, PM_{10}
NX	Number of east-west grid cells	140 (Class II modeling)
NY	Number of north-south grid cells	140 (Class II modeling)
DGRIDKM	Meteorology grid spacing (km)	1.5 km (Class II modeling)
NZ	Number of Vertical layers of input meteorology	12
ZFACE	Vertical cell face heights (m)	0, 20, 40, 80, 120, 180, 260, 400, 600, 800, 1200, 2000, 3000.
IBCOMP	Southwest X-index of computational domain	1
JBCOMP	Southwest J-index of computational domain	1
IECOMP	Northeast X-index of computational domain	140
JECOMP	Northeast Y-index of computational domain	140
Dry Gas Dep	Chemical parameters of gaseous deposition	CALPUFF default
Dry Part. Dep	Chemical parameters of particle deposition	CALPUFF default
Wet Dep	Wet deposition parameters	CALPUFF default
MOZ	Ozone background	From multiple stations
BCKNH3	Ammonia background	1 ppb (for arid lands)
IRESPLIT	Hours when puff are eligible to split	Default
NPT1	Number of point sources	Application-specific
NREC	Number of user-defined receptors	Consistent with receptors provided by the FLMs
Receptors	Location (with elevation)	Class I Area specific

Both the height and the width of the building are determined through a vertical cross-section perpendicular to the wind direction. In all instances, the GEP formula height is based upon the highest value of H_g as determined from H and L over all nearby buildings over the entire range of possible wind directions. For the purposes of determining the GEP formula height, only buildings within 5L of the source of interest are considered.

The GEP analysis will be conducted with EPA's BPIP program, version 95086. The building-specific wind directions will then be used as input to CALPUFF.

5.6 Building Cavity Analysis

If any of the stacks associated with the proposed project are below GEP formula height, a cavity analysis will be considered to determine the potential for cavity region impacts. The SCREEN3 model (Version 96043), which incorporates the Scire-Schulman cavity algorithm, is available as a screening tool to estimate the extent of the building cavity, if any. Since the project buildings and stacks are located far from the plant fenceline, it is likely that any building cavity will not extend to ambient air.

5.7 Local Area Topography and Receptors

The proposed facility's central location is noted by the UTM coordinates of the main stack, which are, 721,703.3 m (Easting) and 4,040,903.95 m (Northing) (UTM zone 12, North American Datum 1983 [NAD83]). The Lambert Conformal location of this stack is, 129.21 km (east) and 54.14 km (north), based on reference coordinates of 36° N latitude and 110° W longitude along with 30° N and 60° N as the two standard parallels. The Class II CALPUFF analysis will use receptors based on this Lambert Conformal projection and the main stack as the center of the grid (see Figure 5-4). Receptors will be placed along the proposed facility fence line spaced at every 50 meters. A multi-layered Cartesian grid combined with a polar grid will extend out from the main stack as far as to resolve the SIA. The Cartesian receptor grid will consist of 100-meter spaced receptors beyond the fenceline out to 1.5 km, 250-meter spacing will be used beyond 1.5 km out to 4 km, and 500-meter spacing will be used beyond 4 km out to 8 km, and 1000-meter spacing will be used beyond 8 km out to 10 km. Beyond 10 km, polar grid receptors will be used. The polar grid receptors will be placed along 36 10^{o} radials extending from the central location of the main stacks. Receptors between 10 km and 20 km will be placed along each radial every 1000 meters, and from 20 km to 50 km, 5000-meter spacing will be used. Additional densely spaced receptors will be placed in one area of complex terrain (in the Ute Mountains to the north, in the direction where the proposed facility, the Four Corners Power Plant, and the San Juan Generating Station line up) to ensure resolution of the maximum impacts in that area. If peak modeled impacts for determination of significance and PSD or NAAQS compliance are not within an area with receptor spacing of 100 meters or less and the impacts are more than 50% of the significance or compliance levels, then those impacts will be refined with 100-meter spaced receptors.

Receptor elevations will be developed from 7.5 minute (~30 meter spaced) and 10-meter Digital Elevation Model (DEM) files for the near-field grid and 90-meter spaced DEMs for the coarse polar grid

5.8 Worst-Case Load Determination

SCREEN3 modeling will be conducted to determine the operating load for which the highest modeled impacts are obtained. Modeling will be conducted for four load cases: 40, 60, 80, and 100 percent. The emission rates and stack exhaust parameters used to determine the worst-case operating load are described in Section 3 and shown in Table 2-1.

The operating load resulting in the highest ground-level impacts will be the case used for subsequent significance and cumulative source modeling. However, if the highest ground-level impacts are not associated with 100 percent load operation, then the significance and cumulative modeling will assess the 100 percent load-operating scenario along with the operating scenario resulting in the highest ground-level impacts. SCREEN3 modeling results show that the 40 and 100 percent load cases cause the highest impacts. The input and output files for SCREEN3 are located in Appendix D.

5.9 Distant Class II Areas

CALPUFF will be used to assess impacts at distant Class II areas (beyond 50 kilometers) as requested by the FLMs. These areas are shown in Figure 5-4 and include:

- Aztec Ruins National Monument
- Canyon de Chelly National Monument
- Chaco Culture National Historic Park
- Colorado National Monument
- Cruces Basin Wilderness Area
- Curecanti National Recreation Area
- El Malpais National Monument
- El Morro National Monument
- Glen Canyon National Recreation Area
- Hovenweep National Monument
- Hubbel Trading Post National Historic Site
- Lizard Head Wilderness Area
- Mount Sneffels Wilderness Area
- Natural Bridges National Monument
- Navajo National Monument
- Pecos National Historic Park
- Petroglyph National Monument
- Rainbow Bridge National Monument
- Salinas Pueblo Missions National Monument
- South San Juan Wilderness Area
- Sunset Crater National Monument
- Wupatki National Monument
- Yucca House National Monument
- Zuni-Cibola NHP
- Wilson Mountain Primitive Area
- Uncompahgre Wilderness Area

Figure 5-4 Class II Receptor Grid

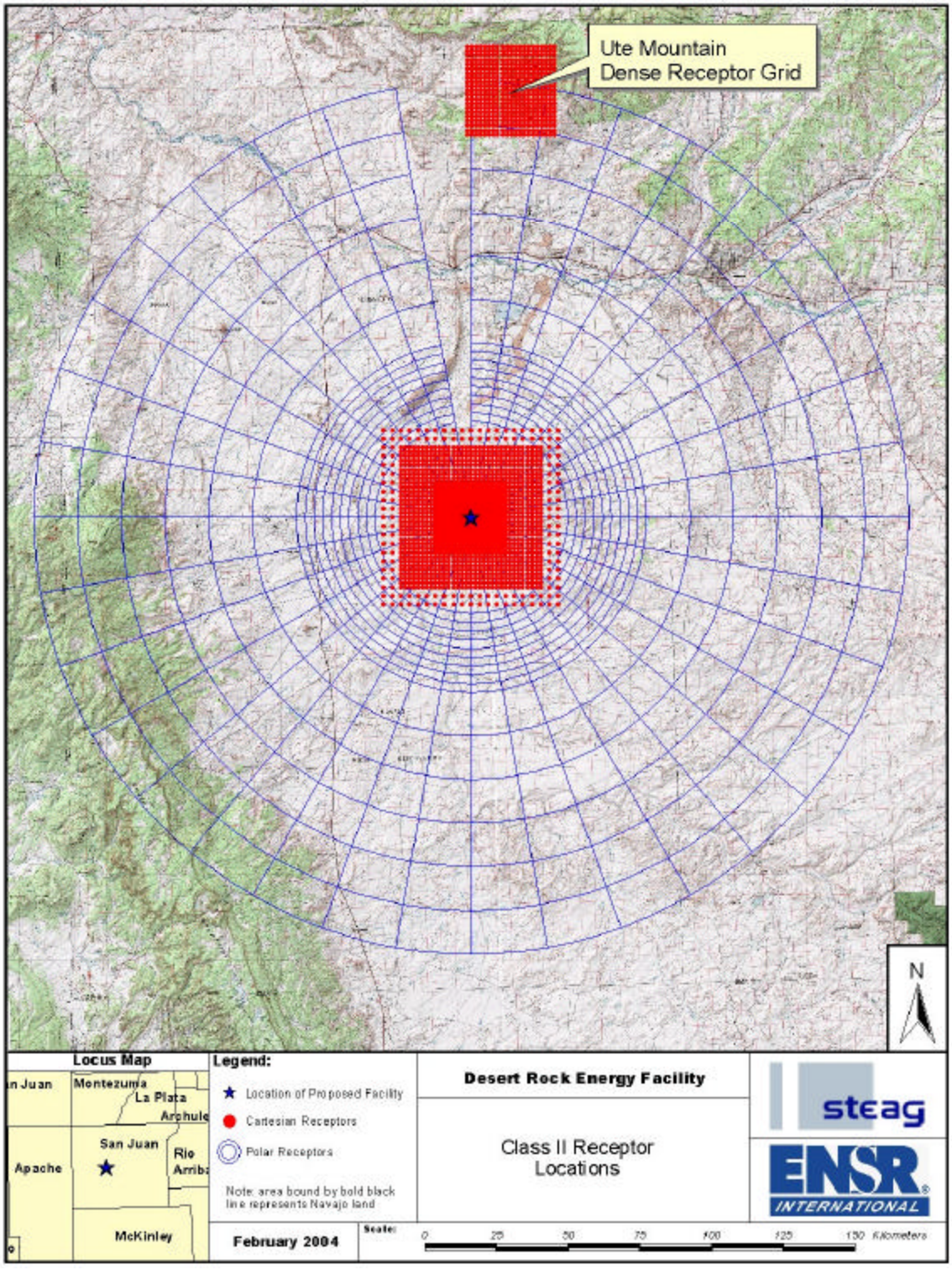

Except where noted below, impacts at these areas will be addressed in terms of PSD Class II increment, regional haze, and acidic deposition. For pollutants and averaging periods at each area shown to have an insignificant modeled increment, no further modeling will be required (Class II significance thresholds are shown in Table 3-1). For those pollutants and averaging period at each area that exceed the PSD increment significance thresholds, a cumulative modeling analysis will be preformed and compared to the Class II significance thresholds.

Since these areas are not Class I designated, regional haze and acidic deposition results associated with emissions from the main stacks alone will be reported for informational purposes and will not be compared to thresholds that are applicable for a Class I area.

However, Colorado National Monument, Wilson Mountain Primitive Area, and Uncompahgre Wilderness Area are Class I protected areas for SO_2 PSD increment. Therefore, the SO_2 Class I significance thresholds and increments will apply to these Class II areas only. Class I significance thresholds and increment values can be found in Table 3-1 and Class I increment values are in Table 3-3.

This modeling analysis will assess the impacts at the specified Class II areas from the proposed project's two main stacks alone operating at 100 percent load. Other small ancillary or fugitive sources that are either emergency or start-up in nature will not be included in this portion of the modeling analysis because the effects of these sources are typically confined within the first few kilometers of the project site.

Receptor grids for these areas will be generated based on the suggestions of John Notar of the NPS. A description of each area's receptor grid is shown in Table 5-3. Receptor elevations will either be picked from a topographic map or calculated using 90-meter spaced Digital Elevation Model (DEM) files. Receptors for Glen Canyon will be modeled out to 200 kilometers from the proposed project location.

Table 5-3
Distant Class II Area Receptors

Park	Receptor(s) Description
Aztec Ruins Nat. Mon.	one receptor(1)
Canyon de Chelly Nat. Mon.	use 2-km grid for extensive coverage
Chaco Culture NHP	use 2-km grid for extensive coverage--be sure to capture high point near Pueblo Alto, as well as canyon bottom
Colorado Nat. Mon.	use 2-km grid for extensive coverage
Cruces Basin NWA	use 2-km grid for extensive coverage
Curecanti NRA	one receptor(1)
El Malpais Nat. Mon.	use 2-km grid for extensive coverage
El Morro Nat. Mon.	one receptor at ruins on top of monument
Glen Canyon NRA	use 5-km grid for extensive coverage out to 200 km
Hovenweep Nat. Mon.	one receptor(1)
Hubbel Trading Post NHS	one receptor(1)
Lizard Head NWA	use 2-km grid for extensive coverage
Mount Sneffels NWA	use 2-km grid for extensive coverage
Natural Bridges Nat. Mon.	one receptor(1)
Navajo Nat. Mon.	one receptor at Betatakin overlook
Pecos NHP	one receptor(1)
Petroglyph Nat. Mon.	one receptor(1)
Rainbow Bridge Nat. Mon.	one receptor(1)
Salinas Pueblo Missions Nat. Mon.	one receptor(1)
South San Juan NWA	use 2-km grid for extensive coverage
Sunset Crater Nat. Mon.	one receptor(1)
Wupatki Nat. Mon.	one receptor(1)
Yucca House Nat. Mon.	one receptor(1)
Zuni-Cibola NHP	one receptor(1)
Wilson Mountain Primitive Area	use 2-km grid for extensive coverage
Uncompahgre NWA	use 2-km grid for extensive coverage
(1) Receptor will be located on the park boundary closest to the proposed project site	

6.0 DISPERSION MODELING APPROACH: PSD CLASS I ANALYSIS

The evaluation of impacts at PSD Class I areas within 300 kilometers of the proposed plant will be modeled with CALPUFF. The PSD Class I areas will include Arches, Bandelier, Black Canyon of the Gunnison, Capitol Reef, Canyonlands, Grand Canyon, Great Sand Dunes, Mesa Verde, and Petrified Forest National Parks, along with La Garita, Pecos, San Pedro Parks, West Elk, Weminuche, and Wheeler Peak Wilderness Areas. The use of CALPUFF in a screening mode will not be used and we will proceed directly to the use of CALPUFF in a refined mode to assess impacts from the proposed Desert Rock Energy Facility. The long-range analysis will address ambient air impacts on Class I PSD Increments and Air Quality Related Values (AQRVs) at all above mentioned Class I areas. See Figure 6-1 for the location of the proposed project in relation to nearby PSD Class I areas.

6.1 Selection of Dispersion Model

ENSR will run CALPUFF in a refined mode to determine the project impacts on PSD increments and AQRVs at Arches, Bandelier, Black Canyon of the Gunnison, Capitol Reef, Canyonlands, Grand Canyon, Great Sand Dunes, Mesa Verde, and Petrified Forest National Parks, along with La Garita, Pecos, San Pedro Parks, West Elk, Weminuche, and Wheeler Peak Wilderness Areas. EPA has recently promulgated CALPUFF as the approved model for long-range transport beyond 50 kilometers, and for local complex winds situations on a case-by-case basis.

6.2 Use of CALPUFF and RUC Data

ENSR proposes to use CALPUFF and RUC data for 2001-2003 in the PSD Class II modeling. The same years of data will be used as input to CALPUFF for the PSD Class I modeling, but the modeling domain will be expanded to include PSD Class I areas within 300 kilometers of the proposed plant site.

Even for the high quality RUC data, EPA (Irwin, 2004) recommends a comparison of the winds derived from the use of the RUC data with observed surface winds at a few locations to verify that the RUC winds are reasonably comparable. Irwin acknowledges that there will be significant sample-to-sample noise in the wind speed and especially the wind direction because of horizontal variations. However, we would expect a relatively unbiased comparison between wind speed and wind direction of the *average* RUC and surface winds.

Although Tim Allen of the Fish & Wildlife Service recommended a specific test using software available from Environ (METSTAT), we found this software to be incompatible with both the RUC data and CALMET output, and that there would be an extensive effort needed to adapt the program to these datasets. Instead, we simply used Excel spreadsheets to conduct this test, using a total of four surface stations distributed over the modeling domain for the three years being modeled. The four stations compared were:

Figure 6-1 Proposed Location of the Desert Rock Energy Facility in Relation to Nearby PSD Class I Areas

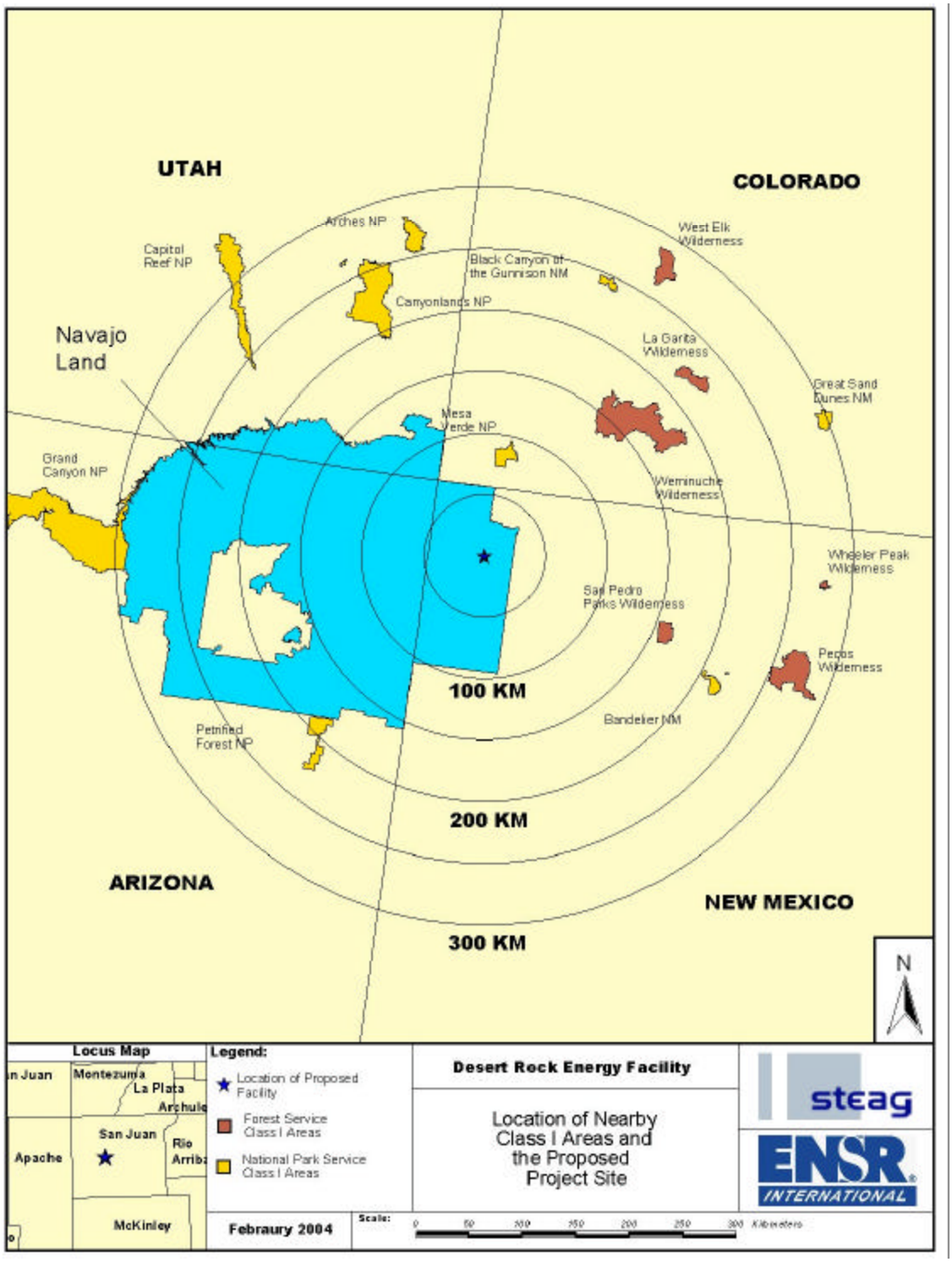

- Farmington, NM
- Moab, UT
- Flagstaff, AZ and
- Santa Fe, NM.

The comparison was done by taking the PRTMET output of CALMET for nearby grid points to these airports. With the assignment of R1 in CALMET to just 1 kilometer, we made sure that the influence zone of the airport data in the Step 2 wind field process was beyond each grid point used (so that the RUC data dominated), but that the grid point was sufficiently close to the airports to provide a meaningful comparison.

The wind speed plots were comprised of ratios of hourly RUC/CALMET values divided by the airport values (calms were not included). The ratios were displayed as "box" plots, with the x-axis (comprised of the observed airport wind speed) divided into 4 "bins", as shown in the example in Figure 6-2. The box plots provide a range of y-axis values in which the center of the box represents the 50% ranked value, the upper and lower box limits are the 10% and 90% ranked values. This figure shows that, on average, the CALMET wind speeds are within about 20% of the Farmington wind speeds over the range of speeds. The airport speeds are slightly higher than the CALMET speeds for high winds, and are slightly lower than the CALMET speeds for low winds.

The wind direction plots were comprised of the difference of the hourly CALMET values minus the airport values (differences were set to values between –180 and +180 degrees). The x axis (airport wind direction) was divided into four quadrants, centered at north, east, south, and west, as shown in the example in Figure 6-3. This figure shows that the CALMET and airport wind directions are, on average, within 5-10 degrees of each other over all wind direction sectors.

The complete set of plots generated is provided in Appendix G. The overall results indicate the following:

- There is a moderate tendency for the ratio of CALMET to airport wind speeds to decrease as the wind speeds increase. The finite starting threshold speed at airports may play a role in this regard.

- In general, over the entire wind speed range and all stations used in the comparison, the CALMET wind speeds are relatively unbiased. However, some wind speed ratios above or below 1.0 are evident for different stations and years.

Figure 6-2 Example of RUC Wind Speed Comparison with Airport Data

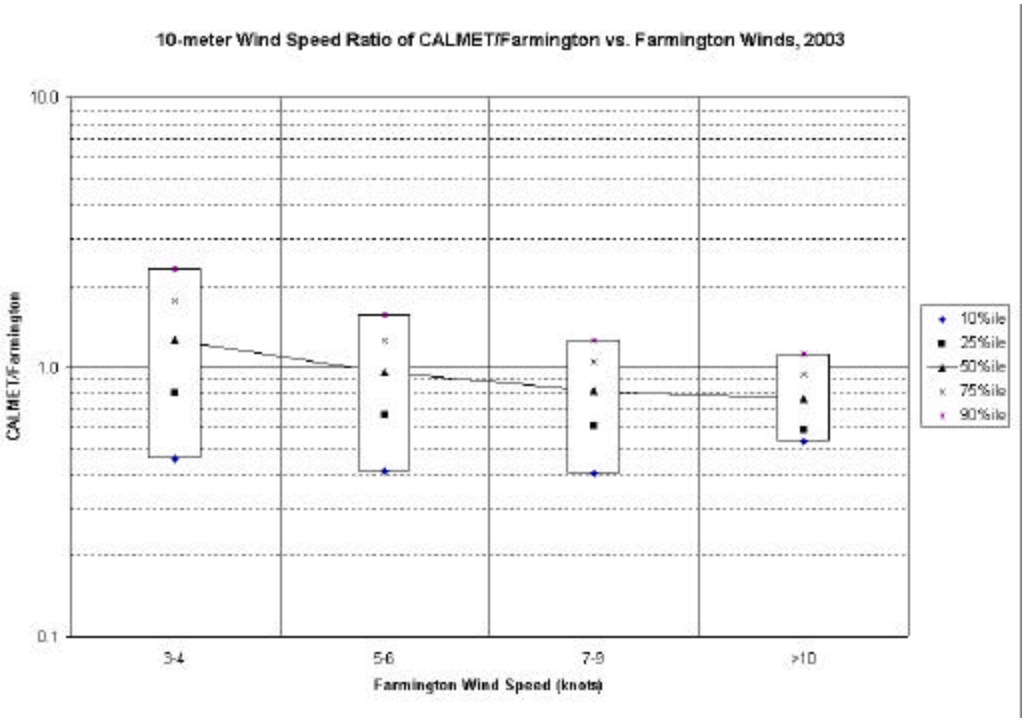

Figure 6-3 Example of RUC Wind Direction Comparison with Airport Data

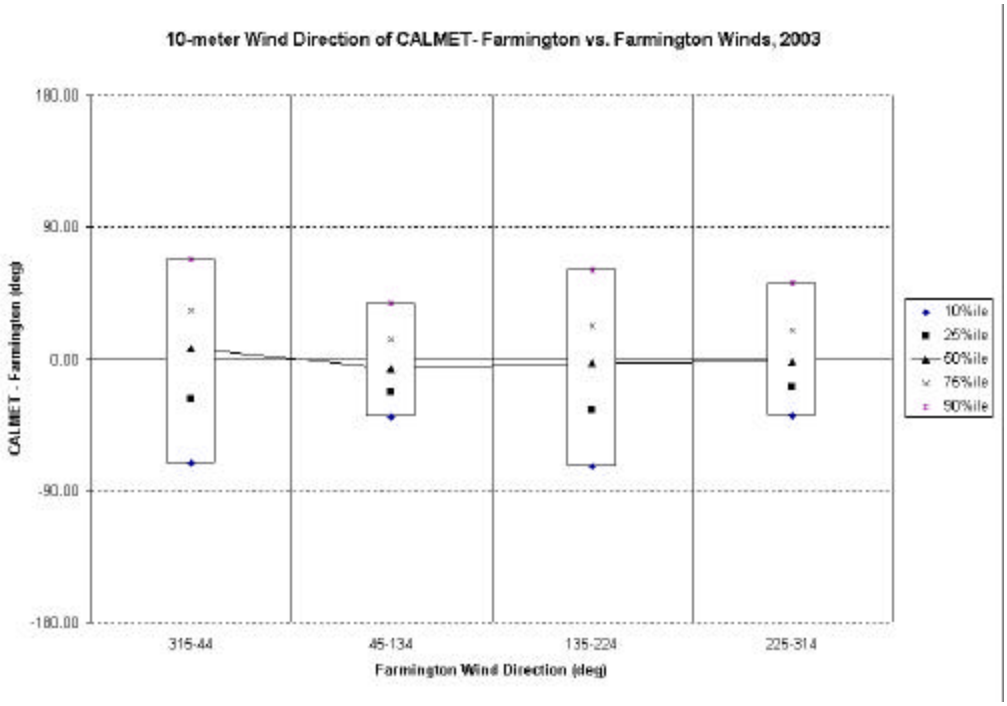

- In general, over the entire wind direction range and all stations used in the comparison, the CALMET wind directions are relatively unbiased. Biases are generally site-specific, as would be expected.

- Overall, the CALMET winds compare reasonably well with the airport stations selected for this comparison. Due to the availability of state-of-the-art remote data sources for NOAA, we would expect that the accuracy of the RUC data for levels well above the surface would be very good.

6.3 Class I Modeling Domain

The CALPUFF modeling grid system was designed to extend approximately 50 kilometers east of Great Sand Dunes National Park, north of West Elk Wilderness, south of Petrified Forest, as well as 350 kilometers west of the project site. The modeling domain proposed for this analysis is shown in Figure 6-4. The additional buffer distances beyond the Class I areas will allow for the consideration of puff trajectory recirculations. This design allows for a 680 km x 552 km (E-W / N-S) grid with a 4-km grid element size. The southwest corner of the grid is located at approximately 34.28° N latitude and 112.46° W longitude. The Class I modeling domain is described in Section 5.3.

6.4 Receptors

The receptors used in the refined CALPUFF analysis will be limited to those actually along the PSD Class I boundary. However, if the park boundary extends more than 300 kilometers from the project site, then only those receptors within 300 kilometers will be assessed in this CALPUFF analysis. The receptors for Arches, Bandelier, Black Canyon of the Gunnison, Capitol Reef, Canyonlands, Grand Canyon, Great Sand Dunes, Mesa Verde, and Petrified Forest National Parks, along with La Garita, Pecos, San Pedro Parks, West Elk, Weminuche, and Wheeler Peak Wilderness Areas will be obtained from a database of receptors for all Class I areas produced by the National Park Service.

6.5 CALMET Processing

CALMET (version 5.5), the CALPUFF meteorological pre-processor will be used to simulate three years (2001, 2002 and 2003) of meteorological conditions. For the hourly wind field initialization, CALMET will use gridded prognostic RUC40 data for 2001 and 2002 and RUC20 data for 2003. This information will be combined with terrain data with a 4-km grid resolution to more accurately characterize the wind flow throughout the modeling domain. The Step 2 wind field will be produced with the input of all available National Weather Service hourly surface and upper air twice daily balloon sounding data within and just outside the modeling domain. Data from some second-order hourly surface stations will be used where there are gaps in the coverage of the NWS stations. Other sources of meteorological data may be explored to supplement areas lacking NWS or second-order data. Similarly, relative humidity data from the RUC MM5 input data may be used to supplement areas with poor coverage for this important parameter. Hourly precipitation data from stations within and just

Figure 6-4 Class I CALPUFF Modeling Domain

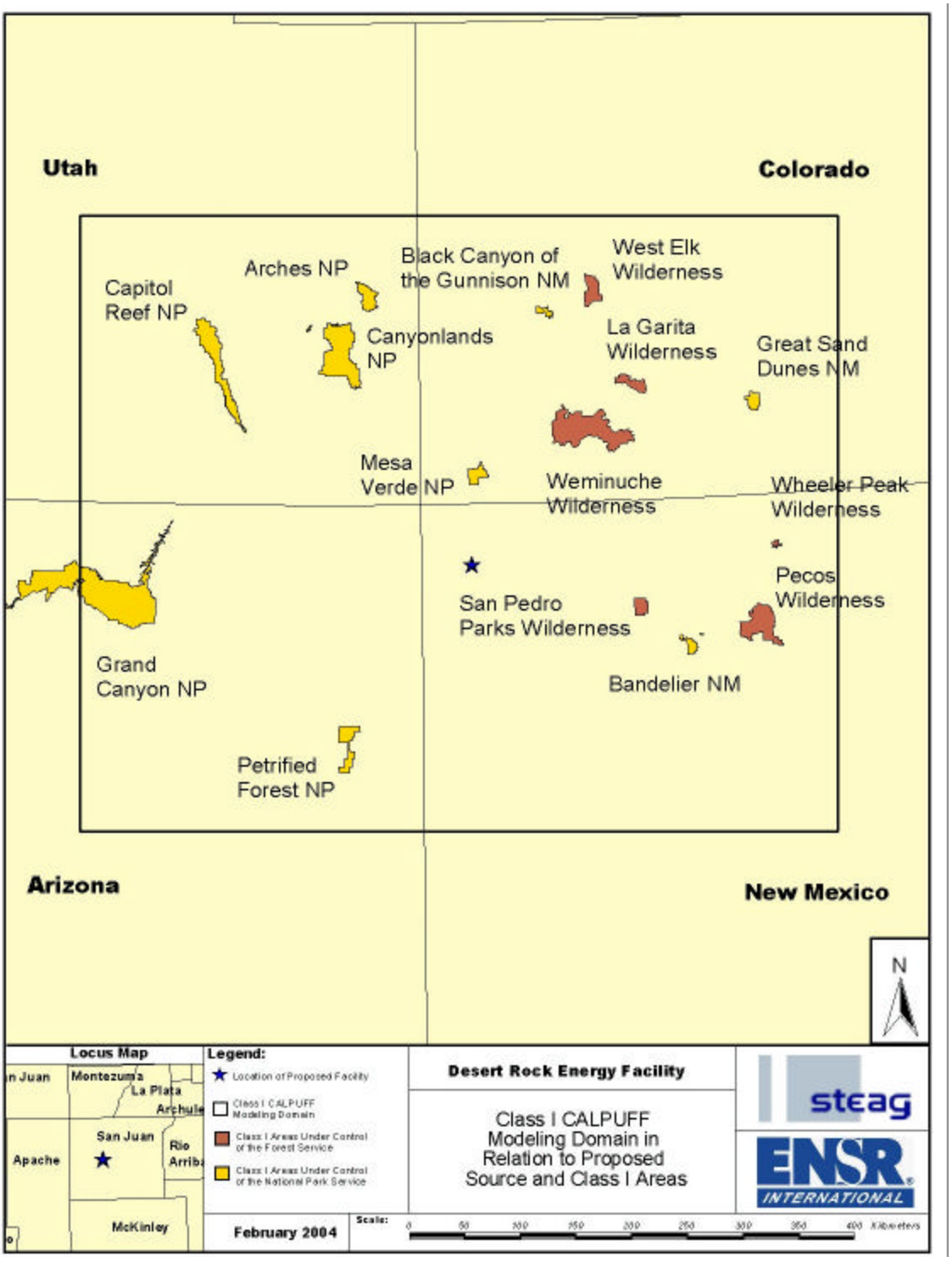

outside of the modeling domain will be taken from an NCDC data set. For 2001 and 2002, RUC40 data is available every 40 km within the modeling domain and for 2003, RUC20 data is available every 20 km within the modeling domain. Figure 6-5 shows the location of the surface and upper air stations, Figure 6-6 shows the location of the precipitation stations, and Figure 6-7 shows the location of the RUC40/RUC20 nodes used to produce the 2001, 2002, and 2003 CALMET, CALPUFF-ready, meteorological data. Note, availability of the surface, upper air, and precipitation stations may vary from year to year.

Except where noted in Table 6-1, the CALMET model parameter settings will follow the recommendations in Appendix A of the IWAQM Phase II report. Due to the size of the modeling domain, a Lambert Conformal coordinate system will be used. The Lambert Conformal grid will be based on the reference coordinates of 36° N latitude and 110° W longitude along with 30° N and 60° N as the two standard parallels.

Table 6-1
CALMET User-Defined Fields Not Specified in IWAQM Appendix A (Class I Modeling)

Variable	Description	Value
NX	Number of east-west grid cells	170 (Class I modeling)
NY	Number of north-south grid cells	138 (Class I modeling)
DGRIDKM	Meteorology grid spacing (km)	4 km (Class I modeling)
NZ	Number of Vertical layers of input meteorology	12
ZFACE	Vertical cell face heights (m)	0, 20, 40, 80, 120, 180, 260, 400, 600, 800, 1200, 2000, 3000.
IEXTRP	Extrapolation of surface winds to upper layers	-4
RMAX1	Max surface over-land extrapolation radius (km)	10
RMAX2	Max aloft over-land extrapolation radius (km)	20
RMAX3	Maximum over-water extrapolation radius (km)	500
TERRAD	Radius of influence of terrain features (km)	10
R1	Relative weight at surface of Step 1 field and obs	1
R2	Relative weight aloft of Step 1 field and obs	10
ISURFT	Surface station to use for surface temperature	Farmington, NM
IUPT	Station for lapse rates	Albuquerque, NM
IPROG	Gridded initial prognostic wind field – 3D.DAT (RUC) data	14
RMIN	Min radius of influence for wind field interpolation	0.1

Figure 6-5 Location of Surface and Upper Air Meteorological Data Used for CALPUFF Class I Modeling

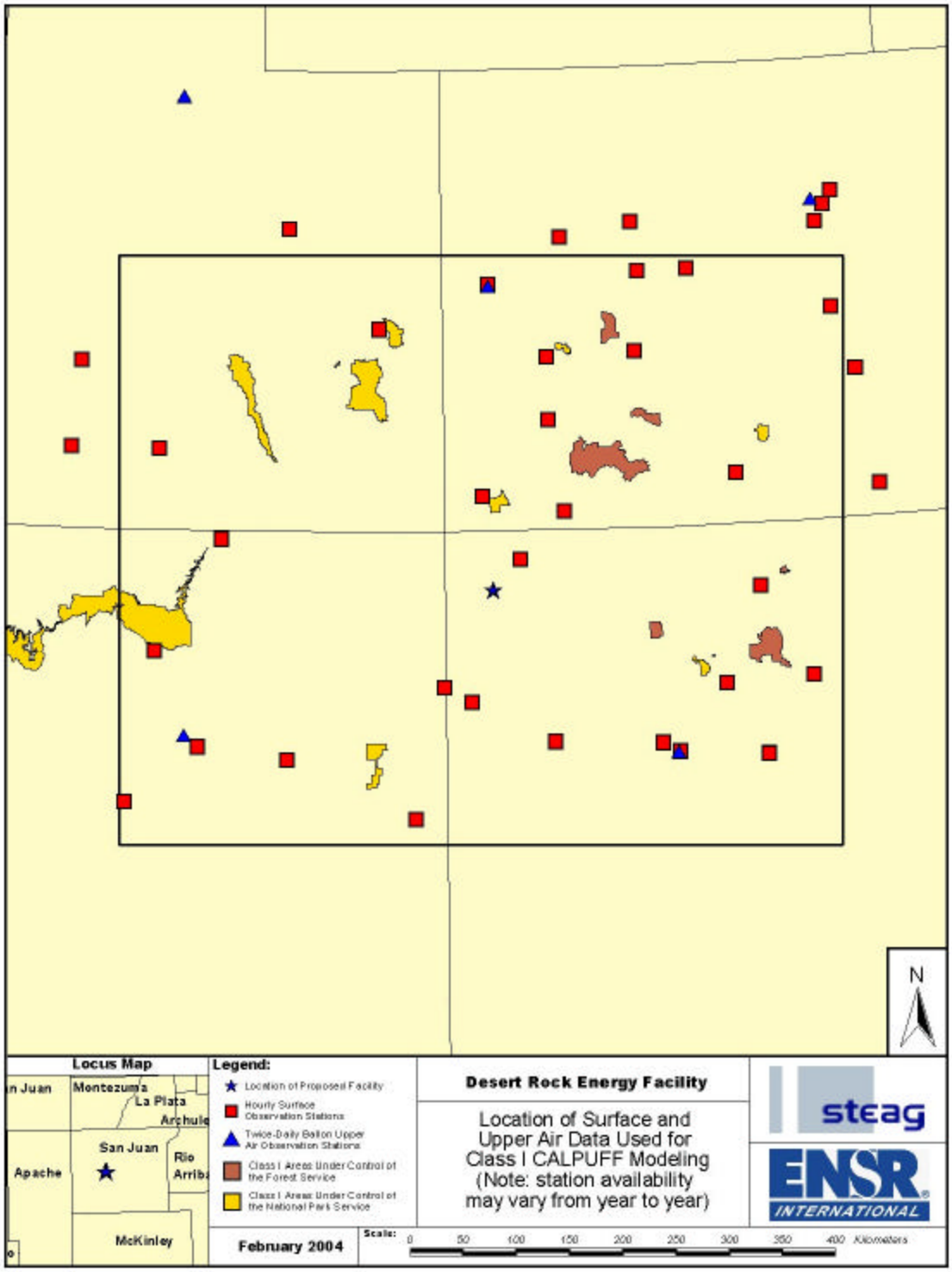

Figure 6-6 Class I Precipitation Data Used for CALPUFF Modeling

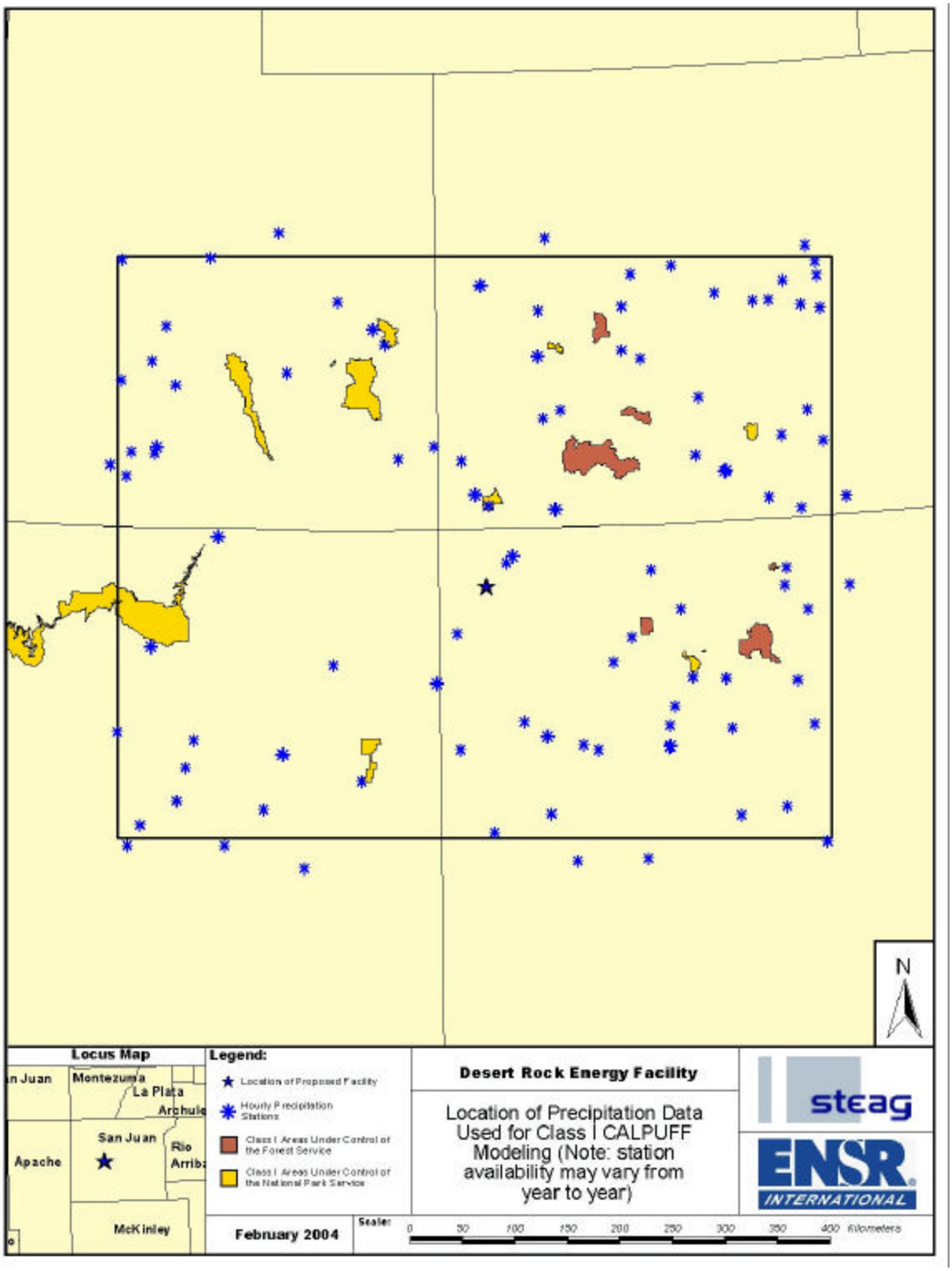

Figure 6-7 Class I RUC20/RUC40 Used for CALPUFF Modeling

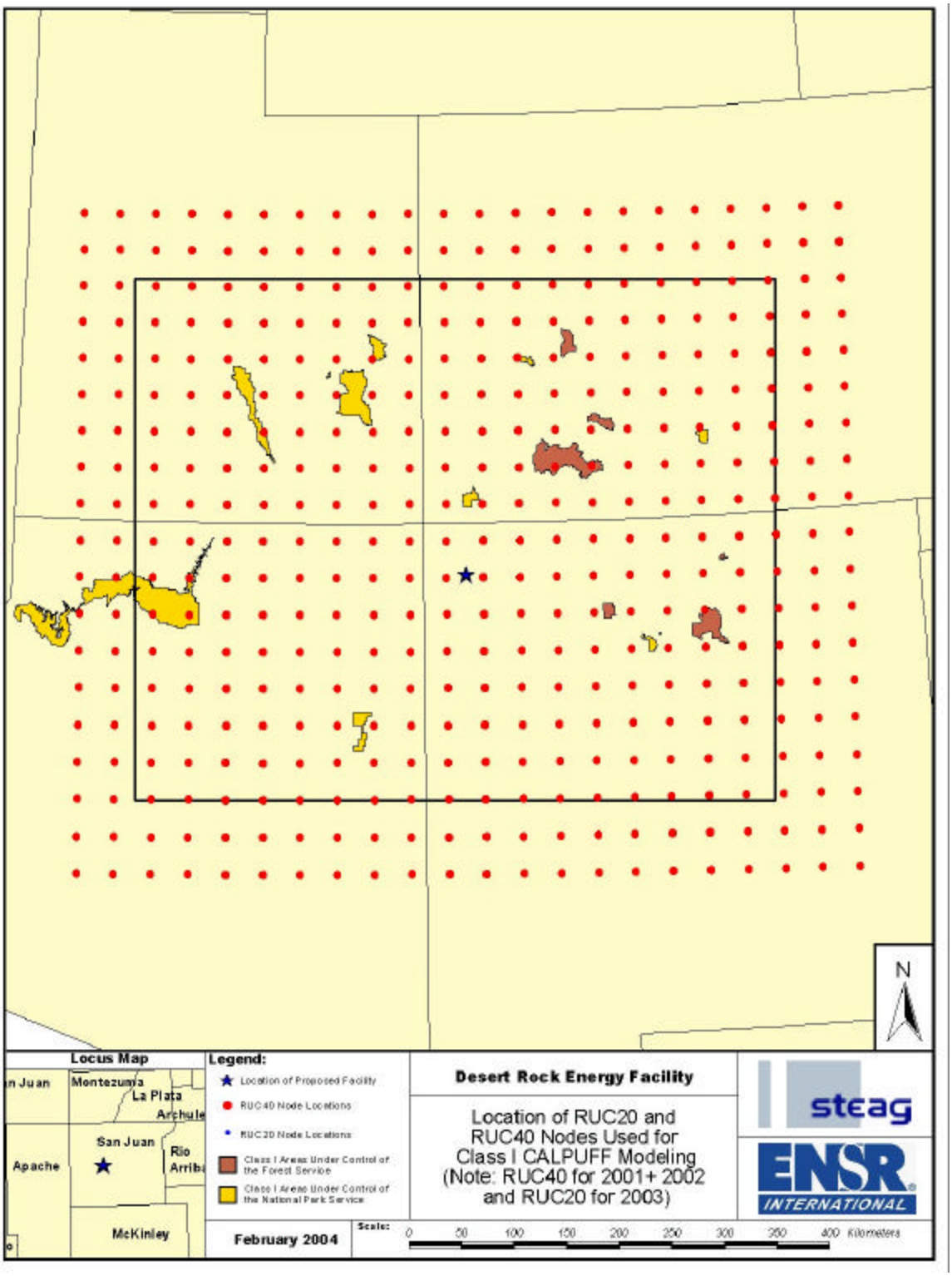

6.6 CALPUFF and CALPOST Processing for Significance Determination at Class I Areas

The evaluation of PSD Increment and AQRVs at Arches, Bandelier, Black Canyon of the Gunnison, Capitol Reef, Canyonlands, Grand Canyon, Great Sand Dunes, Mesa Verde, and Petrified Forest National Parks, along with La Garita, Pecos, San Pedro Parks, West Elk, Weminuche, and Wheeler Peak Wilderness Areas will be addressed by modeling the emissions from proposed plant's main stacks alone. All other ancillary sources are either emergency or start-up in nature or are very small, so they are likely to have negligible impacts at all of the distant Class I areas and will not be included in the Class I increment consumption, acidic deposition or regional haze analysis. The maximum impacts of these smaller sources will be localized to within a few kilometers of the plant. The auxiliary boiler is generally used only if no steam is available from the main boilers, so it will not be used for the worst-case modeled conditions.

For those PSD Increments or AQRVs that are shown to be insignificant, no further modeling is required. Significance for PSD Increment is based on thresholds that are listed in Table 6-2. For other AQRVs, significance thresholds are described in later sections. If the project is shown to be significant for any PSD Increments or AQRV(s), then a cumulative analysis will be performed for that PSD Increment or AQRV after consultation with the reviewing agencies. The results of the multi-source assessment will then be compared to applicable Class I Area PSD Increments or respective AQRV adverse impact thresholds that are established by the Federal Land Manager.

Table 6-2
Proposed PSD Class I Area Significant Impact Levels (µg/m3)

Pollutant	3 – Hour	24 – Hour	Annual
SO_2	1.0	0.2	0.1
PM_{10}	N/A	0.3	0.2
NO_x	N/A	N/A	0.1
Note: All values are compared to the highest concentration when determining significance. N/A = not applicable.			

Proposed facility emissions from the main stacks alone will be modeled with CALPUFF (version 5.5) following the model input parameters recommended in Appendix B of the IWAQM Phase II report, except where noted in Table 6-3. CALPOST (version 5.2) will then be used to post process the results from the binary CALPUFF output files. Hourly ozone data, concurrent with the meteorological data, will be used in the modeling. Figure 6-8 shows the location of all ozone stations used for each of the three years (2001, 2002, and 2003).

6.6.1 PSD Increments

CALPUFF and CALPOST will be used in a refined mode with CALMET meteorological data for 2001, 2002, and 2003 to assess maximum concentrations of SO_2, NO_x, and PM_{10} at Arches, Bandelier, Black Canyon of the Gunnison, Capitol Reef, Canyonlands, Grand Canyon, Great Sand Dunes, Mesa Verde, and Petrified Forest National Parks, along with La Garita, Pecos, San Pedro Parks, West Elk, Weminuche, and Wheeler Peak Wilderness Areas. It will be conservatively assumed that 100 percent of the NO_x emissions are converted to NO_2, but a national default conversion rate of 75 percent will be used to more accurately assess modeled NO_2 impacts, if a refined analysis is necessary. PM_{10} increment consumption will be based on the proposed source's primary PM_{10} emissions along with the secondary particulate formed from the proposed source's SO_2 and NO_X emissions. If modeled concentrations at all receptors with in the PSD Class I Areas are below the proposed significant impact levels (SILs) (see Table 6-2), then no further modeling will be required. However, if the project shows significant impacts for any pollutant/averaging time, then a cumulative analysis for that pollutant/averaging time will be performed in consultation with the reviewing agencies.

6.6.2 Regional Haze

CALPUFF and CALPOST processing will be used for the regional haze analysis to compute the maximum 24-hour average light extinction at Arches, Bandelier, Black Canyon of the Gunnison, Capitol Reef, Canyonlands, Grand Canyon, Great Sand Dunes, Mesa Verde, and Petrified Forest National Parks, along with La Garita, Pecos, San Pedro Parks, West Elk, Weminuche, and Wheeler Peak Wilderness Areas associated with emissions from the modeled sources and then compare it to the background extinction. The dry hygroscopic and non-hygroscopic values make up the "natural" background conditions (extinction) from which the modeled extinction will be compared too when determining the percent change due to the project's emissions. As noted in FLAG (2000), if a project-related change in extinction is less than 5 percent of the background extinction, then the project regional haze impact is determined to be insignificant and no further modeling is required.

If the project-related change in extinction exceeds 5 percent, then ENSR will consider a number of refinements to the default FLAG process. These refinements may include the new f(RH) curves published by EPA in September 2003 and adjusting the natural background extinction to account for naturally occurring salt particles. ENSR may also investigate whether the associated days involve natural obscuration due to meteorological interferences: precipitation, fog, high relative humidity, and/or a cloud ceiling during nighttime hours. During such events, the natural background visual range is much lower than that assumed by the FLAG procedure, and should be adjusted accordingly. If all days with a prediction of more than a 5 percent change in extinction due to the proposed project (following the FLAG procedures) are associated with meteorological interferences, and the associated adjustments in the natural background visibility result in no days with an extinction change over 5 percent, this finding will be documented and submitted to the USDA Forest Service and the National

Table 6-3
CALPUFF User-Defined Fields Not Specified in IWAQM Appendix B (Class I Modeling)

Variable	Description	Value
CSPECn	Names of Species	SO_2, SO_4, NO_x, HNO_3, NO_3, PMF, SOA
NX	Number of east-west grid cells	170 (Class I modeling)
NY	Number of north-south grid cells	138 (Class I modeling)
DGRIDKM	Meteorology grid spacing (km)	4 km (Class I modeling)
NZ	Number of Vertical layers of input meteorology	12
ZFACE	Vertical cell face heights (m)	0, 20, 40, 80, 120, 180, 260, 400, 600, 800, 1200, 2000, 3000.
IBCOMP	Southwest X-index of computational domain	1
JBCOMP	Southwest J-index of computational domain	1
IECOMP	Northeast X-index of computational domain	190
JECOMP	Northeast Y-index of computational domain	155
Dry Gas Dep	Chemical parameters of gaseous deposition	CALPUFF default
Dry Part. Dep	Chemical parameters of particle deposition	CALPUFF default
Wet Dep	Wet deposition parameters	CALPUFF default
MOZ	Ozone background	From multiple stations
BCKNH3	Ammonia background	1 ppb
IRESPLIT	Hours when puff are eligible to split	Default
NPT1	Number of point sources	Application-specific
NREC	Number of user-defined receptors	Consistent with receptors provided by the FLMs
Receptors	Location (with elevation)	Class I Area specific

Figure 6-8 Class I Ozone Stations Used for CALPUFF Modeling

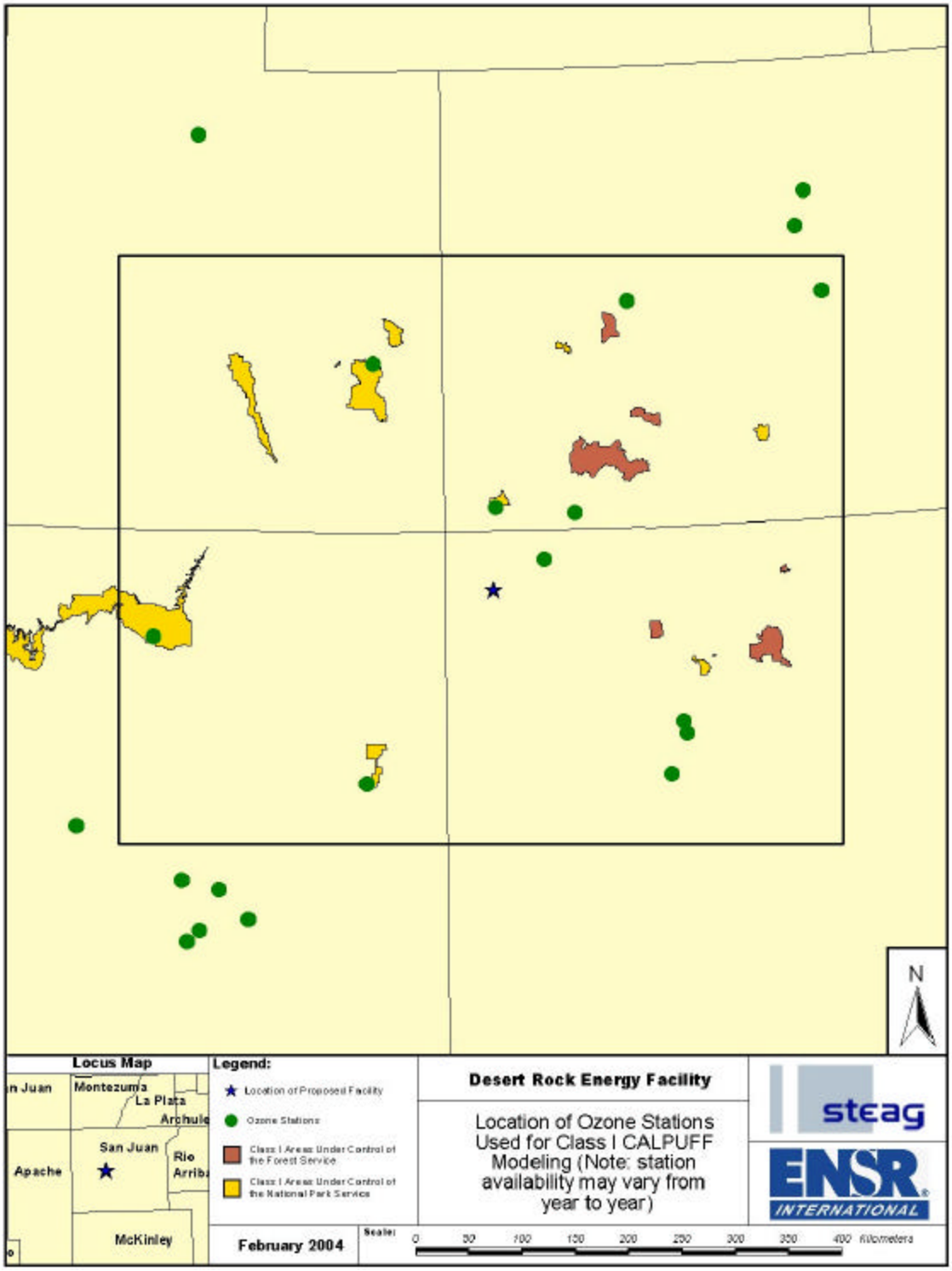

Park Service. Other refinements as noted in the technical paper provided in Appendix E will be considered, such as adjustments to natural conditions that consider naturally occurring salt particles, as well as adjustments to the extinction efficiency for ammonium sulfate and nitrate. If, however, there are still days with a change in extinction that exceeds 5 percent, then a cumulative modeling analysis will be performed for the regional haze assessment, after consultation with the reviewing agencies.

Seasonal average values of the dry hygroscopic and non-hygroscopic components of the background extinction coefficient for each PSD Class I area will be input to CALPOST as ammonium sulfate and soil, respectively. The annual values of dry hygroscopic, which is divided by 3 (FLAG 2000), and non-hygroscopic used in CALPOST for this regional haze analysis will be taken from FLAG (2000) and are shown in Table 6-4. All PSD Class I areas considered in the analysis have the same hygroscopic and non-hygroscopic values.

Table 6-4
Hygroscopic and Non-Hygroscopic Extinction Coefficients (from FLAG, 2000)

	Hygroscopic[(1)]	Non-Hygroscopic
Annual	0.2	4.5

(1) Hygroscopic values shown are those listed in FLAG divided by three, as recommended by FLAG 2000.

The CALPUFF refined modeling will be conducted with hourly background ozone data from the closest monitors (see Figure 6-8 for location of ozone stations) and an ammonia background taken from the IWAQM Phase II Report. IWAQM lists only three possible ammonia background concentrations: 10 ppb for grasslands, 1.0 ppb for arid lands at 20°C, and 0.5 ppb for forest. Since the modeling domain is mostly a mixture of arid lands and forest, a weighted average ammonia background concentration could be determined to be less than 1.0 ppb. However, to be conservative, the modeling analysis will use 1.0 ppb as its ammonia background concentration.

The computation of incremental background light extinction due to the proposed project will use the option to calculate extinction from speciated particulate matter measurements, by applying the FLAG-recommended hourly relative humidity adjustment factors to observed and modeled sulfate and nitrate (MVISBK=2). RHMAX will be capped at 95 percent.

6.6.3 Acid Deposition

CALPUFF and CALPOST will be applied to obtain upper limit estimates of annual wet and dry deposition of sulfur and nitrogen compounds (kg/ha/yr) associated with emissions of SO_2 and NO_x from the proposed facility at Arches, Bandelier, Black Canyon of the Gunnison, Capitol Reef, Canyonlands, Grand Canyon, Great Sand Dunes, Mesa Verde, and Petrified Forest National Parks, along with La

Garita, Pecos, San Pedro Parks, West Elk, Weminuche, and Wheeler Peak Wilderness Areas. Specifically, CALPUFF will be used to model both wet and dry deposition of SO_2, SO_4, NO_3 and HNO_3 as well as dry deposition of NO_x to estimate the maximum annual wet and dry deposition of sulfur (S) and nitrogen (N) at the Class I Areas.

There are no published thresholds for acidic deposition for any of the above PSD Class I areas in which acidic deposition impacts will be addressed. The deposition results will be documented for evaluation by the FLM in the Application. However, it is noted that the United States Department of Agriculture Forest Service web site (http://www.fs.fed.us/r6/aq/natarm/document.htm) indicates that the minimum detectable level for measuring an increase in wet deposition of sulfates or nitrates is 0.5 kg/ha/yr. For conservatism, the Forest Service recommends a significance level of one tenth of this minimum detectable level, or 0.05 kg/ha/yr. The FLM has also recently developed a Deposition Analysis Threshold (DAT) for nitrogen of 0.005 kg/ha/yr (FLAG, 2001) to be used as a threshold for further FLM analysis, rather than as an adverse impact threshold (Porter, 2004).

6.6.4 Lake Acid Neutralizing Capacity Analysis

Sulfur and nitrogen deposition can impact lakes in and near Class I and sensitive Class II areas. The Forest Service will provide ENSR with a screening methodology to calculate the change in lake acid neutralizing capacity (ANC) from a baseline value at several lakes within the modeling domain. The values for baseline ANC are given in units of micro-equivalent per liter (μeq/l). The threshold values for change in ANC are as follows:

- If the baseline ANC > 25 μeq/l, a 10% increase in ANC is allowed
- If the baseline ANC < 25 μeq/l, a 1 μeq/l increase in ANC is allowed
- If the baseline ANC < 0 μeq/l, no increase in ANC is allowed

The screening procedure documentation is presented in Appendix H.

7.0 PSD BACKGROUND AIR QUALITY

7.1 Determination of Significant Impacts

Predicted impacts from the Project's major sources will be compared to the significant impact levels (SILs) for each applicable pollutant and averaging period. If there is no significant impact, no further modeling is required. The Class I and II area SILs are shown in Table 3-1.

The overall maximum concentration for each pollutant and averaging period over the three years (2001, 2002, and 2003) of CALPUFF modeling will be used to determine significance.

For those pollutants with a significant impact in PSD Class II areas, the Project's significant impact area (SIA) will be determined. The SIA is defined as the circular area whose radius is equal to the greatest distance from the source that dispersion modeling predicts a significant impact (EPA 1990), with a maximum possible SIA distance of 50 kilometers. The farthest extent of the SIA for each pollutant will likely be determined by peak load emissions from the two main boiler stacks.

7.2 Compliance with Ambient Air Quality Standards and PSD Increments

For those pollutants and averaging periods and areas determined to be less than the SILs, no further analysis will be required. The discussion below applies only to those pollutants and averaging periods for which a significant impact is predicted with CALPUFF.

Compliance with the PSD increments and NAAQS will be based on the sum of the following:

1. Modeled impacts attributable from the Project

2. Modeled impacts from "nearby" appropriate background sources, to be determined in consultation with the reviewing agencies.

3. For NAAQS, representative ambient background concentration, representing small local sources or other distant sources not explicitly modeled.

Impacts on PSD Class II increment consumption attributable to the Project and "nearby" PSD increment consuming and expanding background sources will be estimated using CALPUFF. Modeling will be performed only for receptors within the SIA distance from the project source. An inventory of sources will be obtained for each pollutant that exceeds the SIL, covering all facilities within 50 km of the SIA that could contribute significantly to ambient concentrations within the SIA radius. For the evaluation of NAAQS, all sources identified to be within 50 km of the SIA that could contribute significantly to ambient concentrations within the SIA radius will be evaluated. A regionally representative ambient background concentration representing small local sources or other distant sources not explicitly modeled will be added to modeled values to determine overall NAAQS compliance.

PSD increment and NAAQS compliance will be based on modeled highest-second-highest concentrations using CALPUFF for those pollutants and averaging periods with predicted significant impacts due to the Project's impacts. Tables 3-1 and 3-3 list the applicable NAAQS and PSD increments for determining compliance. The Project will also be required to demonstrate compliance with the NMAAQS (Table 3-4) for receptors with significant impacts located in New Mexico that extend beyond the Navajo Nation.

7.3 Regional Background Monitors

Ambient air quality data are used to represent the contribution to total ambient air pollutant concentrations from non-modeled sources. In addition, the PSD regulations require applicants to evaluate existing ambient air quality in the Project area.

The closest NO_x SO_2, PM_{10}, and O_3 monitors are located in Farmington, NM and the closest CO monitor is located in Rio Rancho, NM as shown in Figure 7-1.

A summary of the ambient background measurements is provided in Table 7-1. The background data are from the three most recent years (2000-2002) available from the EPA AirData Website (http://www.epa.gov/air/data). Table 7-1 lists the second-highest short-term (≤ 24-hours) concentrations and the highest annual concentrations observed for each monitor. The highest of the second-highest short-term and highest annual concentrations over the three-year period for the most representative monitor(s) will be used in the NAAQS/NMAAQS compliance analysis (see concentrations in bold in Table 7-1).

A discussion of the air quality data measured at the representative sites as they relate to the AAQS is provided below. For each pollutant and averaging period, the highest of the second-highest short-term concentrations and/or the highest long-term concentrations measured at the monitors in the years 2000, 2001, and 2002 are compared to their respective AAQS. The highest second-highest measured short-term concentration is considered because one exceedance of the short-term AAQS is allowed.

7.3.1 Sulfur Dioxide (SO_2)

Ambient air quality standards for SO_2 have been established for three averaging periods: annual, 24-hour and 3-hour. The two closest monitors relative to the proposed facility are the Shiprock Substation in Farmington located 22 miles north of the Project and 1300 W. Navajo in Farmington located 23 miles northeast of the Project. The Shiprock monitor is located in the vicinity of the San Juan Generating Station and the Shiprock Substation and therefore would not be most representative of the background air quality in the vicinity of the Project site. This is reflected by the higher observed concentrations at the Shiprock monitor compared to those at the 1300 W. Navajo, Farmington monitor. Therefore, the measured concentrations at the 1300 W. Navajo, Farmington monitor are proposed to be most representative of the Project site. If a multi-source compliance analysis is required, data from

the 1300 W. Navajo, Farmington monitor will be used to represent the non-modeled portion of background.

Table 7-1 Summary of Ambient Background Measurements

Pollutant	Monitor Site	Averaging Period	Measured Concentrations ($\mu g/m^3$)		
			2000	2001	2002
SO_2	1300 W. Navajo, Farmington, San Juan County ID 35-045-0008-42401-1	3-hour	62.9	65.5	**68.1**
		24-hour	18.3	18.3	**21.0**
		Annual	5.2	5.2	**5.2**
PM_{10}	W. Animas, Farmington, San Juan County ID 35-045-0006-81102-1	24-hour	27.0	27.0	**38.0**
		Annual	16.0	17.0	**17.0**
NO_2	Shiprock Substation, Farmington, San Juan County ID 35-045-1005-42602-1	Annual	16.9	16.9	**16.9**
CO	Rio Rancho, Sandoval County ID 35-043-1003-42101-1	1-hour	2529	**2989**	2069
		8-Hour	1149	1379	**1609**
O_3[(1)]	Shiprock Substation, Farmington, San Juan County ID 35-045-1005-42602-1	1-hour[(2)]	0.09	0.09	0.09
		8-hour[(3)]	0.08	0.07	0.08

(1) Units are in ppm.
(2) Highest measured each year.
(3) 4th highest measured each year.

Figure 7-1 Monitoring Station Locations

All data measured at the 1300 W. Navajo, Farmington monitor are less than the NAAQS. The maximum annual average concentration of 5.2 micrograms of SO_2 per cubic meter ($\mu g/m^3$) is 7 percent of the NAAQS. The highest second-highest 3-hour and 24-hour average concentrations are 68.1 µg/m3 and 21.0 $\mu g/m^3$, respectively. These represent 5 percent and 6 percent of their respective NAAQS.

7.3.2 Particulate Matter (PM_{10})

Ambient air quality standards for PM_{10} have been established for two averaging periods: annual and 24-hour. The closest monitor located relative to the proposed facility is the W. Animas, Farmington monitor located 24 miles northeast of the Project. If a multi-source compliance analysis is required, data from the 1300 W. Navajo, Farmington monitor will be used to represent the non-modeled portion of background.

All data measured at the Farmington monitor are less than the NAAQS. The maximum annual average concentration of 17 $\mu g/m^3$, is 34 percent of the NAAQS. The highest second-highest 24-hour average concentration of 38 $\mu g/m^3$, is 25 percent of the NAAQS.

7.3.3 Nitrogen Dioxide (NO_2)

An ambient air quality standard for NO_2 has been established for the annual averaging period. The only nearby monitor located relative to the proposed facility is the Shiprock, Farmington monitor, located 22 miles northeast of the Project. If a multi-source compliance analysis is required, data from the Farmington monitor will be used to represent the non-modeled portion of background.

The data measured at the Shiprock Farmington monitor are less than the NAAQS. The maximum annual average concentration of 16.9 $\mu g/m^3$, is 17 percent of the NAAQS.

7.3.4 Carbon Monoxide (CO)

Ambient air quality standards for CO have been established for two averaging periods: 1-hour and 8-hour. The closest monitor located relative to the proposed facility is the Rio Rancho monitor located 136 miles southeast of the Project. If a multi-source compliance analysis is required, data from the Rio Rancho monitor will be used to represent the non-modeled portion of background.

The data measured at the Rio Rancho monitor are less than the NAAQS. The maximum 1-hour and 8-hour average concentrations are 2989 $\mu g/m^3$ and 1609 $\mu g/m^3$, respectively. These represent 7 percent and 16 percent of their respective NAAQS.

7.3.5 Ozone

Ambient air quality standards for O_3 have been established for two averaging periods: 1-hour and 8-hour. The closest monitor located relative to the proposed facility is the Shiprock/ Farmington monitor, located 22 miles northeast of the Project.

The data measured at the Shiprock/Farmington monitor do not exceed the NAAQS. The highest 1-hour and fourth highest 8-hour average concentrations are 0.09 ppm and 0.08 ppm, respectively. These represent 75 percent and 100 percent of their respective NAAQS.

In summary, all measured concentrations of criteria pollutants subject to PSD review do not exceed the NAAQS, indicating that the full PSD increments are available.

7.3.6 Pre-Construction Monitoring Waiver

The PSD regulations require that a PSD permit application contain an analysis of existing air quality for all regulated pollutants that the source has the potential to emit in significant amounts. The definition of existing air quality can be satisfied by air measurements from either a state-operated or private network, or by a pre-construction monitoring program that is specifically designed to collect data in the vicinity of the proposed source. A source may be allowed an exemption from the pre-construction monitoring program if the ambient impacts from the source are less than the *de minimis* levels established by the EPA (see Table 7-2) or if existing data are representative of the air quality in the site vicinity.

Table 7-2
PSD Monitoring Threshold Concentrations

Pollutant	Avg. Period	Threshold Concentration ($\mu g/m^3$)
CO	8-hour	575
NO_2	Annual	14
SO_2	24-hour	13
PM/PM_{10}	24-hour	10
O_3	NA	(1)
Lead	3-month	0.1
Fluorides	24-hour	0.25
Total Reduced Sulfur	1-hour	10
Reduced Sulfur Compounds	1-hour	10
Hydrogen Sulfide	1-hour	0.2
(1) Exempt if VOC emissions less than 100 tpy		

A source-specific pre-construction monitoring program should not be required for this Project. This is supported by the existence of representative air quality data as discussed in the previous section. The Project therefore requests written confirmation that a pre-construction monitoring program is not required for this Project.

7.4 PSD and NAAQS Cumulative Modeling Assessment

For pollutants with impacts greater than the Class II SILs, multi-source modeling will be conducted, after consultation with the reviewing agencies, to demonstrate compliance with the NAAQS and PSD increments. As noted, receptors with significant impacts outside of the Navajo lands will be evaluated relative to the New Mexico AAQS as well as the NAAQS. Compliance with the NAAQS and NMAAQS will be based on the modeled concentrations of the proposed project sources and nearby major sources within 50 kilometers of the SIA, plus ambient background concentrations to represent sources in the area not included in the modeling. PSD increment compliance will be based on the multi-source modeling of the proposed Project sources plus PSD increment sources from the NAAQS inventory. The minor source baseline dates for San Juan County, New Mexico are:

- NO_2 – June 6, 1989
- SO_2 – October 2, 1978
- PM_{10} – October 2, 1978

For pollutants with impacts greater than PSD Class I SILs, multi-source modeling for those affected Class I areas will be conducted after consultation with reviewing agencies. The receptors to be used in the cumulative modeling will be a subset of the receptors used for the impact analysis of the proposed facility that are within the SIA distance of the Desert Rock Generating Station. If peak modeled impacts for PSD increment or NAAQS compliance are not within a receptor area with a spacing of 100 meters or less and the impacts are more than 50% of the compliance levels, then those impacts will be refined with 100-meter spaced receptors.

This page intentionally left blank

8.0 ADDITIONAL IMPACT CONSIDERATIONS

8.1 Growth Analysis

The potential growth impacts due to the Project will be evaluated. The number of permanent new employees will likely be on the order of 200 persons, a number that can easily be accommodated within the local infrastructure. Contributors to growth could involve activities related to additional coal mining and preparation facilities. These impacts are likely to be very localized, and would likely not significantly affect off-site air quality.

8.2 Soils and Vegetation

PSD regulations require analysis of air quality impacts on sensitive vegetation types, with significant commercial or recreational value, and sensitive types of soil. Evaluation of impacts on sensitive vegetation will be performed by comparing the predicted impacts attributable to the Project with the screening levels presented in *A Screening Procedure for the Impacts of Air Pollution Sources on Plants, Soils, and Animals* (EPA 1980); see Table 8-1.

Most of the designated vegetation screening levels are equivalent to or less stringent than the NAAQS and/or PSD increments, therefore satisfaction of NAAQS and PSD increments assures compliance with sensitive vegetation screening levels.

Table 8-1
Screening Concentrations for Soils and Vegetation

Pollutant	Averaging Period	Screening Concentration ($\mu g/m^3$)
SO_2	1-Hour	917
	3-Hour	786
	Annual	18
NO_2	4-Hours	3,760
	1-Month	564
	Annual	94
CO	Weekly	1,800,000

Source: "A Screening Procedure for the Impacts of Air Pollution Sources on Plants, Soils, and Animals". EPA 450/2-81-078, December 1980

This page intentionally left blank

9.0 DOCUMENTATION OF RESULTS

The PSD permit application that documents the air quality impact analysis will describe the input data, the modeling procedures, and the results in tabular and graphical form. Much of the information regarding locations, plot plans, etc., associated with the Project that is included in this modeling protocol will be included in the permit application report. The document will be presented in loose-leaf format in a 3-ring binder so that additions or revisions can easily be made. Any process information deemed to be confidential by Steag would be so noted.

The computer files associated with the air quality analysis will be submitted on CD-ROMs. Meteorological and modeling data will be presented so that a reviewer can check the documented modeling results. Descriptions of files on the CD will be included in the computer documentation, and the use of binary files will be avoided to promote portability of the files to other computer systems.

This page intentionally left blank

10.0 REFERENCES

Federal Land Manager's Air Quality Related Values Workgroup (FLAG). 2001. Guidance on Nitrogen Deposition Analysis Thresholds.

Federal Land Manager's Air Quality Related Values Workgroup (FLAG). 2000. Phase I Report. December 2000.

Interagency Workgroup on Air Quality Modeling (IWAQM). 1998. Phase 2 Summary Report and Recommendations for Modeling Long Range Transport Impacts. EPA-454/R-98-019. December 1998.

Moore, G.E., R.G. Ireson, C.S. Liu, T.W. Tesche, R.E. Morris, A.B. Hudischewskyj, 1982. Air Quality and Meteorology of Northwest New Mexico. SAI No. 82014. Contract No. EC80-3396-001.80. Systems Applications, Inc. San Rafael, CA.

Porter, E. (Fish & Wildlife Service) 2004. Personal communication with Robert Paine of ENSR.

Scire, J.S., D.G. Strimaitis, R.J. Yamartino, 2000: A User's Guide for the CALPUFF Dispersion Model (Version 5). Earth Tech, Inc. Concord, MA.

Scire, J.S., F.R. Robe, M.E. Fernau, R.J. Yamartino, 2000: A User's Guide for the CALMET Meteorological Model (Version 5). Earth Tech, Inc. Concord, MA.

Seitz, John S., October 1997. Interim Implementation of New Source Review Requirements for PM2.5.

U.S. Environmental Protection Agency, 1980. *A Screening Procedure for the Impacts of Air Pollution Sources on Plants, Soils, and Animals.* EPA-450/2-81-078. U.S. Environmental Protection Agency, Research Triangle Park, NC 27711.

U.S. Environmental Protection Agency, 1983. *EPA Complex Terrain Model Development: Third Milestone Report - 1983*. USEPA Publication No. EPA-600/3-83-101. USEPA, Research Triangle Park, North Carolina.

U.S. Environmental Protection Agency, 1985. *Guideline for Determination of Good Engineering Practice Stack Height (Technical Support Document for Stack Height Regulations).* EPA-450/4-80-023R. Office of Air Quality Planning and Standards, Research Triangle Park, North Carolina. June 1985.

U.S. Environmental Protection Agency, 1990. *New Source Review Workshop Manual*. Draft October 1990. U.S. Environmental Protection Agency, Research Triangle Park, NC 27711.

This page intentionally left blank

APPENDIX A

AIR QUALITY AND METEOROLOGY OF NORTHWEST NEW MEXICO

Final Report

AIR QUALITY AND METEOROLOGY OF NORTHWESTERN NEW MEXICO

SAI No. 82014

Contract No. EC80-3396-001.80

28 January 1982

Prepared for

Arizona Public Service
411 North Central Avenue
Phoenix, Arizona 85004

Prepared by

G. E. Moore
R. G. Ireson
C. S. Liu
T. W. Tesche
R. E. Morris
A. B. Hudischewskyj

Systems Applications, Inc.
101 Lucas Valley Road
San Rafael, California 94903

48900-ef-81336r

4 METEOROLOGICAL ANALYSIS OF THE FOUR CORNERS REGION

4.1 HISTORICAL REVIEW OF METEOROLOGICAL ANALYSES

Over the past 10 to 15 years, several monitoring programs have been carried out in the Four Corners region. The data that were collected have been analyzed by several consulting firms. Stearns-Roger Corporation (1970) produced one of the earliest reports, which summarizes some of the meteorological phenomena found in the Farmington-San Juan River basin area. Primary Stearns-Roger Corporation report findings included the following information:

- The radiative heating and cooling of the surface drove a diurnal drainage-upslope wind cycle, a condition which was predominant in most of the areas in the basin regardless of synoptic wind direction aloft.

- Drainage patterns were disrupted when storm systems moved in or when clouds acted as a control on radiative cooling.

- Drainage flow thickness was normally 300 m to 700 m and the power plant plume did not penetrate drainage flow caused by ground-based inversions.

Another consulting agency--Loren Crow Associates--has long been involved in the study of the Four Corners meteorology and air quality. Between 1970 and 1979, this group issued a number of reports covering several aspects of the meteorological measurement programs taking place under the auspices of APS.

One of the principal analytic contributions made by this firm is a meteorological classification scheme. First introduced by Crow (1975), the following six meteorological types can be used to describe over 95 percent of the days occurring in the Four Corners region during a year:

- Western synoptic airflow (WS)

- Western synoptic airflow with cold air dropout (WS-DO)

> Eastern synoptic airflow (ES)

> Afternoon linkage with gusty east winds (PML)

> Drainage days (D)

> Turnaround days (TA).

Western synoptic airflow days are characterized by winds blowing persistently from the western quadrant over the course of an entire day. Generally, the wind speeds are high (7 m/s or greater) with strong mechanically turbulent coupling of the air right down to the surface. Western synoptic flow with dropout occurs when radiative cooling is strong enough to stabilize the air near the surface, thus eliminating mechanical turbulence. The air near the surface is relatively slow-moving and can meander as it is uncoupled from the western synoptically driven air aloft. The slow-moving air retains a westerly component of motion as a result of a small residual coupling just large enough to offset gravitationally driven drainage flow tendencies.

The easterly synoptic airflow seems to occur during the passage of a front, or a nonstationary low pressure system, moving south of the Four Corners area. Crow (1975) found that the eastern synoptic wind flows did not generally persist beyond 24 hours, as might be expected as a result of the transient meteorological phenomena driving these winds. Another nonpersistent wind flow is the afternoon linkage with gusty east winds. During the summer, late afternoon easterly winds of a variable (gusty) nature sometimes appear. These winds possibly result from the drawing influence of the persistent heat lows to the southwest of the Four Corners area and the thunderstorms that are spawned by such lows. The terrain, such as the Chuska mountain range, is sometimes the site of thunderstorms whose inflow is aided by upslope air motion in the region.

Drainage days are simply those days during which easterly downslope flow continues all day with nearly calm wind speeds occurring during the afternoon. The wind speeds are generally low all day, not exceeding 4 m/s. Stagnation subsidence from high pressure centers in the region during the wintertime is a possible driving mechanism for drainage days. Turnaround days represent the most frequently occurring type of airflow pattern (Crow, 1975). Cooling in the evening and morning results in a strong surface inversion. The dense surface air flows from high to low terrain. The inversion air is stable and mechanically uncoupled from the synoptic-scale airflow aloft. The inversion is rapidly destroyed by the sun during the late morning. Eventually, the thermally driven turbulence breaks up the surface inversion, and the airflow at the ground is coupled with the westerly synoptic flow aloft. The direction of the wind, thus,

turns around during the late morning/early afternoon hours and turns again during the late evening hours.

Crow (1975) catalogued over 1000 days and the frequency distribution is shown in figure 4-1. He found that turnaround flow occurred most often, and that western synoptic flow and drainage were next in occurrence. Furthermore, most high SO_2 measurements during that period occurred under the turnaround and the drainage meteorological regimes. In a study of 23 episodes of high NO_x measured concentrations, he found similar results.

Crow also examined some of the characteristics of the stable drainage layer with the aid of minisondes, pibals, airplane observations, and acoustic sounder measurements. The characteristics of the drainage airflow layer are discussed in Crow (1975, 1978, and 1979). The findings of these reports are summarized by the following points.

- The average depth of the drainage inversion layer was about 500 m to 550 m. The buildup of the layer took place from 1900 LST to 0800 LST during the winter.

- The plume would rise above the inversion layer if the winds within the inversion layer were less than 2 m/s.

- Minimum wind speed occurred at the top of the drainage layer inversion.

- Wind directional shear reached a maximum at the top of the drainage layer inversion with the wind direction veering 20° to 40° between 61 m and the top of the inversion.

- The acoustic sounder and the minisonde estimates of inversion height did not agree when the minisonde indicated a drainage layer greater than 300 m. The deep layers of nearly isothermal temperature lapses posed a difficult measurement problem for acoustic sounder technology.

- The ground-based drainage inversion was generally eliminated by 1300 LST during turnaround days. During the afternoons, the wind direction varied little with height and was usually west-northwesterly from 850 m to the ground.

Crow has also investigated some of the dispersive processes leading to high episodes of SO_2 or NO_x (Crow, 1974, 1978, and 1979). The main findings of these reports are

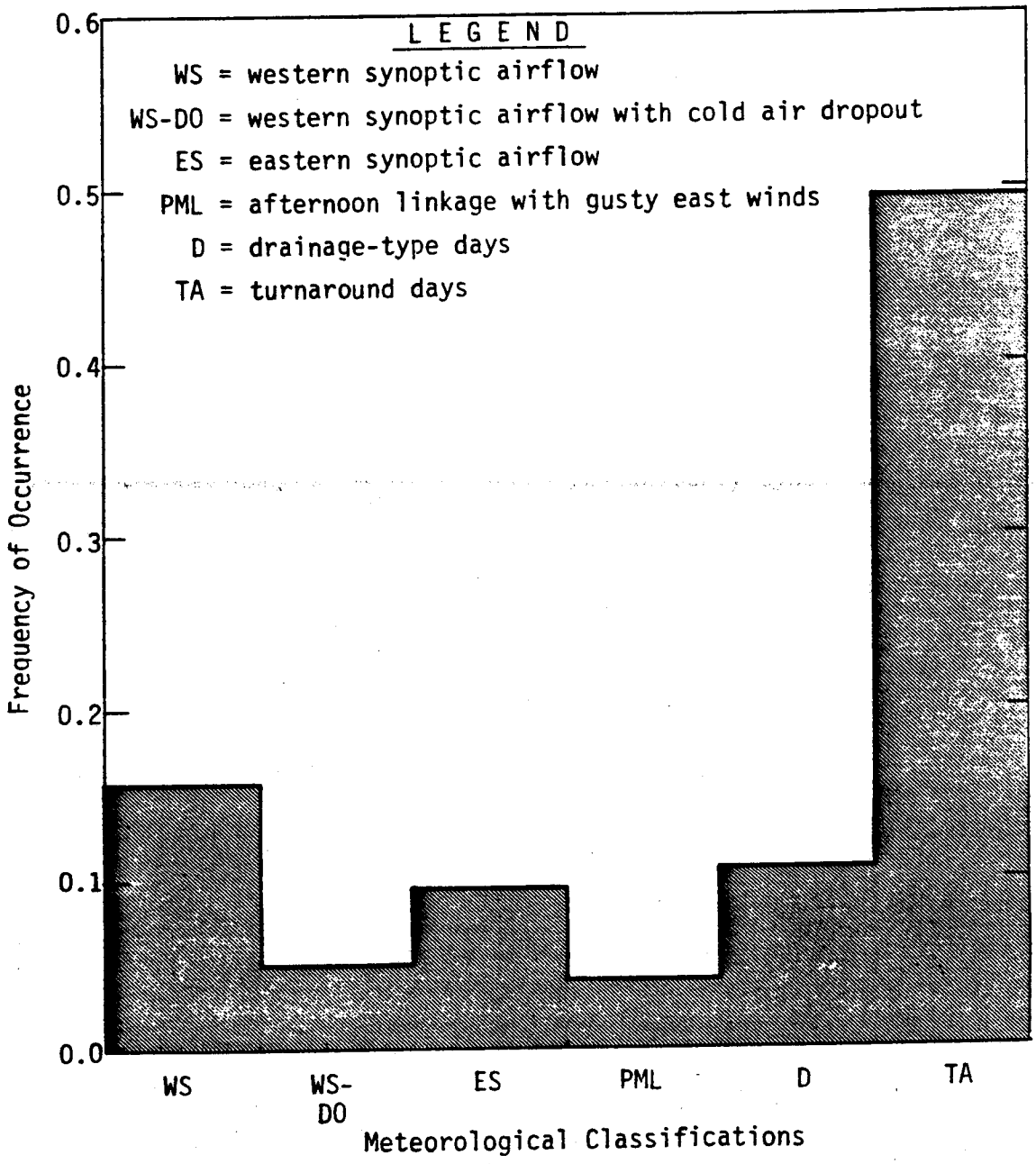

Source: Crow (1975).

FIGURE 4-1. FREQUENCY DISTRIBUTION OF VARIOUS CROW METEOROLOGICAL REGIMES FOR 1974 AT THE FOUR CORNERS POWER PLANT

- Higher wind speeds, associated with either western synoptic or eastern airflow, resulted in rapid dilution and consequently low SO_2 concentrations at any of the monitoring stations, as of 1974.

- Strong surface heating with a superadiabatic lapse rate between 20 ft and 200 ft was generally required to initiate and sustain sufficient vertical mixing to envelope the elevated plume leaving the Four Corners Power Plant, consequently leading to high surface SO_2 concentrations.

- Direct fumigation during morning transition periods of turnaround days resulted in large concentrations to the northwest of the Four Corners Power Plant.

- During turnaround days, material carried to the west of the Four Corners Power Plant by the drainage flow was simultaneously pushed east-southeastward and mixed down to the surface by the solar-insolation-caused upslope wind flow and thermal convection. Figure 4-2, taken from Crow (1974), schematically indicates the turnaround flow.

The HTMP meteorological and air quality data have been examined by both York Research Corporation (York, 1979) and Systems Applications, Inc. (SAI, 1979). In the York report (1979), only some summary statistics concerning the air quality and some comments regarding acoustic sounder data are discussed. The only discussion of the meteorological information gathered during the HTMP is found in the SAI report (1979). In this report, a total of four episodes of high SO_2 concentration are discussed in some detail; an analysis of the meteorological conditions leading to the elevated SO_2 resulted in the following conclusions:

- On 10 December 1978, there were impacts at the Ute Mountain Mesa monitors. A turnaround flow drained plume material downslope toward the San Juan River valley; then, a synoptically guided southwesterly upslope flow brought plume material from both the San Juan and Four Corners power plants onto the Ute Mountain Mesa during the midmorning hours.

- On 15 December 1978, direct line-of-flight traversal of the Four Corners plume in the isothermal (stable) drainage layer led to elevated SO_2 concentrations at the Hogback monitor in the early morning.

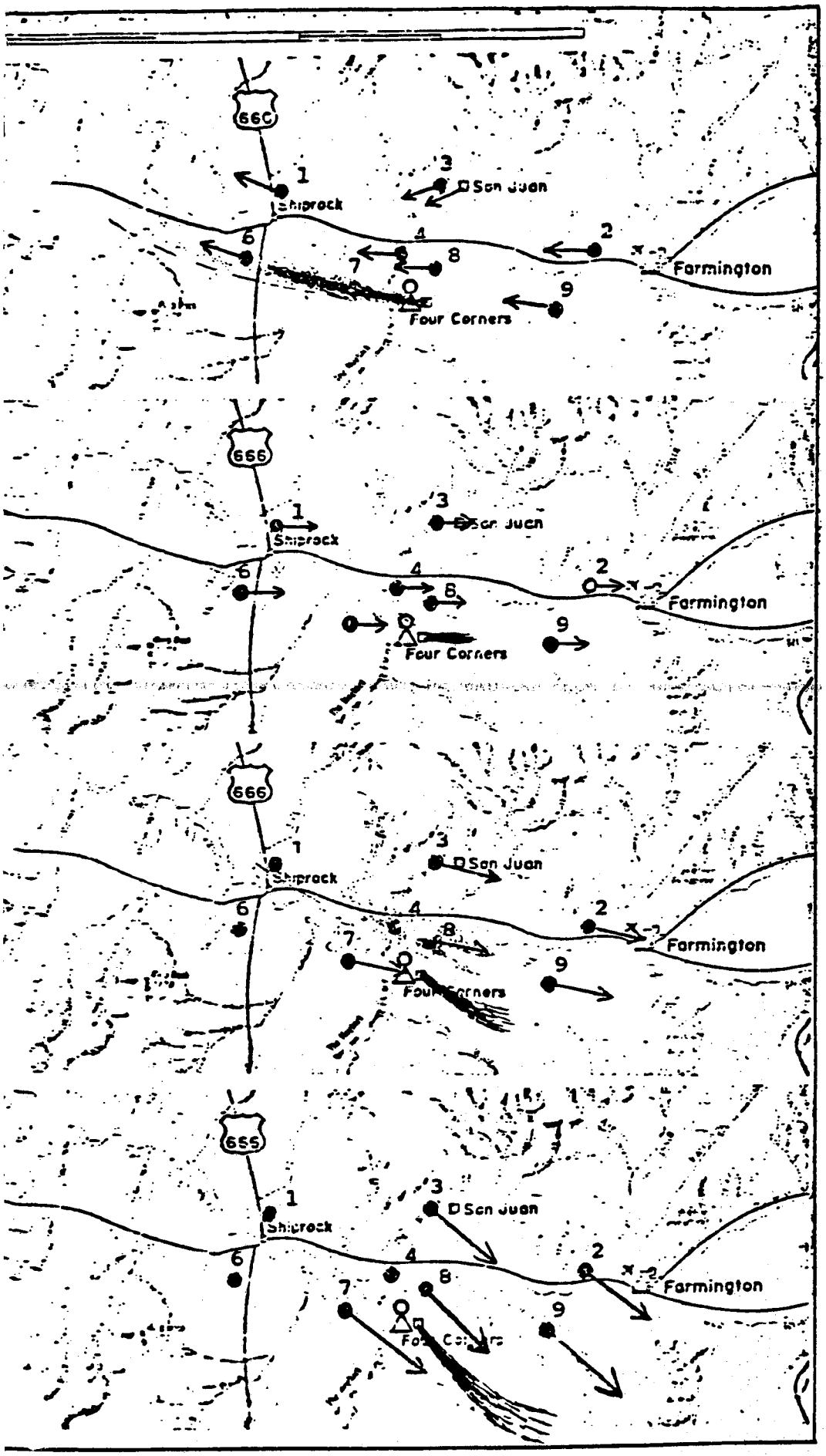

1100

End of downslope stable airflow and beginning of "turn-around" air motion.

1200

"Old" plume gradually fumigates and then moves eastward 4 miles in 1 hour.

New and higher plume moves toward east from Four Corners Plant.

1300

"Old" plume, deeper and thinner, moves 6 miles toward ESE.

New plume also moves toward ESE.

1400

"Old" plume spreads across 8 miles toward SE.

New plume moves toward SE.

FIGURE 4-2. Schematic pattern of sequential paths of plume dispersal on a typical "turn-around" day. Arrows show flow pattern. Numbers identify monitoring stations. (from Crow (1974))

- On 10 February 1979 direct line-of-flight traversal of the San Juan plume in the isothermal (stable) drainage layer led to elevated SO_2 concentrations at Ute Mountain Mesa in the evening hours.

- On 12 and 13 February 1979, it appeared that indirect curved flow brought material from the Four Corners Power Plant to the Hogback monitor late in the evening. During the afternoon and early evening, plume material was transported in a southeasterly direction as a result of the western synoptic flow. The drainage flow that set in earlier in the evening brought the material back to the Hogback monitor via easterly-southeasterly winds, which brought gravitationally dense air down Chaco wash. During transport, the air in which the plume was imbedded was neutral or slightly stable.

In summary, previous investigations have shown the probable existence of four dispersive meteorological regimes that led to elevated SO_2 concentrations. The low terrain monitors are affected by direct line-of-flight fumigation and turnaround flow, which also result in fumigation of plume material to the ground. The high terrain is affected by two types of plumes--one resulting from direct line of flight and one resulting from a turnaround.

4.2 THE METEOROLOGICAL DATA ARCHIVE

Five principal sources of data were used in the meteorological analysis: monitoring sites, meteorological towers, minisonde and pibals, NWS three-hour data, and NWS daily meteorological map data. The monitor siting data consisted exclusively of wind speed and wind direction information taken at roughly 7 to 10 m above the surface. The meteorological tower data consisted of wind speed, wind direction, and temperature at one or more levels and, in addition, solar insolation, and dewpoint temperature. The minisonde-pibal data were generally taken twice daily. The pibals were theodolite-tracked and wind speed and wind direction were inferred from tracking results. The minisondes were pibals with a temperature sensor and a transmitter that broadcast a continuous record of temperature. Farmington Airport was a primary surface NWS station. Consequently, data reported every three hours (not averages) were saved on NCC climatic tapes. Some of the variables that were estimated by NWS-certified observer were wind speed, wind direction, temperature, pressure, relative humidity, visibility, sky cover, and

precipitation. The NWS weather maps reported surface and 500-mb conditions at 0500 LST. Spatial patterns of surface pressure and 500-mb geopotential were presented. Surface and 500-mb winds were presented as well as surface pressure, temperature, and sky cover.

The air quality monitors that indicated wind speed and wind direction are given in table 4-1 along with the dates over which the record extended. Two separate monitoring programs were in effect: the low terrain was monitored by the Joint Ambient Air Quality Program (JAAP), and the high terrain was monitored by the High Terrain Monitoring Program* (HTMP). The monitoring sites are shown from a northerly perspective in the raised topography map in figure 4-3. Note the clustering of the Ute Mountain Mesa (UMM) monitors on the south lip of the mesa. Note also that the low terrain monitors were based along the axis of the San Juan River basin. Figure 4-3 also shows that the Hogback monitor sits at nearly the highest point on Hogback Ridge.

The last column of table 4-1 indicates the degree of data capture. One can see that three of the Joint Ambient Air Quality Program sites--TWIN, RATW, and DUCT--captured substantially fewer data than the other stations. TWIN, in particular, rarely seemed to have both the wind vane and the anemometer working simultaneously. Since instruments were inoperable for so long, the data may not be of any value. The HTMP monitoring sites seem to have had a uniformly acceptable level of data capture, indicating that the instruments probably were working as intended.

During the period that the Four Corners meteorological tower was operational, most of the variables had a sufficient (> 75 percent) level of data capture. The only exceptions were σ_θ, σ_ϕ, W_S (7-m), W_D (7-m) and T_D (7-m). Considering notation by Erbes (1979) of problems related to the operation of the FCMT sigma meter, the low data recovery for σ_θ and σ_ϕ was expected. The Ute Mountain Mesa tower did not recover data well, possibly as a result of the operational failure of the instruments mounted on the meteorological tower.

Farmington Airport is shown on the map in figure 4-3. Table 4-2 summarizes the types and record lengths of available data at different stations. The recovery of NWS data was excellent. Total sky cover was monitored, but it was improperly archived and the values of -1, 0, or 1 were only assumed. NWS data were recorded through the end of 1976.

---

* Later changed to HUMMP, the Hogback and Ute Mountain Monitoring Program.

TABLE 4-1. WIND DATA MONITORS AND RECORDS

Monitor Site Designation	Period of Record	Valid Hours of Data--with Wind Speed and Direction	
		Number	Percentage
DRIL	4/77-3/80	21,180	82%
PUMP	4/77-3/80	19,779	77
RIVR	4/77-3/80	22,344	87
TWIN*	4/77-3/80	1,164*	49
SUBE	4/77-3/80	20,087	78
RATW	4/77-3/80	14,115	55
DUCT	4/77-3/80	9,560	37
SHIP	4/77-3/80	20,519	80
UMM1 (E)	9/78-9/80	13,453	77
UMM3	9/78-9/80	13,812	79
UMM5	9/78-9/80	13,224	75
UMM7	9/78-9/80	14,173	81
UMM9 (W)	9/78-9/80	15,212	87
HOGB	9/78-9/80	14,763	84

* Was moved part way through the period of record.

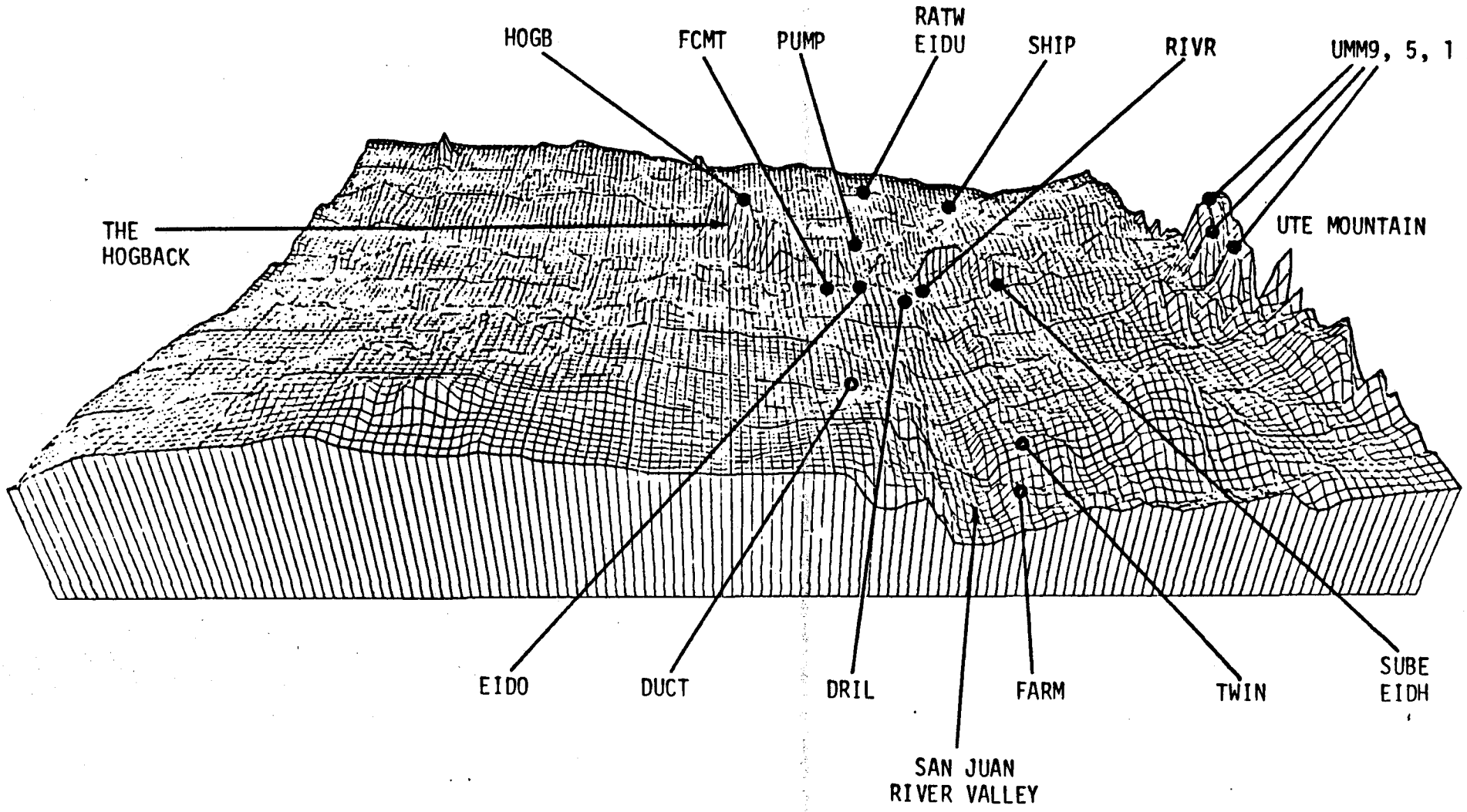

FIGURE 4-3. FOUR CORNERS AREA VIEWED FROM THE EAST WITH VARIOUS AIR QUALITY STATIONS AND METEOROLOGICAL MONITORING

TABLE 4-2. LENGTH OF RECORD AND VARIABLES MEASURED AT EACH SITE

Monitoring Site	Record Length	Variables Monitored*	Valid Hours of Data	
			Number	Percentage
FCMT	1/74-5/79	7-m WS	31247	66%
		7-m WD	30992	65
		30-m WS	-	
		30-m WD	-	
		61-m WS	35625	75
		61-m WD	35617	75
		7-m T	42169	89
		30-m T	-	
		61-m T	42615	80
		7-m TD	34756	73
		I	40974	86
		σ_θ	16772	35
		σ_ϕ	15034	32
UMMT	4/75-3/77	10-m WS	9298	55
		10-m WD	9290	55
FARM	1/70-12/76	WD	61365	100
		WS	61365	100
		T	61098	100
		RH	59970	89
		TD	61368	100
		P	61335	100
		Visibility	61368	100
		Rainfall	61368	100
		Fog	61368	100

WD = wind direction
WS = wind speed
T = temperature
RH = relative humidity
TD = dewpoint temperature
P = precipitation

81336r 13

The pibals and minisondes were clustered just north of Lake Morgan. Generally, there were two launches during a day. The available archive of wind speed and direction soundings was begun in August 1976 and was completed in March 1979; the temperature soundings were begun in January 1978 and were concluded in March 1979. Table 4-3 summarizes the number of wind and temperature soundings for each year. There were over one thousand soundings in the archive. In most cases, if one sounding was made during a day, another one was also performed; thus, if a morning sounding were made, an afternoon sounding would be available. With the exception of the last part of 1978 and the first part of 1979, the soundings were relatively infrequent, occurring in clusters separated by several days without soundings. The average number of soundings per week for each year is shown in table 4-3.

The full set of NWS daily weather maps was obtained for January 1973 through November 1980. Table 4-4 displays the yearly breakdown of NWS weather map availability. The map recovery rate was high except for 1977 when maps for several months were missing from the library.

4.3 ANALYSIS OF THE SURFACE WIND DATA

Wind speed and wind direction statistics indicate the preferred rates and direction of plume material travel. The wind speed in the surface layer is indicative, to some degree, of the amount of mechanical turbulence; high winds suggest a large degree of mechanical turbulence. With the low wind speeds, when the solar insolation is significant, the convective turbulence can become substantial. If direct line-of-sight impact is being considered, it is important to know whether winds are blowing at an angle formed by the line extending from the source to the receptor. Wind direction also indicates whether or not topographically channeled wind flows are occurring.

A climatological study of wind speed and direction at any site addresses several questions:

- Are there preferred wind directions? If so, what are they, and how preferred are they? Does the wind blow only rarely from some directions?
- From what directions do the strongest and weakest winds tend to blow?
- How often do calms and small winds occur? What is the median wind speed?

TABLE 4-3. NUMBER OF WIND AND TEMPERATURE SOUNDINGS PER YEAR

Period	Type of variable	Number of soundings
1/78-12/78	T	263 (5.0/wk)
1/79-3/79	T	116 (9.0/wk)
1/76-12/76	WS, WD	83 (1.6/wk)
1/77-12/77	WS, WD	132 (2.5/wk)
1/78-12/78	WS, WD	323 (6.2/wk)
1/79-3/79	WS, WD	132 (10.0/wk)

T = temperature
WS = wind speed
WD = wind direction

TABLE 4-4. AVAILABILITY OF NWS WEATHER MAPS

Year	Available Maps	
	Number	Percentage
1973	334	91%
1974	365	100
1975	365	100
1976	300	82
1977	251	69
1978	341	93
1980	337	92

- Does there seem to be an appreciable interannual variability in wind statistics?

In addition to analyzing multiannual and annual wind statistics, seasonal and diurnal comparisons are conducted. Several questions are addressed by these additional analyses.

- Do preferred wind directions (often caused by channeled wind flows, like drainage) vary from season to season in frequency of occurrence?

- Does the median wind speed and the frequency of calms and weak winds vary from season to season?

- Do the strongest and weakest winds tend to come from different directions during different seasons?

- When broken down by time of day during a given season, do the frequencies of wind speed and wind direction show the predominance of a particular group of wind flows as defined by Crow (1975)?

- When broken down by time of day, are the wind statistics different from one time period to another?

- Do the wind statistics of similar time periods in different seasons show major differences?

These seasonal and time-of-day analyses are carried out for the following temporal groupings:

- Winter (December, January, February)

- Spring (March, April, May)

- Summer (June, July, August)

- Fall (September, October, November)

- Morning (0000 - 0859) LST

- Midday (0900 - 1559) LST

- Evening (1600 - 2359) LST.

The intent of the finer temporal breakdown is to explore the wind statistics for meteorological conditions that are biased by a particular group of wind flows. This approach gives the most information about how often a specific wind flow type, like drainage flow, occurs at a given station, without requiring a classification and grouping analysis.

Considering the number of stations providing wind statistics, some preliminary lumping of stations was necessary for simplification. The JAAP stations were lumped into several groups:

> Stations west of the Hogback ridge--SHIP, RATW, PUMP

> Stations in the San Juan River valley--RIVR

> Stations north of the San Juan River valley--SUBE

> Stations closest to the Four Corners Power Plant--DRILL

> Stations near Farmington--TWIN, FARM

> Other stations--DUCT.

The HTMP and HUMMP stations were divided into two groups

> Ute Mountain stations--UMM1(E), UMM3, UMM5, UMM7, UMM9(W)

> Hogback station--HOGB.

The two meteorological towers (FCMT, UMMT) were treated separately.

To introduce further simplification into the analysis, the data comparisons were summarized in tables. The reader is referred to these tables for details; the salient points are summarized in the text.

4.4 SYNTHESIS OF STATION WIND STATISTICS INTO WIND PATTERNS

The dominance of certain wind flows can be felt over most, if not all, of the Four Corners area. There are two primary ways to determine wind patterns from basic wind statistics:

- Analysis of principal components of wind vectors using a method similar to that of Hardy (1978).
- Reconstruction of wind patterns using wind roses and a meteorological explanation of the occurrence of predominant wind vectors and their relationship to wind vectors at other sites.

The analysis of principal components is more objective than the reconstruction method. However, as Hardy and Walton (1978) points out, stratification by time or some other variable is often necessary to determine the preferred orientation when plotting the geometric representation of an eigenvector as a N two-dimensional vector; thus, stratification by time of day and season would be required. Furthermore, data sets for all stations would have to chronologically overlap. Unfortunately, data sets overlap only slightly during the latter part of 1978 and the beginning of 1979. Considering the lack of data set overlap and the lengthy stratification that would be required, the reconstructive method was selected instead of the analytical method. (The analysis of wind roses at the various stations did not require a complete series of chronologically overlapping observations.)

Information on the geographical peculiarities of the area and the major features of the time-stratified wind statistics made it possible to determine the relationships between wind statistics at each station. The wind roses illustrated the most probable direction(s) at a site, and plotting these wind roses on a map allowed visual analysis of the most probable paths of air parcels. The aerodynamics of air masses determined the pairing of the favored directions for a given time of day.

The strategy of the present analysis included several steps:

> Stratify wind roses by time of day and season (for the winter and summer only).

> Overlay wind roses for each station on a topographic map.

> From basic meteorological data for the region and wind rose maximums, draw wind flow arrows to represent wind flow patterns.

> Draw a directional cone to represent the most probable direction of plume travel influence, given the wind flow.

> Relate wind flow pattern to the Loren Crow classification scheme.

Figures 4-22 through 4-31 illustrate the various wind flow patterns that prevail in the Four Corners area. This analysis synthesizes the information presented in the previous section.

The wind flow patterns for winter mornings are apparent in figure 4-22. The wind roses at each station were used to determine a net airflow through the region; the airflow is represented by the arrows. When bimodality or trimodality occurred in the wind roses, similar peaks between stations were inferred (thus minimizing convergences and divergences since $\Delta \cdot \underset{\sim}{V} \sim 0$). The reconstructed airflow (figure 4-22) indicates a downslope component of wind flow that occurred at every station with a definite maximum. This downslope flow during the morning was aided strongly by drainage, and could be a drainage (katabatic) wind caused by cooling at the surface.

Figure 4-23 indicates a second prevalent wind flow for winter mornings. This was not really an upslope flow, but rather a flow driven from the west-northwest up the San Juan River valley by a western synoptic wind caused by pressure gradients of large-scale weather features. This wind did not shift direction with increasing height. Several easternmost stations (FARM, DUCT, and DRIL) were not influenced by this wind flow. Here, the wind probably fanned out, lost velocity, and failed to effectively resist the drainage flow that was taking place. The lower terrain stations tended to have a smaller frequency of west-northwest winds due to sheltering and/or the surface drainage layer opposition. The wind at the effective plume height tended to be more affected by the west-northwest wind; the more frequently this wind occurred, the less probability there was of "blow back" of plume material and of impact at the high terrain monitoring sites.

The upslope wind flow that took place during winter middays is visible in figure 4-24. Again, the average wind flow (particularly at higher elevations) seemed to be from the west-northwest. There are several interesting features in this airflow: (1) evidence from SUBE indicates that the lower portion of the Hogback ridge did not act as a strong barrier to the west-northwest wind, (2) upslope winds from the south-southwest near Ute Mountain were recorded by the monitors there, and (3) DRIL seemed to be under the influence of west-northwest winds and northerly upslope winds, which resulted in a blurred wind rose.

The west-northwest wind at the effective plume height of the Four Corners Power Plant plume moved the plume away from possible impacts at most of the monitoring sites. However, if drainage flow occurred during morning hours and western synoptic flow occurred during midday, the old plume material blown to the west-northwest in the morning "blew back" during midday. This turnaround flow occurred because downslope flow predominated during morning hours; west-northwest flow occurred as often as downslope flow during midday.

The winter midday downslope and eastern synoptic flow (figure 4-25) were approximately about one-third as frequent as the western synoptic upslope flow. This flow was not a true drainage flow; often the surface was unstable, as we will discuss later. With generally low wind conditions, downslope motion tended to waft plume material from the Four Corners Power Plant out toward PUMP, RATW, and SHIP. In the event that the plume was convectively entrained, impacts would occur at PUMP or some of the other westerly monitoring sites.

During winter evenings, the western synoptic winds were apparent (see figure 4-26). This wind flow was the most uniform; the wind was from the west-northwest and covered the whole region except for the San Juan River valley proper (e.g., FARM). The west-northwest wind flow provided good ventilation; plume material from the Four Corners region moved toward the southeast away from all of the monitoring sites.

Downslope drainage flow also occurred during winter evening hours (figure 4-27). As a result of gradual buildup, the drainage flow was not as prevalent or as frequent as the western synoptic flow during morning hours. During late evening hours, as the wind shifted from west-northwest to east-southeast, the possibility of "blow back" appeared again. The site most affected was HOGB, particularly when several hours of weak winds with stable conditions occurred. There was potential for the air flow to "button hook" and for the Four Corners Power Plant plume to be brought back from the south-southeast to impact HOGB.

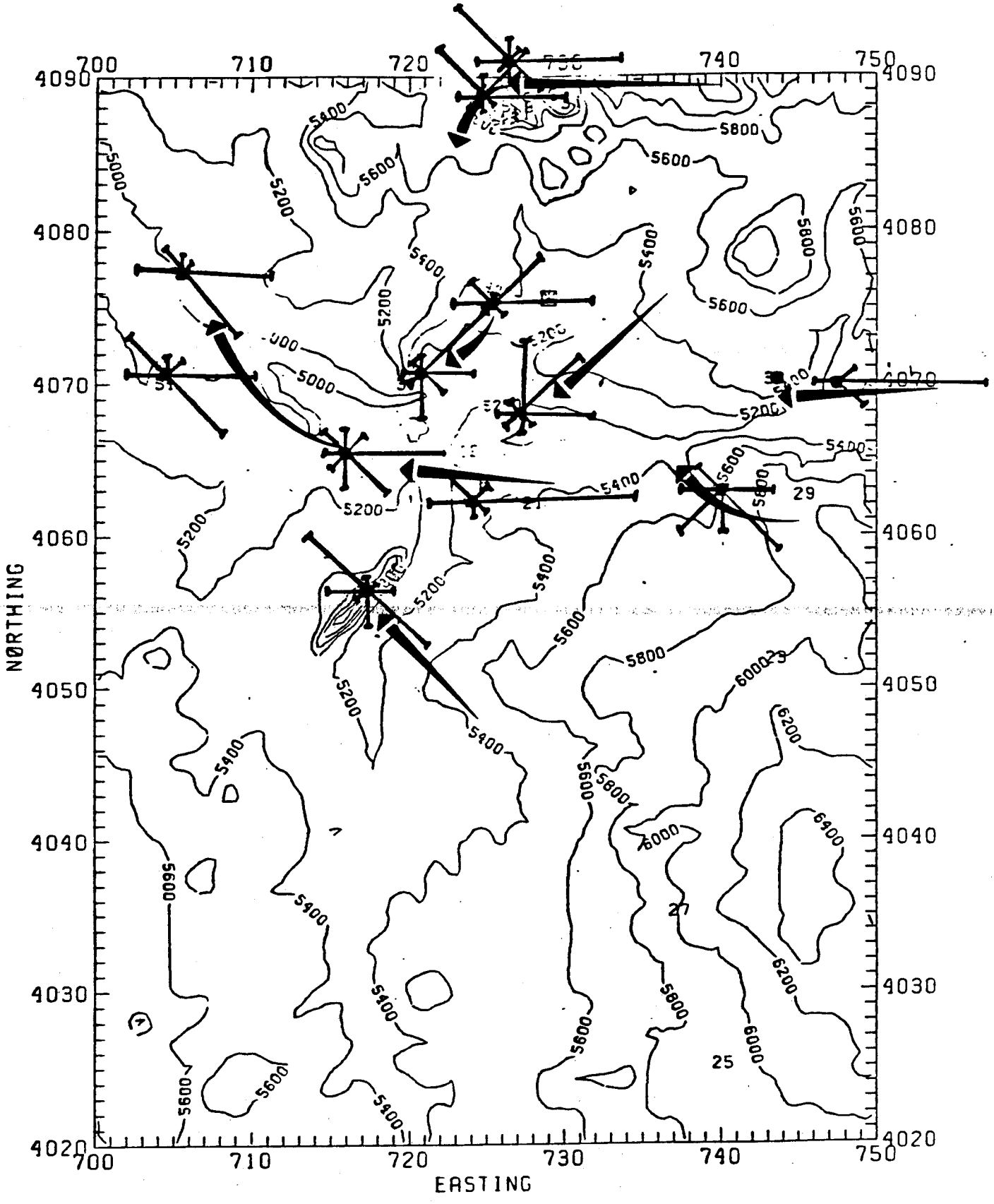

FIGURE 4-22. WINTER MORNING DOWNSLOPE (DRAINAGE) FLOW PATTERN (FROM STATION WIND ROSES)

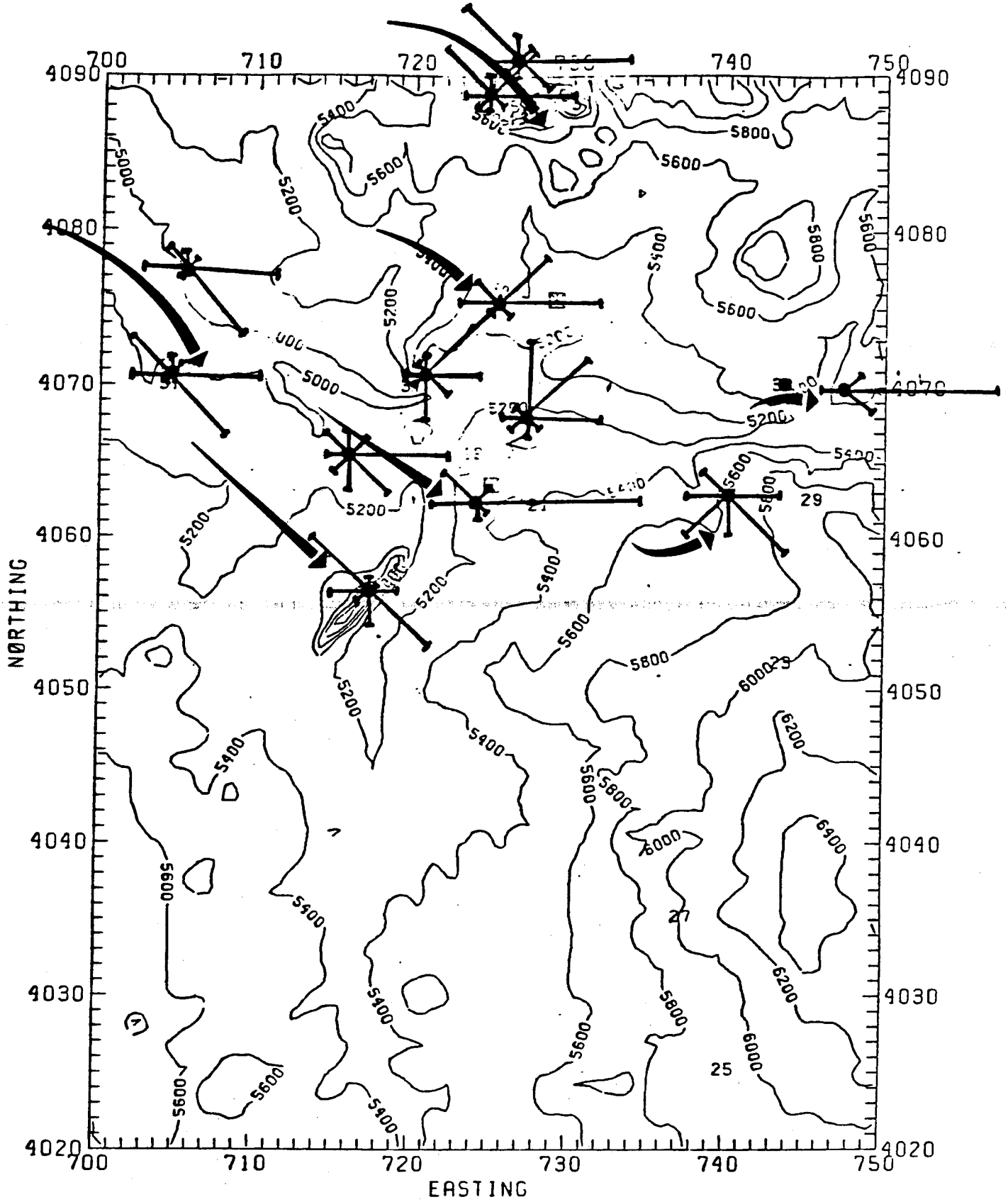

FIGURE 4-23. WINTER MORNING WESTERN SYNOPTIC FLOW PATTERN (FROM STATION WIND ROSES)

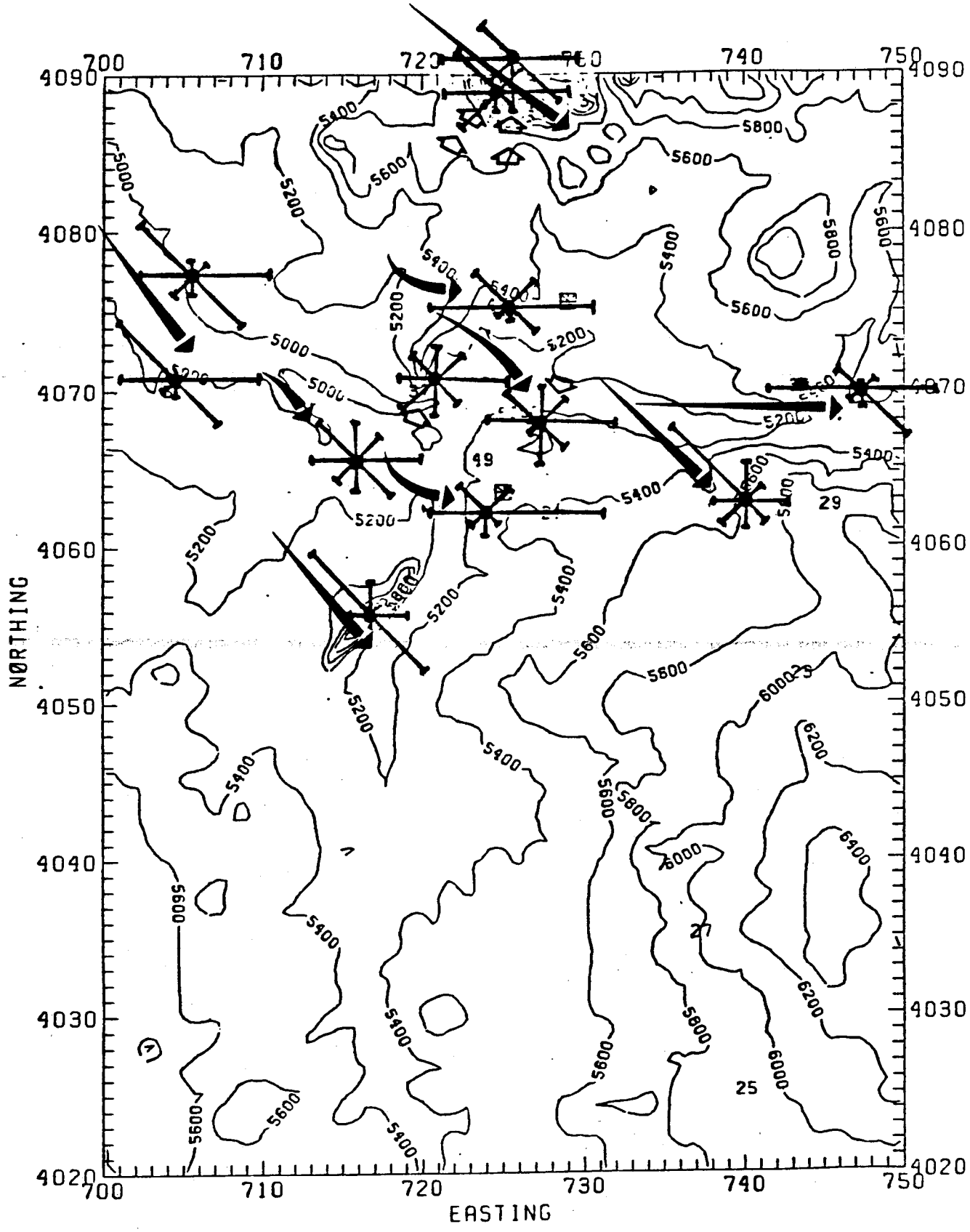

FIGURE 4-24. WINTER MIDDAY WESTERN SYNOPTIC (UPSLOPE) FLOW DEVIATIONS (SHOWN BY OPEN ARROWS)

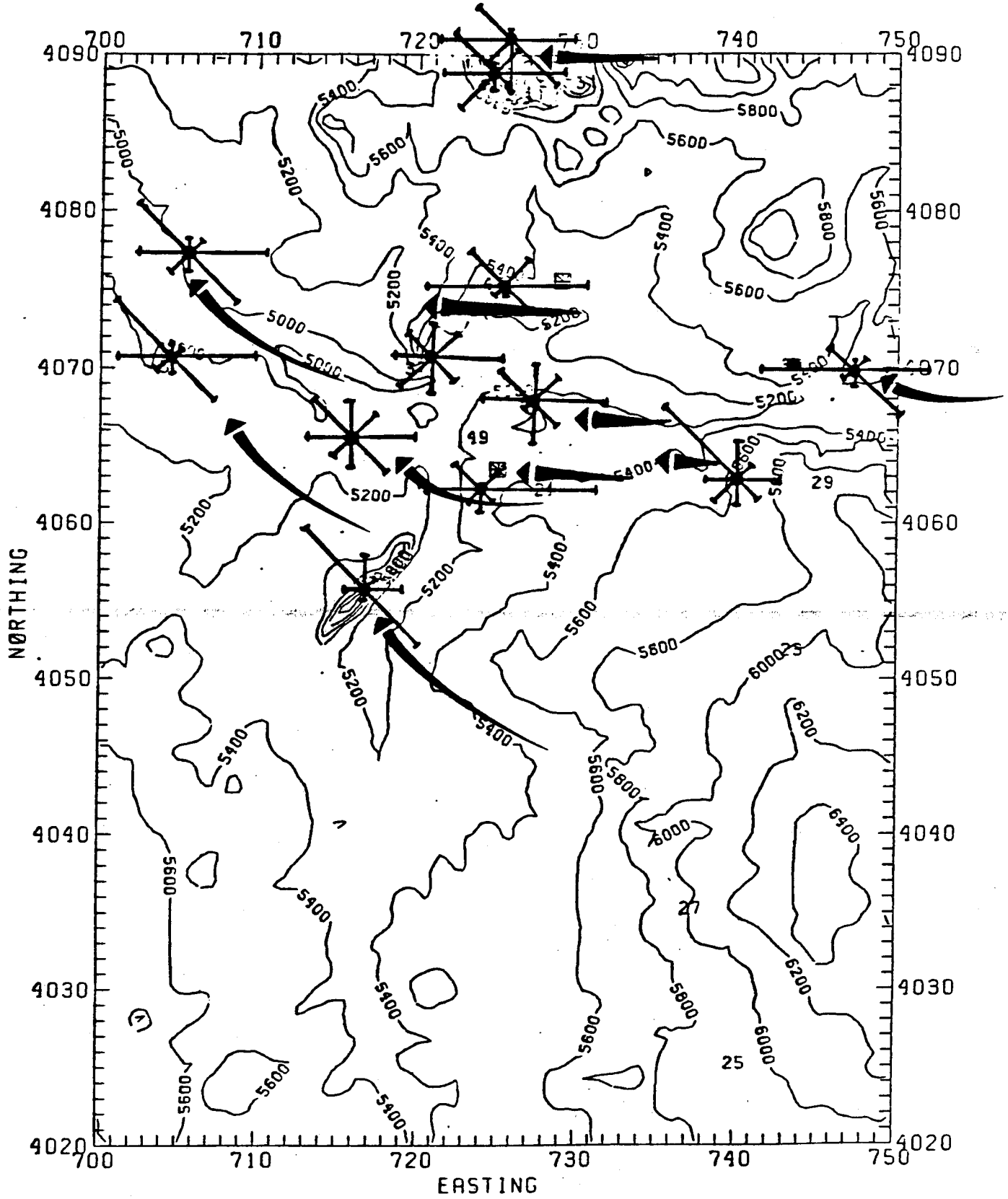

FIGURE 4-25. WINTER MIDDAY DOWNSLOPE AND EASTERN SYNOPTIC FLOW (FROM STATION WIND ROSES)

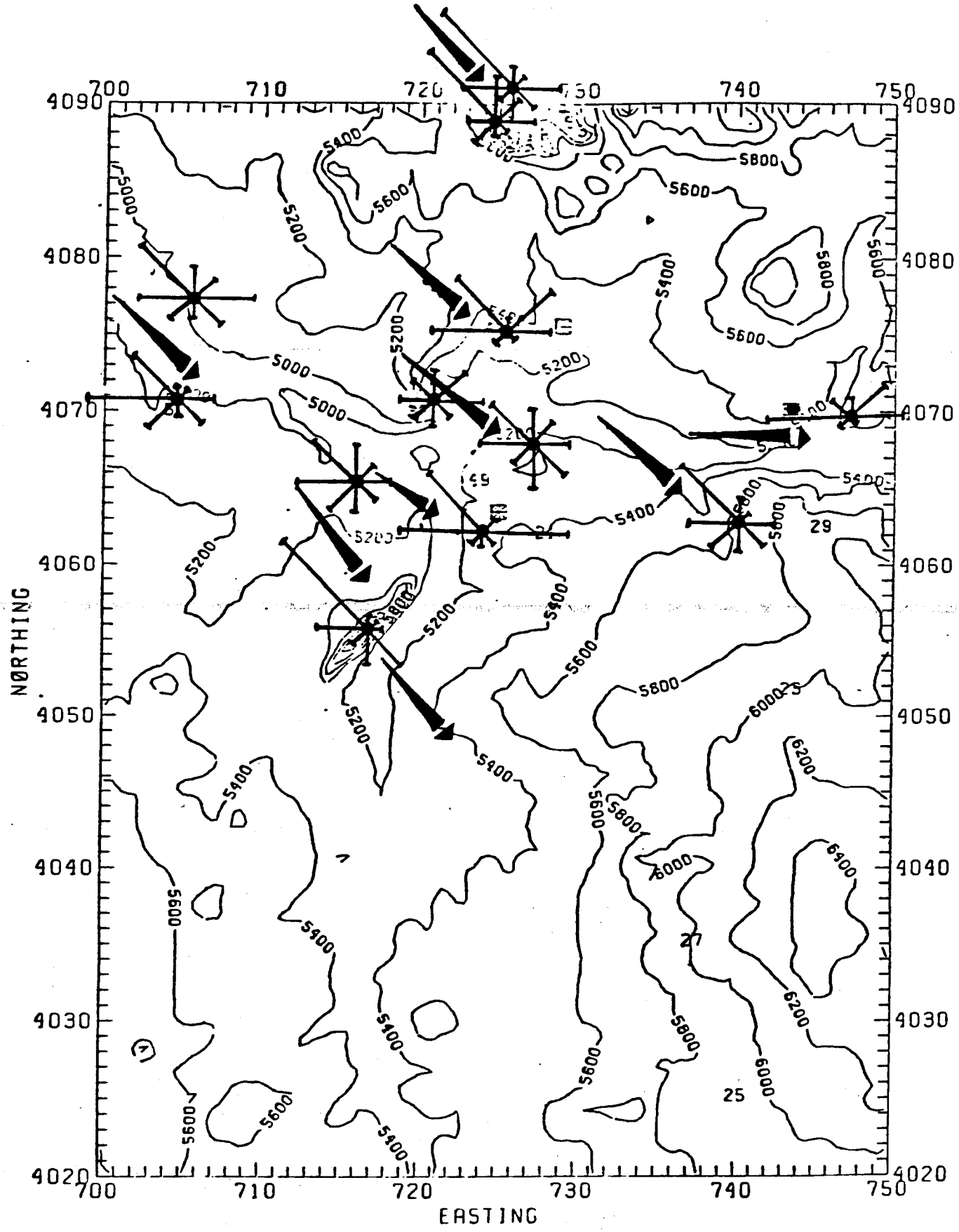

FIGURE 4-26. WINTER EVENING WESTERN SYNOPTIC FLOW (FROM STATION WIND ROSES)

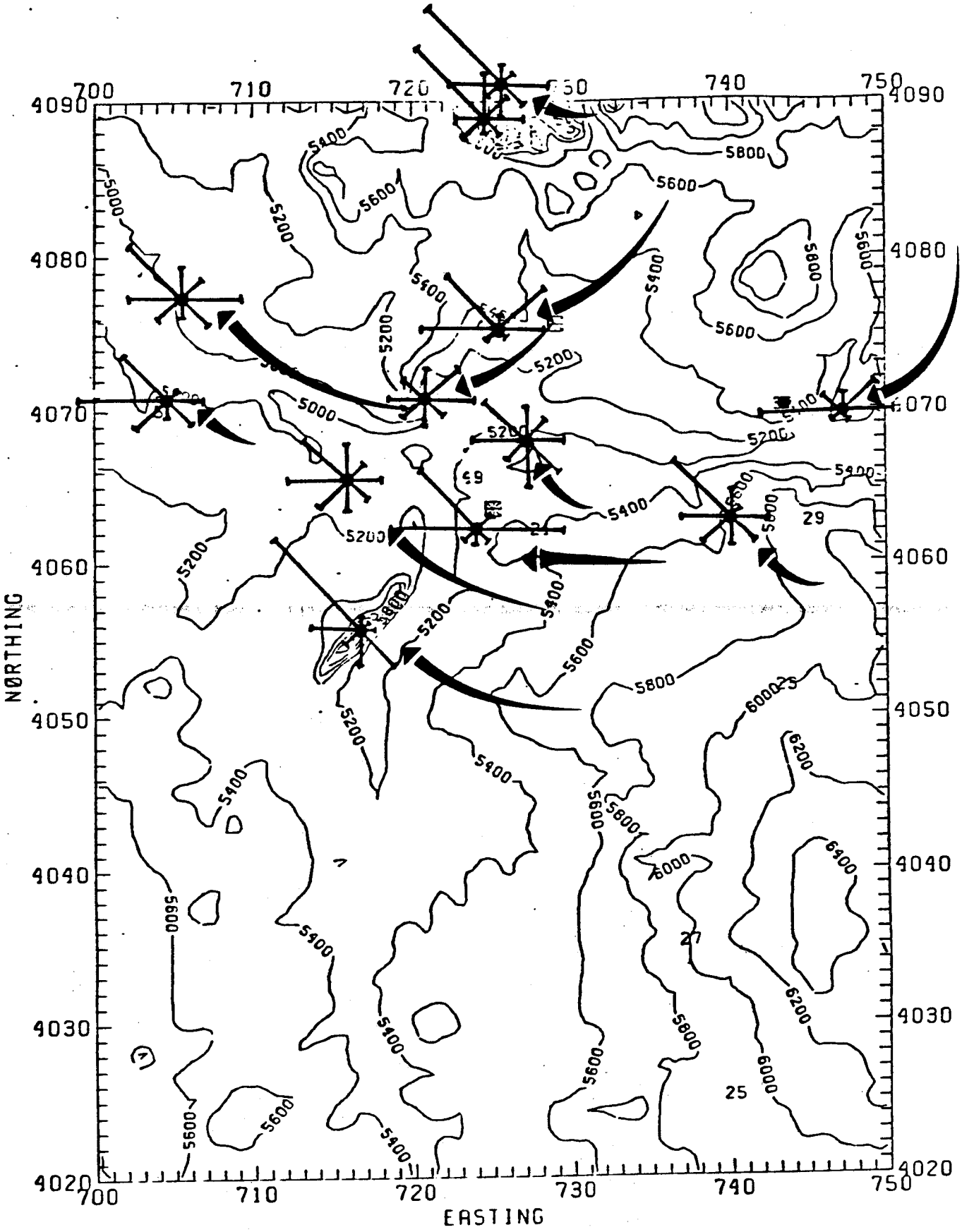

FIGURE 4-27. WINTER EVENING DOWNSLOPE DRAINAGE FLOW (FROM STATION WIND ROSES)

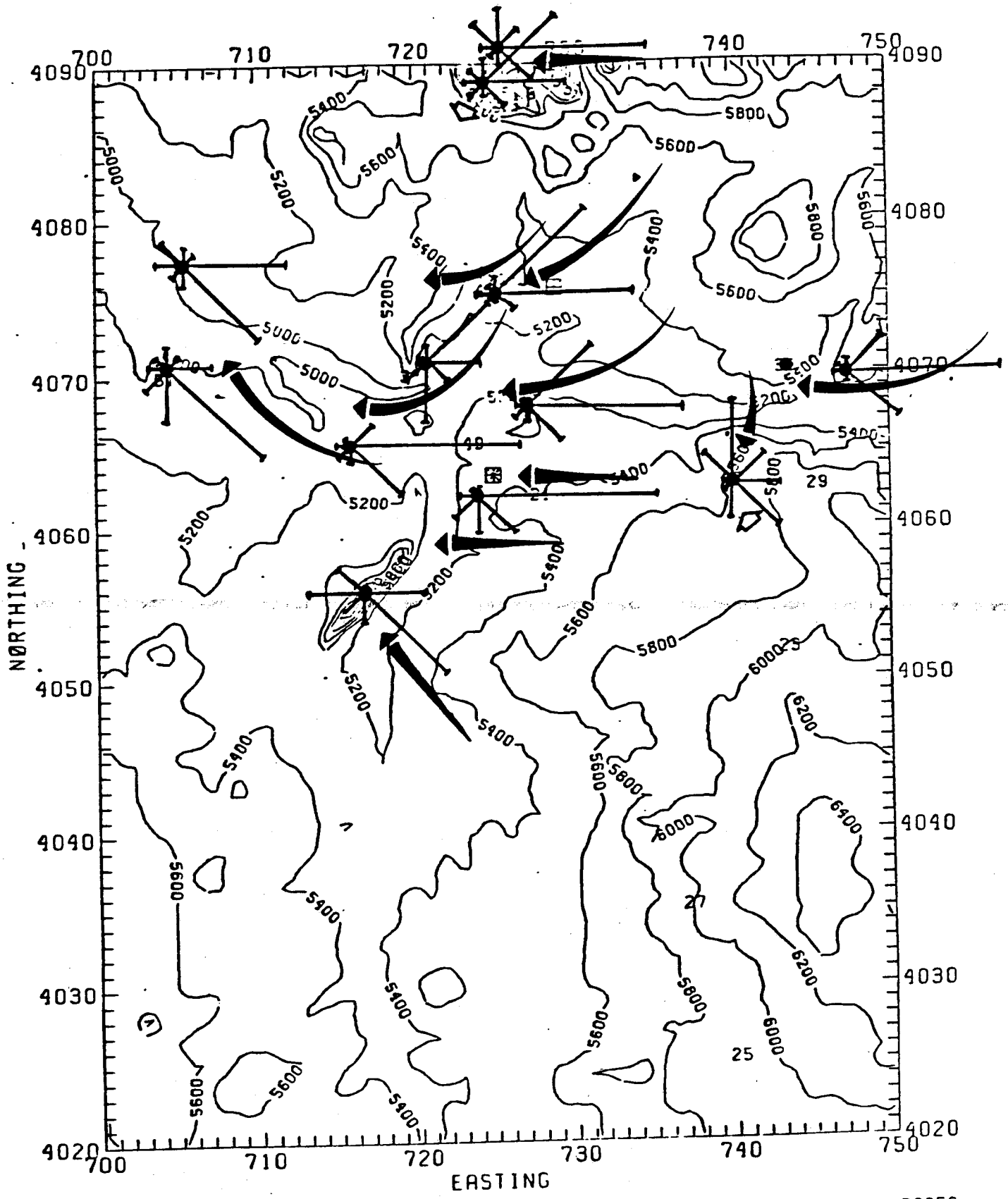

FIGURE 4-28. SUMMER MORNING DOWNSLOPE DRAINAGE FLOW (FROM STATION WIND ROSES; OPEN ARROWS DENOTE LOCAL TOPOGRAPHIC EFFECTS)

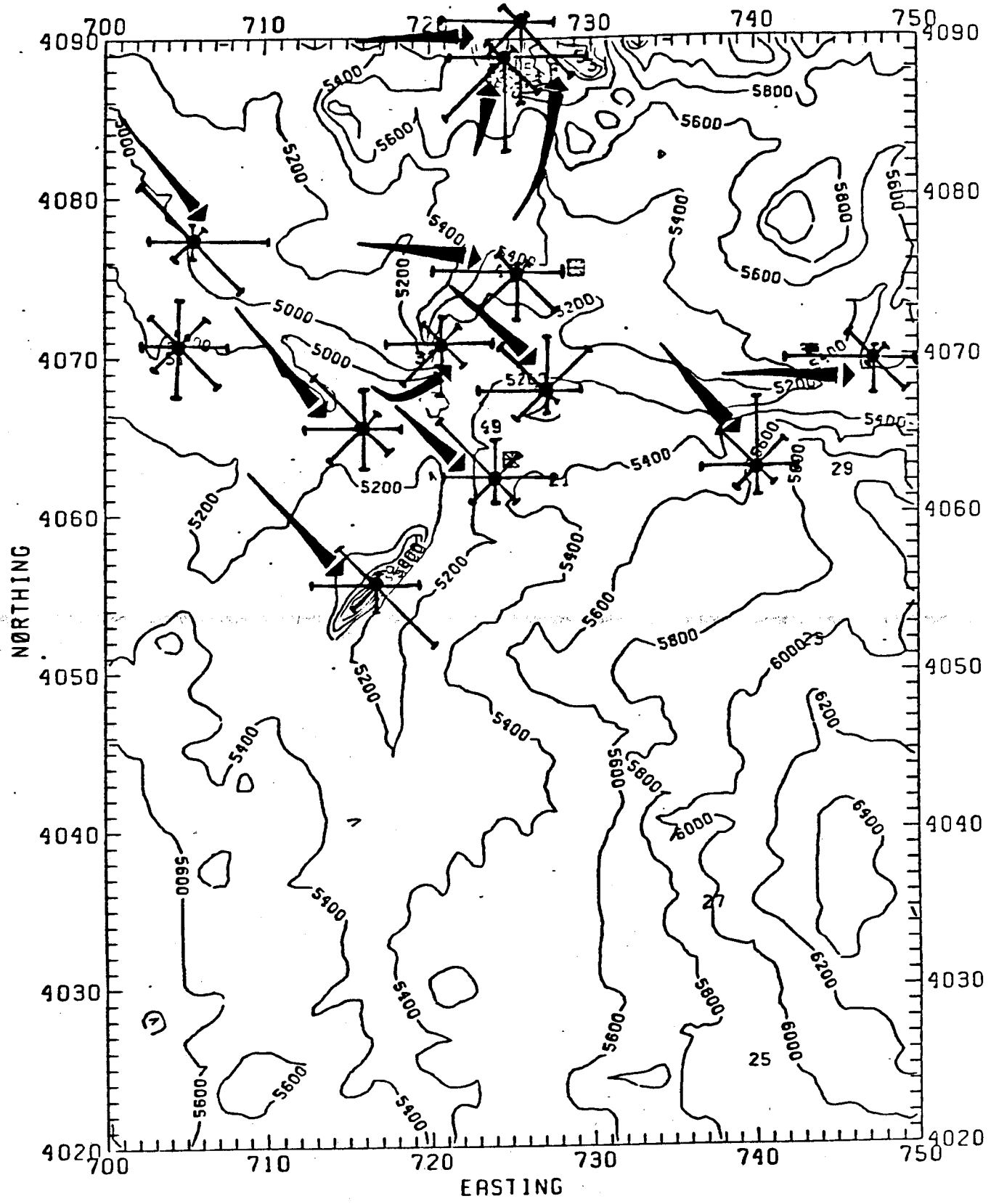

FIGURE 4-29. SUMMER MIDDAY UPSLOPE FLOW AIDED BY NORTHWESTERN SYNOPTIC FLOW ALOFT

6 14

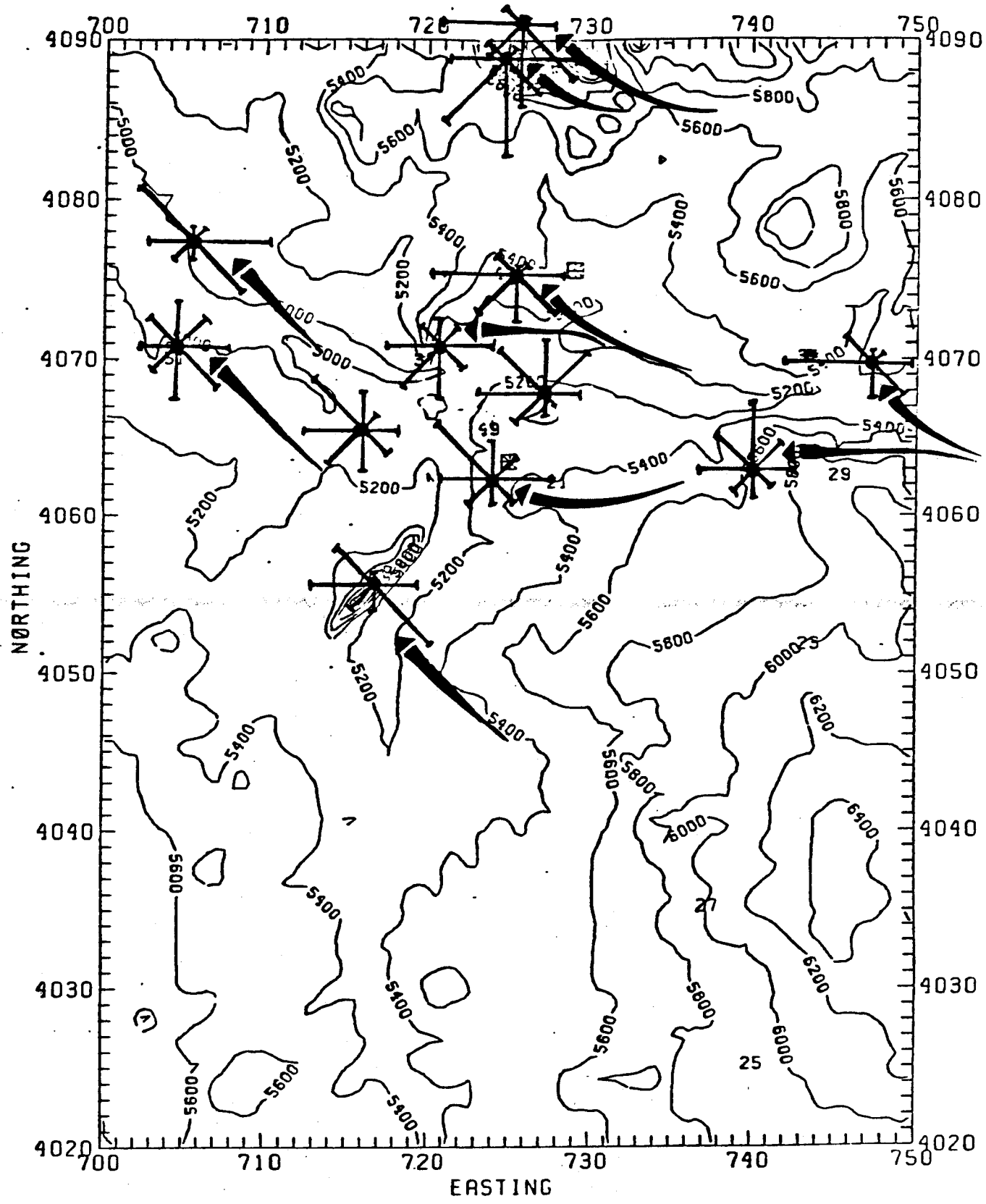

FIGURE 4-30. SUMMER MIDDAY DOWNSLOPE FLOW (FROM STATION WIND ROSES)

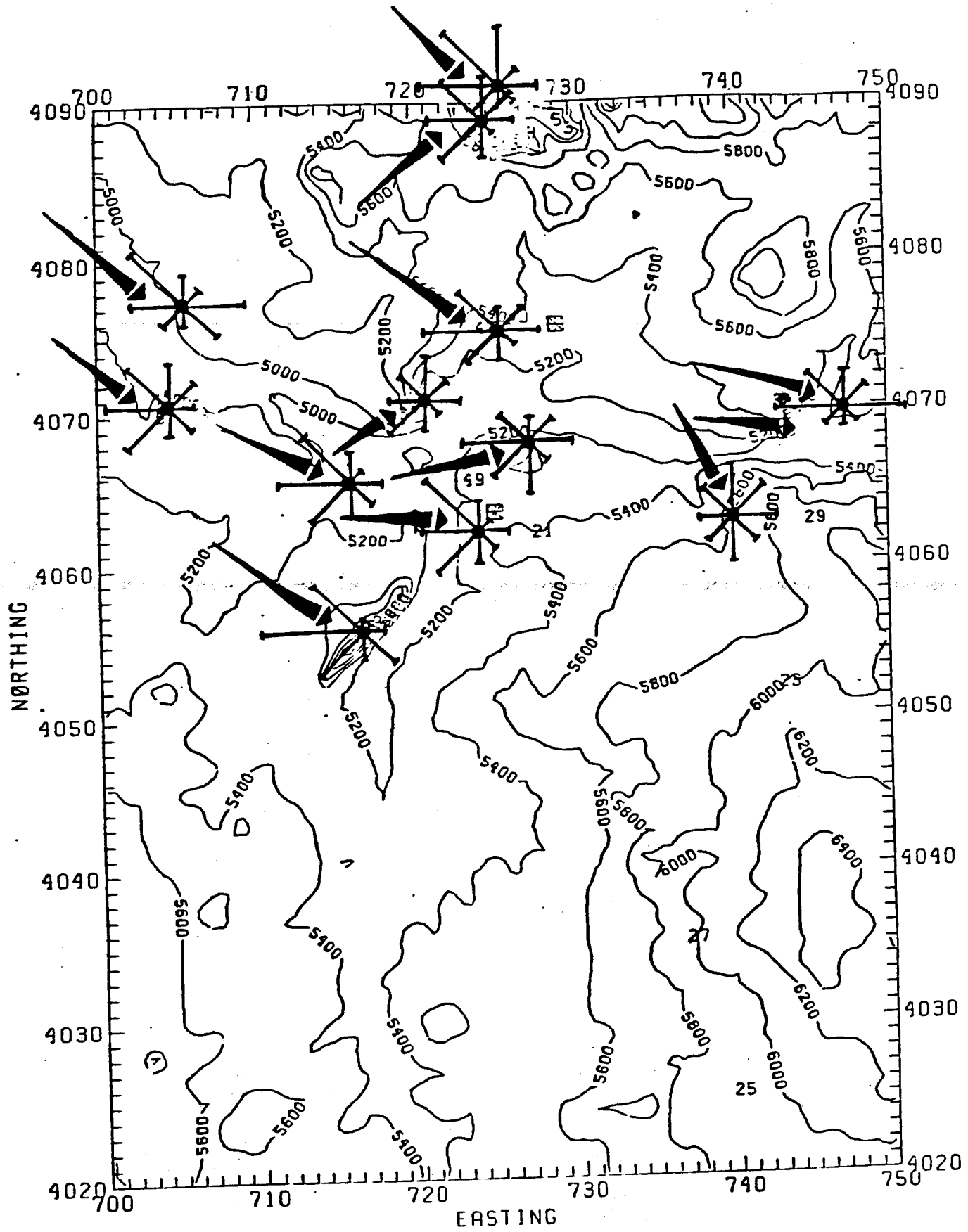

FIGURE 4-31. SUMMER EVENING UPSLOPE WESTERN SYNOPTIC FLOW

Infrared cooling occurred at a faster rate during dry, clear summer evenings and mornings; consequently, summer morning downslope drainage flow was strongly predominant (figure 4-28). The flow was almost consistently downslope at most stations except for DUCT. The wind direction at DUCT seemed dependent on the degree to which dense air moving downhill overshot the normal downslope motion of air from the southeast. Almost every morning, the plume from Four Corners moved out through the gaps in the Hogback ridge towards the stations to the west (PUMP, RATW, SHIP, etc.).

Figure 4-29 indicates that during almost half of the summer middays, some form of western synoptic upslope flow took place at many of the stations. The airflow assumed the nature of upslope flow, possibly assisted by a weak synoptic flow aloft. Upslope flow frequently develops as a response to surface heating and expansion of air columns at the surface. This upslope flow was responsible for the turnaround flow that caused the blow-back of plume material that had originally moved west-northwest during the morning, This caused the plume material to move southeast during midday.

There was also a persistent downslope flow that was not a drainage flow, but rather, an outflow from a persistent high pressure region to the northeast and an inflow to a thermal low to the west and southwest (figure 4-30). The airflow manifested itself most strongly in the wind roses of monitoring sites at high elevations or with good exposure. On a day when downslope flow was continuous, the Four Corners Power Plant plume simply moved westward and did not return.

During the evening, there was a tendency for the downslope motion to cease or at least be minimized, and for an upslope-western synoptic flow to dominate (figure 4-31). This upslope motion cannot be clearly explained but there are several possibilities:

- Outflow from convective activity in the mountains to the west.
- Synoptic flow aloft coupling to the ground.
- Dissipation of residual buoyancy as a result of mid-evening solar heating.

Only the elevated or exposed sites showed the highest occurrence of evening upslope winds. Other stations seemed to be altered by the sheltering and channeling effects of their topography.

The evening upslope flow provided the setting for a secondary turnaround that would occur infrequently. Here, downslope air motion moved the power plant plume westward; then, in the early evening, the downslope air shut off and the west wind brought the plume material back. Mixing was so extensive during the daytime convective activity that the returning plume was highly diluted. The evening upslope wind also resulted in the button hook turnaround that carried material southeast back toward HOGB. If the air at effective plume height were relatively stable, moderate impacts could occur on the elevated Hogback ridge terrain.

The evening upslope flow provided the setting for a secondary turnaround that would occur infrequently. Here, downslope air motion moved the power plant plume westward; then, in the early evening, the downslope air shut off and the west wind brought the plume material back. Mixing was so extensive during the daytime convective activity that the returning plume was highly diluted. The evening upslope wind also resulted in the button hook turnaround that carried material southeast back toward HOGB. If the air at effective plume height were relatively stable, moderate impacts could occur on the elevated Hogback ridge terrain.

4.10 SUMMARY

The detailed summary of the meteorological data presented in this section strongly supports the existence of most of the meteorological dispersion regimes described by Crow. In most cases, the differences in the local meteorology of a station result because the terrain tends to shelter areas and to contain horizontally moving airflows.

The results of the analysis indicated no significant annual variation. The whole air mass over the Four Corners area frequently moves in a day-night cycle that Crow called "turnaround." Regardless of local terrain phenomena, the following cycle of events takes place:

- Sunset to Sunrise--The surface air radiatively cools off and in the process becomes more dense. The denser air settles gravitationally and moves down the San Juan River Valley. Here, the air resists displacement and is neither easily trasnported by air aloft nor stirred by surface variations. The cooling air grows thicker approximately 500 m deep, and becomes a layer of stable westward moving air. The wind above this layer is from a westerly direction.

- Sunrise to Sunset--The surface air radiatively heats up, expands, and rises like a hot air balloon. This air is then pulled upslope to replace the rising air, and as a result, it moves eastward through the San Juan River valley. The heated air becomes unstable causing convective overturning that destroys the remnants of the stable drainage layer. The convection tends to couple air at the surface to air aloft. Eventually, all the surface is moving in an easterly direction, the same general direction as the air aloft.

During the late morning or the early afternoon, most monitoring sites experience a change in wind direction from a downslope (easterly) to an upslope (westerly) wind direction. In the late evening, a more gradual reversal from upslope (westerly) to downslope (easterly) wind direction takes place. The thickness and stability of the drainage layer is greater

during the summer than the winter as a result of greater summer heating and cooling rates.

The turnaround airflow cycle leads to a sloshing effect in which air is pushed back and forth. Generally, in the morning, the power plant plumes are trapped in the drainage layer, lateral and vertical dispersion is suppressed by the stability of the air, and the airflow is constrained by topography. When a morning transition occurs, the meteorological analysis indicates that two dispersion phenomena can occur:

- The air mass with the previous evening emissions moves over the source region again and is mixed downwards by the evolving convective overturning (blow back).

- New source material can be vigorously mixed downward by the evolving convective overturning (fumigation).

These dispersion conditions result in high impacts of low terrain regions along a northwest-southeast corridor over the Four Corners Power Plant (figure 4-2).

The present meteorological analysis indicates that the air aloft is usually from the west, and the arrangement of high and low air pressure regions near the Four Corners area seems to force the surface air to come from the west-northwest, particularly during the winter. Crow calls this airflow a "western synoptic flow" that has the following characteristics:

- The airflow persists all day without any cyclic behavior.

- The air is neutrally stable with little temperature change.

- There are few significant inversions in the boundary layer.

- Winds are moderate to high (> 4 m/s) at the surface and increase with height with no significant maxima or minima in the sounding.

- The airflow occurs most often and is stronger during the winter.

The western synoptic flow strongly dilutes and moves plume material eastward, away from the high terrain and most of the low terrain monitors. The only phenomenon that resulted in plume impacts at the surface was observed when the wind became so strong that it suppressed plume

rise. The drag on the surface then caused the plume to mix downward as the air tended to roll up (similar to the way one rolls up dough).

There is a western synoptic flow in which the air at ground level accrues the characteristics of a drainage flow layer. However, since the gravitational forcing of the air is westward, it is not sufficient to overcome the pressure gradient, and drag forces act to move the air continually eastwards. This airflow, called "western synoptic flow with dropout", seemed to appear in the present meteorological analysis statistics. The characteristics of this airflow are similar to western synoptic flow except that

- Surface wind speeds vary diurnally; low wind speeds occur from sunset to sunrise, and higher speeds are observed during midday.
- There appears to be a ground-level inversion present in the mornings when moderate cooling rates occur.
- At ground level, the wind speed remains low and suddenly increases with height.

The meteorological analysis also seemed to indicate the presence of several types of noncyclic easterly flows that tended to occur more often during the summer. One form of this easterly flow occurred under clear skies and persisted all day, even though the air at the ground was unstable and convectively overturning. Crow referred to this condition as "drainage" whereas, in fact, air that tends to move down the San Juan valley is not draining gravitationally like a river; instead, a horizontal pressure gradient seems to be moving the air mass slowly southwestward. Consequently, drainage is a slight misnomer. This airflow appears to have the following characteristics:

- The wind direction has an easterly component all day.
- A normal drainage flow develops in the evening with the accompanying ground-based inversion.
- Solar heating causes the surface air to convectively overturn during the day; the depth of this layer seems to be limited.
- Local upslope flows oppose the overall easterly wind during the midday and often dominate some stations.

> Wind speeds are generally lower during midday than at other times, usually less than 3 m/s to 4 m/s.

This type of airflow has some potential for poor dispersion since (1) the wind speeds are generally low to moderate, (2) there is depth-limited convective overturning, and (3) there is some evidence of descending air.

A second type of easterly airflow was discovered to occur widely during the winter. Crow noted this also, and called it "eastern synoptic flow." He linked this airflow to the passage of low pressure regions to the south of the Four Corners that resulted in cloudiness, precipitation, and high winds. This analysis found this winter-type of easterly airflow to have the following characteristics:

> The wind blows from an easterly direction all day.

> The wind speeds are moderate to high.

> The air mass is generally neutrally stable.

> There seems to be a lack of evening drainage flow and its accompanying ground-based inversion.

> A reduction in solar radiation tends to occur during the daytime (cloudiness).

This airflow has excellent dispersive and dilutive potential; pollutant episodes would not normally be expected under such circumstances.

Observations were made concerning the nature of the space and time variability of the dispersion conditions near the Four Corners Power Plant:

> The hourly averaged wind direction persistence within a 22.5° sector was small; it lasted only one or two hours.

> The hourly averaged wind direction varied significantly with height (typically ± 20°/100 m).

These inhomogeneities tend to add to the dispersive ability of the atmosphere. The analysis indicates that the ground-based drainage layer often becomes so thick that it pours over and around Hogback much like water over and around a spillway. The average inversion height was found to be about 500 m, generally high enough to entrain the Four Corners plant plumes.

APPENDIX B

CALPUFF MODELING AND EVALUATION USING RUC DERIVED MM5 DATA

CALPUFF Modeling and Evaluation Using RUC-Derived MM5 Data

Paper # 69570

Mary M. Kaplan and Robert J. Paine

ENSR Corporation, 2 Technology Park Drive, Westford, MA 01886

Dennis A. Moon

SSESCO, Itasca Technology Exchange, 201 NW 4th St., Grand Rapids, MN, 55744

ABSTRACT

In recent years, EPA has recommended the use of initialization wind data from National Weather Service (NWS) prognostic forecast techniques in the CALPUFF dispersion model. One such prognostic model, the Rapid Update Cycle 2 (RUC), incorporates traditional observations (hourly surface and twice-daily upper air soundings) with new sources of data, such as cloud drift winds, NEXRAD radar, profiler data, and aircraft ascent and descent observations. In 1999, the NWS increased the output of the RUC2 from every three hours to every hour. The hourly output has been archived by some interested parties since that time for future uses, such as dispersion modeling.

Recently, the North Dakota Department of Health (NDDH) conducted a modeling study using CALPUFF with wind data for the year 2000 derived from traditional surface and upper air sounding meteorological observations. NDDH modeled sources with hourly emissions data in North Dakota and Eastern Montana with receptors located at two SO_2 monitors and compared the results to observed concentrations. The authors have conducted an alternative CALPUFF analysis using RUC2-derived winds supplied by Software Solutions and Environmental Services Company (SSESCO). This paper compares the results of the alternative CALPUFF analysis to those of the NDDH study and presents model evaluation results from the two approaches. The authors also mention some of the ways in which the use of RUC2 Mesoscale Model 5 (MM5) data avoids underestimates in wind speeds during relatively light wind conditions that can occur with the use of traditional sources of meteorological data.

INTRODUCTION

The U.S. Environmental Protection Agency (EPA) proposed CALPUFF[1] as the preferred long-range transport model in April 2000. Plume transport beyond 50 kilometers is considered long range and beyond the capabilities of steady-state models such as the Industrial Source Complex (ISC) model. CALPUFF is a non-steady-state transport and dispersion model designed to advect plumes or "puffs" emitted from sources using a four-dimensional (x, y, z, and time) meteorological grid. CALPUFF contains algorithms to compute wet and dry pollutant removal, vertical wind shear, chemical

transformation, and dispersion coefficents, as well as the effects of building downwash and terrain on the plume. The Interagency Workgroup for Air Quality Modeling (IWAQM) conducted limited evaluations of CALPUFF and found[2] that the model is mostly unbiased out to 100 kilometers. At distances of 300-400 kilometers, however, IWAQM found that CALPUFF shows an over prediction bias of a factor of 3-4. Accordingly, IWAQM cautioned the use of CALPUFF at distances beyond 200-300 kilometers due to the effects of wind shear. Even at a distance of 200 kilometers, a significant over prediction tendency for CALPUFF is possible.

A meteorological model, CALMET, provides the hourly three-dimensional wind field and other meteorological data used in CALPUFF. CALMET processes available meteorological and geophysical data and computes hourly micro-meteorological variables, wind and temperature fields for the entire modeling domain. Hourly surface observations and twice-daily balloon soundings at scattered locations require CALMET to interpolate between these observations. To reduce the amount of interpolation necessary in CALMET, prognostic wind field data from a mesoscale model (MM), such as the RUC2[3], can be introduced as the initial guess field. The observations are added into the initial guess field as part of an objective analysis procedure. IWAQM has reported improved CALPUFF results when MM data are employed in the model as the initial guess field.

This paper addresses the types of observations assimilated into the RUC2 data and the advantages of using this data as input into CALMET. The authors compare results from a CALPUFF modeling evaluation performed with and without the RUC2 data.

NEW SOURCES OF METEOROLOGICAL DATA INPUT TO CALPUFF

CALMET builds the wind field in two steps. In Step 1, MM5[4] prognostic wind field data is usually incorporated as a superior initial wind field estimate prior to correction from actual observations (in Step 2). The Step 1 process takes the initial wind field estimate and subjects it to refinements due to terrain effects and minimization of divergence (to preserve conservation of mass laws). The result of this Step 1 process is far superior to that using a crude initial wind field estimate, which then would require a substantial correction to observations in the Step 2 process. With the use of traditional observations (widely scattered airports and balloon sounding stations,), the CALMET Step 2 process needs to have a large radius of influence for the correction of a crude initial wind field estimate. This tends to smooth out the wind field relative to what is available as details in an MM5 data set. As an alternative, the use of the MM5 data for Step 1 is often associated with very local corrections in the Step 2 process. As noted above, IWAQM[2] has observed improved CALPUFF performance with the prognostic wind field model used as a Step 1 initial guess field.

Prognostic (predictive) models are well known to have significant advantages over diagnostic wind field models. Dynamic constraints are those resulting from the application of conservation laws involving time derivatives, such as conservation of momentum. The chief drawback of prognostic models is the computational expense of running them. Computational stability considerations require that the models be stepped forward with a time-step that is proportional to the grid cell size. Thus, high-resolution grids require an extremely large number of time-steps to be computed in order to cover the needs of a long-

term air quality study. For this reason, high-resolution prognostic models are most often applied to episodic case studies.

While the application of customized prognostic meteorological models to long-term air quality studies can in some cases be prohibitively expensive, data from the National Oceanographic and Atmospheric Administration (NOAA) prognostic model outputs and analyses can be combined with mesoscale data assimilation systems to produce high-resolution data sets of long duration. NOAA runs a suite of models at varying initial times, resolutions, domains of coverage, and forecast duration. Each model run starts with results from a previous run, combined with all available observed data, including surface and upper air observations, satellite, and radar data. This process of combining the various data sources to yield a unified representation of the three-dimensional atmosphere is termed assimilation.

Assimilation has been an area of active research over the years. As increasingly accurate analyses become available, combining more data types is one of the principal means for improving forecast quality. A promising data archive for air quality applications is NOAA's RUC2 model data. RUC2, or Rapid Update Cycle 2, is a short-term forecast model that is re-initialized each hour based on previous model results and actual meteorological readings. The RUC2 model[3] grid contains 40 km cells, with over 40 layers of data in the vertical dimension (see Figure 1). This resolution is sufficient to easily represent the upper air features captured by the rawinsonde network. Interested parties, including private companies such as SSESCO, can download the RUC2 model data from a NOAAPORT server.

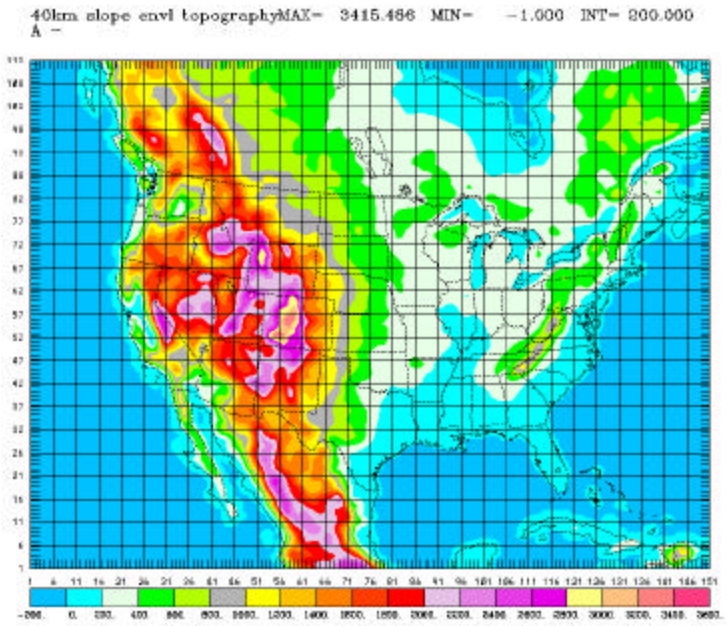

Figure 1. Horizontal Resolution and Domain of the 40-Kilometer RUC2 Model[3]

While NOAA has been advancing the assimilation and modeling process as applied to synoptic scale weather systems, a parallel effort in mesoscale modeling systems has been proceeding at a number of governmental and educational research institutions. Foremost among those efforts has been the work done at the Center for the Analysis and Predictions of Storms (CAPS), at the University of Oklahoma. This group, funded by NSF and the FAA, is focused on research and the development of software tools related to small-scale weather phenomenon. In some cases, the RUC2 data with its 40-km grid may not be of high enough resolution to capture all of the relevant flow and thermal structures that arise near the earth's surface (although the RUC2 has been available since April 2002 on a 20-km grid). To avoid this problem, some investigators have taken advantage of a technique to introduce high-resolution terrain data and surface observations using a "mesoscale assimilation system". We have chosen the Advanced Regional Prediction System[5] (ARPS) Data Assimilation System (ADAS), for use as a mesoscale assimilation tool.

SSESCO applied the ADAS system by starting with a "first-guess" field derived from the RUC2 archives of NOAA model data, then factoring in observational meteorological data and performing climatological, spatial, and temporal continuity checking of the data. The key to the assimilation process was the blending of different data sources, each with their own error characteristics into a unified, "most probable" three-dimensional distribution of the target variable. Taking into account the error characteristics of the first-guess gridded data and each of the observational sources, an objective analysis onto the target CALMET model grid is performed by employing a highly efficient iterative approach to the widely used Statistical or Optimal Interpolation (OI) technique, known as the Bratseth[6] technique. Mass conservation and boundary conditions are then applied to derive the vertical motion fields.

In many CALPUFF applications, even those using MM5 prognostic model output with traditional airport and balloon sounding data, the area between the major sources and the receptor locations lack significant meteorological coverage. The model has to interpolate the data and fill in the grid points that have no data. The model must interpolate in space and time between the twice-daily balloon soundings, which fall near the times of sunrise and sunset in the continental United States. Due to interpolation, the model may underestimate wind speeds by missing diurnal features such as the daytime diurnal wind speed maximum or the low-level jet stream after sunset. During periods when the wind shifts nearly 180 degrees between sounding times, interpolation of vector winds could potentially yield near-calm winds at the midpoints of the 12-hour periods between sounding times. Even accounting for balloon sounding data, the 3-dimensional wind field is mostly devoid of real measurements, as shown in Figure 2.

Figure 2. Three-Dimensional View of Data Coverage During Sounding Periods – Traditional Meteorological Data

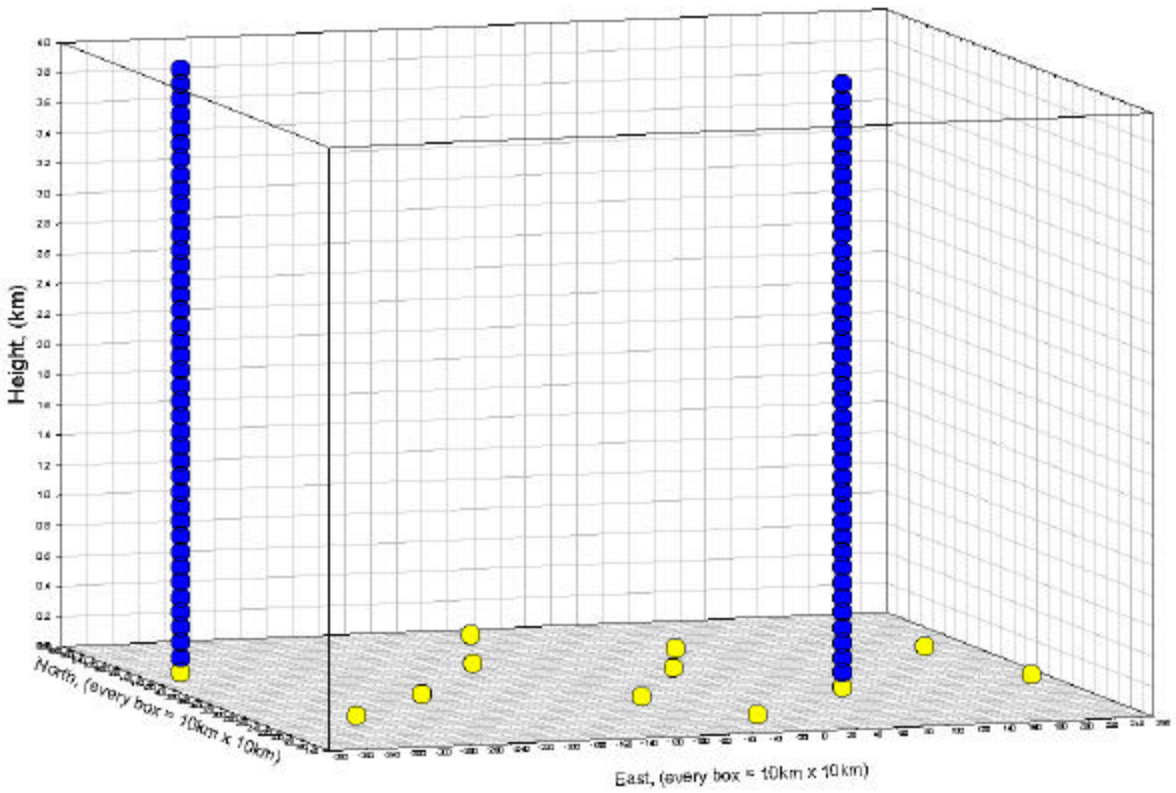

While most forecast models are initialized every three to twelve hours, the RUC2 model began in 1999 to be initialized every hour, making it ideal for input to dispersion models. It is a short-term weather data assimilation and forecast model that is re-initialized each hour based on the projected analysis from the previous hour and updated meteorological data readings. The major advantage of the RUC2 model over all other prognostic models is that it incorporates new sources of data, many of which are only available to NOAA, in addition to the hourly surface observations and twice-daily balloon soundings, such as:

- satellite derived-wind data;
- Next Generation radar (NEXRAD) that provides newly available Doppler wind data in three dimensions from several radar sweeps each hour;
- wind profilers that probe the atmosphere vertically; and
- aircraft ascent-descent reports, newly available from several hundred commercial flights per day in the U.S.

Satellites such as Geo-stationary Operational Environmental Satellite (GOES)-East and GOES-West derive wind speed and direction from cloud movement under all weather and cloud conditions over the Earth's surface using Infra-Red (IR), Water Vapor (WV), and Visible channels. Figure 3 shows one hour of wind speed and direction derived from GOES-East Visible channel.

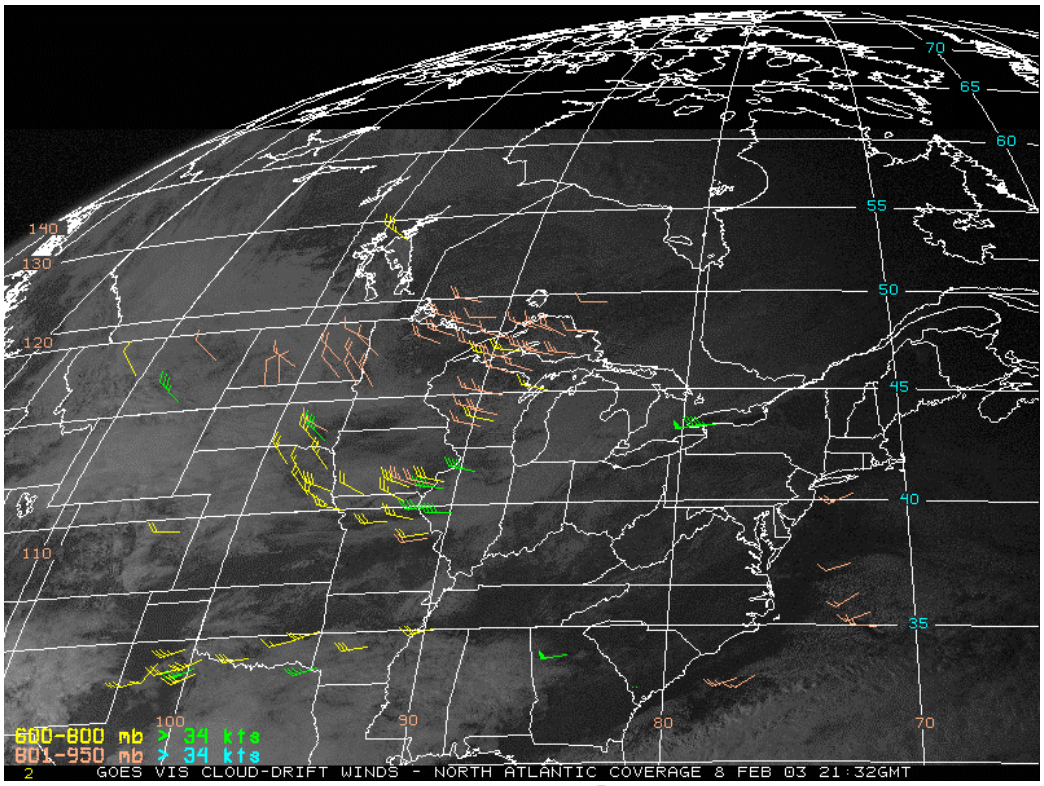

Figure 3. GOES – East Satellite Derived Winds[7]

NEXRAD (Next Generation Radar) Doppler Radar (see Figure 4) measures precipitation and wind based upon the energy and the "shift in the phase" returned to the radar when it bounces off a target. The VAD (Velocity Azimuthal Display) winds are derived from geometry and trigonometry (assuming uniform winds in the radar volume) and are incorporated into the RUC2 model. An advantage of VAD winds is the widespread coverage of NEXRAD radar across the country (Figure 6). A complete sweep of NEXRAD radar is made every 10 minutes. The availability of the NEXRAD data greatly increases the actual wind data available to the RUC2 prognostic model every hour over that of traditional data (compare Figures 7 and 2).

Figure 4. NEXRAD Doppler Radar Installation[8]

Figure 5. Doppler-derived Radial Velocity Field from NEXRAD Radar (Green Moving Towards the Radar, Red Moving Away from the Radar)[9].

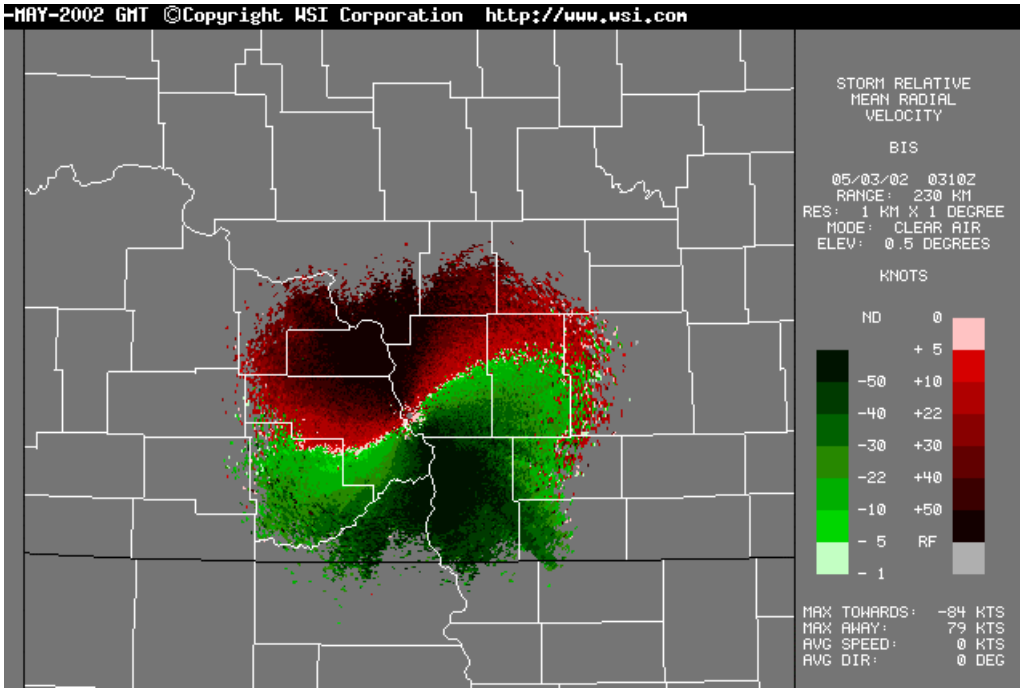

Figure 6. Completed NEXRAD Doppler Radar Installations Within the United States[10]

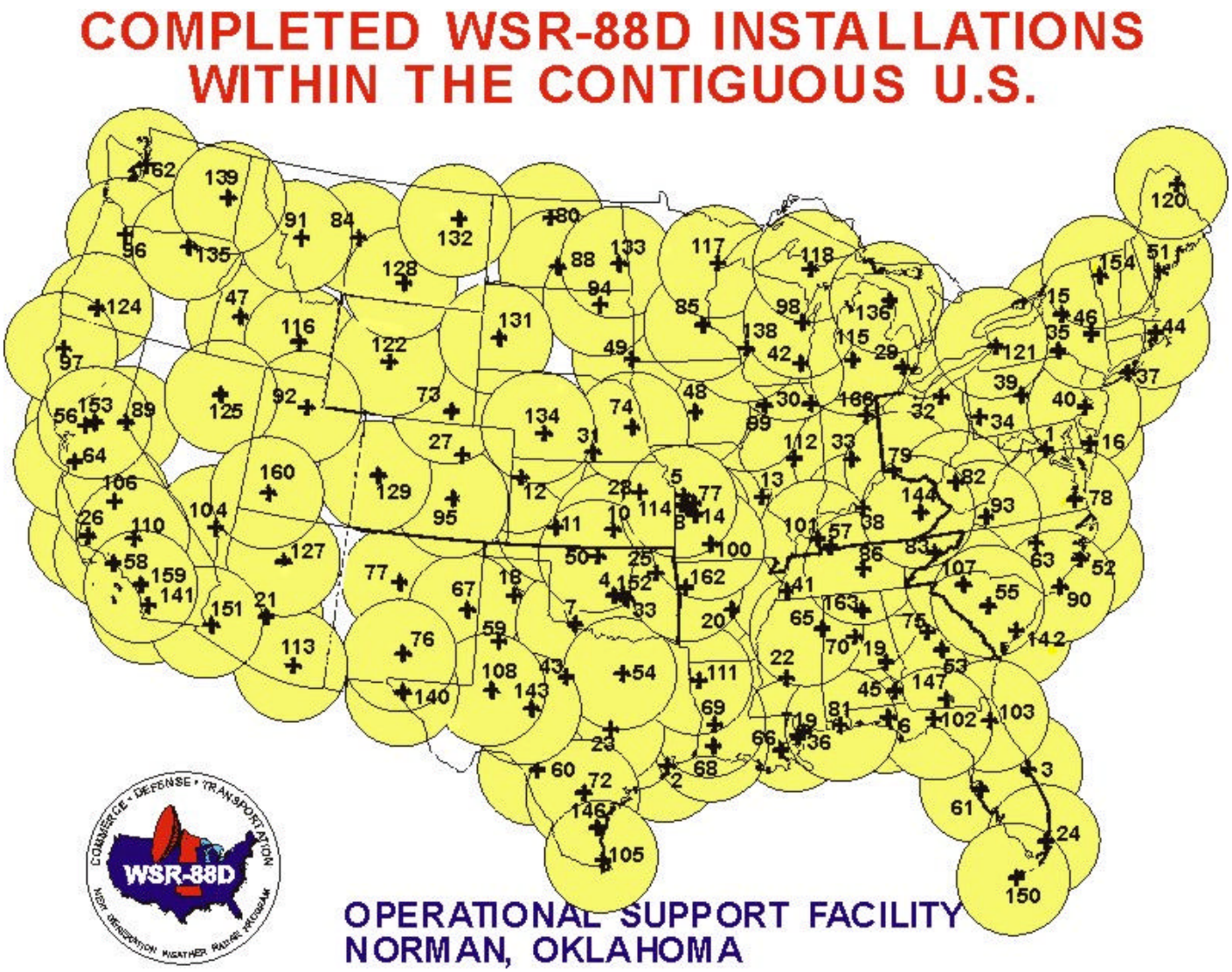

Figure 7. Hourly Meteorological Data Coverage with Clear-Air NEXRAD

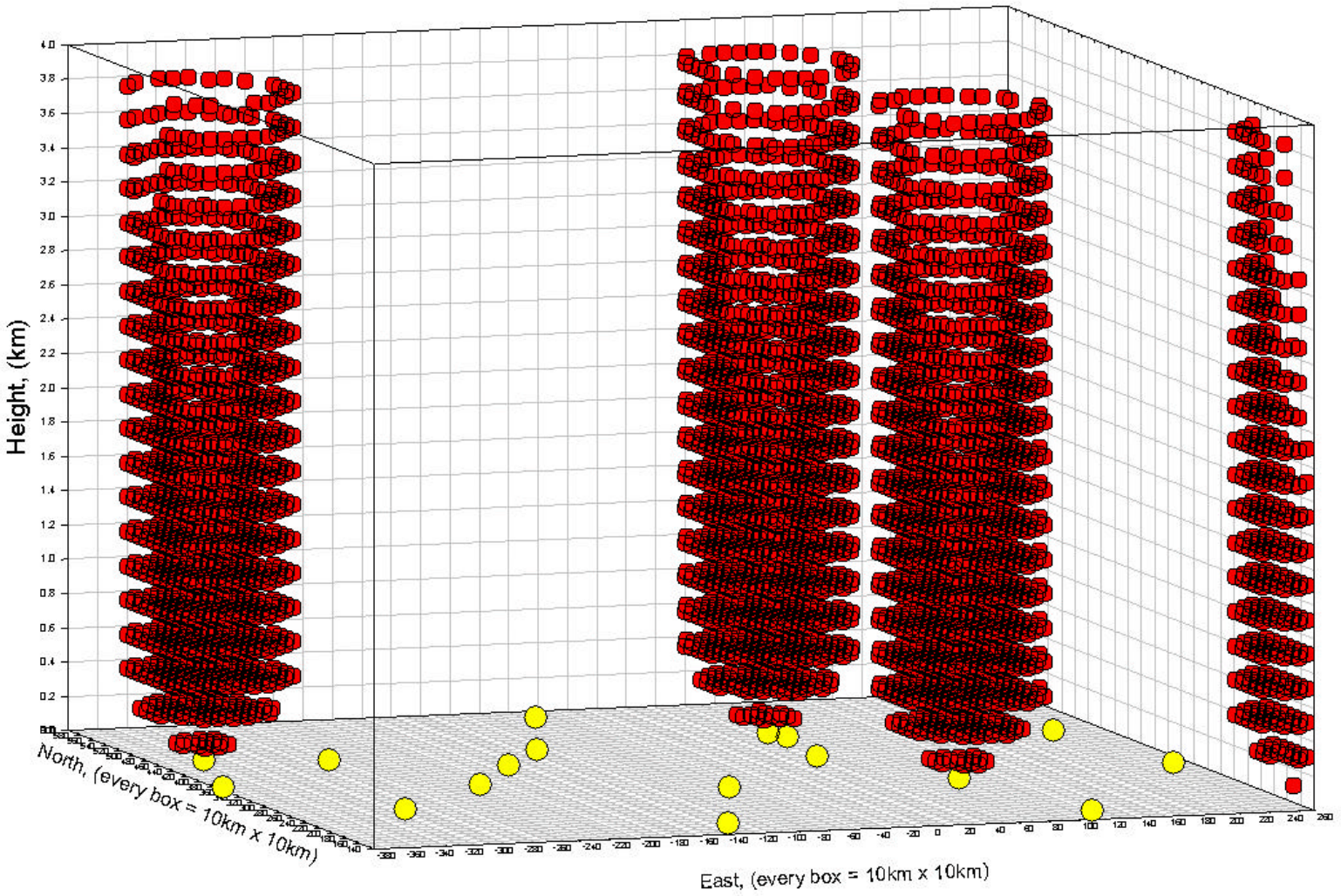

In addition to NEXRAD and satellite data, the RUC2 model incorporates aircraft ascent and descent data from over 500 flights each day (see Figure 8). Airlines such as Delta, Northwest, United, and Federal Express transmit the flight's latitude, longitude, altitude, time, temperature, wind speed and direction.

The wind profiler installations across the United States are shown in Figure 9. The profilers provide hourly soundings of wind, temperature, and turbulence data at many levels in the vertical.

The RUC2 model assimilates all available data, performs a quality assurance check, reads in the previous 1-hour RUC2 model forecast, and outputs a forecast for the next 12 hours. The data analysis and model forecast account for terrain, land/water interaction, mountain circulations, sea/lake breezes, snow cover, vegetation, soil moisture, and a host of other variables.

These new meteorological observations have the potential to increase the accuracy of CALPUFF model simulations. The use of the enhanced meteorological data, specifically the NEXRAD winds, has been found to reduce MM5 model wind errors[11], and was recommended in presentations at the EPA's Seventh Modeling Conference[12]

Figure 8. Typical ACARS Coverage for a 24-Hour Period Up to 5000 Feet[13]

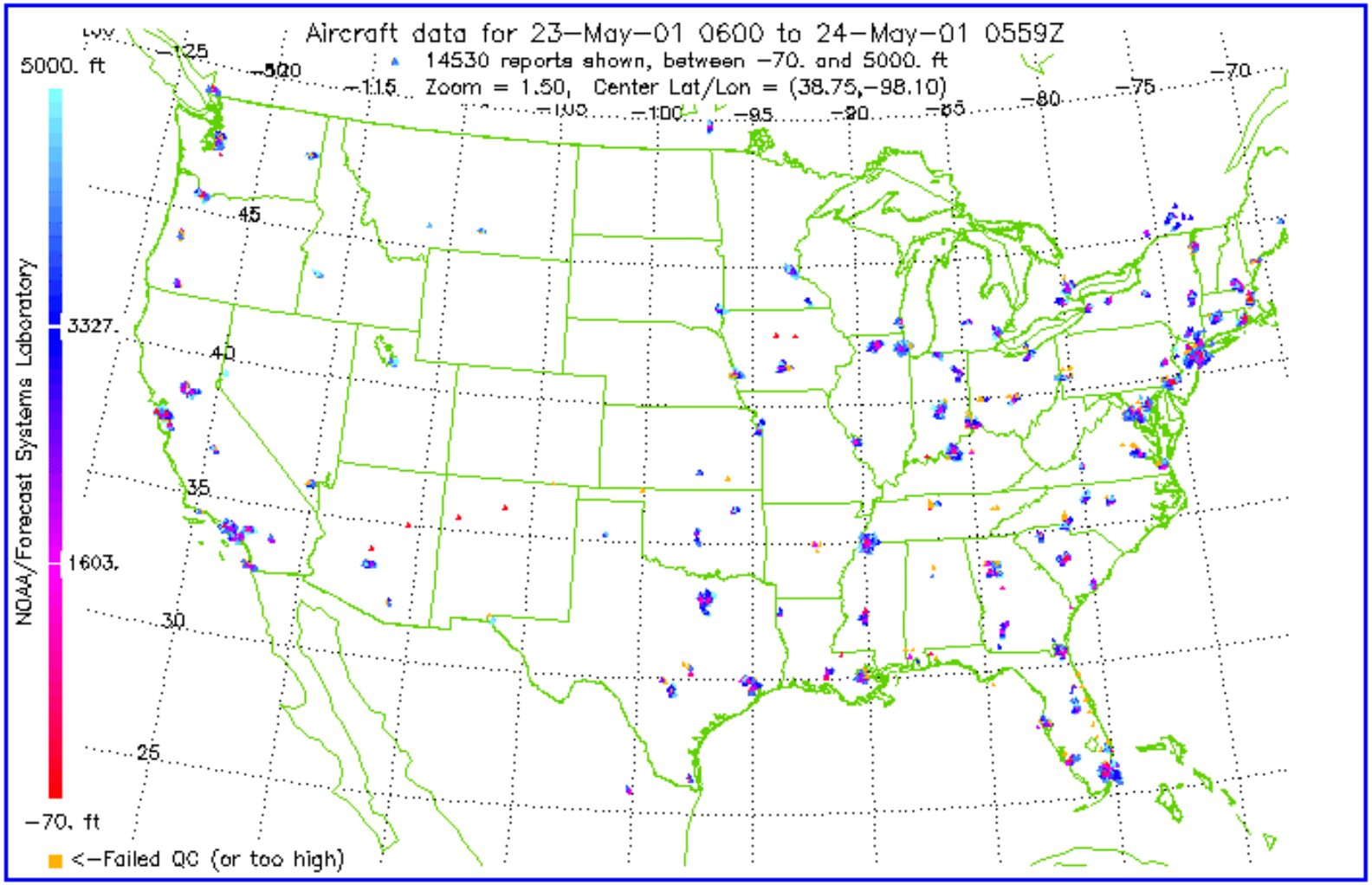

Figure 9. Coverage of Profiler Wind Data Stations in the United States[14]

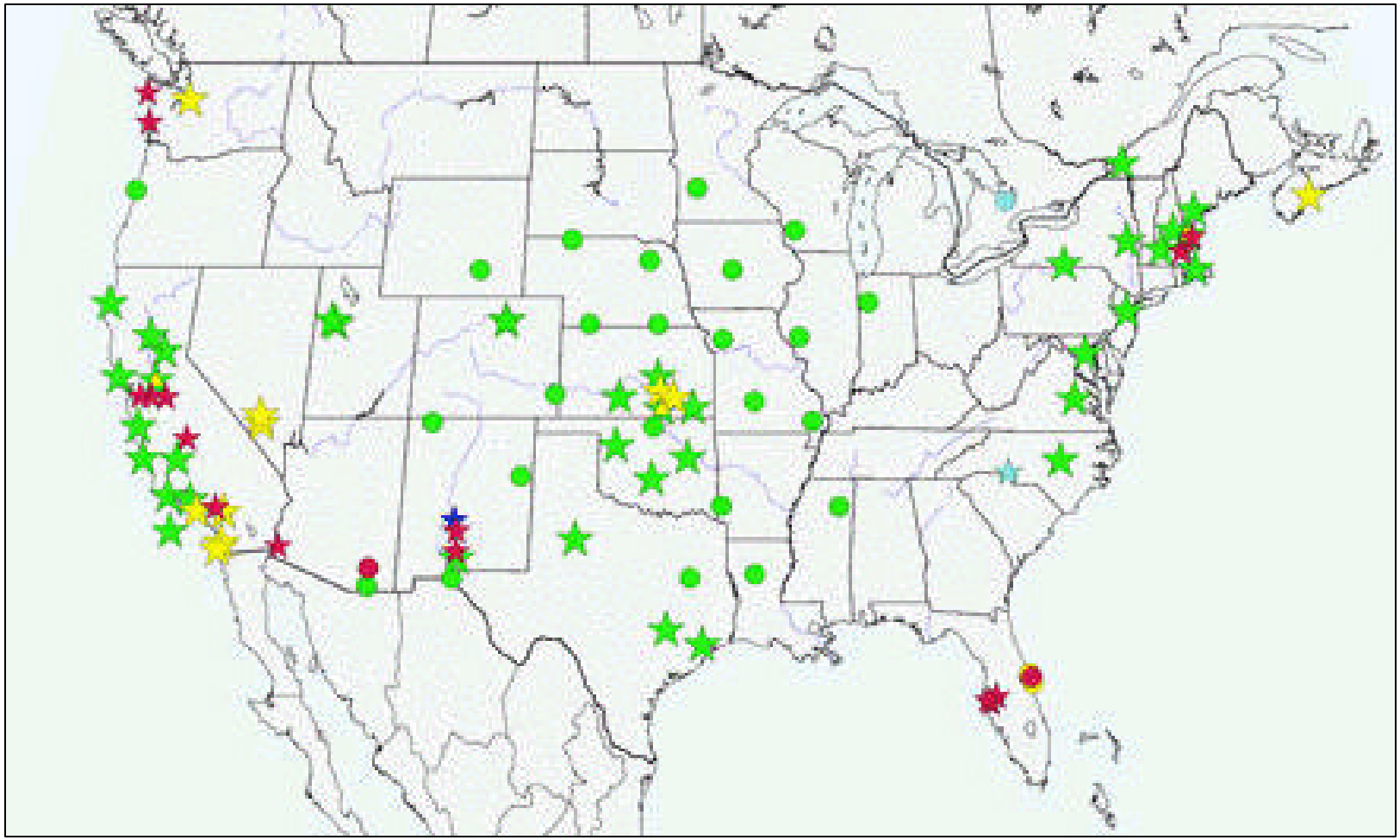

COMPARISON OF WIND SPEED AND DIRECTION IN BISMARCK SOUNDING VS. RUC2 MODEL

Mr. John Irwin[15] of the United States Environmental Protection Agency (USEPA) has recommended that MM5 databases in general be tested against traditional data such as balloon soundings to assure data compatibility. One concern expressed by the North Dakota Department of Health was that the RUC2 data showed systematically higher wind speeds at plume height (about 300-400 meters), leading to lower modeled predictions. We decided to compare the RUC2 MM5 wind speed and direction with Bismarck balloon sounding data at several levels within the boundary layer. Bismarck is the closest upper-air sounding to the major emissions sources and would be most influential for plume trajectories. The closest grid point in the RUC2 CALMET output was only 0.7 kilometers away from the Bismarck airport, with an elevation difference of four meters. The data at this grid point was extracted from the CALMET output using the PRTMET program.

The PRTMET program extracts data for specific grid points, time periods, vertical layers, and variables. The wind speed and direction data were extracted hourly for all available vertical layers in the model output. The CALMET output has twelve vertical layers. The CALMET output and the Bismarck airport soundings were linearly interpolated (consistent with the CALMET interpolation approach) to eight selected heights before comparing the wind speed and direction (Table 1). The eight interpolated layers are based on the approximate height of mandatory or frequently available sounding levels from the Bismarck soundings. The heights were selected to adequately cover the expected heights of the plumes emitted from the stacks in the emissions inventory. A FORTRAN program was written to interpolate and format the data for use in Excel spreadsheets.

Table 1. Heights used in the wind speed comparison.

RUC Vertical Layer (m)	Interpolated Vertical Layer (m)
10	100
30	
60	
100	
150	200
220	
330	300
500	400
700	700
1000	1000
1600	1500
3000	3000

The interpolated CALMET wind speed and direction were compared to the Bismarck airport sounding wind speed and direction every twelve hours (from January 4th to December 31st (AM), 2000) for a total of 725 data points at each level. Scatter plots of Bismarck vs. RUC2 (MM5) wind speed (Figure 10) and direction (Figure 11) and box and whisker plots of Bismarck vs. the ratio of RUC2 to Bismarck wind speed (Figure 12) and RUC2-Bismarck vs. Bismarck wind direction (Figure 13) were prepared for all eight levels. These plots subdivide the domain of the variable of interest (e.g., Bismarck sounding wind speed or direction) into "bins" and present a distribution of wind speed ratios as a box plot for each bin. The plot provides an indication of the following cumulative frequency data for each population sampled: 10%, 25%, 50%, 75%, and 90%.

The linear regression calculation available in Excel determined the trend in each scatter plot with the slope and y-intercept labeled next to the regression line. A slope of 1.0 indicates that the RUC2 data are in agreement with the Bismarck sounding data. In general, the RUC2 wind speed and direction do not show a significant bias, although the wind speeds in the 0-4 meters/second category are slightly higher than the Bismarck sounding data (y-intercept of nearly one meter per second). The RUC2 wind speed and direction show more scatter about the one-to-one line because of the other data sources incorporated into the RUC model.

The box and whisker plots subdivide the Bismarck sounding wind speeds into four categories and depict the ratio of the RUC2 to Bismarck wind speeds as a frequency distribution (centered at 50%, with extremes at 10% and 90%). Tables 2 and 3 indicate the number of data points in each "bin" for our examples at 400 meters. Tables 4 and 5 tabulate the 10th, 50th, and 90th percentile in each bin. A value of one at the 50th percentile would indicate agreement between the RUC2 and Bismarck data sets (at the median). The plot indicates that the RUC2 wind speeds are less than 20% higher than the Bismarck winds in the lowest wind speed category (0-4 m/s). The relative difference between the RUC2 and the Bismarck sounding wind speeds drops to less than 10% in the 4-8 m/s category.

Table 2. Box plot observation counts.

Level (meters)	Bismarck Sounding Wind Speed (meters/second)			
	0.00-4.00	4.01-8.00	8.01-12.00	>12.01
400	140	261	183	141

Table 3. Box plot observation counts.

Level (meters)	Bismarck Sounding Wind Direction (degrees)			
	315-44	45-134	135-224	225-314
400	227	98	217	183

Figure 10: Scatter Plot of Twice-Daily MM5 Wind Speed vs. Bismarck Sounding Wind Speed at the 400-meter Level

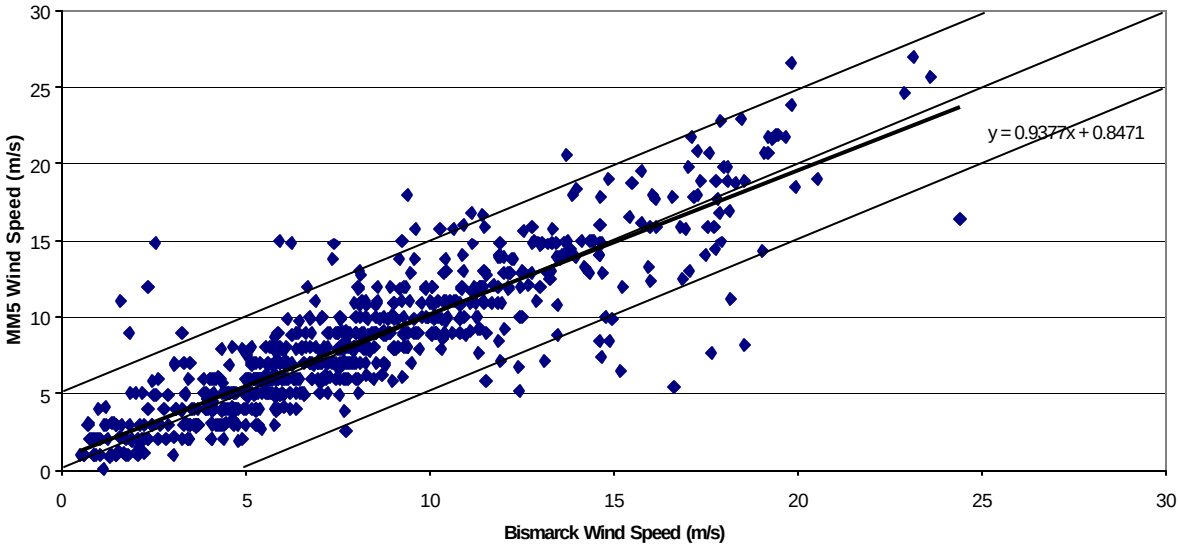

Figure 11: MM5-Bismarck vs. Bismarck Wind Direction at the 400-meter Level (adjusted for cross-over at 360 degrees

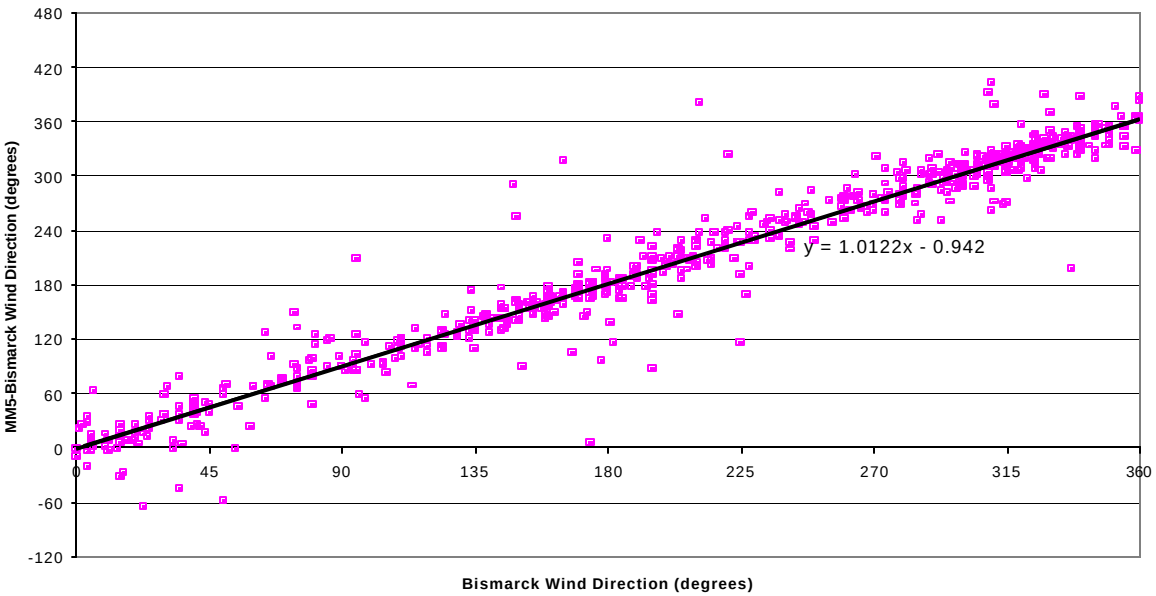

Table 4. Ratio of RUC2/Bismarck to Bismarck sounding wind speed (meters/second).

Level (meters)	Box Plot Frequency Data – 50% (10%,90%)			
	0.00-4.00	4.01-8.00	8.01-12.00	>12.01
400	1.18(0.66,2.05)	1.07(0.81,1.37)	1.02 (0.80,1.26)	1.00 (0.80,1.17)

Table 5. RUC2-Bismarck to Bismarck sounding wind direction (degrees).

Level (meters)	Box Plot Frequency Data – 50% (10%,90%)			
	315-44	45-134	135-224	225-314
400	1.0(-16.0,13.4)	1.0(-14.3,32.0)	1.0 (-15.4,17.0)	4.0 (-14.0,19.8)

Figure 12: 400-meter Wind Speed Ratio of MM5/Bismarck vs. Bismarck Sounding

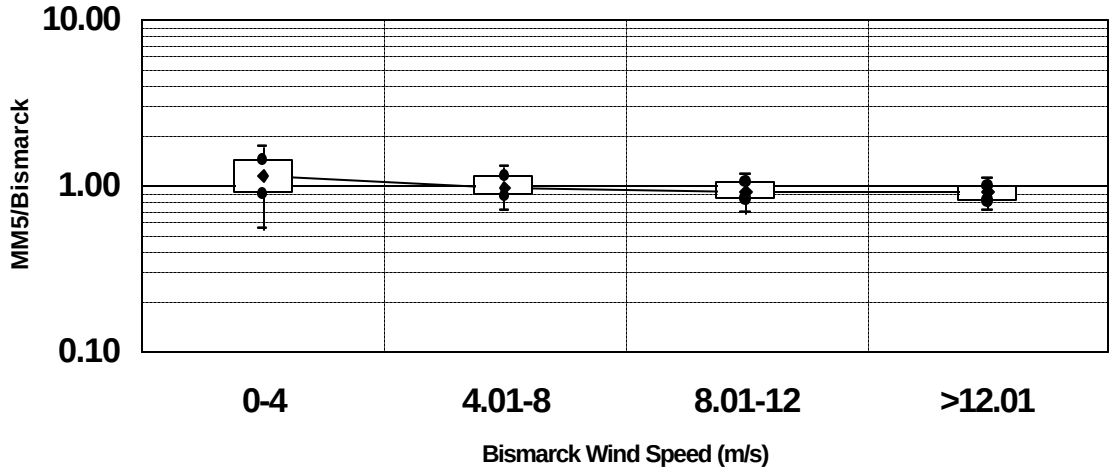

Figure 13: 400-meter Wind Direction of MM5-Bismarck vs. Bismarck Sounding

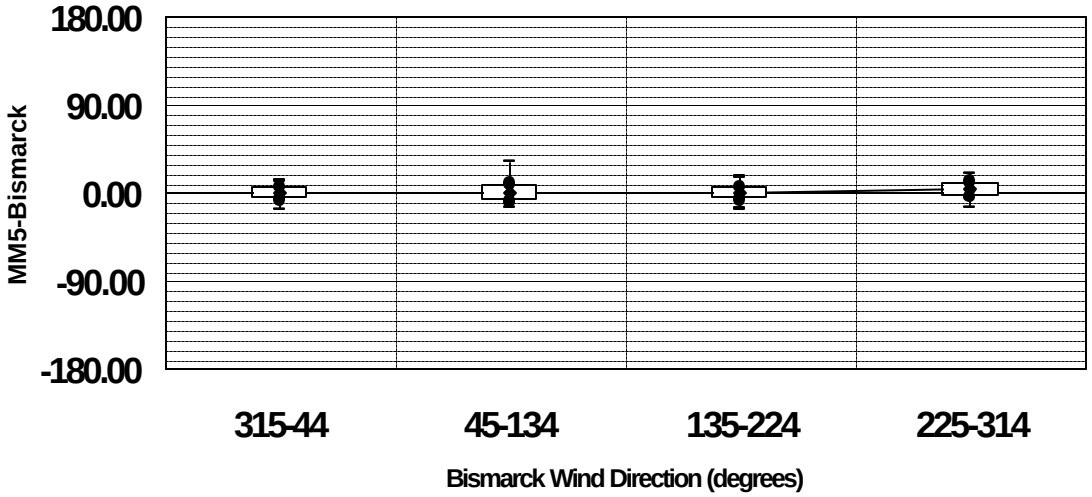

For rawinsonde measurements, the Federal Meteorological Handbook #3[16] (Rawinsonde and Pibal Observations) states that wind speed measurements derived from a Radio Direction Finding (RDF) antenna or radiotheodolite are accurate to within 1 meter per second. This means, for example, that a wind speed reported as 2 meters per second could actually range between 1 and 3 meters per second and be within the acceptable tolerance of the reported data. The Bismarck station is equipped with VIZ-B2 radiosondes and a Weather Bureau RadioTheodolite (WBRT-57). The balloon sounding instrument accuracy of 1 m/s would translate to $\pm$50% uncertainty for the mean wind speed of the first bin (2 m/s), $\pm$17% for the mean of the second bin (6 m/s), $\pm$10% for the mean of the third bin (10 m/s), and $\pm$8% for the fourth bin. This implies that the limitations in the balloon sounding instrument accuracy could account for the difference between the RUC2 and Bismarck wind speeds.

The Federal Meteorological Handbook #3 lists the accuracy of wind direction measurements as 5 degrees, but the precision of the measurement varies with wind speed. The Meteorological Monitoring Guidance for Regulatory Modeling Applications published by EPA[17] suggests data quality objectives of ±5 to ±18 degrees for radiosondes. The 50th percentile in each quadrant is less than 5 degrees, indicating good agreement between the RUC2 and Bismarck wind direction data.

The results presented indicate that there is no significant difference between the RUC2 wind speed and direction and the Bismarck sounding data. It is also apparent that systematic wind speed differences between the two data sets do not exist, and are not the cause of the lower prediction in the year 2000 modeling results. While the RUC2 database wind speeds are slightly higher at low wind speeds, the balloon sounding instrumentation accuracy limitation would have the most impact in the 0-4 m/s category. The diversity of the measurements incorporated into the RUC2 data may imply that the wind measurements derived from the rawinsonde location underestimate the wind speed. Several other modeling variables could contribute to the large difference in the modeling results. The 10-kilometer horizontal grid provides improved resolution allowing a more accurate depiction of the terrain in the modeling domain. A primary contributor to the difference could be the additional observational data in the RUC2 data, which incorporates observations every hour in three dimensions over much of the modeling domain.

MODELING PROCEDURES

Modeling Domain and Setup

The modeling study involved modeling emissions sources located in North Dakota, Eastern Montana and Southern Canada, as depicted in Figure 14. The receptor locations coincided with two SO_2 monitors located at Dunn Center (145 km northwest of Bismarck) and Theodore Roosevelt National Park – South Unit (200 km west of Bismarck). A 630-km (east-west) by 450-km (north-south) modeling domain with twelve vertical layers was designed to accommodate all emissions sources with a sufficient buffer. Thirty-seven hourly surface stations and five twice-daily upper air stations were

located in or near the modeling domain as depicted in Figure 15. Several options in CALMET are important to balancing the surface and balloon

Figure 14: Major Emissions Sources and Receptor Locations

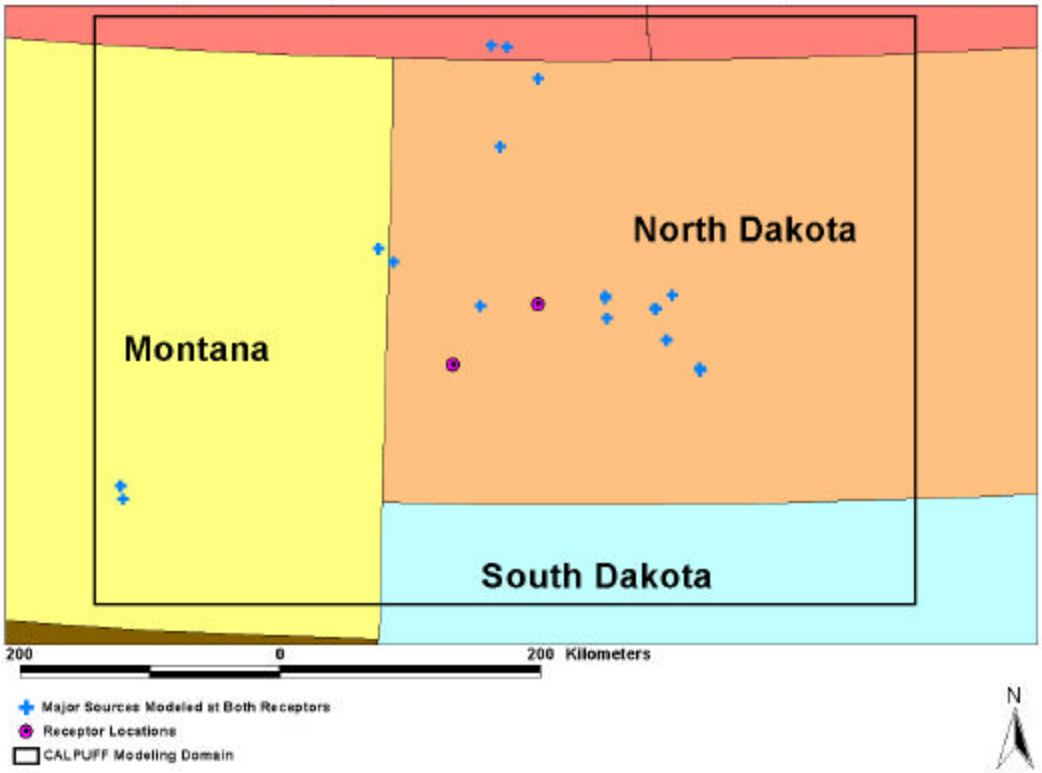

Figure 15: Modeling Domains and Meteorological Data Coverage

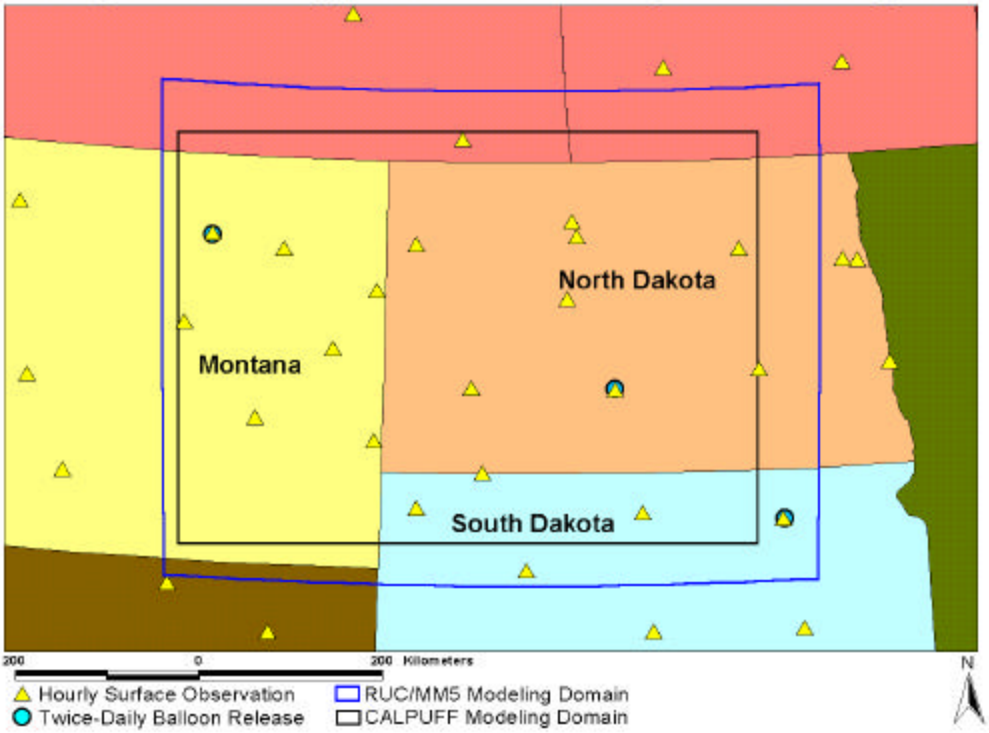

sounding observations with the prognostic data available in the RUC2 model. These options include:

TERRAD – TERRAD controls the distance out from a hill or valley wall that the terrain-flows can have an effect on local winds. John Irwin recommends a value of 3 grid spaces (for a 3 km grid - 10 km, for a 10 km grid - 30 km).

IPROG – CALMET[1] contains the option to allow prognostic meteorological models, such as the RUC or MM5, to be used as input to the model in one of three capacities:

- As the initial guess field, where the RUC2 data are interpolated to the CALMET grid and are adjusted for the fine-scale terrain in the CALMET grid. In this case, the 10-kilometer RUC2 data are interpolated to the 3-kilometer CALMET grid. The interpolated data become the Step 1 wind field which is subject to an objective analysis that adds the observed surface and balloon sounding wind data to produce the Step 2 wind field.
- As the Step 1 wind field, where the RUC2 data are interpolated to the CALMET grid but are not adjusted for the fine scale terrain. It is assumed that the data already contain terrain effects and adjustment is not necessary. As in the first option, an objective analysis adds the observed wind data to form the Step 2 wind field.
- As "observations", where the RUC2 data would be treated like observations. The Step 1 wind field is created by adjusting the RUC2 data for fine scale terrain effects, but in Step 2 the RUC2 data would be used in the objective analysis procedure. Surface and balloon sounding data would be weighted equally with the RUC2 data.

EPA guidance recommends the use of prognostic data in the initial guess field and not as observations.

RMAX1 – RMAX1 controls the distance to which a surface station has any effect on the wind field. From the actual surface station location to a radial distance prescribed by the value of "R1", the first guess wind field and surface observations are weighted equally. Once past the distance designated by "R1", the wind field is still affected by the surface observations. However, the weight of the first guess wind field decreases as a function of distance away from the surface station until the "RMAX1" distance is reached and the surface observation has no weight in the final wind field.

RMAX2 – Similar to RMAX1, but it is used for the wind field aloft. RMAX2 should be larger than RMAX1 due to the decreasing effect of surface friction and terrain features as height increases. Making RMAX2 larger provides more continuity in the upper levels as the drop off is not as sharp in the equal weighting and damping out of the surface observations and the first guess wind field.

R1 and R2 – R1 and R2 affect how the surface and upper air observations are blended into the Stage 1 winds. They define a radial distance to which the Stage 1 winds are equal in weight to the observed surface and upper air winds. The effect of R1 and R2 is to reintroduce the observations where they exist, but not have them erase the terrain effects created during the Stage 1 processing. By selecting large R1 and R2 values, it essentially negates the Stage 1 terrain adjustments.

MODEL EVALUATION

The NDDH[18] conducted a limited model evaluation study for the year 2000 with hourly emissions data

available for that year and meteorological data from hourly surface observations and twice-daily balloon sounding data. Hourly SO_2 observations from two monitors, Dunn Center and Theodore Roosevelt National Park - South Unit, were used in the model evaluation analysis. The evaluation study was repeated with the same hourly emissions and observed SO_2 data, but using the updated year 2000 RUC2 data. The purpose of the evaluation study was to demonstrate that the evaluation results would be at least as good as those without the benefit of the MM5 data, showing predictions at or above observations.

Although all major point sources within 250 km were modeled by NDDH, local minor sources and mobile source emissions were not included in the modeling. It is important to consider a background concentration in the evaluation process because this procedure is required by EPA's Guideline on Air Quality Models[19]. The two monitors involved in the study are close to local, unmodeled sources. For example, statistics from the North Dakota Department of Transportation[20] show that an average of 3,000 vehicles and 690 trucks travel I-94 near Dickinson and Theodore Roosevelt National Park – South Unit every day.

The annual average concentration for SO_2 observations at TRNP South Unit and Dunn Center for the year 2000 are 2.1 and 3.4 $\mu g/m^3$, respectively, if one assumes that when the value is non-detectable, it is half the detection limit (which may be an underestimate). Natural background levels of SO_2 are difficult to estimate due to the thresholds of monitoring instruments. A search of references that discuss this issue provide the following comments:

- Background levels of SO_2 in the ambient air are as low as 1 part per billion[21] (ppb), or 2.6 $\mu g/m^3$.
- Sources of atmospheric sulfur dioxide are 30% (by mass) anthropogenic and 70% natural (from biological decay on land and in the oceans, sea spray, and from volcanic activity)[22].
- A significant contributor of on-land decay are peat bogs, which are numerous in North Dakota and are the basis for lignite formation[23]. The area of the "prairie potholes" that comprise the wetland regions where the peat bogs exist cover much of the state of North Dakota.

Due to the presence of important natural sources of SO_2 as well as unmodeled SO_2 emissions, we recommend an unmodeled background of 2 $\mu g/m^3$ for SO_2. This value is still below the detection limit of the monitors and is lower than the computed annual average, even assuming that nondetects are assigned half the detection limit.

The results of adding a natural background of 2 $\mu g/m^3$ to the NDDH modeled predictions and the RUC2 modeled predictions for the year 2000 are shown in Figures 16 through 23. The results of the evaluation show the RUC2 data are acceptable because the predictions match closely with the observed data or over-predict slightly. To determine the ratio of over prediction in each graph, the top ten predicted concentrations were divided by the top ten observed concentrations. The geometric mean of the ratios were calculated for comparison purposes. Table 6 lists the geometric mean[24] of the ratios for each receptor and averaging period. The NDDH model concentrations are 25-35% higher than the observed concentrations at Dunn Center and 60-70% higher at TRNP-South Unit. The RUC model concentrations are less than 15% higher than the observed concentrations at Dunn Center and less than 25% higher at TRNP – South Unit. Overall, the NDDH modeling results are 20% higher than the RUC2 modeling results at Dunn Center and 40% higher at TRNP-South Unit.

Table 6. Geometric mean of the ratio of the top ten concentrations.

		Dunn Center	TRNP – South Unit
3-hour	NDDH/Observed	1.35	1.61
	RUC/Observed	1.13	1.16
24-hour	NDDH/Observed	1.25	1.70
	RUC/Observed	1.06	1.24

Figure 16: NDDH CALPUFF Predicted + 2 ug/m³ Background vs TRNP-SU Observed (3-hour)

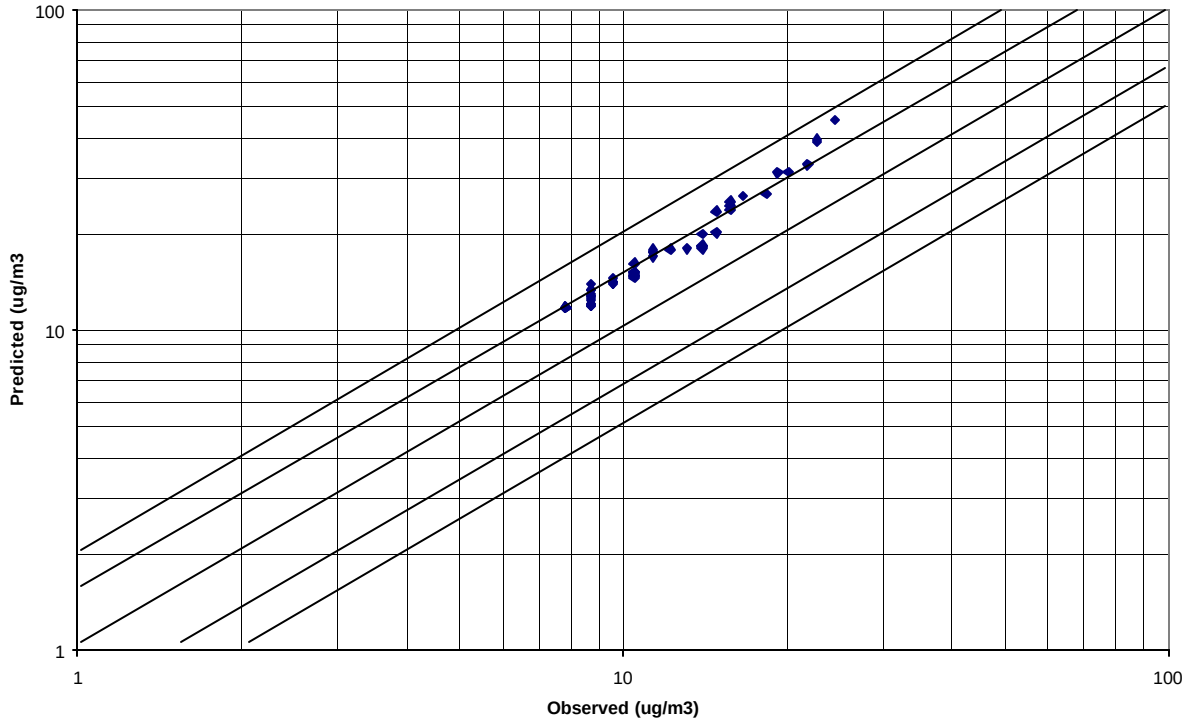

Figure 17 - RUC CALPUFF Predicted + 2 ug/m³ Background vs. TRNP - South Unit (3-hour)

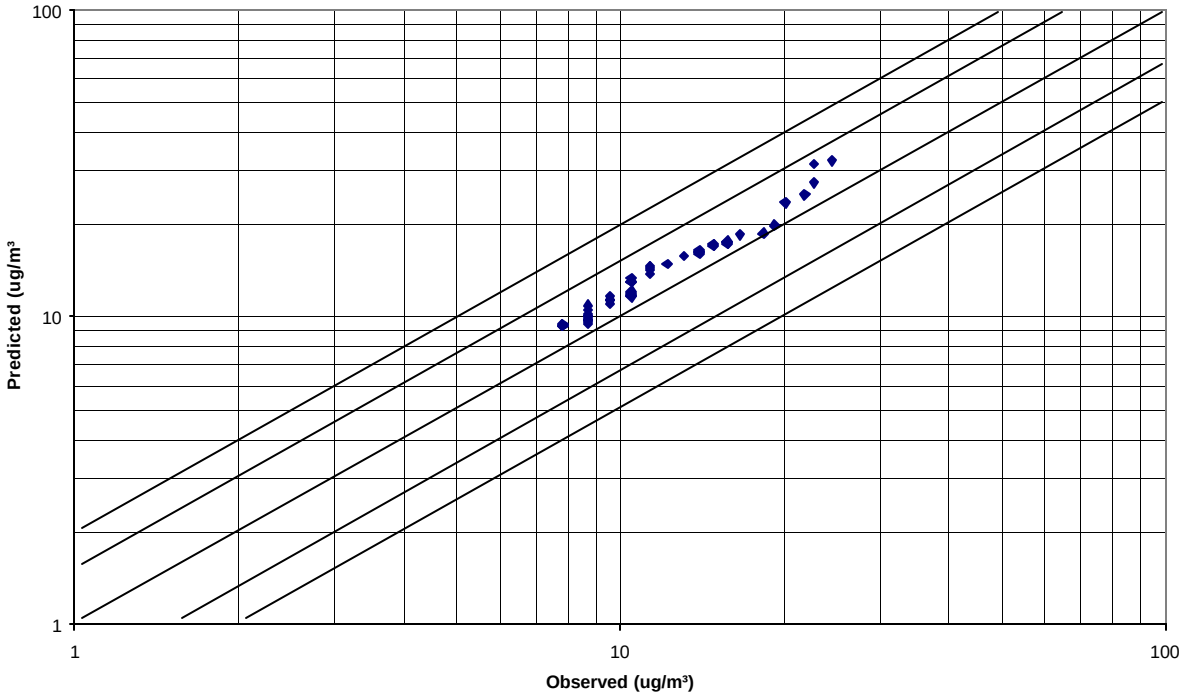

Figure 18: NDDH CALPUFF Predicted + 2 ug/m³ Background vs Dunn Center Observed (3-hour)

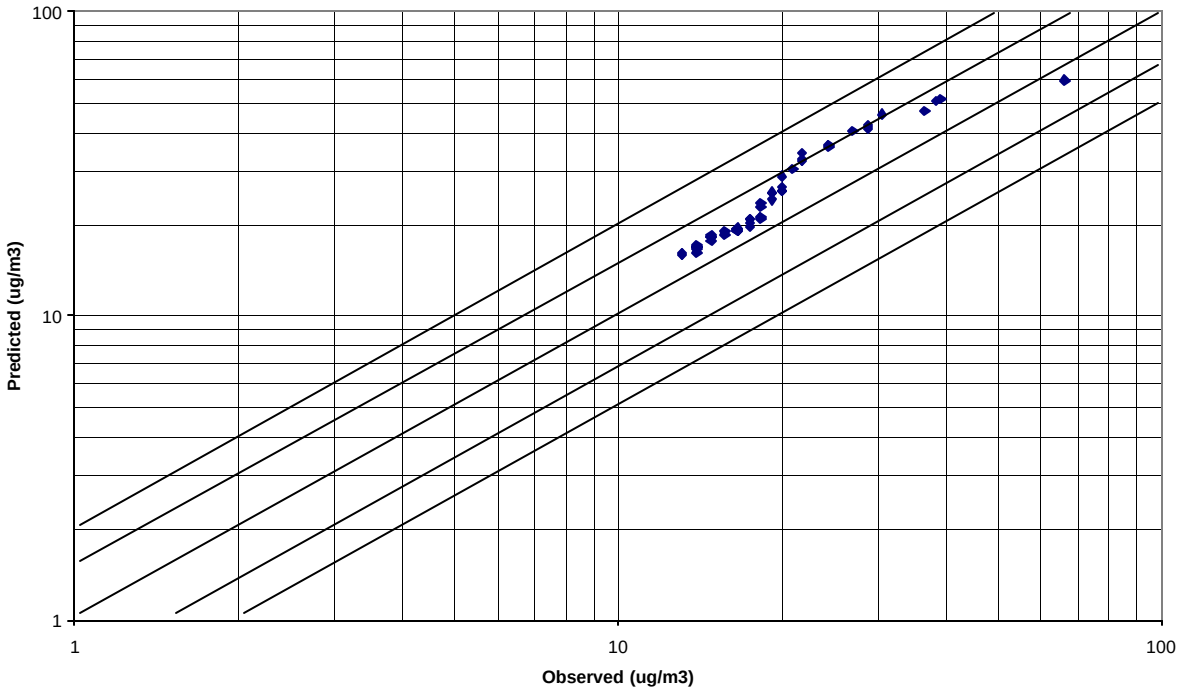

Figure 19 - RUC CALPUFF Predicted + 2 ug/m³ Background vs. Dunn Center Observed (3-hour)

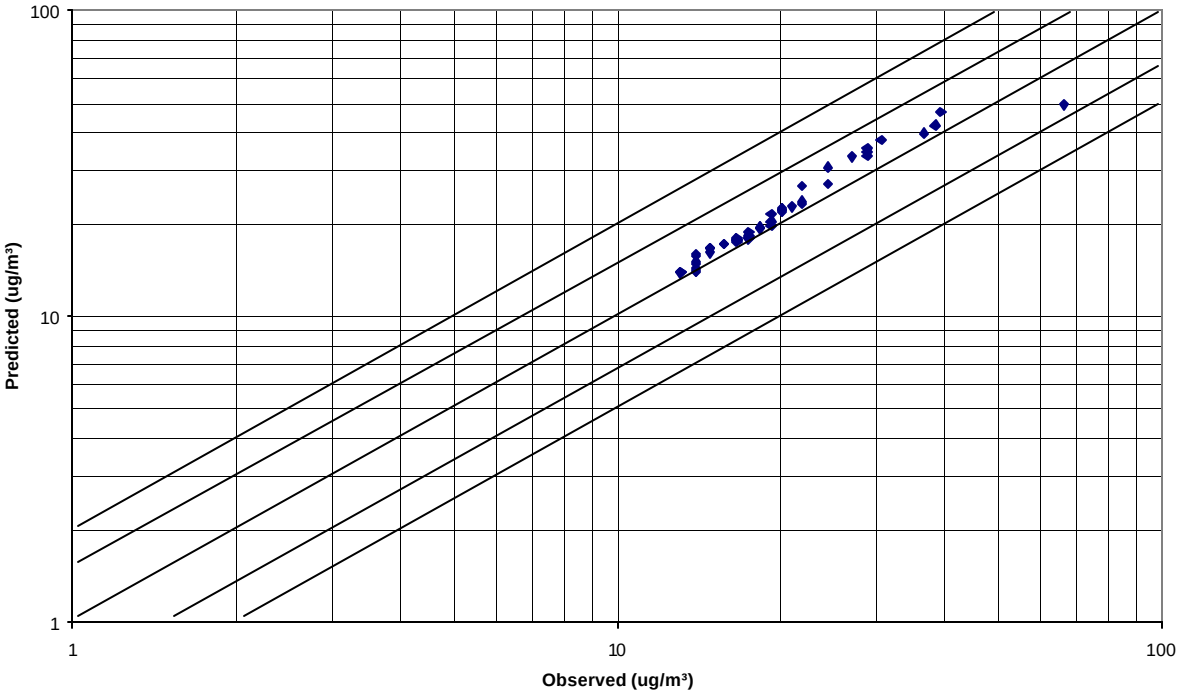

Figure 20: NDDH CALPUFF Predicted + 2 ug/m³ Background vs TRNP-SU Observed (24-hour)

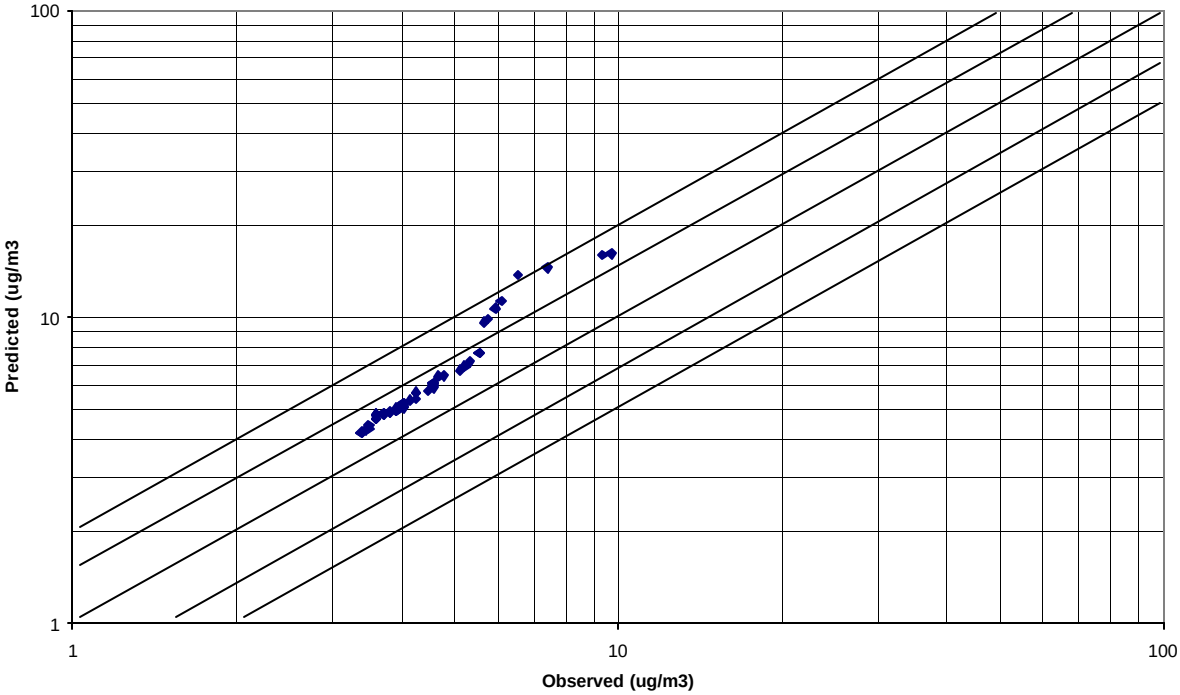

Figure 21 - RUC CALPUFF Predicted + 2 ug/m³ Background vs. TRNP - SU Observed (24-hour)

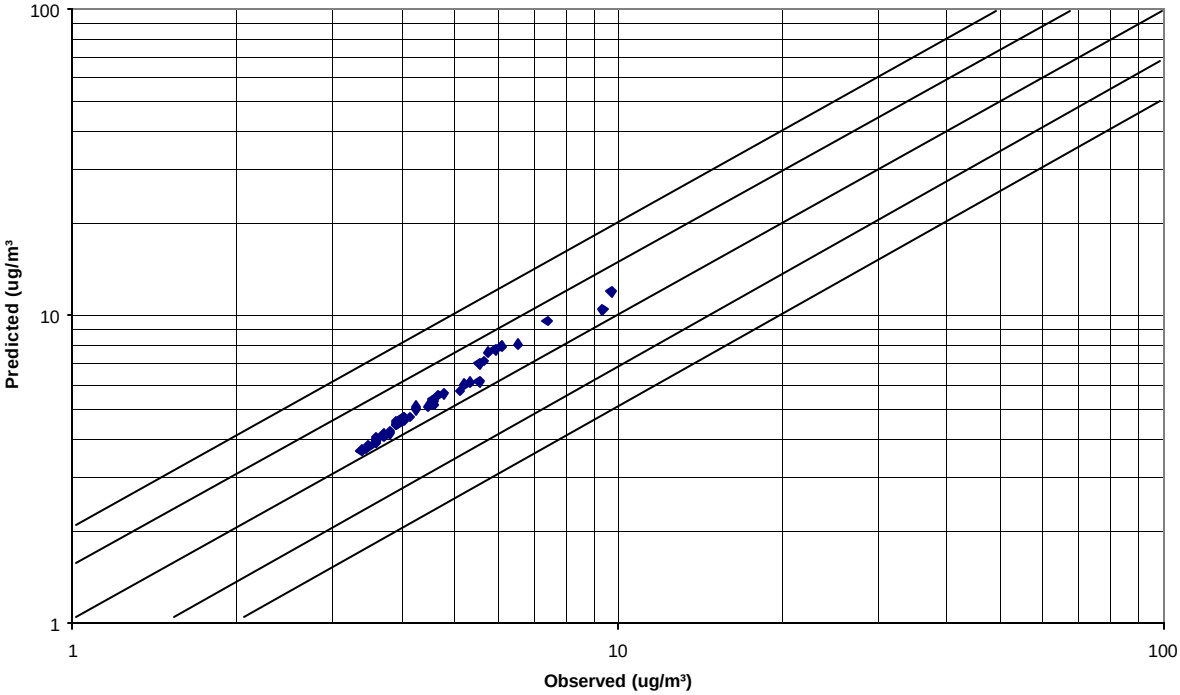

Figure 22: NDDH CALPUFF Predicted + 2 ug/m³ Background vs Dunn Center Observed (24-hour)

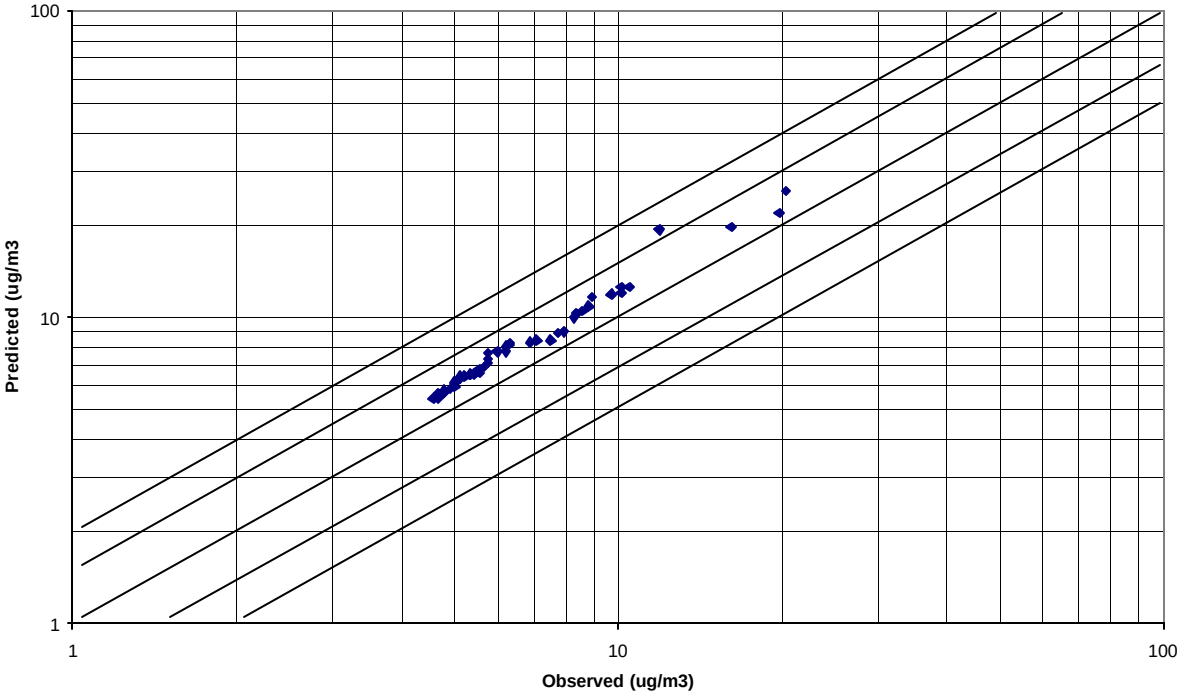

Figure 23 - RUC CALPUFF Predicted + 2 ug/m³ Background vs. Dunn Center Observed (24-hour)

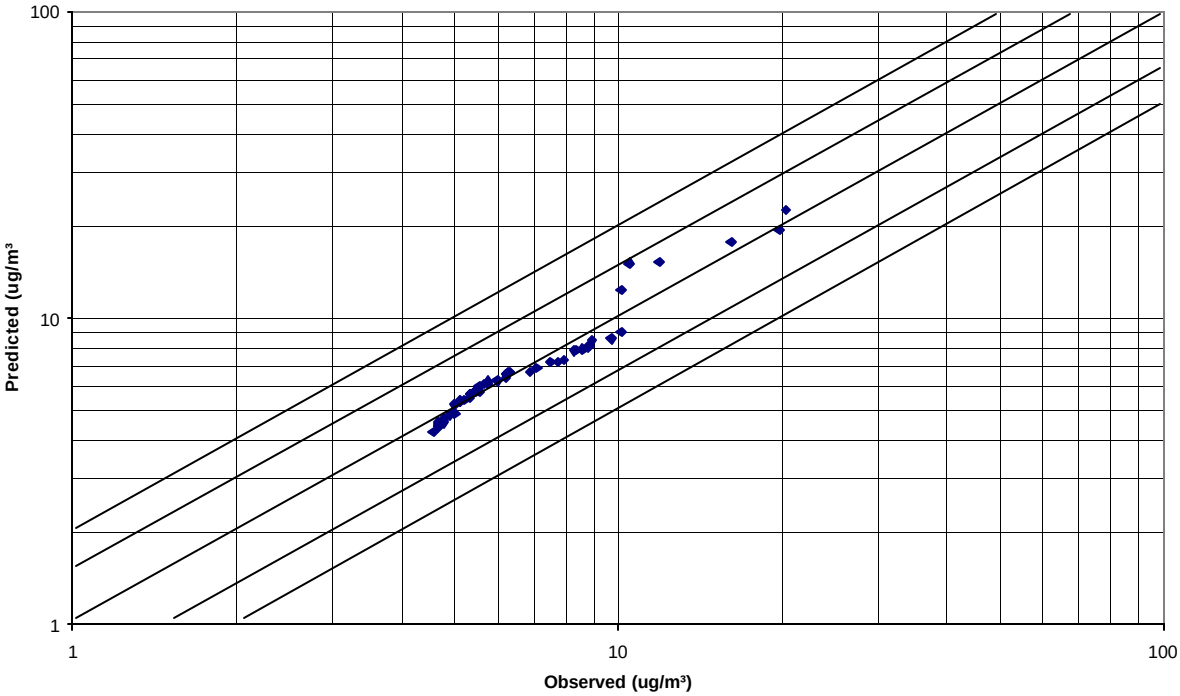

CONCLUSIONS

EPA has recommended the use of initialization wind data from National Weather Service (NWS) prognostic forecast techniques in the CALPUFF dispersion model, such as the RUC2. At the 7th Modeling Conference in June, 2000, the use of prognostic data in CALPUFF was discussed at length. The three-dimensional RUC2 data are a valuable resource that can improve the way dispersion models characterize wind fields and disperse plumes. One concern with using prognostic data is that any bias in the data is carried over to the dispersion modeling. In this example, the RUC2 data were compared with the Bismarck balloon soundings. The results compared well within the tolerances of the instrumentation.

IWAQM found that the CALPUFF model tends to over predict beyond 100 kilometers, but the use of the prognostic data improved the wind fields and consequently the CALPUFF modeling results. We found that at the more distant monitor (TRNP – South Unit), the CALPUFF model overover prediction with traditional data is 60-70% for the short-term concentrations (top 10 values). This significant over prediction tendency is mitigated to some extent (to be less than 25%) with the use of the RUC2 data. The evaluation results reflect IWAQM's findings in that the results improved with the use of the RUC2 data but that significant over prediction is possible at a distance of 200 kilometers. The RUC2 data's lower wind speeds tended to be somewhat higher than the Bismarck data, allowing for less stagnation and more dilution resulting in lower concentrations for the evaluation. The CALPUFF modeling with the RUC2 data still over-predicts compared to observations, such that it is still protective of air quality.

REFERENCES

1. CALPUFF Dispersion Model (Version 5.4). http://www.epa.gov/scram001 (under 7th Modeling Conference link to Earth Tech web site). (accessed December 2000).

2. Interagency Workgroup on Air Quality Modeling. *Interagency Workgroup On Air Quality Modeling (IWAQM) Phase 2 Summary Report and Recommendations for Modeling Long Range Transport Impacts*. EPA-454/R-98-019. (December, 1998).

3. Benjamin, S.G., J.M. Brown, K.J. Brundage, B.E. Schwartz, T.G. Smirnova, and T.L. Smith. RUC-2 - The Rapid Update Cycle Version 2 (Technical Procedures Bulletin – draft). http://maps.fsl.noaa.gov/ruc2.tpb.html. (accessed February 2003)

4. MM5 Community Model. http://www.mmm.ucar.edu/mm5/overview.html (accessed April 2003).

5. ARPS Webpage. http://www.caps.ou.edu/ARPS/arpsoverview.html (accessed April 2003)

6. Bratseth, A.M. Statistical interpolation by means of successive corrections. *Tellus, 38A*, 439-447. (1986).

7. National Oceanographic and Atmospheric Administration. GOES-East/West Satellite Derived Wind Product. http://orbit-net.nesdis.noaa.gov/goes/winds/ (accessed February 2003).

8. National Oceanographic and Atmospheric Administration. Radar Operations Center NEXRAD WSR-88D. http://www.osf.noaa.gov/ (accessed February 2003).

9. WSI Corporation. Sample NEXRAD Azimuth Wind Display for Bismarck, ND. www.wsi.com. (accessed November 2002).

10. National Oceanographic and Atmospheric Administration. Radar Operations Center NEXRAD WSR-88D. http://www.roc.noaa.gov/maps.asp (accessed November 2002).

11. Michelson, S.A. and N.L. Seaman. Assimilation of NEXRAD-VAD Winds in Summertime Meteorological Simulations over the Northeastern United States. *J. App. Met. 39*: 367-383. (2000).

12. USEPA. Verbatim transcripts from the EPA Seventh Conference on Air Quality Modeling. Volume II (June 29, 2000). http://www.epa.gov/scram001/7thconf/information/proc6-29.pdf (accessed February 2003).

13. National Oceanographic and Atmospheric Administration. Experimental Aircraft Data Display. http://acweb.fsl.noaa.gov/may_01_coverage/data/may23_lvl1.gif (accessed February 2003).

14. National Oceanographic and Atmospheric Administration. NOAA Forecast Systems Laboratory Demonstration Division Home Page http://www.profiler.noaa.gov/jsp/index.jsp (accessed February 2003).

15. Personal Communication from John Irwin of EPA to Steve Weber of North Dakota Department of Health. (November 26, 2002).

16. Office of the Federal Coordinator of Meteorology. *Federal Meteorological Handbook #3, Rawinsonde and Pibal Observations.* FCM-H3-1997. (May, 1997).

17. Environmental Protection Agency. *Meteorological Monitoring Guidance for Regulatory Modeling Applications.* EPA-454/R-99-005. (February, 2000).

18. North Dakota Department of Health. *Evaluation of CALPUFF Model Performance Using Year 2000 Data.* (November, 2001).

19. Environmental Protection Agency. *Appendix W to Part 51 - Guideline on Air Quality Models.* 40CFR51. http://www.epa.gov/scram001/guidance/guide/appw_01.pdf, (accessed January 2003).

20. North Dakota Marketing Website. http://www.ag.ndsu.nodak.edu/ced/resources/farmranch/section3.htm (accessed February 2003).

21. Minnesota Pollution Control Agency Website. http://www.pca.state.mn.us/air/emissions/so2.html (accessed February 2003).

22. Manahan, Stanley. *Environmental Chemistry*. Northern Arizona University. http://jan.ucc.nau.edu/~doetqp-p/courses/env440/env440_2/lectures/lec41/lec41.htm (accessed February 2003).

23. Environmental Protection Agency. *EPA Region 1 Student Center*. http://www.epa.gov/region01/students/pdfs/wetaccp2.pdf (accessed February 2003).

24. Giese, B. Arithmetic Mean, Harmonic Mean, Combined Average, Geometric Mean. http://people.ne.mediaone.net/delilama/dc_mean.html, accessed January 2002.

KEYWORDS

CALPUFF

Prognostic Meteorological Model

RUC Model

APPENDIX C

RUC40 AND RUC20 INFORMATION FROM THE FORECAST SYSTEMS LABORATORY

RUC-2 - The Rapid Update Cycle Version 2

Technical Procedures Bulletin - draft

Stanley G. Benjamin, John M. Brown, Kevin J. Brundage, Barry E. Schwartz, Tatiana G. Smirnova, and Tracy L. Smith

NOAA/ERL Forecast Systems Laboratory, Boulder, CO

Lauren L. Morone

Environmental Modeling Center, National Centers for Environmental Prediction, Camp Springs, MD

Revised 31 Mar 98, a few small updates. Change log link added 16 June 1998. Use of tropical storm reconnaissance data added 31 Aug 98.

ABSTRACT - Summary of RUC-2 vs. RUC-1 differences
Horizontal and vertical domain
Data assimilated
Assimilation frequency
Model physics
Surface analyses/forecasts
Variables available
Output formats available
Verification stats for 40km MAPS vs. 60km MAPS and 48km Eta

Change log for operational RUC-2 running in real-time at NCEP

To RUC/MAPS homepage, including real-time images

1. INTRODUCTION AND HISTORY

A number of significant weather forecasting problems exist in the 0-12 hour range, including severe weather in all seasons (tornadoes, severe thunderstorms, crippling snow and ice storms) and hazards to aviation (clear air turbulence, icing, downbursts). Accurate short-term forecasts are clearly indispensable for the protection of life and property, but they also have tremendous economic value even under non-threatening conditions, for example, for agriculture and the recreation and power-generation industries. The Rapid Update Cycle (RUC) was designed to provide accurate numerical forecast guidance for weather-sensitive users for the next 12 hour period. The RUC runs at the highest frequency of any forecast model at the National Centers for Environmental Prediction (NCEP), assimilating recent observations aloft and at the surface to provide very high frequency updates of current conditions and short-range forecasts using a sophisticated mesoscale model.

This bulletin describes a new version of the RUC, called RUC-2, implemented at NCEP in April 1998. The RUC-2 produces new 3-d analyses and short-range forecasts every hour, compared to the 3-h updating in RUC-1. The original Rapid Update Cycle (RUC-1, Benjamin et al. 1994a (TPB) ,1994b) was implemented in September 1994 at NCEP. Some number of smaller changes were made to RUC-1 over the 1995-1996 period, but the RUC-2 is a significant advance over RUC-1, not just in assimilation frequency, but also in resolution, types of data assimilated, and model physics. These changes (summarized in the TPB Abstract) allow the RUC-2 to more accurately represent significant weather systems across the United States in all seasons.

Rapid Update Cycle - Present and Next Version **Summary of characteristics in RUC-2 compared to RUC-1.** Also see the TPB Abstract.

Uses of the RUC

- **Explicit use of short-range forecasts** - The RUC forecasts are unique in that they are initialized with very recent data. Thus, the majority of the time, the most recent RUC forecast has been initialized with more recent data than the other forecast model runs available. Even at 0000 and 1200 UTC, when other model runs are available, the RUC forecasts are useful for comparison over the next 12-h since they have some unique aspects regarding the isentropic coordinate, hourly data assimilation, and model physics.
- **Monitoring current conditions with hourly analyses** - Hourly analyses are particularly useful when overlaid with hourly satellite and radar images, or hourly observations such as from surface stations or profilers.
- **Evaluating trends of longer-range models** - RUC-2 analyses and forecasts are useful to confirm (or call into question) the short-term predictions of the Eta, NGM, and AVN models. This is often helpful in establishing which of the 48-72-h models is verifying most accurately in the first 12-h period.

Some key users of the RUC

- Aviation Weather Center/NCEP, Kansas City, MO
- Storm Prediction Center/NCEP, Norman, OK
- NWS Weather Forecast Offices
- FAA/DOT, including use for air traffic management and in ITWS

2. DOMAIN, RESOLUTION, TERRAIN FOR RUC-2

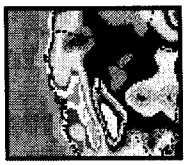

2.a. Domain

The RUC-2 domain (Fig.1a) is on a Lambert conformal projection matching that used for the AWIPS 212 NWS distribution grid. The mesh is rectangular on this projection, and its size is 151 by 113 grid points (compared to 81x62 for RUC-1 (Fig.1b)). The grid length is 40.635 km at 35 deg N. Due to the varying map-scale factor from the projection, the actual grid length in RUC-2 varies from about 40.6 km at 35 deg N to 33 km at the north boundary. The grid length is about 38 km at 43 deg N.

The RUC-2 domain was designed to:

- provide higher horizontal resolution than RUC-1
- move the lateral boundaries slightly farther off the east and west coasts than in RUC-1 to improve coastal forecasts (a weakness of RUC-1)
- match the AWIPS 212 distribution grid to avoid interpolation and give field users the highest resolution possible.

The 40-km RUC-2 domain covers about 50% more area than the 60-km RUC-1 domain. It extends farther than the RUC-1 domain in all directions, but especially in the southeast, owing to use of the Lambert conformal projection and the need to cover slightly east of the state of Maine. It covers considerably more oceanic areas than the RUC-1 domain.

The RUC-2 latitude/longitude at each point in an ASCII file can be downloaded from http://maps.fsl.noaa.gov/MAPS.domain.html. The lower left corner point is (1,1), and the upper right corner point is (151,113), as shown in the table below.

RUC-2 point	AWIPS-212 point	Latitude	Longitude
(1,1)	(23,7)	16.2810 N	126.1378 W
(1,113)	(23,119)	54.1731 N	139.8563 W
(151,1)	(173,7)	17.3400 N	69.0371 W
(151,113)	(173,119)	55.4818 N	57.3794 W

RUC-2 domain parameters

2.b. Horizontal resolution

Horizontal resolution in RUC-2 is 40 km compared to 60 km for the RUC-1. The higher resolution allows considerable improvement in resolution of topography and also in shapes of coasts and lakes. These improvement improve the ability of the RUC-2 to resolve local circulations and orographic precipitation patterns. Because the RUC-2 model has less internal smoothing than the Eta or NCAR/Penn State MM5 models, these features tend to be fairly well depicted considering its 40-km resolution.

2.c. Vertical resolution

The RUC-2 has 40 vertical levels compared to 25 levels in RUC-1. The RUC-2 continues to use a generalized vertical coordinate configured as a hybrid isentropic-sigma coordinate in both the analysis and model. This coordinate has proven to be very advantageous in RUC-1 in providing sharper resolution near fronts and the tropopause (e.g., Benjamin 1989, Johnson et al. 1993, Zapotocny et al. 1994). Some of the other advantages include:

- All of the adiabatic component of the vertical motion on the isentropic surfaces is captured in flow along the 2-d surfaces. Vertical advection, which usually has somewhat more truncation error than horizontal advection, does much less "work" in isentropic/sigma hybrid models than in quasi-horizontal coordinate models. This characteristic results in improved moisture transport and very little precipitation spin-up problem in the first few hours of the forecast.
- Improved conservation of potential vorticity. The potential vorticity and tropopause level (based on the 2.0 PV unit surface) show very good spatial and temporal coherence in RUC-2 grids.
- Observation influence in the RUC-2 analysis extends along isentropic surfaces, leading to improved air-mass integrity and frontal structure.

A sample cross section of RUC-2 native levels is displayed in Fig. 2. The cross-section is across the United States, passing south of San Francisco, through Boulder (where a downslope windstorm occurred that morning) and through southern Virginia on the East Coast. The cross section is for a 12-h forecast valid at 1200 UTC 30 November 1995.

The typical RUC-2 resolution near fronts is apparent in this figure, as well as the tendency for more terrain-following levels to "pile up" in warmer regions (the eastern part of the cross section, in this case). The hybrid isentropic-sigma coordinate is defined by a 20-line section of code in both the analysis and forecast model. The rest of the code treats the analysis/model processes as a generalized vertical coordinate. The 20-line section of code can be changed to define a pure sigma terrain-following coordinate and has been tested in this mode.

In the RUC-2 (as well as in RUC-1), analysis/model levels which are isentropic in part of the domain can become terrain-following in other parts, as shown in Fig. 2. A reference potential temperature is assigned to each of the 40 levels (Table 1).

Table 1. RUC-2 reference potential temperatures

224.	232.	240.	245.	250.	255.	260.	265.
270.	274.	278.	282.	286.	290.	294.	297.
300.	302.	304.	306.	308.	310.	312.	314.
316.	318.	320.	322.	325.	328.	331.	334.
337.	341.	347.	355.	364.	375.	400.	450.

The prespecified pressure spacing in RUC-2, starting from the ground is 2, 5, 8, and 10 mb, followed by as many 15-mb layers as are needed. (Near-surface pressure spacing in RUC-1 was 20 mb.) This terrain-following spacing compacts somewhat as the terrain elevation increases. Excellent resolution of the boundary layer is provided in all locations, including over higher terrain. The lowest atmospheric level in RUC-2 is set at 5 m above the model terrain height. The effects of this choice are discussed in the analysis and model sections, but since the RUC-2 has an explicit level actually *at* the surface, no extrapolation from higher levels is necessary to diagnose values at the surface. The minimum potential temperature spacing occurs through much of the troposphere and is 2 K instead of 4 K as in RUC-1. The top level in RUC-2 is at 450 K as opposed to 410 K in RUC-1. Overall, the vertical resolution is somewhat higher both in the boundary layer and free atmosphere, and the domain extends farther into the stratosphere.

2.d. Terrain

The most obvious difference, of course, between terrain in RUC-2 (Fig. 3a) and that in RUC-1 (Fig. 3b) is that finer-scale topographical features are distinct in the RUC-2 terrain. RUC-2 analyses and forecasts can depict many significant topographically induced features, including mountain/valley circulations, mountain waves, sea breezes, and orographic precipitation patterns. The surface elevation of the RUC-2 is defined by a "slope envelope" topography instead of the previous full envelope topography used in RUC-1. The envelope topography is defined by adding the sub-grid-scale terrain standard deviation (calculated from a 10-km terrain field) to the mean value over the grid box. In the slope envelope topography, the terrain standard deviation is calculated with respect to a plane fit to the high-resolution topography within each grid box. This gives more accurate terrain values, especially in sloping areas at the edge of high-terrain regions. It also avoids a tendency of the standard envelope topography to project the edge of plateaus too far laterally onto low terrain regions. Using the slope envelope topography gives

lower terrain elevation at locations such as Denver and Salt Lake City which are located close to mountain ranges. The RUC-2 topography at each point in an ASCII file can be downloaded from http://maps.fsl.noaa.gov/MAPS.domain.html.

3. ANALYSIS METHOD FOR RUC-2

3.a. Data assimilated

The new data sets assimilated in the 40-km RUC-2 include:

- VAD wind profiles
- high-resolution ascent-descent aircraft reports
- ship reports
- GOES integrated precipitable water retrievals
- SSM/I integrated precipitable water retrievals
- GOES high-density cloud drift winds
- tropical storm dropwindsonde data - reconnaissance

These new data sets already assimilated in the experimental 40-km RUC/MAPS at FSL will also be ingested into the RUC-2 as soon as available at NCEP:

- boundary-layer (915 MHz) profiler winds
- RASS (Radio Acoustic Sounding System) temperatures

Satellite-based precipitable water retrievals and cloud-drift winds are currently used only over water points. Satellite observations over land will be ingested in the near future. Wind profiler, rawinsonde, aircraft, and surface (land and buoy) observations continue to be utilized in the RUC-2, as they were for RUC-1, except that the wind profiler and rawinsonde data are used with higher vertical resolution due to the 40 levels in RUC-2. Here is a summary of the actual measurements used from other data sets:

- Rawinsonde/dropwindsonde - temperature, height, moisture, wind
- Aircraft - wind, temperature
- Surface - wind, temperature, dewpoint, altimeter setting

More information on the use of wind data in RUC-2 is available in Smith and Benjamin (1998).

3.b. Optimum interpolation analysis

The optimal interpolation multivariate analysis used in RUC-1 has been substantially modified for the RUC-2, providing, among other things, closer fit to observations, better use of aircraft ascent/descent winds and temperatures, and greater efficiency. A discussion of optimal interpolation analysis in isentropic coordinates is provided in Benjamin (1989).

Sequence in RUC-2 analysis

- Read in observations
- Subject to gross quality control (range limits, wind shear, lapse rate)
- Read in background (previous 1-h forecast, if available). RUC-2 will "cold start" with Eta forecast background if RUC-2 has not been running within last 12 hours.

  This background field is defined at the (x,y,p) points of the hybrid coordinate surfaces for the

background field. The quality control and analysis steps below are carried out at these (x,y,p) points. This will result in changes to virtual potential temperature at these points. For the RUC-2, the next-to-last step (bullet) is in effect a repositioning of the coordinate surfaces to correspond to the results of the analysis steps that preceed it.

- Perform precipitable water analysis and modify background moisture values according to precipitable water observations (currently -- GOES and SSM/I, future - GPS). In this precipitable water "pre-analysis", the shape of the water vapor mixing ratio in the background grid field is left intact, but is either moistened or dried out according to the observations. (See Benjamin et al. 1998 - GPS precipitable water paper, NWP conference.)
- Perform buddy-check quality control. Flag suspicious observations. (See quality control section below.)
- Calculate super-observations. This procedure combines observations that are near to each other in space. It prevents against the possibility of ill-conditioned matrices in the optimum interpolation analysis.
- Multivariate z/u/v analysis at all levels. A level-dependent partial geostrophic constraint is applied, weakest at the surface and in the boundary layer. The wind analysis is anisotropic and oriented along the flow, according to the geostrophically derived horizontal covariances of forecast error (Benjamin 1989).
- Height analysis increment (z') calculated in last step is vertically differentiated to obtain a temperature increment. This temperature increment is added to the temperature field. Now the temperature (virtual potential temperature) background is an updated field which has taken into account the height observations and wind observations through the partial geostrophic constraint.
- Calculate surface pressure increment from multivariate z' increment at surface. This provides an updated background field for the univariate surface pressure analysis a few steps down. The height analysis is essentially ignored from this step on, since a hydrostatic integration will occur at the end of the analysis to calculate heights.
- Perform univariate temperature (theta-v) analysis at all levels using temperature observations. Now the direct temperature observations (e.g., surface, aircraft, rawinsonde, RASS) have also been incorporated.
- Perform univariate wind analysis at lowest 5 levels. This analysis uses the result of the previous multivariate analysis as its background. This step forces close matching to surface wind observations. No geostrophic constraint is applied at this step.
- Perform univariate analysis for pressure at surface. This step forces close fitting to surface pressure observations (calculated through the altimeter setting).
- Perform univariate moisture (condensation pressure) analysis at all levels. The moisture variable stored in RUC-2 is water vapor mixing ratio, but inside the RUC-2 analysis, values are converted to condensation pressure, since this variable varies with fewer orders of magnitude over the depth of the troposphere than water vapor mixing ratio.
- All calculations up to this point have been done to change values at the (x,y,p) points of the background field. The exact same procedure could have been applied to a background from a sigma or eta coordinate model. In the case of the RUC-2, we adjust (vertically interpolate) these values to the hybrid isentropic-sigma coordinates.
- Hydrostatic integration to recalculate z (height) at all levels. Thus, the RUC-2 mass field changes are all made through the virtual potential temperature field at all levels and the surface pressure field. The height observations influence these fields, as described above.
- Diagnose other variables from analysis - e.g., special levels such as freezing level, maximum wind level, tropopause level...

The RUC-2 analysis provides de facto analyses of cloud variables and soil variables by using the previous 1-h forecast of these variables as initial conditions for the next run. Although use of

observations will later provide improved fields for these variables (e.g., Kim and Nychka 1998), this "cycling" provides substantial improvement over zero initial clouds and climatology for soil variables.

3.c. Incorporation of the surface analysis within the 3-d analysis

With the 1-h assimilation cycle, the RUC-2 integrates into one system the RUC-1 and RSAS (RUC Surface Analysis System) from the 60-km era. The RUC-2 surface analyses are improved over those from RUC-1 due to the use of a forecast background combined with new design features to ensure that the 40km surface analyses not only draw more closely to the data, but also have better consistency and reliability. Specific advantages of RUC-2 surface analyses over those from RUC-1 are:

- use of a forecast background rather than persistence
- multivariate/univariate two-pass analysis for winds/pressure instead of a single-pass univariate analysis
- consistency in data-void regions with terrain-induced dynamics and surface physics in the 40-km version, allowing features of the background (forecast) fields such as mountain/valley circulations, drainage winds, effects of variations in soil moisture, vegetation type, land use, roughness length, snow cover, land/water contrast, and explicit clouds to be present in the analysis.
- improved quality control due to the forecast background. This is a fairly significant item, as the 60km QC led to frequent bullseyes that could only be eliminated by black-listing problematic stations
- lack of spurious temperature, moisture, and wind gradients at ocean or data-void boundaries.

The following new features are added to ensure that the 40km surface analyses draw very closely to surface data:

- All station pressure (altimeter) and surface wind observations are used regardless of the difference between station and model elevation. The pressure is reduced to the model elevation using the local lapse rate over the bottom 5 levels in the background field.
- Temperature and dewpoint observations are reduced, via the local lapse rate, from model terrain height to actual station elevation, provided, however, that the reduction does not exceed 70 mb. With this change and the higher-resolution 40km terrain, a far higher percentage (95%) of surface temperature and dewpoint observations in the western U.S. are used in the 40km 3-d analysis than in the 60km RUC-1 3-d analysis. Click here for a list of surface stations used in the RUC-2 at a particular time and the pressure separation between station pressure and model pressure for each.
- The surface wind analysis is performed in two passes, as noted earlier. The first pass is a multivariate wind/height analysis with weak geostrophic coupling since some correlation between the actual and geostrophic winds is expected at the surface, especially over water. The second pass uses the first pass as its background and is univariate, so that local details, particularly in the wind observations, are drawn for.
- Expected surface observation errors for the 40km RUC-2 (a parameter in the analysis) have been reduced from values in the 60km RUC to force closer fit to observations.
- Through use of a minimum topography field, surface temperature and dewpoint are diagnosed at close to the station elevation in both the RUC-1 and RUC-2. The minimum topography field is determined from a high-resolution 10km topography field, with the value for the grid box being the *minimum* 10km elevation, which is representative of valley elevations in rough terrain. The rationale is that surface stations in mountainous areas are usually located in valleys or open parks at lower elevation.
- The reduction from the model topography to the minimum topography is done using the model lapse rate limited to be between the dry adiabatic and isothermal.

Comparison of 60km RUC-1 and 40km RUC-2 surface temperature analyses for 1200 UTC 19 February 1997.

3.d. Quality control

As in RUC-1, quality control in RUC-2 involves a buddy check. The buddy check is of observation residuals, the differences betwen the observation and the background field interpolated to the observation point, and not of the observations alone. This is an important distinction, since it means that any known anomaly in the previous forecast has already been subtracted out, improving the sensitivity of the QC procedure to actual errors.

At each observation point, the parameter in question is estimated via optimum interpolation of values from surrounding observation points. If the estimated and measured values differ by more than a prescribed amount, further checks determine whether the central observation or one of its neighbors is erroneous.

Bird contamination for radar/profiler winds

Checks are made for bird contamination for both VAD and profiler winds in RUC-2. A careful check for bird (and other) contamination in profiler winds is made at the Profiler Hub in Boulder, CO. This check includes use of second-moment data to examine for likelihood of bird contamination. If the quality control flag produced by this check indicates suspicious data, the profiler data at that level is not used by RUC-2. For VAD winds, no second-moment data is available, so a cruder and more conservative check is made. A solar angle is calculated, and if the sun is down and the temperature is warmer than -2 deg C, VAD winds are not used if they have a northerly component between 15 August and 15 November or a southerly component between 15 February and 15 June.

3.e. Future improvements

A new 3-d variational analysis (Devenyi and Benjamin 1998) is nearing completion for the RUC-2 and will follow the rest of the RUC-2 into operations with a lag time of several months.

4. ONE-HOUR ASSIMILATION CYCLE FOR RUC-2

See also information on **1-h cycle and data used** for more differences.

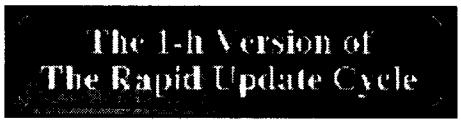

1-h assimilation cycle. The background for each analysis is the previous 1-h forecast. The 1-h cycle allows much more complete use of profiler, surface, and VAD data, which are all available at least hourly. The time window for aircraft data is now -1h to 0h instead of -2h to +1h, meaning that aircraft data are now applied closer to the time that they are actually reported.

Grids from RUC-2 will be available almost 1 hour earlier than those from RUC-1. The data cut-off time from the 40km system is 20 min after the analysis valid time. A catch-up cycle at 0000 and 1200 UTC runs at +55 min to catch late-arriving rawinsonde data. Twelve-hour forecasts from these times are run from the catch-up cycle analysis, rather than the "early look" analysis at 20 min after.

5. RUC-2 FORECAST MODEL

The RUC-2 forecast model is an updated version of the generalized vertical coordinate model described by Bleck and Benjamin (1993). Modifications to a 20-line section of code in the model are sufficient to modify it from the hybrid isentropic-sigma coordinate described in section 2.c to either a pure sigma or pure isentropic model.

The RUC-2 model is considerably different from the RUC-1 model in its parameterizations of physical processes such as cloud microphysics (stable precipitation), turbulent mixing, radiation, and convective precipitation. To some extent, this was made possible by changing the RUC-2 model to use the code structure of the NCAR/Penn State Mesoscale Model version 5 (MM5, Grell et al. 1994). This allowed relatively easy transfer of MM5 parameterizations (cloud microphysics, radiation) into the RUC-2 model, and will continue to do so in the future as new MM5 parameterizations are developed.

5.a. Basic dynamics/numerics Here are some of the basic numerical characteristics of the RUC-2 model:

- Arakawa-C staggered horizontal grid (Arakawa and Lamb 1977); u and v horizontal wind points offset from mass points to improve numerical accuracy.
- No vertical staggering.
- Time step is 60 seconds at 40-km resolution.
- Positive definite advection schemes used for continuity equation (advection of pressure thickness between levels) and for horizontal advection (Smolarkiewicz 1983) of virtual potential temperature and all vapor and hydrometeor moisture variables.

The atmospheric prognostic variables of the RUC-2 forecast model are:

- pressure thickness between levels
- virtual potential temperature
- horizontal wind components
- water vapor mixing ratio
- cloud water mixing ratio
- rain water mixing ratio
- ice mixing ratio
- snow mixing ratio
- graupel (rimed snow) mixing ratio
- number concentration for ice particles
- turbulence kinetic energy
- turbulent variance of potential temperature
- turbulent variance of water vapor mixing ratio
- turbulent covariance of potential temperature perturbations with water vapor mixing ratio perturbations

The soil prognostic variables (at six levels) of the RUC-2 forecast model are:

- soil temperature
- soil volumetric moisture content

Other surface-related prognostic variables are snow water equivalent moisture and snow temperature.

5.b. Physical parameterizations

Explicit cloud/moisture processes. The explicit microphysics from the NCAR/Penn State mesoscale model MM5 (level 4, Reisner et al. 1997) is used, with five hydrometeor species -- cloud water, rain water, snow, ice, graupel (mixing ratios for each) and also with an explicit prediction of ice particle number concentration. This improvement was made to provide improved forecasts of clouds, icing, and precipitation from RUC-2. In the 60km RUC-1, stable precipitation was defined simply by supersaturation removal, with no knowledge of cloud or ice processes. All of the cloud variables are cycled in the 40-km MAPS, meaning that there are initial cloud fields for each run. In the RUC-2 model, all six cloud variables are advected using the positive definite scheme of Smolarkiewicz (1983) on the isentropic-sigma levels with adaptive vertical resolution. The incorporation of this scheme into RUC-2 is described in detail by Brown et al. (1998).

Improved surface physics. The RUC-2 includes a 6-layer soil/vegetation/snow model (schematic) to improve forecasts of low-level conditions. Surface (shelter/anemometer level) forecasts are often critically dependent on accurate estimates of surface fluxes, and in turn, on reasonably accurate soil moisture and temperature estimates. The RUC-2 soil model contains heat and moisture transfer equations solved at 6 levels at each grid point together with the energy and moisture budget equations for the ground surface (Smirnova et al. 1997a,b). The heat and moisture budgets are applied to a thin layer spanning the ground surface and including both the soil and the atmosphere with corresponding heat capacities and densities. A treatment of the evapotranspiration process, developed by Pan and Mahrt (1987), is implemented in the MAPS/RUC soil/vegetation scheme.

In the presence of snow cover, snow is considered to be an additional upper layer of soil that interacts with the atmosphere, significantly affecting its characteristics (Smirnova et al 1998).

The snow model contains a heat-transfer equation within the snow layer together with the energy and moisture budget equations on the surface of the snow pack. This budget is applied to the entire snow layer if the snow depth is less than a threshold value, currently set equal to 7.5 cm, or to the top 7.5 cm layer of snow if the snow pack is thicker. Snow evaporates at a potential rate unless the snow layer would all evaporate before the end of the time step. In this case the evaporation rate is reduced to that which would just evaporate all the existing snow during the current time step. A heat budget is also calculated at the boundary between the snow pack and the soil, allowing melting from the bottom of the snow layer. Melting at the top or bottom of the snow layer occurs if energy budgets produce temperatures higher than the freezing temperature (0 deg C). In this case the snow temperature is set equal to the freezing point, and the residual from the energy budget is spent on melting snow. Water from melting snow infiltrates into the soil, and if the infiltration rate exceeds the maximum possible value for the given soil type, then the excess water becomes surface runoff.

The accumulation of snow on the ground surface is provided by the microphysics algorithm of the MAPS/RUC forecast scheme (Reisner et al. 1997, Brown et al. 1998). It predicts the total amount of precipitation and also the distribution of precipitation between the solid and liquid phase. The subgrid-scale ("convective") parameterization scheme also contributes to the liquid precipitation. With or without snow cover, the liquid phase is infiltrated into the soil at a rate not exceeding maximum infiltration rate, and the excess goes into surface runoff. The solid phase in the form of snow or graupel is accumulated on the ground/snow surface and is unavailable for the soil until melting begins. The RUC-2 surface package provides surface temperature and dewpoint forecasts that are clearly superior to those of the RUC-1 due to improved surface heat and moisture fluxes. The soil temperature and moisture has been evolving since 29 April 1996, leading to fairly accurate estimates of these fields, certainly much better than climatology (Smirnova et al. 1997b). Real-time estimates of soil moisture in the top 2 cm are available on the MAPS/RUC home page, http://maps.fsl.noaa.gov.

Atmospheric radiation. The MM5 atmospheric radiation package (Dudhia 1989, Grell et al. 1994) is

used in the RUC-2, with additions for attenuation and scattering by all hydrometeor types. This scheme is a broadband scheme with separate components for longwave and shortwave radiation. In the RUC-1, there was no atmospheric radiation at all, only a surface radiation budget with clouds diagnosed from relative humidity. The solar flux at the top of the atmosphere is now variable, taking into account the elliptical orbit of the earth around the sun.

Turbulent mixing. In RUC-2, turbulent mixing at all levels, including the boundary layer, is prescribed the explicit turbulence scheme of Burk and Thompson (1989). This scheme is a level-3.0 scheme, with explicit forecast of turbulent kinetic energy and three other turbulence variables, replacing the Mellor-Yamada level-2.0 scheme in RUC-1. The surface layer mixing continues to be prescribed by Monin-Obukhov similarity theory, specifically the three-layer scheme described in Pan et al. (1994).

With the Burk-Thompson scheme, the RUC-2 forecasts TKE amounts of 5-20 J/kg in the boundary layer, and also forecasts TKE maxima aloft, typically localized in frontal zones, corresponding to estimated areas of clear-air turbulence potential.

Convective parameterization. A version of the Grell (1993) convective parameterization is used, updated from that used in the RUC-1, including fixes to downdraft detrainment, calculation of cloud top, minimum cloud depth, and capping criteria. This version gives somewhat larger amounts of precipitation and more coherent patterns in convective areas than the RUC-1 version.

The inclusion of downdrafts in the Grell scheme results in smaller-scale details in RUC-2 warm season precipitation patterns than may be evident in that from the Eta model, which currently uses the Betts-Miller-Janjic convective parameterization. This same difference in character of precipitation forecasts is also evident in NCEP/NSSL experiments comparing the Kain-Fritsch (which also includes downdrafts) and Betts-Miller-Janjic schemes both within the MesoEta model (Kain et al. 1998).

5.c. Lateral boundary conditions Lateral boundary conditions for the RUC-2 model are provided by the early Eta run output at 3-h intervals. The Eta model forecasts are interpolated to the 40-km RUC-2 domain on its hybrid coordinate levels. Values of pressure thickness, virtual potential temperature, and horizontal winds at the edge of the RUC-2 domain (up to 5 grid points from the boundary) are nudged (Davies 1976) toward the Eta values at each time step in a model run.

The accuracy of RUC-2 forecasts is driven to some extent by the time availability of Eta forecasts. RUC-2 forecasts initialized at 0000 or 1200 UTC are forced to use boundary conditions from Eta runs already 12 h old, since the RUC-2 runs before the Early Eta. This means that the 12-h RUC-2 forecasts valid at 0000 or 1200 UTC are nudging toward 24-h Eta forecasts at these times. Typically, the skill of RUC-2 forecasts jumps near the western boundary by the 0300 or 1500 UTC runs, respectively, since the newer Early Eta runs are available by those times.

5.d. Fields for surface boundary conditions

- Daily 50-km resolution sea-surface temperatures- NCEP. The same SST field used for the Eta model is also used for the RUC-2. An up-to-date display of the field used in RUC-2 and Eta is available here .
- Daily 14-km resolution lake-surface temperatures for the Great Lakes - NOAA/Great Lakes Environmental Research Laboratory
- Weekly ice cover - NESDIS/NCEP
- Monthly vegetation fraction data at a resolution of 0.14 degrees latitude - NESDIS/NCEP
- Seasonal (4 seasons) albedo at 1 deg resolution.

- Land use (14 classes) at 1 deg resolution.
- Soil texture at 1 deg resolution

• The snow fields cycled by RUC-2 seem to be more accurate than the daily U.S. Air Force snow cover analysis. A better snow cover analysis from NESDIS is expected early in 1998, and modifications will be made to combine the RUC-2 cycled fields with these data when they become available. Improved surface fields (land use, soil texture) will also added as they become available for the RUC-2 domain.

6. VERIFICATION OF RUC-2 ANALYSES AND FORECASTS

Verification statistics for the RUC-1, RUC-2, and the 48-km Eta models are available at this link.

7. RUC-2 OUTPUT VARIABLES AND FILES

Variables available

- **RUC-2 variables available**
- **Explanation of RUC-2 variables, including diagnostics**

In RUC-2, water vapor mixing ratio replaces condensation pressure (output in RUC-1) as the water vapor moisture variable in the 3-d grids. Height also replaces Montgomery stream function. The use of height and water-vapor mixing ratio instead of the variables they replace facilitates calculation of derived quantities involving these variables. Height also stores more efficiently in GRIB.

40km RUC/MAPS output formats

From the 40km RUC at NCEP, five different formats will be available: Click **here** for more information on 40km RUC-2 variables.

RUC-2 GRIB table - parameters for all RUC-2 variables

- isobaric main (25-mb) grids of primary six 3-d variables plus about 77 2-d fields (including precipitation, fluxes, CAPE/CIN, tropopause fields, surface fields, fields from special levels - mean layers near surface, freezing level, max wind, etc.)
  (~6 MB in GRIB format per output time)
- native (hybrid coordinate) grids of 3-d variables plus 2-d fields
  (~10 MB in GRIB format per output time)
- surface grids (25 2-d fields)
  (0.35 MB per output time)
- model output (BUFR) soundings at ~486 sites (standard sounding variables plus surface variables).

```
Naming convention

isobaric main:
   RUC/ruc2.yymmdd/ruc2.TXXZ.pgrbanl
     or
   RUC/ruc2.yymmdd/ruc2.TXXZ.pgrbfzz

native:
   RUC/ruc2.yymmdd/ruc2.TXXZ.bgrbanl
     or
```

```
   RUC/ruc2.yymmdd/ruc2.TXXZ.bgrbfzz
     XX = cycle time (01,02,03..)
   - zz = forecast hour (00,01,02...)

surface:
   RUC/ruc2.yymmdd/ruc2.TXXZ.sgrbanl
     or
   RUC/ruc2.yymmdd/ruc2.TXXZ.sgrbfzz

BUFR sounding:
   RUC/ruc2.yymmdd/ruc2.TXXZ.bufranl
     or
   RUC/ruc2.yymmdd/ruc2.TXXZ.bufrfzz
```

- **List of sounding sites available in 40-km RUC/MAPS domain**
- **List of sounding variables/units available in 40-km RUC/MAPS domain** The format of the BUFR sounding data has been set up so that the scripts used for BUFR soundings from the Eta model can also be used for RUC-II sounding data.

(~2.5 MB for each hour for a given run, soundings for all sites)

Use of GRIB gridded input and output. The MAPS database routines used in RUC-1 will no longer be used for grid input and output.

8. DIAGNOSTIC FIELDS FROM RUC-2

Explanation of diagnosed RUC-2 variables , including surface fields, stability indices, precipitation products, special level fields (tropopause, freezing level).

9. PLANS FOR THE FUTURE

- 3-d variational analysis
- 3-d cloud analysis using satellite, radar, and surface observations combined with explicit RUC-2 multi-hydrometeor cloud forecast.
- Assimilation of new data types - radial winds from radar, satellite radiances, GPS precipitable water, local mesonets.
- Improved physical parameterizations, including cloud microphysics, surface physics (frozen soil, high-resolution soil and surface data sets), and turbulence physics.
- 20-km horizontal resolution - planned for NCEP's Class 8 computer about 1999.
- Non-hydrostatic version of RUC forecast model - Development underway in collaboration with University of Miami.

10. REFERENCES

• Arakawa, A., and V.R. Lamb, 1977: Computational design of the basic dynamical processes of the UCLA general circulation model. Methods in Computational Physics, Vol. 17, Academic Press, 174-265, 337 pp.

• Benjamin, S.G., J.M. Brown, K.J. Brundage, B.E. Schwartz, T.G. Smirnova, and T.L. Smith, 1998: The operational RUC-2. Preprints, 16th Conference on Weather Analysis and Forecasting, AMS, Phoenix, 249-252.

• Benjamin, S.G., T.L. Smith, B.E. Schwartz, S.I. Gutman, and D. Kim, 1998: Precipitation forecast sensitivity to GPS precipitable water observations combined with GOES using RUC-2. 12th Conf. on Num. Wea. Pred., AMS, Phoenix, 73-76.

• Benjamin, S.G., J.M. Brown, K.J. Brundage, D. Devenyi, D. Kim, B.E. Schwartz, T.G. Smirnova, T.L. Smith, and A. Marroquin, 1997: Improvements in aviation forecasts from the 40-km RUC. Preprints, 7th Conference on Aviation, Range, and Aerospace Meteorology, Long Beach, February, 411-416.

• Benjamin, S. G., K. J. Brundage, and L. L. Morone, 1994a: The Rapid Update Cycle. Part I: Analysis/model description. Technical Procedures Bulletin No.~416, NOAA/NWS, 16 pp. [National Weather Service, Office of Meteorology, 1325 East-West Highway, Silver Spring, MD 20910]. This is the TPB for the original 60-km RUC-1.

• Benjamin, K.J. Brundage, P.A. Miller, T.L. Smith, G.A. Grell, D. Kim, J.M. Brown, and T.W. Schlatter, 1994b. The Rapid Update Cycle at NMC. Preprints, Tenth Conference on Numerical Weather Prediction, Portland, OR, July 18-22, 1994. American Meteorological Society, Boston, 566-568.

• Benjamin, S. G., K. A. Brewster, R. L. Brummer, B. F. Jewett, T. W. Schlatter, T. L. Smith, and P. A. Stamus, 1991: An isentropic three-hourly data assimilation system using ACARS aircraft observations. Mon. Wea. Rev., 119, 888-906. The original MAPS description -- an early pure isentropic version.

• Benjamin, S. G., 1989: An isentropic meso-alpha scale analysis system and its sensitivity to aircraft and surface observations. Mon. Wea. Rev., 117, 1586-1603.

• Bleck, R., and S.G. Benjamin, 1993. Regional weather prediction with a model combining terrain-following and isentropic coordinates. Part I: model description. Mon. Wea. Rev., 121: 1770-1785. Primary journal article on the dynamic framework for the MAPS/RUC hybrid coordinate model.

• Brown, J.M., T.G. Smirnova, and S.G. Benjamin, 1998: Introduction of MM5 level 4 microphysics into the RUC-2. Preprints 12th Conf. on Num. Wea. Pred., AMS, Phoenix.

• Burk, S.D., and W.T. Thompson, 1989: A vertically nested regional numerical prediction model with second-order closure physics. Mon. Wea. Rev., 117, 2305-2324.

• Davies, H.C., 1976: A lateral boundary formulation for multi-level prediction models. Tellus, 102, 405-418.

• Devenyi, D. and S.G. Benjamin, 1998: Application of a 3DVAR analysis in RUC-2. 12th Conf. on Num. Wea. Pred., AMS, Phoenix, 37-40.

• Dudhia, J., 1989: Numerical study of convection observed during the winter monsoon experiment using a mesoscale two-dimensional model. J. Atmos. Sci., 46, 3077-3107.

• Grell, G.A., 1993: Prognostic evaluation of assumptions used by cumulus parameterizations. Mon. Wea. Rev., 121, 764-787.

• Grell, G.A., J. Dudhia, and D.R. Stauffer, 1994: A description of the fifth-generation Penn State/NCAR Mesoscale Model (MM5). NCAR Technical Note, NCAR/TN-398 + STR, 138 pp.

• Johnson, D.R., T.H. Zapotocny,F.M. Reames, B.J. Wolf, and R.B. Pierce, 1993: A comparison of simulated precipitation by hybrid isentropic-sigma and sigma models. Mon. Wea. Rev., 121, 2088-2114.

• Kain, J.S., D.J. Stensrud, M.E. Baldwin, and G.S. Manikin, 1998: A comparison of two convective parameterizations schemes in NCEP's MesoEta model and the implications for quantative precipitation forecasting.

• Kim. D., and D. Nychka, 1998: Comparisons of density smoothers to combine satellite imager and sounder data. 14th Conf. on Prob. and Stat. in the Atmos. Sci., AMS, Phoenix

• Marroquin, A., T.G. Smirnova, J.M. Brown, and S.G. Benjamin, 1998: Forecast performance of a prognostic turbulence formulation implemented in the MAPS/RUC model. 12th Conf. on Num. Wea. Pred., AMS, Phoenix.

• Pan, H.-L. and L. Mahrt, 1987: Interaction between soil hydrology and boundary-layer development. Bound.-Layer Meteorol., 38, 185-202.

• Pan, Z., S.G. Benjamin, J.M. Brown, and T. Smirnova. Comparative experiments with MAPS on different parameterization schemes for surface moisture flux andb oundary- layer processes. Monthly Weather Review 122:449-470 (1994)

• Reisner, J., R.M. Rasmussen, and R.T. Bruintjes, 1997: Explicit forecasting of supercooled liquid water in winter storms using a mesoscale model. Quart. J. Roy. Meteor. Soc.

• Schwartz, B.E. and S.G. Benjamin, 1998: Verification of RUC-2 and Eta model precipitation forecasts. 16th Conf. on Wea. Analysis and Forecasting, AMS, Phoenix, J19-J22.

• Smirnova, T.G., J.M. Brown, and S.G. Benjamin, 1998: Impact of a snow physics parameterization on short-range forecasts of skim temperature in MAPS/RUC. 12th Conf. on Num. Wea. Pred., AMS, Phoenix.

• Smirnova, T. G., J. M. Brown, and S. G. Benjamin, 1997a: Performance of different soil model configurations in simulating ground surface temperature and surface fluxes. Mon. Wea. Rev., 125, 1870-1884.

• Smirnova, T. G., J. M. Brown, and S. G. Benjamin, 1997b: Evolution of soil moisture and temperature in the MAPS/RUC assimilation cycle. Preprints, 13th Conference on Hydrology, Long Beach, AMS, 172-175.

• Smith, T.L., and S.G. Benjamin, 1998: The combined use of GOES cloud-drift, ACARS, VAD, and profiler winds in the RUC-2. 12th Conf. on Num. Wea. Pred., AMS, Phoenix.

• Smolarkiewicz, P.K., 1983: A simple positive-definite advection transport algorithm. Mon. Wea. Rev., 111, 479-486.

• Zapotocny, T.H., D.R. Johnson, and F.M. Reames, 1994: Development and initial test of the University of Wisconsin global isentropic-sigma model. Mon. Wea. Rev., 122, 2160-2178.

This page prepared by Stan Benjamin

NWS Technical Procedures Bulletin No. 490

RUC20 - The 20-km version of the Rapid Update Cycle

11 April 2002 (updated 16 May)

Stanley G. Benjamin, John M. Brown, Kevin J. Brundage, Dezső Dévényi, Georg A. Grell, Dongsoo Kim, Barry E. Schwartz, Tatiana G. Smirnova, and Tracy Lorraine Smith, and Stephen S. Weygandt

NOAA/OAR Forecast Systems Laboratory, Boulder, CO

Geoffrey S. Manikin

Environmental Modeling Center, National Centers for Environmental Prediction, Camp Springs, MD

Abstract

A major revision to the Rapid Update Cycle (RUC) analysis/model system was implemented into operations at the National Centers for Environmental Prediction Center (NCEP) on 17 April 2002. The new RUC version with 20-km horizontal resolution (RUC20) replaces the previous 40-km version of the RUC (RUC40).

Summary of RUC20 vs. RUC40 (RUC-2) differences

1. Horizontal resolution
The RUC20 has a 20-km horizontal resolution, compared to 40 km for the previous RUC40 (RUC-2). The area covered by the computational grid has not changed. The RUC20 has a 301x225 horizontal grid, compared to 151x113 for the RUC40.

2. Vertical resolution
The RUC20 has 50 computational levels, compared to 40 levels for the RUC40, and continues to use the hybrid isentropic-sigma vertical coordinate as in previous versions of the RUC.

3. Improved moist physics
Improved quantitative precipitation forecasts have been the primary focus for changes in the RUC20 model, including a major revision in the MM5/RUC mixed-phase microphysics cloud routine, and a new version of the Grell convective parameterization with an ensemble approach to closure and feedback assumptions. The main effect of the microphysics change is to decrease overforecasting of graupel and ice and improve the precipitation type forecast. The new Grell scheme provides in considerable improvement in convective precipitation forecasts from the RUC.

4. Assimilation of GOES cloud-top data
The RUC20 includes a cloud analysis that updates the initial 3-d cloud/hydrometeor fields by combining cloud-top pressure data from GOES with the background 1-h RUC hydrometeor field. Cloud clearing and building is done to improve the initial cloud water/ice/rain/snow/graupel fields for the RUC.

5. Better use of observations in analysis
The RUC20 assimilates near-surface observations more effectively through improved algorithms for calculating observation-background differences. Assimilation of surface observations is improved by diagnosing background forecasts for surface temperature and dewpoint at 2 m and for winds at 10 m. It is also improved by matching land-

use type between the background and the observation for near-coastal stations. The RUC20 continues to use an optimal interpolation analysis as in the RUC40 – implementation of a 3-d variational analysis has been deferred.

6. Improved land-surface physics
The RUC20 land-surface model is changed from that of the RUC40. It uses more detailed land-use and soil texture data, in contrast to 1-degree resolution fields used in the RUC40. It includes improved cold-season processes (soil freezing/thawing) and a 2-layer snow model. These changes improve the evolution of surface moisture and temperature and snow cover, which in turn improve forecasts of surface temperature and moisture and precipitation.

7. Lateral boundary conditions
The RUC40 used lateral boundary conditions specified from the Eta model initialized every 12 h. The RUC20 adds updates of its lateral boundaries from the 0600 and 1800 UTC Eta runs.

8. Improved post-processing
The RUC20 includes improved diagnostic techniques for 2-m temperature and dewpoint, 10-m winds, helicity, visibility, convective available potential energy, and convective inhibition.

Most significant improvements in RUC20 fields over those from RUC40 (RUC-2).

- **Precipitation – both summer and winter –** From improved precipitation physics and higher resolution
- **All surface fields - temperature, moisture, winds** – Reduced bias and RMS error in comparison with METAR observations. From improved surface and cloud/precipitation physics and higher resolution
- **Upper-level winds and temperatures** – From higher vertical and horizontal resolution, better physics
- **Orographically induced precipitation and circulations** – From higher horizontal resolution, cloud physics, and better use of surface data near mountains.

1. INTRODUCTION

A new version of the Rapid Update Cycle (RUC) has been implemented at the National Centers for Environmental Prediction (NCEP) on 17 April 2002 with a doubling of horizontal resolution (40km to 20km), an increased number of vertical computational levels (40 to 50), and improvements in the analysis and model physical parameterizations. A primary goal in development of the 20-km RUC (or RUC20) has been improvement in warm-season and cold-season quantitative precipitation forecasts. Improvements in near-surface forecasts and cloud forecasts have also been targeted. The RUC20 provides improved forecasts for these variables, as well as for wind, temperature, and moisture above the surface.

The RUC20 provides improved short-range numerical weather guidance for general public forecasting as well as for the special short-term needs of aviation and severe-weather forecasting. The RUC20 continues to produce new analyses and short-range forecasts on an hourly basis, with forecasts out to 12 h run every 3 h. The implementation of the RUC20 in 2002 follows previous major implementations of a 60-km 3-h cycle version in 1994 (Benjamin et al 1994, 1991) and a 40-km 1-h cycle version in 1998 (Benjamin et al 1998).

The uses of the RUC summarized below continue with the RUC20:

- **Explicit use of short-range forecasts** - The RUC forecasts are unique in that they are initialized with very recent data. Thus, usually, the most recent RUC forecast has been initialized with more recent data than other available NCEP model forecasts. Even at 0000 or 1200 UTC, when other model runs are available, the RUC forecasts are useful for comparison over the next 12 h. Although there are many differences between the RUC and other NCEP models, the key unique aspects of the RUC are its hybrid isentropic vertical coordinate (used in the analysis and model), hourly data assimilation, and model physics.
- **Monitoring current conditions with hourly analyses** - Hourly analyses are particularly useful when overlaid with hourly satellite and radar images, or hourly observations such as from surface stations or profilers.
- **Evaluating trends of longer-range models** - RUC analyses and forecasts are useful for evaluation of the short-term predictions of the Eta and AVN models.

The users of the RUC include:

- Aviation Weather Center/NCEP, Kansas City, MO
- Storm Prediction Center/NCEP, Norman, OK
- NWS Weather Forecast Offices
- FAA/DOT, including use for air traffic management and other automated tools, and for FAA workstations
- NASA Space Flight Centers
- Private sector weather forecast providers

Sections below describe changes in the RUC with the RUC20 implementation regarding spatial resolution, data assimilation, model, changes to lower and lateral boundary condition, and diagnostics / post-processing. Comments from a field test for the RUC20 held March-April 2002 are included in an appendix.

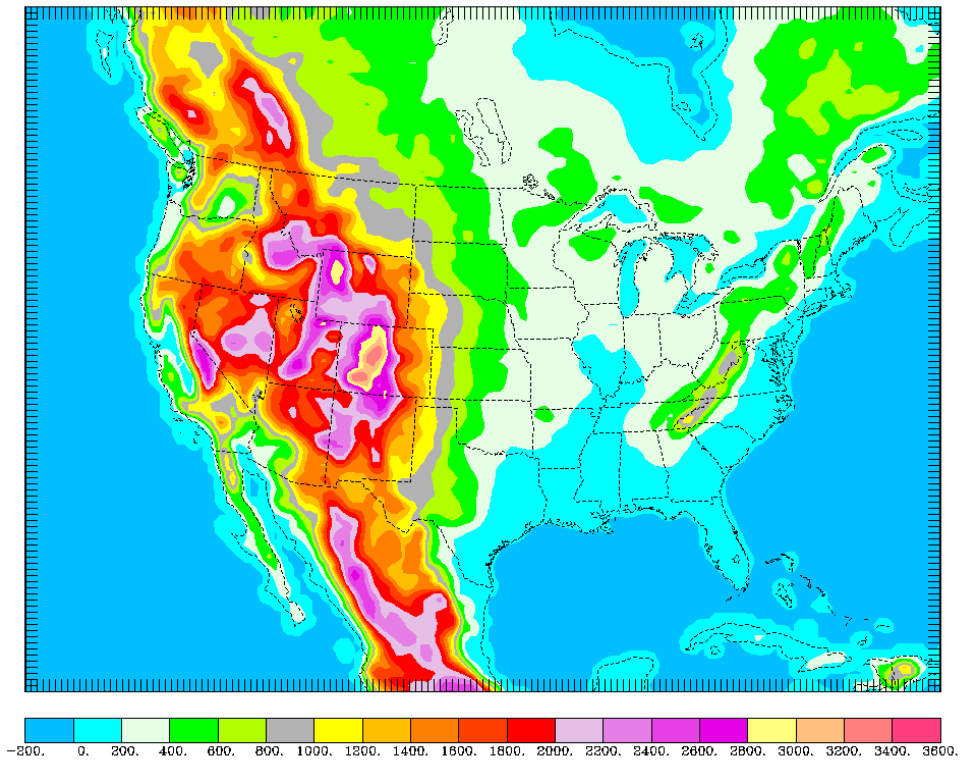

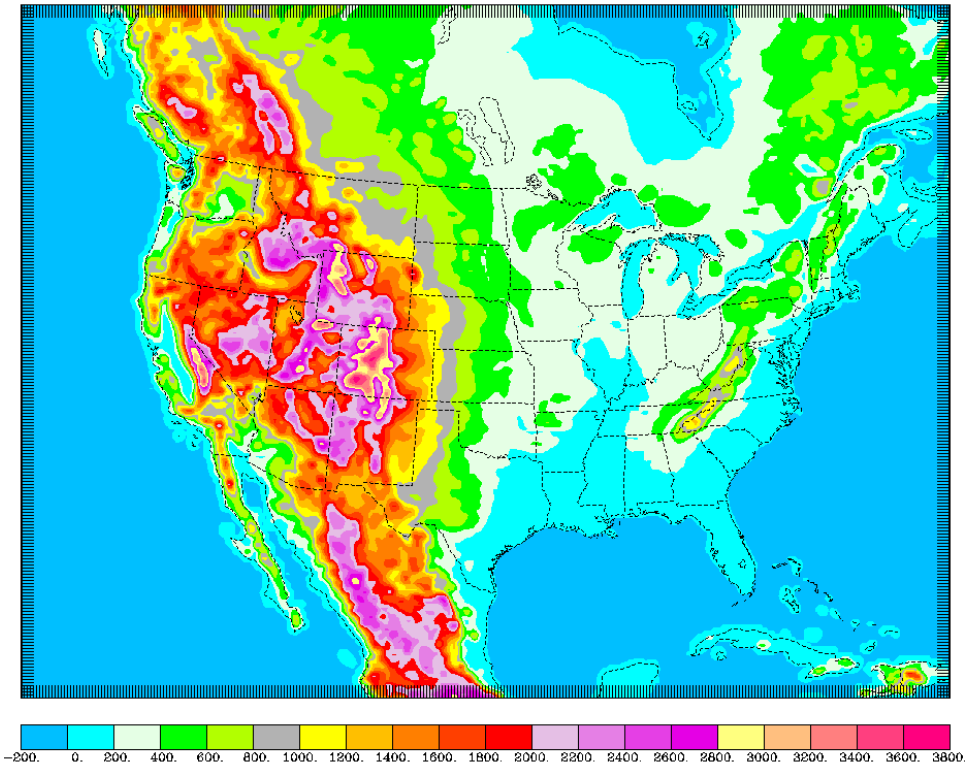

Figure 1. Terrain elevation for a) 40-km RUC-2, b) 20-km RUC20

2. SPATIAL RESOLUTION

The RUC20 occupies the same spatial domain as the previous RUC40 (40-km RUC-2), as shown in Figs. 1a,b. The RUC20 grid points are still a subset of the AWIPS Lambert conformal grid (AWIPS/GRIB grid 215 for 20 km) used as a distribution grid by the National Weather Service. Direct use of the AWIPS grid reduces the number of distribution grids for the RUC. The AWIPS grid ID for the RUC20 grid is 252, compared to 236 for the RUC40 grid. Thus, the 252 grid for the RUC20 is a subset of the 215 grid. The RUC20 grid size is 301 x 225 grid points (compared to 151 x 113 for RUC40).

2.a. Horizontal resolution

The 20-km grid spacing allows better resolution of small-scale terrain variations, leading to improved forecasts of many topographically induced features, including low-level eddies, mountain/valley circulations, mountain waves, sea/lake breezes, and orographic precipitation. It also allows better resolution of land-water boundaries and other land-surface discontinuities. While the most significant differences in the terrain resolution of the RUC20 (Fig. 1b) vs. RUC40 (Fig. 1a) are in the western United States, a number of important differences are also evident in the eastern part of the domain.

The surface elevation of the RUC20, as in the RUC40, is defined as a "slope envelope" topography. The standard envelope topography is defined by adding the sub-grid-scale terrain standard deviation (calculated from a 10-km terrain field) to the mean value over the grid box. By contrast, in the slope envelope topography, the terrain standard deviation is calculated with respect to a plane fit to the high-resolution topography within each grid box. This gives more accurate terrain values, especially in sloping areas at the edge of high-terrain regions. It also avoids a tendency of the standard envelope topography to project the edge of plateaus too far laterally onto low terrain regions. Using the slope envelope topography gives lower terrain elevation at locations such as Denver and Salt Lake City which are located close to mountain ranges. As shown in Table 1, the RUC20 more closely matches station elevations in the western United States.

Rawinsonde station	**Station elevation minus RUC40 elevation (m)**	**Station elevation minus RUC20 elevation (m)**
Edwards AFB, CA	300	41
Denver, CO	354	26
Grand Junction, CO	679	323
Boise, ID	274	253
Great Falls, MT	157	29
Reno, NV	381	144
Elko, NV	352	152
Medford, OR	544	346
Salem, OR	233	51
Rapid City, SD	153	45
Salt Lake City, UT	630	438
Riverton, WY	225	119

Table 1. Terrain elevation difference between station elevation and interpolated RUC elevation for selected rawinsonde stations in western United States.

The grid length is 20.317 km at 35 deg N. Due to the varying map-scale factor from the projection, the actual grid length in RUC20 decreases to as small as 16 km at the north boundary. The grid length is about 19 km at 43 deg N. The RUC20 latitude/longitude (and terrain elevation) at each point in an ASCII file can be downloaded from http://ruc.fsl.noaa.gov/MAPS.domain.html. The lower left corner point is (1,1), and the upper right corner point is (301,225), as shown in Table 2.

An example is shown below (Fig. 2) of the improved orographic effect on low-level wind circulation comparing 3-h forecasts from RUC20 and RUC40, both displayed at 40-km resolution. The RUC20 shows a better depiction of the

Denver-area cyclonic circulation, strong southerly flow up the San Luis Valley into southern Colorado near Alamosa, and winds of greater than 20 knots near higher terrain in central Colorado and south central Utah. The verifying analysis in Fig. 3 shows that all of these features appear to be better depicted in the RUC20 3-h forecasts.

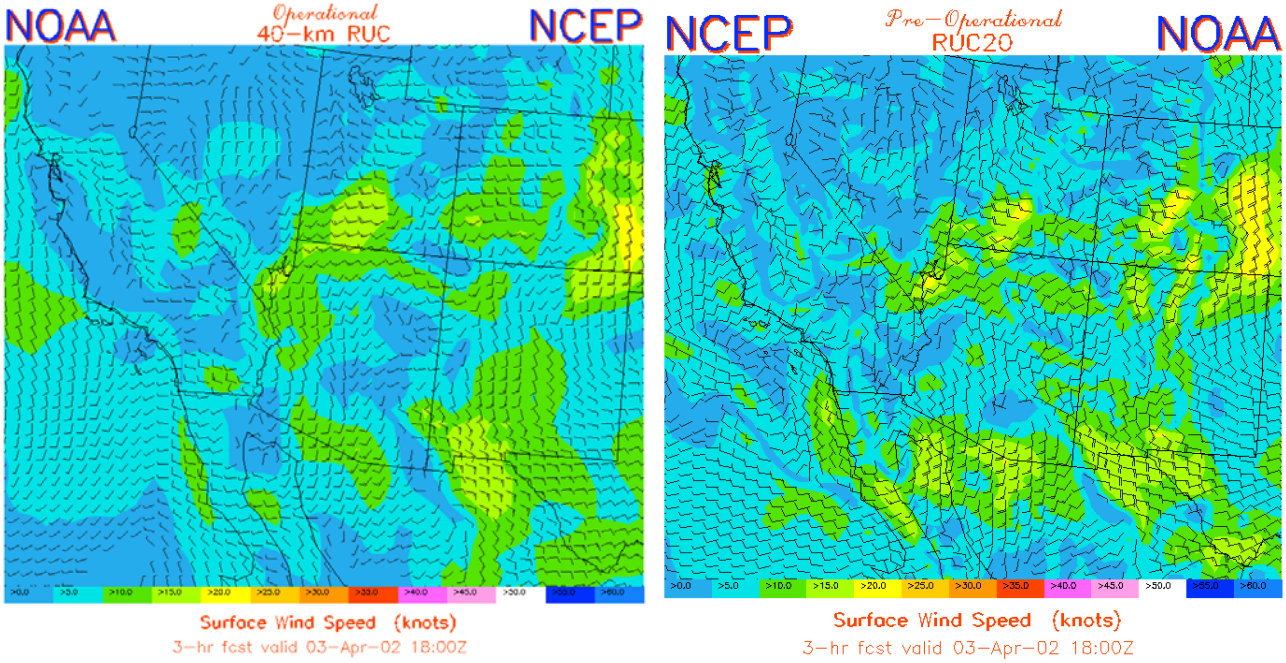

Figure 2. RUC 3-h surface wind forecasts from a) RUC40 and b) RUC20. Forecasts valid at 1800 UTC 3 April 2002.

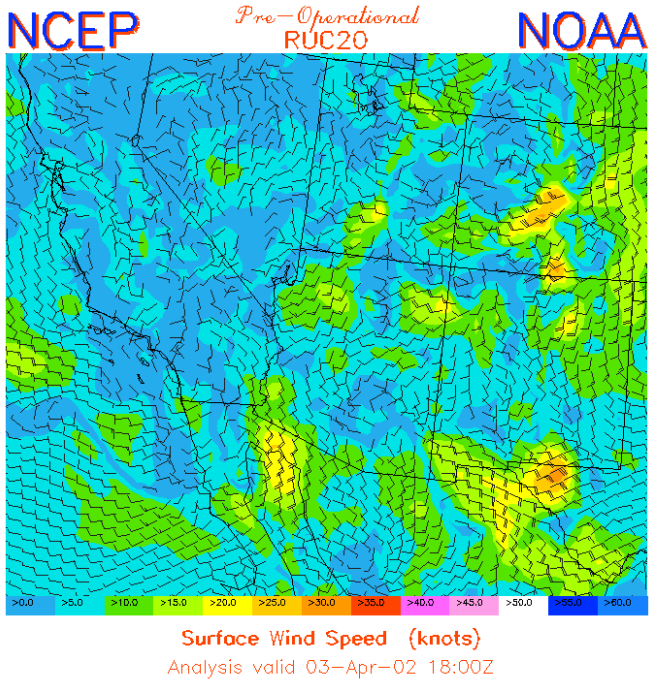

Figure 3. Verifying analysis of surface winds at 1800 UTC 3 April 2002 from RUC20.

RUC20 point	AWIPS-212 point	Latitude	Longitude
(1,1)	(23,7)	16.2810 N	126.1378 W
(1,225)	(23,119)	54.1731 N	139.8563 W
(301,1)	(173,7)	17.3400 N	69.0371 W
(301,225)	(173,119)	55.4818 N	57.3794 W

Table 2. Latitude/longitude and AWIPS-212 positions of corner points for the RUC20 domain.

b. Vertical resolution

The RUC20 continues to use the generalized vertical coordinate configured as a hybrid isentropic-sigma coordinate (Bleck and Benjamin 1993) used in previous versions of the RUC. This coordinate is used for both the analysis and the forecast model. The RUC hybrid coordinate has terrain-following layers near the surface with isentropic layers above. This coordinate has proven to be advantageous in providing sharper resolution near fronts and the tropopause (e.g., Benjamin 1989, Johnson et al. 1993, 2000). Some of the other advantages are:

- All of the adiabatic component of the vertical motion on the isentropic surfaces is captured in flow along the 2-D surfaces. Vertical advection through coordinate surfaces, which usually has somewhat more truncation error than horizontal advection, is less prominent in isentropic/sigma hybrid models than in quasi-horizontal coordinate models. This characteristic results in improved moisture transport and less precipitation spin-up problem in the first few hours of the forecast.
- Improved conservation of potential vorticity. The potential vorticity and tropopause level (based on the 2.0 PV unit surface) show very good spatial and temporal coherence in RUC grids (Olsen et al 2000).
- Observation influence in the RUC analysis extends along isentropic surfaces, leading to improved air-mass integrity and frontal structure. From an isobaric perspective, the RUC isentropic analysis is implicitly anisotropic (Benjamin 1989).

The RUC20 has 50 vertical levels, compared to 40 levels in RUC40. Extra levels are added near the tropopause and lower stratosphere and also in the lower troposphere. The RUC hybrid coordinate is defined as follows:

- Each of the 50 levels is assigned a reference virtual potential temperature (θ_v) that increases upward (Table 3).
- The lowest atmospheric level (k=1) is assigned as the pressure at the surface (the model terrain elevation).
- Each of the next 49 levels is assigned a minimum pressure thickness between it and the next level below. This thickness will apply to coordinate surfaces in the lower portion of the domain where the coordinate surfaces are terrain-following. For grid points with surface elevation near sea level, the minimum pressure thickness is 2.5, 5.0, 7.5, and 10 hPa for the bottom 4 layers, and 15 hPa for all layers above. These minimum pressure thicknesses are reduced over higher terrain to avoid "bulges" of sigma layers protruding upward in these regions.
- The pressure corresponding to the reference θ_v for each (k) level is determined for each (i,j) column. (For lower θ_v values, this pressure may be determined via extrapolation as beneath the ground.)
- At this point, there are two choices for the assignment of pressure to the (i,j,k) grid point, corresponding to:
    1) the reference θ_v value (the *isentropic* definition), and
    2) the minimum pressure spacing, starting at the surface pressure (the *sigma* definition)

If the isentropic pressure (1) is less than sigma pressure (2), the grid point pressure is defined as isentropic, or otherwise as terrain-following (sigma).

224	232	240	245	250	255	260	265	270	273
276	279	282	285	288	291	294	296	298	300
302	304	306	308	310	312	314	316	318	320
322	325	328	331	334	337	340	343	346	349
352	355	359	365	372	385	400	422	450	500

Table 3. Reference θ_v values (K) for the RUC20 (50 levels).

The maximum θ_v value in the RUC20 is 500 K, compared to 450 K for the RUC40. The 500 K surface is typically found at 45-60 hPa. As with the RUC40, a greater proportion of the hybrid levels are assigned as terrain-following in warmer regions and warmer seasons. This is shown in Figs. 4a,b below.

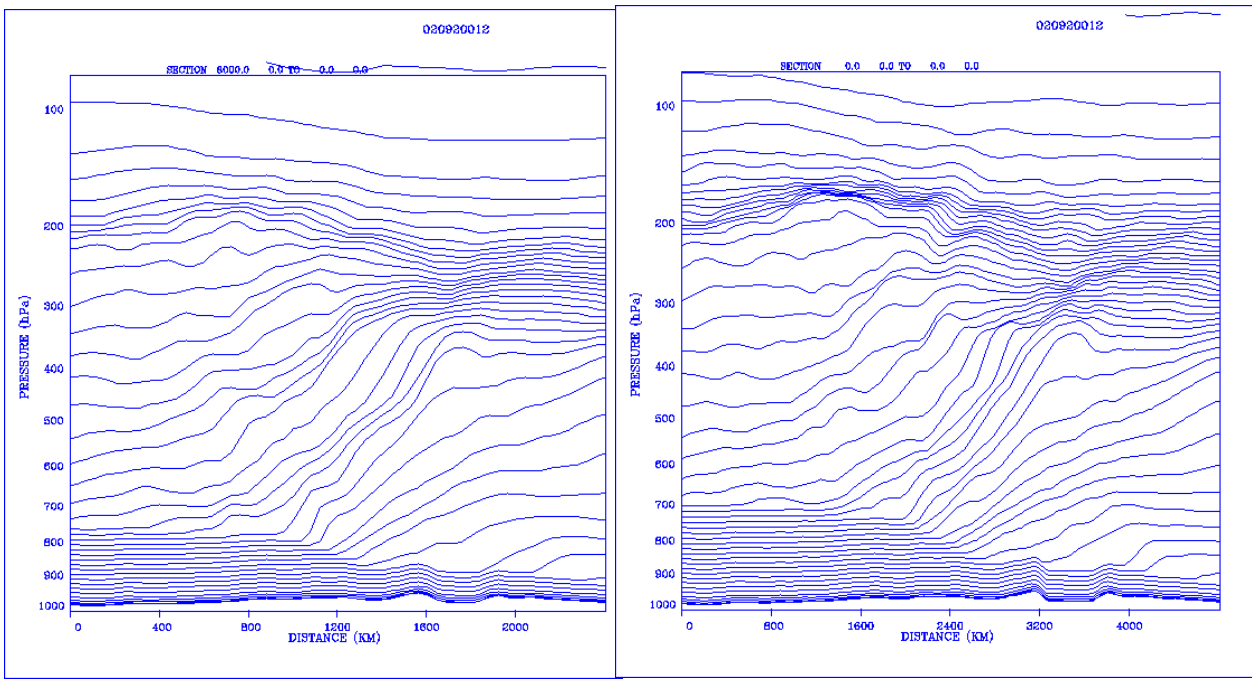

Figure 4. Vertical cross sections showing RUC native coordinate levels for a) RUC40 – 40 levels, and b) RUC20 – 50 levels. Data are taken from RUC 12-h forecasts valid at 1200 UTC 2 April 2002. Cross sections are oriented from south (Mississippi) on left to north (western Ontario) on right

In this example (Fig. 4), north-south vertical cross sections are shown depicting the pressure at which the RUC native levels are found for a particular case. The case shown is from April 2002, with the cross section extending from Mississippi (on the left) northward through Wisconsin (center point), across Lake Superior (slightly higher terrain on each side), and ending in western Ontario. A frontal zone is present in the middle of the cross section, where the RUC levels (mostly isentropic) between 700 and 300 hPa are strongly sloped.

In the RUC20, seven new levels have been added with reference θ_v values between 330 K and 500 K. Three new levels with reference θ_v in the 270—290 K range have also been added. In the RUC20 depiction (Fig. 4b), the tropopause is more sharply defined than in the RUC40, and there are more levels in the stratosphere, resulting from the additional levels in the upper part of the domain. In the RUC20, the isentropic levels from 270-355 K are now resolved with no more than 3 K spacing.

3. FORECAST MODEL CHANGES IN RUC20

The RUC20 forecast model is similar to that for the RUC40 but with important changes in physical parameterizations and smaller changes in numerical approaches. The model continues to be based upon the generalized vertical coordinate model described by Bleck and Benjamin (1993). Modifications to a 20-line section of code in the model are sufficient to modify it from the hybrid isentropic-sigma coordinate described in section 2.b to either a pure sigma or pure isentropic model.

3.a. Basic dynamics/numerics

First, the basic numerical characteristics of the RUC model are reviewed (italicized where different in the RUC20 from the RUC40).

- Arakawa-C staggered horizontal grid (Arakawa and Lamb 1977); u and v horizontal wind points offset from mass points to improve numerical accuracy.
- Generalized vertical coordinate equation set and numerics for adiabatic part of model following Bleck and Benjamin (1993)
- No vertical staggering.
- *Time step is 30 seconds at 20-km resolution.*
- Positive definite advection schemes used for continuity equation (advection of pressure thickness between levels) and for horizontal advection (Smolarkiewicz 1983) of virtual potential temperature and all vapor and hydrometeor moisture variables.
- Application of adiabatic digital filter initialization (DFI, Lynch and Huang 1992) for 40-min period forward and backward before each model start. The use of the DFI in the RUC is important for producing a sufficiently "quiet" (reduced gravity wave activity) 1-h forecast to allow the 1-h assimilation cycle. *A problem in application of digital filter weights is corrected in the RUC20.*

The atmospheric prognostic variables of the RUC20 forecast model are:

- pressure thickness between levels
- virtual potential temperature - θ_v
- horizontal wind components
- water vapor mixing ratio
- cloud water mixing ratio
- rain water mixing ratio
- ice mixing ratio
- snow mixing ratio
- graupel (rimed snow, frozen rain drops) mixing ratio
- number concentration for ice particles
- turbulence kinetic energy

The soil prognostic variables (at six levels) of the RUC forecast model are:

- soil temperature
- soil volumetric moisture content

Other surface-related prognostic variables are snow water equivalent moisture and snow temperature *(at 2 layers in RUC20*), and canopy water.

Other differences in the RUC20 vs. RUC40 model numerics or design are as follows:

- The order of solution in each time step:

RUC40	**RUC20**
Continuity	Continuity
Horizontal advection of θ_v / moisture	Horizontal advection of θ_v / moisture
Physics (sub-grid-scale parameterizations)	Physics
Coordinate adjustment	Momentum
Momentum	Coordinate adjustment

- The vertical advection for all variables is now calculated in a consistent manner using upstream differencing. The placement of the call for coordinate adjustment at the end of the time step allows this consistent treatment.
- More robust and flexible hybrid coordinate algorithm
- Much improved modularization
- *Use of new version of Scalable Modeling System (SMS) message-passing library with non-intrusive compiler directives (Govett et al. 2001) and improved modularization led to a significant reduction in lines of code in the RUC20 model.*

3.b. Physical parameterizations

3.b.1. Explicit mixed-phase cloud/moisture processes.

The RUC20 uses an updated version (Brown et al 2000) of the explicit microphysics from the NCAR/Penn State MM5 mesoscale model MM5 (level 4, Reisner et al. 1998). An earlier version of this scheme was also used in the RUC40. This scheme explicitly predicts mixing ratios for five hydrometeor species -- cloud water, rain water, snow, ice, graupel and also the ice particle number concentration. This explicit mixed-phase prediction is different than the diagnostic mixed-phase prediction used in the Eta-12. In the RUC model, all six cloud/hydrometeor variables are advected horizontally using the positive definite scheme of Smolarkiewicz (1983) on the isentropic-sigma levels with adaptive vertical resolution and advected vertically using upstream differencing (see section 3.a.). The hydrometeor variables cycled without modification in the RUC40 1-h cycle are modified by GOES cloud-top pressure assimilation in the RUC20, as described in section 4.

Significant changes to the RUC/MM5 microphysics (Brown et al. 2000) have been introduced with the RUC20. These changes address unreasonable behavior in the RUC40 regarding excessive graupel and lower than expected amounts of supercooled liquid water. The modifications, developed jointly by NCAR and FSL, include a different curve for ice nucleation as a function of temperature (Cooper replacing Fletcher), new assumed particle size distributions for graupel to reduce the number of small particles, a modified procedure for graupel formation as a result of riming of cloud ice, and revisions to the calculation of cloud-ice particle number concentration. These modifications have been successful in reducing excessive graupel (e.g., Fig. 5) and in improving the precipitation-type forecast (less sleet) in the RUC20.

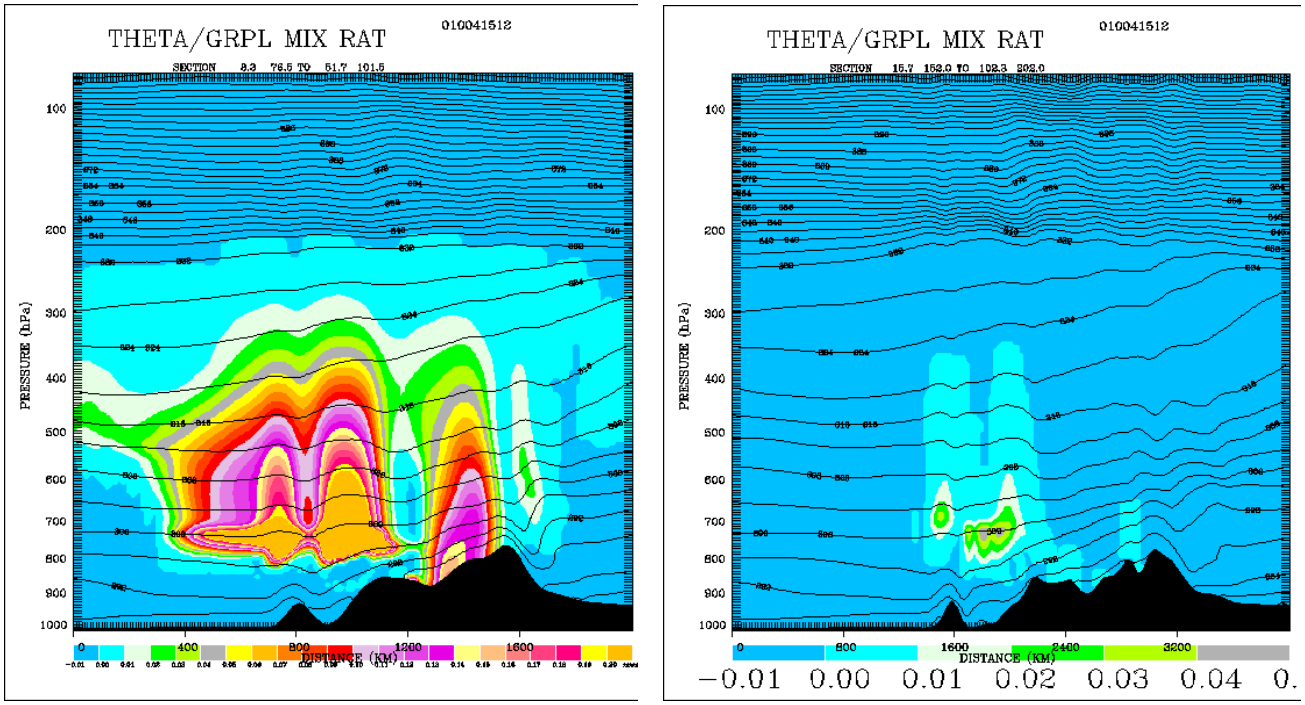

Figure 5. Graupel and potential temperature in vertical cross sections from a) RUC40 and b) RUC20. For 12-h forecasts valid 0300 UTC 5 January 2001. Cross section is oriented SW (left) to NE (right) across Washington (Olympic Peninsula) into British Columbia and Alberta.

3.b.2. Convective parameterization.
A new convective parameterization (Grell and Devenyi 2001) based on an ensemble approach is used in the RUC20. This scheme is based on the Grell (1993) scheme but draws on other schemes by using an ensemble of various closure assumptions. The version of the Grell/Devenyi scheme used in the RUC20 includes the following closures:

- $\frac{\partial(CAPE)}{\partial t}$, where CAPE is convective available potential energy.
- removal of total CAPE (Kain and Fritsch 1992) in a specified time period.
- low-level horizontal moisture convergence.
- low-level mass flux at cloud base.

with different parameters applied to each of these closures. In the RUC20, a total of 108 closure assumptions are used in the Grell/Devenyi convective scheme. The RUC20 convective scheme also now includes:

- detrainment of cloud water and cloud ice
- entrainment of environmental air into the updraft
- relaxation of stability (convective inhibition) constraints at downstream points based on downdraft strength
- removal of stability constraint at initial time of each model forecast in areas where GOES sounder effective cloud amount (Schreiner et al 2001) indicates that convection may be present. This technique can aid convection in starting more accurately at grid points where there is positive CAPE, although it cannot create positive CAPE
- correction to exaggerated effects of surface processes in forcing convection. This bug in RUC40 resulted in too widespread convective precipitation over land in summer, especially in the southeastern U.S., and widespread light precipitation over warm ocean areas.

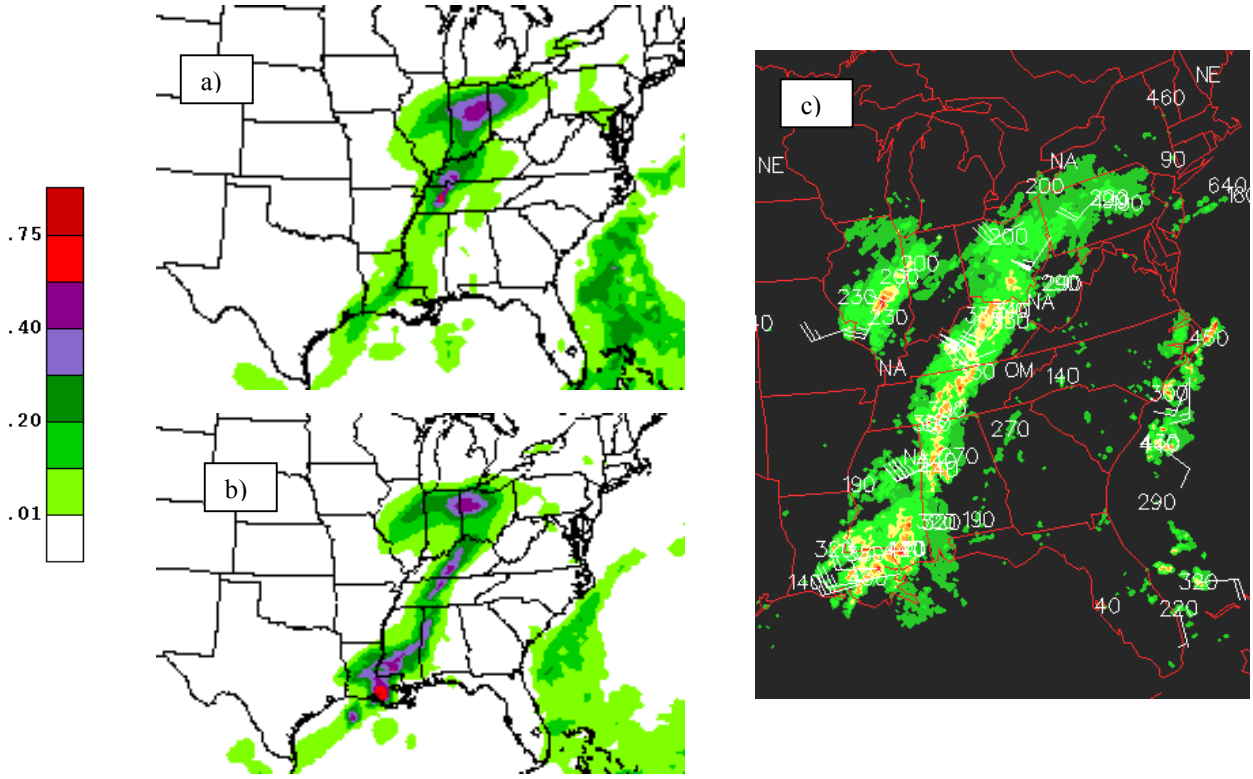

Figure 6. Precipitation (in) forecasts initialized at 0000 UTC 26 March 2002 from a) RUC40 and b) RUC20 for 0900-1200 UTC (9-12 h forecasts). c) Radar summary valid at 1115 UTC (verification).

The skill of RUC precipitation forecasts is significantly improved with the RUC20 version, including the Grell/Devenyi ensemble-based convective parameterization. An example of this improvement is presented in Fig. 6, where Figs. 6a,b are 12-h forecasts of 3-h accumulated precipitation from the RUC40 and RUC20 respectively, and Fig. 6c is a radar image in the verifying period. In this case, the RUC20 has accurately forecast much more intensity than the RUC40 to the southern end of a convective line, especially in eastern Louisiana and southern Mississippi. Not only is the intensity improved in the RUC20 forecast, but also the position of the line is more accurately forecast to be farther east than in the RUC40 forecast, stretching from central Ohio into northwestern Alabama before bending back to eastern Louisiana.

Improvement in precipitation forecasts from the RUC20 relative to the RUC40 is also evident in overall precipitation verification statistics over multi-week periods. Daily verification has been performed using the NCEP 24-h precipitation analysis against RUC 24-h totals produced by summing two 12-h forecasts. Two scores traditionally used for precipitation verification, equitable threat score and bias, are used to compare RUC20 and RUC40 forecasts. For a period from spring 2002, the RUC20 has a much higher equitable threat score (Fig. 7a) and bias (Fig. 7b) much closer to 1.0 (preferable) than the RUC40 for almost all precipitation thresholds. Precipitation verification for a November-December 2001 cold season period (Benjamin et al 2002a) also shows a marked improvement for the RUC20.

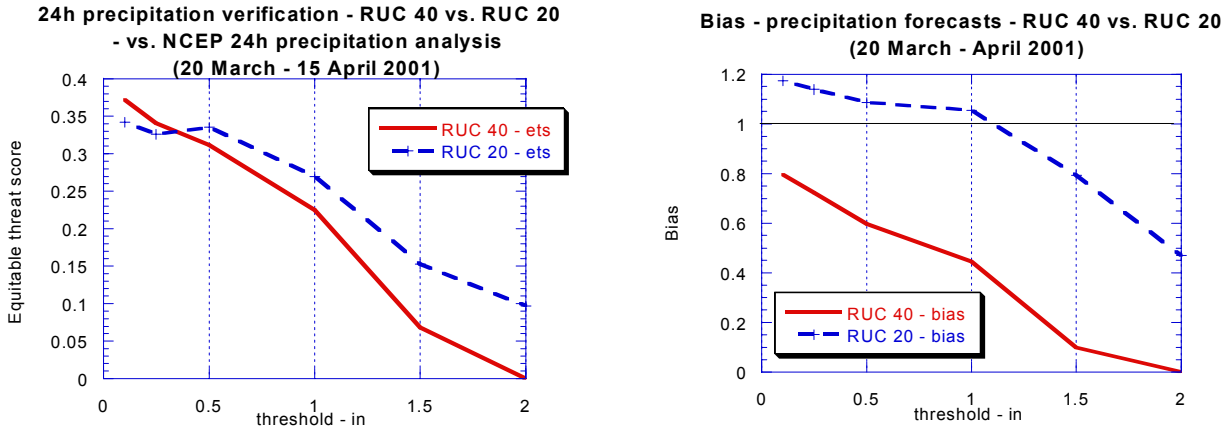

Figure 7. Precipitation verification comparing RUC20 and RUC40 forecasts, a) equitable threat score and b) bias. Verification is against NCEP 24-h precipitation analysis. For period 20 March – 15 April 2001.

As with the RUC40, the inclusion of downdrafts in the Grell scheme results in smaller-scale details in RUC warm season precipitation patterns than may be evident in that from the Eta model using the Betts-Miller-Janjic convective parameterization. This same difference in character of precipitation forecasts is also evident in NCEP/NSSL experiments comparing the Kain-Fritsch (which also includes downdrafts) and Betts-Miller-Janjic schemes both within the MesoEta model (e.g., Kain et al. 1998).

3.b.3. Land-surface physics.

A new version of the RUC land-surface model (LSM) is used in the RUC20, including accounting for freezing and thawing of soil, and using a 2-layer representation of snow (Smirnova et al. 2000b). This updated LSM is a refinement of the previous RUC40 version discussed in Smirnova et al. (1997). Surface (shelter/anemometer level) forecasts are often critically dependent on accurate estimates of surface fluxes, and in turn, on reasonably accurate soil moisture and temperature estimates. The RUC soil model contains heat and moisture transfer equations solved at 6 levels for each column together with the energy and moisture budget equations for the ground surface. These budgets are applied to a thin layer spanning the ground surface and including both the soil and the atmosphere with corresponding heat capacities and densities. (The budget formulation is one of the primary differences between the RUC LSM and LSMs in other operational models.) A treatment of the evapotranspiration process, developed by Pan and Mahrt (1987), is implemented in the RUC LSM. When snow cover is present, snow is considered to be an additional one or two upper layers of soil, depending on its depth.

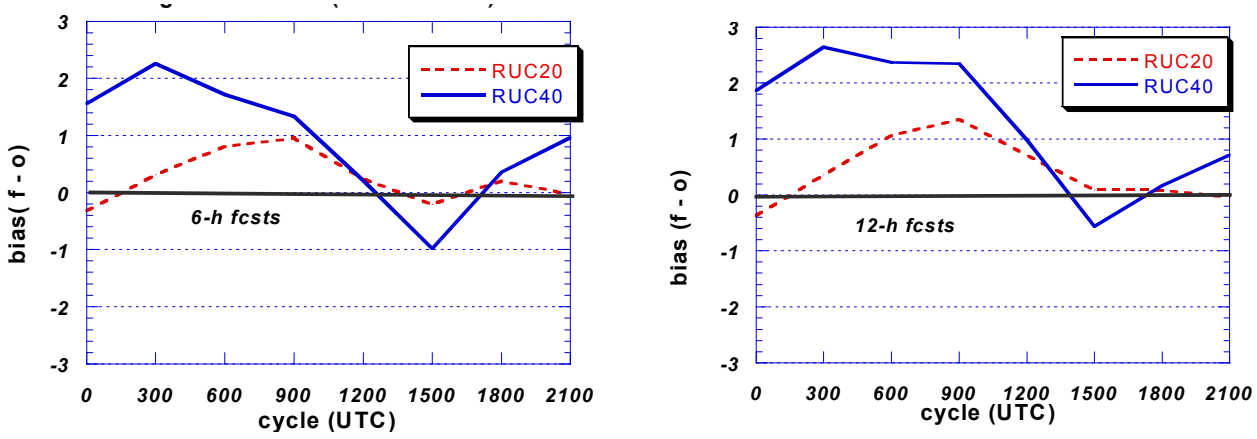

Figure 8. Diurnal variation of 2-m temperature (°C) bias (forecast-obs) in RUC20 and RUC40 forecasts. Forecast valid times on horizontal axis. Verification against METAR observations in RUC domain east of 105°W. a) for 6-h forecasts, b) for 12-h forecasts.

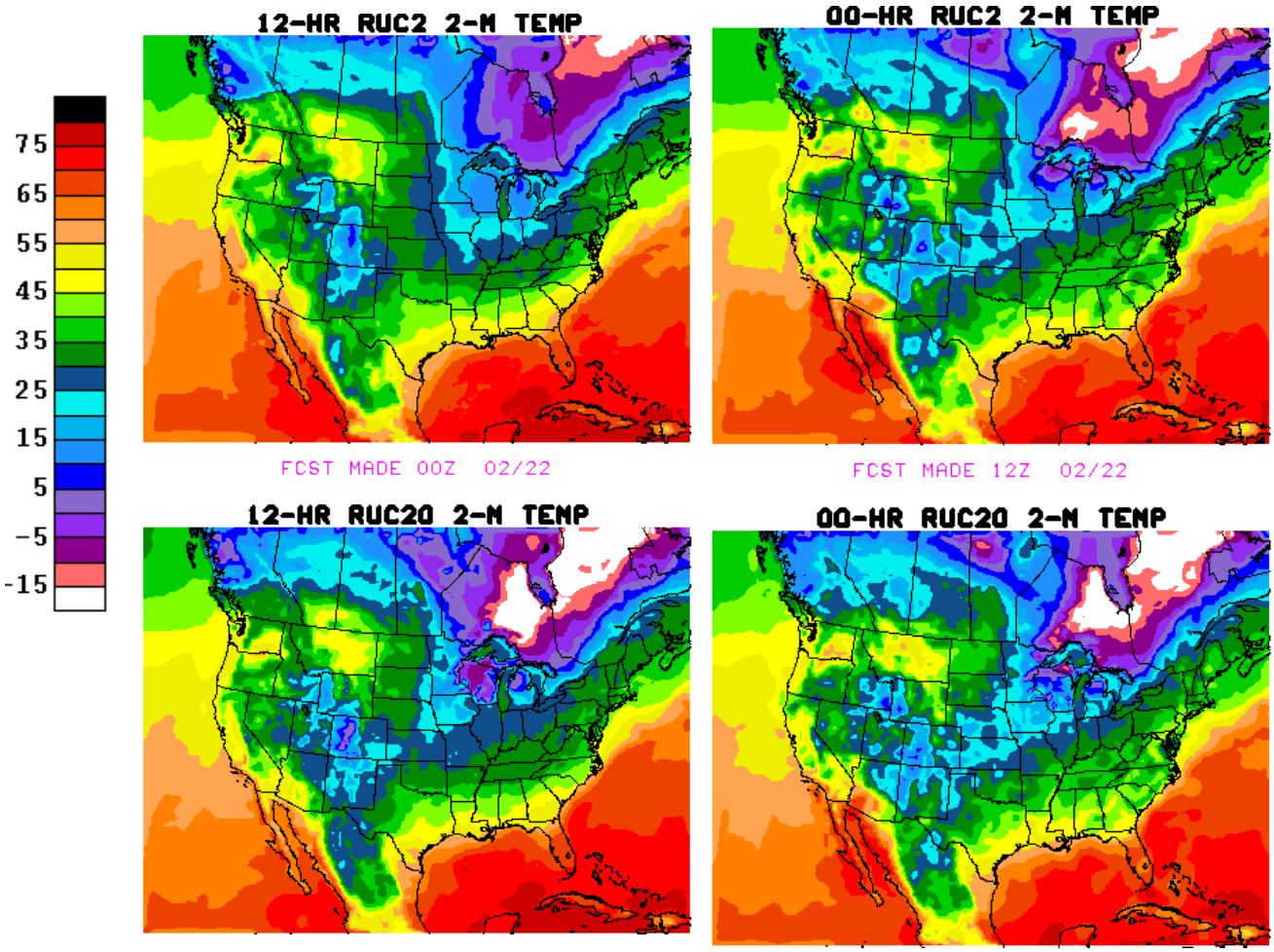

Figure 9. Comparison of 2-m temperature (°F) 12-h forecasts from RUC40 (upper left) and RUC20 (lower left) valid 1200 UTC 22 Feb 2002. Verification analyses from RUC40 (upper right) and RUC20 (lower right).

To provide a more accurate solution of the energy budget through deeper snow, a snowpack thicker than 7.5 cm is split up into two layers where the top layer is set to be 7.5 cm deep, and the energy budget is applied to the top half of this top layer. A heat budget is also calculated at the boundary between the snow pack and the soil, allowing melting from the bottom of the snow layer. Incorporation of a two-layer snow representation into the land-surface scheme in the RUC20 significantly improves the skin temperatures in winter, and therefore, also the 2-m temperature forecasts (Figs. 8, 9).

The accumulation of snow on the ground surface is provided by the mixed-phase cloud microphysics algorithm of the RUC forecast scheme (Reisner et al. 1998, Brown et al. 2000, section 3.b.1 of this document). It predicts the total amount of precipitation and also the distribution of precipitation between the solid and liquid phase. In the RUC20, the Grell/Devenyi convective parameterization scheme now also contributes to the snow accumulation if the surface temperature is at or below 0° C.

As with the RUC40, the RUC20 cycles volumetric soil moisture and soil temperature at the 6 soil model levels, as well as canopy water, and snow temperature. In the RUC20, cycling of the snow temperature of the second layer (where needed) is also performed. The RUC continues to be unique among operational models in its specification of snow cover and snow water content through cycling (Smirnova et al. 2000b). The 2-layer snow model in the RUC20 improves this cycling, especially in spring time, more accurately depicting the snow melting season and spring spike in total runoff, as shown in 1-dimensional experiments with the RUC LSM over an 18-year period from a site in Russia (Smirnova et al 2000b).

The RUC20 also uses a different formulation for thermal conductivity (Johansen 1975, Peters-Lidard 1998) that generally reduces values of this parameter, especially in near-saturated soils, thereby contributing to a stronger diurnal cycle. This change helps to correct an inadequate diurnal cycle (daytime too cool, nighttime too warm) in the RUC40. Figure 8 shows that the diurnal cycle is better depicted in the RUC20 but that there is still some remaining tendency for inadequate nighttime cooling. An example of improved surface temperature forecasts is provided in Fig. 9, where the RUC20 provides more accurate forecasts in the central plains (cooler), northern Indiana and Ohio (warmer), and central California (cooler) than the RUC40 for this overnight 12-h forecast ending at 1200 UTC 22 Feb 2002. Schwartz and Benjamin (2002) show that the RUC20 provides improved 2-m temperature and 10-m wind forecasts, especially during daytime.

3.b.4. Atmospheric radiation.
The RUC20 continues to use the MM5 atmospheric radiation package (Dudhia 1989, Grell et al. 1994) with additions for attenuation and scattering by all hydrometeor types. This scheme is a broadband scheme with separate components for longwave and shortwave radiation. In the RUC20, the calculation of shortwave radiation is corrected for a 30-min mean time lag in solar radiation present in the RUC40. This correction helps to improve morning near-surface temperature forecasts (e.g., Fig. 8 results for forecasts valid at 1500 UTC). The RUC20 also updates shortwave radiation more frequently, every 30 min instead of every 60 min in RUC40 (Table 4). The updating of longwave radiation remains every 60 min in RUC20, same as RUC40.

3.b.5. Turbulent mixing.
The RUC20 continues to prescribe turbulent mixing at all levels, including the boundary layer, via the explicit turbulence scheme of Burk and Thompson (1989). This scheme is a level-3.0 scheme, with explicit forecast of turbulent kinetic energy and three other turbulence variables. The surface layer mixing continues to be prescribed by Monin-Obukhov similarity theory, specifically the three-layer scheme described in Pan et al. (1994). With the Burk-Thompson scheme, the RUC typically forecasts TKE amounts of 5-20 J/kg in the boundary layer, and also forecasts TKE maxima aloft, typically localized in frontal zones, corresponding to likely areas for clear-air turbulence.

3.b.6. Time splitting for physical parameterizations
As with other mesoscale models, the RUC gains efficiency by not calling physical parameterizations at the full frequency of each dynamic time step. Time truncation errors are, however, incurred by this time splitting. In the RUC20, the frequency of calls to physical parameterizations has been increased, as is shown in Table 4. Of these changes, the one for the cloud microphysics is most significant, decreasing time truncation errors associated with microphysical processes and precipitation fallout.

Physical parameterization	RUC40 frequency (min)	RUC20 frequency (min)
Cloud microphysics	10	2
Convection	5	2
Turbulence	5	2
Land-surface	5	2
Shortwave radiation	60	30
Longwave radiation	60	60

Table 4. Frequency of calls to physical parameterizations in RUC40 and RUC20.

The application of tendencies (rate of change to temperature, moisture, wind, etc.) from the physical parameterizations is also different in RUC20. In RUC40, tendencies from each physics routine except for radiation were applied with the parameterization time step only when the parameterization was called instead of being spread evenly over the interval between calls. This technique, which we inelegantly term "chunking", causes some shock to the model, although the effects did not seem harmful. In the RUC20, tendencies are applied at each dynamics time step, thus avoiding "chunking".

4. CHANGES TO LATERAL AND LOWER BOUNDARY CONDITIONS IN RUC20

4.a. Lateral boundary conditions

With the RUC20, lateral boundary conditions are specified from Eta model runs made every 6 h. Thus, the lateral boundaries are updated with more recent data than with RUC40, for which new Eta runs were incorporated only every 12 h. The output frequency from the Eta used for the RUC boundary conditions is 3 h. The Eta data used for RUC lateral boundary conditions are currently from 25-hPa 40-km output grids. The Eta model forecasts are interpolated to the RUC20 domain on its hybrid coordinate levels. Values of pressure thickness, virtual potential temperature, and horizontal winds at the edge of the RUC domain (up to 5 grid points from the boundary) are nudged (Davies 1976) toward the Eta values at each time step in a model run. For the RUC20, fixes have been made in application of lateral boundary conditions, resulting in smoother fields near the boundaries.

It is important to note that since the RUC runs prior to the Eta in NCEP's operational suite, it uses "old" boundary condition data for model forecasts made at 0000 and 1200 UTC. This timing sequence results in a slight degradation of quality of RUC forecasts near the boundaries for runs initialized at these times. Tests at FSL in which the RUC runs at 0000 and 1200 UTC are made *after* Eta boundary conditions are available at those same times show a clear increase in statistical forecast skill.

4.b. Lower boundary conditions

- Sea-surface temperature – Uses same daily analysis as used for Eta runs (currently, the 50-km global real-time SST analysis from the NCEP/EMC Ocean Modeling Branch). Higher-resolution information for the Great Lakes is also incorporated. The RUC's use of SST data is set via scripts to follow any changes made for the Eta model.
    - In the RUC20, a bug has been fixed that was causing 1° lat/lon blockiness in the SST used in the RUC40. This blockiness was also apparent in the 2-m temperatures over oceans (e.g., Fig. 10).
    - Monthly climatological values are used for Great Salt Lake in RUC20 but not RUC40 (L. Dunn, personal communication). Time interpolation is to date of month.

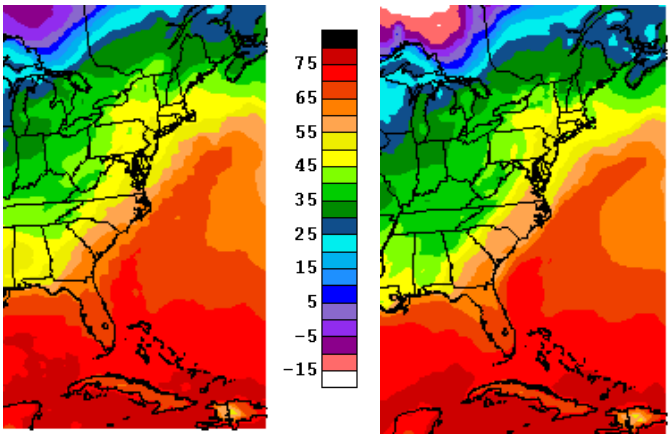

o

Figure 10. 2-m temperature 12-h forecasts from a) RUC40, b) RUC20, valid at 1200 UTC 21 Feb 2001

- Ice cover – RUC20 uses NESDIS daily ice analysis, same as used by Eta model. No change from RUC40.
- Land use – RUC20 land-use (Fig. 11b) is taken from USGS 24-class, 30-second data set used in MM5 and WRF (Weather Research and Forecasting) model pre-processing programs. RUC40 (Fig. 11a) used old MM4 land-use data with 1° lat/lon resolution and caused blockiness in RUC40 surface fields.

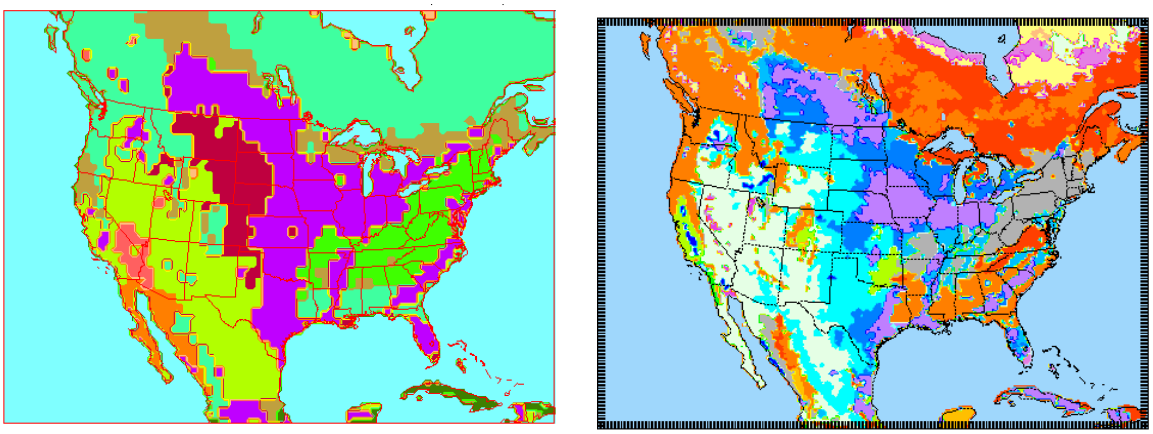

Figure 11. Land-use for a) RUC40 and b) RUC20

- Soil texture – RUC20 uses much higher resolution information than in RUC40. RUC20 soil type data are taken from a global 30-second dataset, accessible from the WRF preprocessor code.
- Vegetation fraction – For both RUC20 and RUC40, this is specified from monthly high-resolution (0.144°) data produced from 5-year climatology (Gutman and Ignatov 1998) of NDVI (normalized digital vegetation index, an AVHRR-based satellite product). This is the same data set used by the Eta model. Values are interpolated by date of month between monthly values assumed to be valid on the 15th of each month.
- Albedo – For RUC20, this is also specified from NESDIS monthly high-resolution (0.144°) data produced from a 5-year climatology (Csiszar and Gutman 1999), and this is the same dataset used by Eta model. In the RUC40, albedo data were from a much coarser 1° seasonal climatology dataset.
- Terrain elevation – As described in section 2.

5. ANALYSIS CHANGES IN RUC20

The RUC20 analysis continues to use an optimal interpolation (OI) analysis applied on the RUC native hybrid isentropic-sigma levels, but with some important modifications from the RUC40 OI analysis, as described below.

[A 3-dimensional variational (3DVAR) analysis has been developed for the RUC (Devenyi et al 2001); some further tuning is needed to squeeze out a little more skill in 3-h forecasts before it can be implemented. It is hoped that the RUC 3DVAR can be implemented 5-6 months after the initial RUC20 implementation.]

5.a. Assimilation of GOES cloud-top pressure data

Toward the goal of improved short-range forecasts of cloud/hydrometeors, icing, and precipitation, an advanced version of the RUC cloud-top pressure assimilation technique (Benjamin et al 2002b) has been developed and tested. This improved technique, using GOES single field-of-view cloud-top pressure and temperature data provided by NESDIS, is being implemented into operations with the rest of the RUC20. As described in section 3.b.1, the RUC uses a bulk mixed-phase cloud microphysics scheme from the NCAR/Penn State MM5 model, with 5 hydrometeor types explicitly forecast (Brown et al. 2000). The prognostic variables in this scheme are mixing ratios of water vapor, cloud water, rain water, ice, snow, and graupel, and number concentration of ice particles. In the RUC40, the initial conditions for the fields were simply those carried over from the previous 1-h RUC forecast. In the RUC20 including assimilation of GOES cloud-top data, these fields are modified each hour as part of the cloud clearing and cloud building.

The RUC20 cloud/hydrometeor analysis technique is an advanced version of the procedures previously described by Kim and Benjamin (2001, 2000). GOES cloud-top pressure data provide information on the horizontal location of cloudy and cloud-free areas, but not on cloud depth. Also, unless there are broken layers, it cannot provide information on multiple cloud layers. Thus, the RUC cloud/hydrometeor assimilation technique is designed to use this partial information. When GOES data indicate that no clouds are present, the technique removes any hydrometeors and reduces water vapor mixing ratio to a subsaturation value. When GOES data indicate that cloud not present in the RUC 1-h forecast at the correct level, cloud water and/or ice is added in a layer of not more than 50 hPa depth. This layer is also saturated with respect to water or ice with a linear variation between these two saturation vapor pressure values in the 248-263 K range.

Other features of the RUC GOES cloud-top assimilation include:

- Rederivation of cloud-top pressure from GOES cloud-top temperature if the original retrieval of cloud-top pressure is closer to the ground than 620 hPa. This rederivation of the cloud-top pressure uses the RUC 1-h temperature/moisture profile at the nearest grid point.
- Use of single field-of-view GOES data (~10-km resolution). The median values from the fields-of-view around each RUC box are used. With this sampling, cloud fraction is calculated in RUC grid volumes.
- Use of stability check to identify possible sub-field-of-view variations from small convective clouds that result in inaccurate cloud-top temperature and pressure determination.
- Remove cloud indicators if they only occur at isolated (noncontiguous) RUC grid points, again on the presumption that GOES may be observing sub-field-of-view clouds.
- Special handling for marine stratus situations to force cloud-top at consistent level with top of marine inversion in RUC background profile.
- Information from the GOES effective cloud amount is used to modify a stability constraint for convection in the subsequent forecast run (see section 3.b.2).

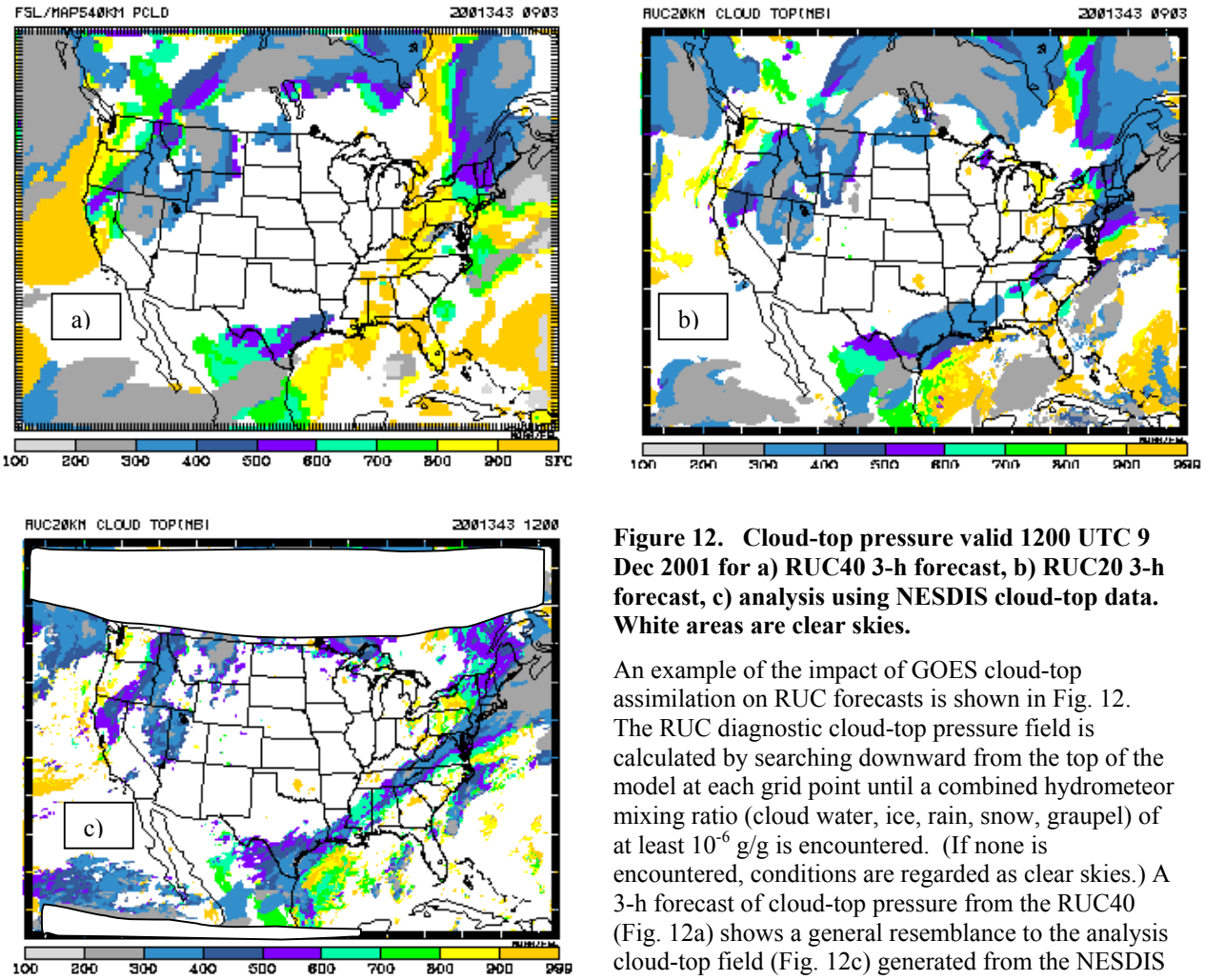

Figure 12. Cloud-top pressure valid 1200 UTC 9 Dec 2001 for a) RUC40 3-h forecast, b) RUC20 3-h forecast, c) analysis using NESDIS cloud-top data. White areas are clear skies.

An example of the impact of GOES cloud-top assimilation on RUC forecasts is shown in Fig. 12. The RUC diagnostic cloud-top pressure field is calculated by searching downward from the top of the model at each grid point until a combined hydrometeor mixing ratio (cloud water, ice, rain, snow, graupel) of at least 10^{-6} g/g is encountered. (If none is encountered, conditions are regarded as clear skies.) A 3-h forecast of cloud-top pressure from the RUC40 (Fig. 12a) shows a general resemblance to the analysis cloud-top field (Fig. 12c) generated from the NESDIS cloud product, but the RUC20 3-h forecast (Fig. 12b) shows much better agreement with the analysis. This improved forecast is due not only to the cloud-top assimilation (and retention in the subsequent forecast), but also to other changes in the RUC20 including improved microphysics and higher resolution.

Ongoing statistical verification has been performed, calculating correlation coefficients between the NESDIS cloud-top product and RUC40 and RUC20 forecasts of durations from 1 h to 12 h. These statistics (Benjamin et al 2002b) show that the RUC20 produces improved cloud-top forecasts over RUC40 not just at 1-h and 3-h projections, but with similar improvement out to 12-h forecasts.

5.b. Improved observation pre-processing

The most important changes in the RUC20 OI analysis are the observation preprocessing and matching to background values. In the observation preprocessing, a more flexible, lower-memory, observation array structure is used in the RUC20 that allows each level of a profile observation (e.g., rawinsonde, profiler, VAD) to be associated with its own metadata (position, time, expected error) if necessary. This structure was developed for the RUC 3DVAR but is also used in the RUC20 OI analysis. It allows, among other things, for use of varying positions to account for balloon drift in rawinsonde observations. However, the decision was made to not incorporate balloon drift in the RUC20 analysis since the effects of time change and position drift largely cancel each other.

The following features are implemented in the RUC20 observation preprocessing to improve the use of observations in the analysis. The goal of these features is to match the information in the observation and background as nearly as possible.

- Surface observations
  - Calculate 2-m temperature and moisture values and 10-m winds from background, instead of simply taking the 5-m background values. The result of this is reduced bias in the analysis.
  - Choose nearest land grid point from background for most surface observations over land, but choose nearest water grid point for buoy surface observations when calculating observation-minus-background values for coastal surface stations. This improves the RUC20 analyzed surface fields in coastal regions.
  - Improve use of background model lapse rate to match observations and background when the elevation is different. This constrained lapse rate reduction is applied for surface temperature observations, and the surface moisture observation is correspondingly modified such that the original dewpoint depression is maintained.
- Rawinsonde/profiler observations
  - Use code to preserve observed near-surface structure when rawinsonde surface elevation does not match that of model background. This logic is similar to that used for surface observations.
  - Use raw level observations now in addition to values interpolated to background levels (also used for wind profiler and VAD observations).
  - Prevent use of interpolated values if significant level data not present. For profilers, prevent use of interpolated values if separation between raw values exceeds 1200 m. This change in the RUC20 prevents a RUC40 problem in which unrealistic linearly interpolated profiles were used when there were large vertical gaps in rawinsonde, profiler, or VAD observation profiles.
- Precipitable water observations
  - Account for elevation differences between observation and background.

5.c. Modifications to optimal interpolation analysis

A detailed description of the RUC OI analysis from the RUC40 is available in the RUC-2 Technical Procedures Bulletin (Benjamin et al 1998, available from the NWS at http://205.156.54.206/om/tpb/448.htm).

Modifications made in the RUC20 to other aspects of the OI analysis are listed below.

- Quality control – Continues to use the OI-based buddy check. In RUC20, a buddy check is now performed for cloud-drift winds and precipitable water observations (not in RUC40) and bugs are fixed. RUC20 honors NCEP observation QC flags, which was not done in RUC40. This means, for instance, that quality flags from the NOAA Profiler Hub are now being used.
- Improved observation search strategy allowing much more complete use of aircraft ascent/descent profiles than in RUC40.
- Moisture analysis looping – In order to force some interconsistency in the RUC20 analysis between different moisture observations, a two-pass loop is performed. Within each loop, the analysis order is as follows: cloud-top observations, precipitable water observations, in situ moisture observations. The observation-minus-background values are recalculated after each part of the moisture analysis, and in situ observations are given the "last say".
- Moisture variable – changed from condensation pressure in RUC40 to natural logarithm of water vapor mixing ratio (ln q). This simplifies the variable transformation needed for precipitable water analysis and cloud-top assimilation. The variable ln q is conserved under motion in adiabatic conditions, considered to be desirable for the choice of an analysis variable. The cycled water vapor variable in the RUC and prognostic variable in the RUC model continues to be water vapor mixing ratio.
- Constraints applied at end of analysis
  - A series of top-down and bottom-up lapse rate checks are applied which are designed to prevent unrealistic lapse rates from occurring in the RUC20 temperature profiles. These checks also improve the retention of surface temperature observations under conditions of a deep boundary layer. A shallow superadiabatic layer near the surface of up to 1.5 K is allowed in these checks.
  - Supersaturation is removed (also performed in RUC40 analysis).

- NCEP quality control flags for individual observations are used, and suspect observations are flagged so that they will not be used in the RUC20 analysis.
- More robust hybrid coordinate adjustment.

The RUC20 OI analysis has been tested extensively at FSL with three additional new observation types:

- GPS ground-based precipitable water values (now over 100 in U.S.)
- 915 MHz boundary-layer profilers (about 25 in RUC domain)
- RASS temperature low-level virtual temperature profiles from selected 405 MHz and 915 MHz profilers

Work by FSL and NCEP is nearly complete to make these observations available to the RUC and other NCEP operational models, and it is likely that they will be added to the RUC20 within 3 months after its initial implementation.

6. RUC20 OUTPUT FILES AND VARIABLES

6.a. Output files

The output files from the RUC20 are essentially the same as those produced by the RUC40, except that they will be available at both 20-km and 40-km resolution. The 40-km files are meant to provide 'look-alike' files so that the change will be relatively transparent to RUC users. A list of the variables in each of these files is provided at http://ruc.fsl.noaa.gov/ruc2vars.html . The gridded files provided by the RUC20 are reviewed below:

- Native (bgrb, bgrb20) files – 14 3-D variables (no change from RUC40) and 46 2-d variables (the last 8 are new, but the first 38 are identical to those being produced currently by the RUC40).
    - There are 50 vertical levels in the bgrb files at both 20-km and 40-km resolution, different from the 40 levels in the RUC40 bgrb files.
- Isobaric (pgrb, pgrb20) files – 6 3-D variables at 25-hPa vertical resolution from 1000-100 hPa and 88 2-d variables (surface, precipitation, mean-layer values, etc.). Surface pressure substituted for altimeter setting. Otherwise, no change from RUC40 variables.
- Surface (sgrb, sgrb20) files – 25 2-D variables (surface, precipitation, precipitation type, stability indices, etc.). Surface pressure substituted for altimeter setting. Otherwise, no change from RUC40 variables. All fields in the sgrb files are also found in the pgrb files.

Improved BUFR data are available from RUC20. Hourly BUFR soundings with the same format as used for the Eta model are available with the RUC20, including individual station files. These individual station files (only ~25-50 KB each) were not available with the RUC40. The hourly output to 12 h is also new with the RUC20. The station list is the same as that used for the Eta model for stations within the RUC domain. (One small difference in the BUFR data is that the RUC uses 6 soil levels compared with 4 levels with Eta BUFR output.) The so-called "monolithic" files with all stations and all output times are also available from the RUC20.

A summary of this information is available at http://ruc.fsl.noaa.gov/ruc20.data-access.html .

6.b. Changes to GRIB identifiers for RUC20

When the RUC40 was implemented, some GRIB parameter values were used on an interim basis until official designations were made. Since the RUC40 implementation, these GRIB parameter values have been officially assigned. These updated parameter values have also been changed (see Table 5) in the RUC20.

Field	Parameter value in RUC40	Parameter value in RUC20
Water vapor mixing ratio	185	53
Gust wind speed	255	180
Soil moisture availability	199	207
Soil volumetric moisture content	86	144

Table 5. Changes in GRIB variable parameters in RUC20

Also, the GRIB level parameter for snow temperature is corrected from 116 in RUC40 to 111 in RUC20.

6.c. Basic 3-D output variables

There is no change in the 3-dimensional variables output by the RUC20 for either bgrb (native) or pgrb (isobaric) fields resulting from post-processing changes except that isobaric heights from the RUC20 are smoother due to extra smoothing passes.

6.d. RUC 2-D diagnosed variables

As with the 3-D fields, the 2-D fields from the RUC20 are different from those produced by the RUC40 due to all of the analysis, model, resolution, etc. changes listed in previous sections. Below are listed 2-D output variables for which there are significant changes from changes in diagnostic techniques or for other reasons not previously addressed in this document.

- *2-m temperature and dewpoint, and 10-m winds*. Similarity theory is used to derive values at these levels rather than the previous approximation of simply using the 5-m values. Note that the RUC20 continues to use a separate topography file (TOPOMINI, recalculated for 20km resolution) designed to more closely match METAR elevations than the model elevation, as shown in Table 6. The 20-km TOPOMINI matches the METAR elevations more closely than the 40-km version. The 2-m temperature and dewpoint temperature values from the RUC are *not* from the model terrain but are instead reduced to the TOPOMINI elevation. Thus, the RUC20 2-m temperature and dewpoint values include effects both from reduction to the TOPOMINI elevation and similarity reduction to 2-m above the surface. In the RUC20, the TOPOMINI is based not only on the minimum 10-km values within each 20-km grid box, but also includes a subsequent correction from METAR station elevations using a very short-length Cressman analysis.
- *convective available potential energy*. Some bug fixes resulting in smoother CAPE and CIN (convective inhibition) fields.
- *helicity* – corrections to helicity and storm-relative motion calculations, including change to Bunkers et al. (2000) formulation.

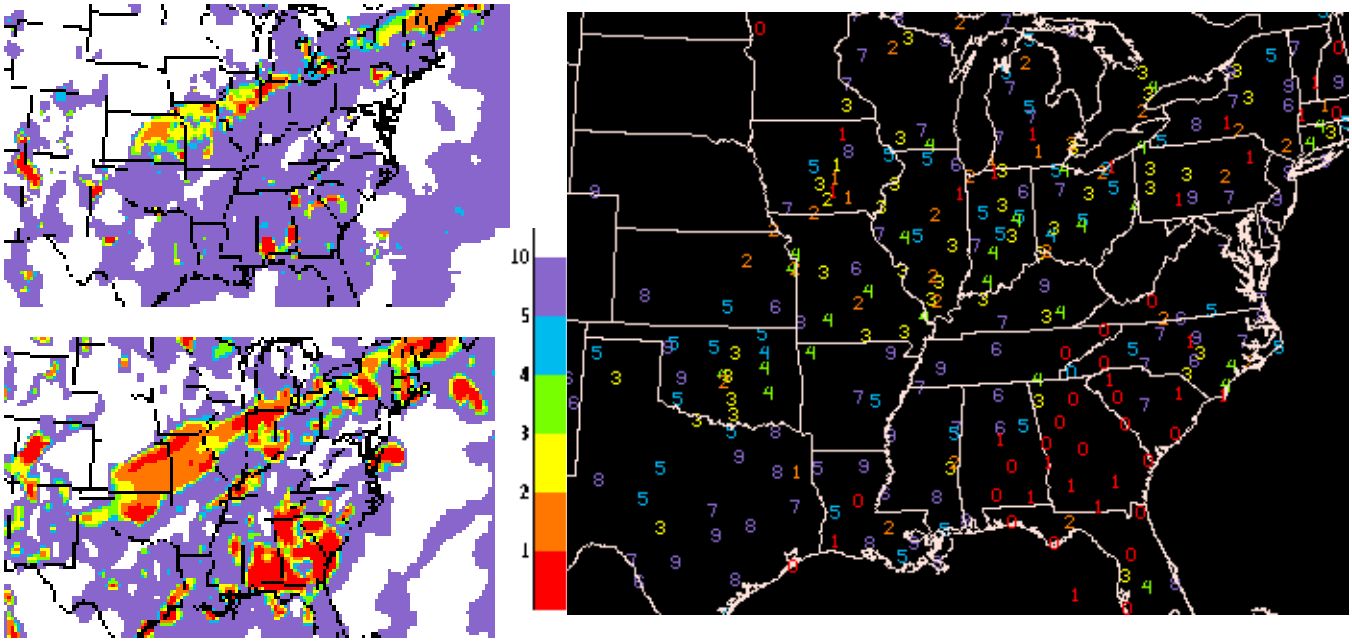

Figure 13. Visibility (mi) valid at 1200 UTC 30 January 2002. a) RUC40 0-h forecast, b) RUC20 0-h forecast, c) METAR observations.

- *MAPS mean sea-level pressure* – Bug fixed for reduction over higher terrain, resulting in more coherent SLP patterns than in RUC40.
- *precipitation type* **–** Less diagnosis of sleet (ice pellets) in RUC20 due to cloud microphysics changes described in section 3.b.1.
- *visibility* (see Smith et al. 2002, Smirnova et al. 2000a) – RUC20 diagnostic changed to use multiple levels near surface for hydrometeor and relative humidity and modification in hydrometeor and relative humidity effects. An example of an improved visibility diagnostic is shown in Fig. 13, a situation with widespread fog in the southeastern U.S.

Rawinsonde station	**Station elevation minus RUC20 model elevation (m)**	**Station elevation minus RUC20 TOPOMINI elevation (m)**
Edwards AFB, CA	41	-20
Denver, CO	26	28
Grand Junction, CO	323	6
Boise, ID	253	69
Great Falls, MT	29	-29
Reno, NV	144	-83
Elko, NV	152	-27
Medford, OR	346	105
Salem, OR	51	6
Rapid City, SD	45	-70
Salt Lake City, UT	438	10
Riverton, WY	119	-74

Table 6. Terrain elevation difference between station elevation and interpolated RUC20 elevation for selected rawinsonde stations in western United States. Column 2 shows this difference for the RUC20 model elevation field, and column 3 shows this difference for the RUC20 TOPOMINI elevation used for reducing 2-m temperature and dewpoint fields.

A detailed description of techniques to derive RUC diagnostic variables is available at http://ruc.fsl.noaa.gov/vartxt.html . Some of these are listed below, and are unchanged from RUC40.

Relative humidity - Defined with respect to saturation over water in the RUC isobaric fields and in the surface relative humidity field.

Freezing levels - Two sets of freezing levels are output from RUC, one searching from the bottom up, and one searching from the top down. Of course, these two sets will be equivalent under most situations, but they may sometimes identify multiple freezing levels. The bottom-up algorithm will return the surface as the freezing level if any of the bottom three native RUC levels (up to about 50 m above the surface) are below freezing (per instructions from Aviation Weather Center, which uses this product). The top-down freezing level returns the first level at which the temperature goes above freezing searching from the top downward. For both the top-down and bottom-up algorithms, the freezing level is actually interpolated between native levels to estimate the level at which the temperature goes above or below freezing.

Tropopause pressure - Diagnosed from the 2.0 isentropic potential vorticity unit (PVU) surface. The 2.0 PVU surface is calculated directly from the native isentropic/sigma RUC grids. First, a 3-D PV field is calculated in the layers between RUC levels from the native grid. Then, the PV=2 surface is calculated by interpolating in the layer where PV is first found to be less than 2.0 searching from the top down in each grid column. Low tropopause

regions correspond to upper-level waves and give a quasi-3D way to look at upper-level potential vorticity. They also correspond very well to dry (warm) areas in water vapor satellite images, since stratospheric air is very dry.

MAPS mean sea-level pressure - This reduction (Benjamin and Miller 1990) is the one used in previous versions of the RUC. It uses the 700 hPa temperature to minimize unrepresentative local variations caused by local surface temperature variations. It has some improvement over the standard reduction method in mountainous areas and gives geostrophic winds that are more consistent with observed surface winds. As noted earlier, a bug fix for reduction over higher terrain is included in the RUC20, improving the coherence of the sea-level pressure pattern in these areas.

3-h surface pressure change - These fields are determined by differencing surface pressure fields at valid times separated by 3 h. Since altimeter setting values (surface pressure) are used in the RUC analyses, this field reflects the observed 3-h pressure change fairly closely over areas with surface observations. It is based on the forecast in data-void regions. The 3-h pressure change field during the first 3 h of a model forecast often shows some non-physical features, resulting from gravity wave sloshing in the model. After 3 h, the pressure change field appears to be quite well-behaved. The smaller-scale features in this field appear to be very useful for seeing predicted movement of lows, surges, etc. despite the slosh at the beginning of the forecast.

2m temperature, dewpoint temperature - Temperature and dewpoint temperatures displayed are extrapolated to a "minimum" topography field to give values more representative of valley stations in mountainous areas, where surface stations are usually located.

Precipitation accumulation - All precipitation values, including the 12-h total, are liquid equivalents, regardless of whether the precipitation is rain, snow, or graupel.

Resolvable and subgrid scale precipitation – The Grell family of convective schemes used in the RUC tends to force grid-scale saturation in its feedback to temperature and moisture fields. One result of this is that for the RUC model, some of the precipitation from weather systems that might be considered to be largely convective will be reflected in the resolvable-scale precipitation. Thus, the subgrid scale precipitation from RUC should *not* be considered equivalent to "convective precipitation."

Snow accumulation - Snow accumulations are calculated using a 10 to 1 ratio between snow and liquid water equivalent. Of course, in reality, the ratio of snow to liquid water equivalent varies, but the ratio used here was set at this constant value so that users will know the water equivalent exactly.

Also, snow accumulation (through the snow liquid water equivalent) is not diagnosed based on temperature, but is explicitly forecast through the mixed-phase cloud microphysics in the RUC model.

Categorical precipitation types - rain/snow/ice pellets/freezing rain - These yes/no indicators are calculated from the explicit cloud microphysics in the RUC model (see section 3.b.1**).** *These values are not mutually exclusive. More than one value can be yes (1) at a grid point. In other words, the RUC can predict mixed precipitation types.* Here is how the diagnostics are done:

Diagnostic logic for precipitation types

- Snow

  There are a few ways to get snow.

  - If fall rate for snow mixing ratio at ground is at least 0.2 x 10^{-9} g/g/second, snow is diagnosed.
  - If fall rate for graupel mixing ratio at ground is > 1.0 x 10^{-9} g/g/s and
    - surface temp is < 0 deg C, and max rain mixing ratio at any level < 0.05 g/kg or the graupel rate at the surface is less than the snow fall rate, snow is diagnosed.
    - surface temp is between 0 - +2 deg C, snow is diagnosed.

- Rain - If the fall rate for rain mixing ratio at ground is at least 0.01 g/g/second, and the temperature at the surface is > or = 0 deg C, then rain is diagnosed. The temperature used for this diagnosis is that at the minimum topography, described above.
- Freezing rain - Same as for rain, but if the temperature at the surface is < 0 deg C **and** some level above the surface is above freezing, freezing rain is diagnosed.
- Ice pellets - If
    - the graupel fall rate at the surface is at least 1.0×10^{-9} g/g/s and
    - the surface temp is < 0 deg C and the max rain mixing ratio in the column is > 0.05 g/kg and
    - the graupel fall rate at the surface is greater than that for snow mixing ratio,

    then ice pellets are diagnosed.

CAPE (Convective available potential energy) - Energy available for buoyant parcel from native RUC levels with maximum buoyancy within 300 hPa of surface. Before the most buoyant level is determined, an averaging of potential temperature and water vapor mixing ratio is done in the lowest seven RUC native levels (about 40 hPa).

CIN (Convective inhibition) -- Negative buoyant energy in layer through which a potentially buoyant parcel must be lifted before becoming positively buoyant.

Lifted index / Best lifted index - Lifted index uses the surface parcel, and best lifted index uses buoyant parcel from the native RUC level with maximum buoyancy within 300 hPa.

Precipitable water - Integrated precipitable water vapor from surface of RUC model to top level (~50 hPa). The precipitable water calculation is performed by summing the product of the specific humidity at each level times the mass of each surrounding layer. This mass layer is bounded by the mid-points between each level, since the native RUC vertical grid is nonstaggered.

7. STATISTICAL VERIFICATION AGAINST RAWINSONDES

RUC20 forecast skill was compared with that of the RUC40 for retrospective periods from February 2001 (cold season, statistics at http://www.emc.ncep.noaa.gov/mmb/ruc2/oiretrostats/) and July 2001 (warm season, statistics at http://www.emc.ncep.noaa.gov/mmb/ruc2/summerretrostats/). In addition, recent real-time runs provide results from cold season and transition season periods (statistics at http://www.emc.ncep.noaa.gov/mmb/ruc2/stats). In general, RUC20 analyses do not fit rawinsonde data quite as closely at this time as RUC40 analyses. This may be due to improved use of aircraft ascent/descent data in the case of wind and temperature analyses, and the use of ln q as a moisture analysis variable in the case of relative humidity.

For wind forecasts (Fig. 14a), the RUC20 provides some improvement over the RUC40 for 3-h forecasts (margin 0 – 0.3 ms^{-1}) and for 12-h forecasts (margin 0.1 – 0.4 ms^{-1}). For temperatures (Fig. 14b), the RUC20 again gives some improvement by this measure, especially in the lower troposphere.

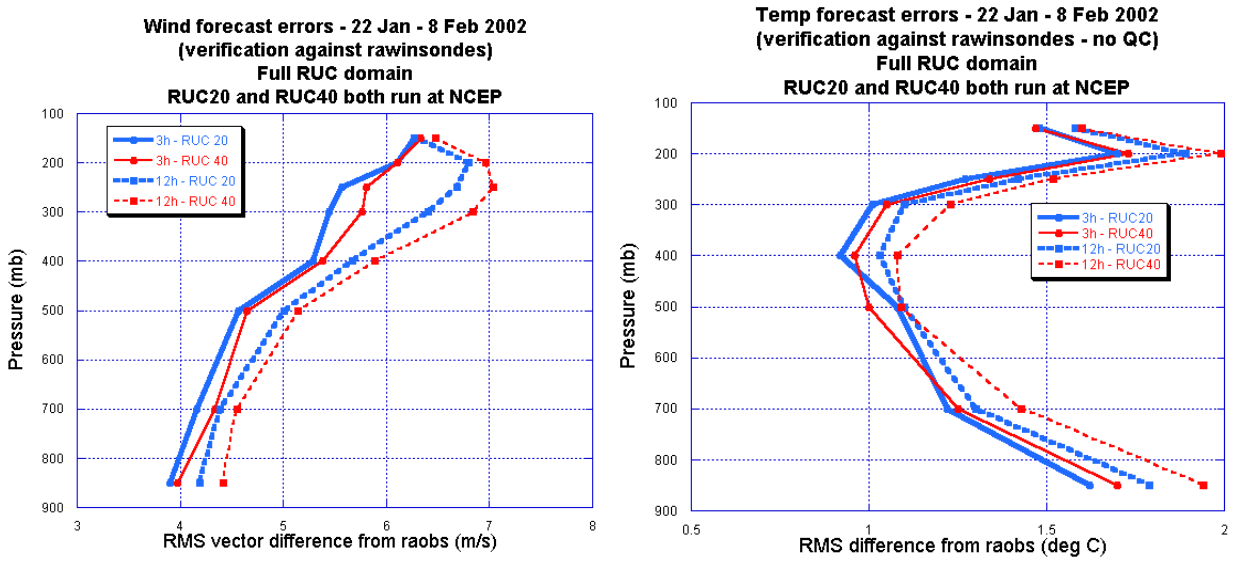

Figure 14. Verification of RUC40 and RUC20 3-h and 12-h forecasts against rawinsonde observations. For a) wind, and b) temperature, and for period 22 January – 8 February 2002.

8. REFERENCES

RUC web page – http://ruc.fsl.noaa.gov - real time products and a great deal of other information including a more complete list of references

Arakawa, A., and V.R. Lamb, 1977: Computational design of the basic dynamical processes of the UCLA general circulation model. *Methods in Computational Physics*, Vol. 17, Academic Press, 174-265, 337 pp.

Benjamin, S.G., J.M. Brown, D. Devenyi, G.A. Grell, D. Kim, T.L. Smith, T.G. Smirnova, B.E. Schwartz, S. Weygandt, K.J. Brundage, and G.S. Manikin, 2002a: The 20-km Rapid Update Cycle--Overview and implications for aviation applications. *10th Conf. on Aviation, Range, and Aerospace Meteorology*, Portland, OR, Amer. Meteor. Soc., 24-27. (available in PDF from http://ruc.fsl.noaa.gov under 'RUC pubs')

Benjamin, S.G., D. Kim, and J.M. Brown, 2002b: Cloud/hydrometeor initialization in the 20-km RUC with GOES and radar data. *10th Conf. on Aviation, Range, and Aerospace Meteorology*, Portland, OR, Amer. Meteor. Soc., 232-235. (available in PDF from http://ruc.fsl.noaa.gov under 'RUC pubs')

Benjamin, S.G., J.M. Brown, K.J. Brundage, B.E. Schwartz, T.G. Smirnova, T.L. Smith, L.L. Morone, 1998: RUC-2 - The Rapid Update Cycle Version 2. NWS Technical Procedure Bulletin No. 448. NOAA/NWS, 18 pp. [National Weather Service, Office of Meteorology, 1325 East-West Highway, Silver Spring, MD 20910] Available online at http://205.156.54.206/om/tpb/448.htm).

Benjamin, S.G., K.J. Brundage, and L.L. Morone, 1994: The Rapid Update Cycle. Part I: Analysis/model description. Technical Procedures Bulletin No. 416, NOAA/NWS, 16 pp. [National Weather Service, Office of Meteorology, 1325 East-West Highway, Silver Spring, MD 20910].

Benjamin, S. G., K. A. Brewster, R. L. Brummer, B. F. Jewett, T. W. Schlatter, T. L. Smith, and P. A. Stamus, 1991: An isentropic three-hourly data assimilation system using ACARS aircraft observations. *Mon. Wea. Rev.*, **119**, 888-906.

Benjamin, S. G., and P. A. Miller, 1990: An alternative sea-level pressure reduction and a statistical comparison of surface geostrophic wind estimates with observed winds. *Mon. Wea. Rev.*, **118**, 2099-2116.

Benjamin, S. G., 1989: An isentropic meso-alpha scale analysis system and its sensitivity to aircraft and surface observations. *Mon. Wea. Rev.*, **117**, 1586-1603.

Bleck, R., and S.G. Benjamin, 1993. Regional weather prediction with a model combining terrain-following and isentropic coordinates. Part I: model description. *Mon. Wea. Rev.*, **121**, 1770-1885.

Brown, J.M., T.G. Smirnova, S.G. Benjamin, R. Rasmussen, G. Thompson, and K. Manning, 2000: Use of a mixed-phase microphysics scheme in the operational NCEP Rapid Update Cycle. *9th Conf. on Aviation, Range, and Aerospace Meteorology*, Amer. Meteor. Soc., Orlando, FL, 100-101.

Bunkers, M.J., B.A. Klimowski, J.W. Zeitler, R.L. Thompson, M.L. Weisman, 2000: Prediction of supercell motion using a new hodograph technique. *Wea. Forecast.*, **15**, 61-79.

Burk, S.D., and W.T. Thompson, 1989: A vertically nested regional numerical prediction model with second-order closure physics. *Mon. Wea. Rev*., **117**, 2305-2324.

Csiszar, I. and G. Gutman, 1999: Mapping global land surface albedo from NOAA/AVHRR. *J Geophys. Res.* **104**, 6215-6228.

Davies, H.C., 1976: A lateral boundary formulation for multi-level prediction models. *Tellus*, **102**, 405-418.

Devenyi, D., S.G. Benjamin, and S.S. Weygandt, 2001: 3DVAR analysis in the Rapid Update Cycle. *14th Conf. on Numerical Weather Prediction,* Fort Lauderdale, FL, Amer. Meteor. Soc., J103-J107.

Dudhia, J., 1989: Numerical study of convection observed during the winter monsoon experiment using a mesoscale two-dimensional model. *J. Atmos. Sci*., **46**, 3077-3107.

Govett, M.W., D.S. Schaffer, T.Henderson, L.B. Hart, J.P. Edwards, C.S. Lior and T.L. Lee, 2001: SMS: A directive-based parallelization approach for shared and distributed memory high performance computers. Proceedings 9th ECMWF Workshop on the Use of High Performance Computing in Meteorology, Volume: Developments in TeraComputing, *World Scientific*, 251-268.

Grell, G.A., 1993: Prognostic evaluation of assumptions used by cumulus parameterizations. *Mon. Wea. Rev*., **121**, 764-787.

Grell, G.A., J. Dudhia, and D.R. Stauffer, 1994: A description of the fifth-generation Penn State/NCAR Mesoscale Model (MM5). NCAR Technical Note, NCAR/TN-398 + STR, 138 pp.

Grell, G.A., and D. Devenyi, 2001: Parameterized convection with ensemble closure/feedback assumptions. *9th Conf. on Mesoscale Processes*, Fort Lauderdale, FL, Amer. Meteor. Soc., 12-16.

Gutman, G. and A. Ignatov, 1998: The derivation of green vegetation fraction from NOAA/AVHRR for use in numerical weather prediction models. *Int. J. Remote Sens*., **19**, 1533-1543.

Johansen, O., 1975: Thermal conductivity in soils. Ph.D. thesis, University of Trondheim, 236 pp. (English translation 637, Cold Reg. Res. and Eng. Lab., Hanover, N.H., 1977).

Johnson, D.R., T.H. Zapotocny, F.M. Reames, B.J. Wolf, and R.B. Pierce, 1993: A comparison of simulated precipitation by hybrid isentropic-sigma and sigma models. *Mon. Wea. Rev*., **121**, 2088-2114.

Johnson, D.R., A.J. Lenzen, T.H. Zapotocny, and T.K. Schaack, 2000: Numerical uncertainties in the simulation of reversible isentropic processes and entropy conservation. *J. Climate,* **13**, 3860-3884.

Kain, J.S., and J.M. Fritsch, 1992: The role of the convective "trigger function" in numerical forecasts of mesoscale convective systems. *Meteor. Atmos. Phys*., **49**, 93-106.

Kain, J.S., M.E. Baldwin, D.J. Stensrud, T.L. Black, and G.S. Manikin, 1998: Considerations for the implementation of a convective parameterization in an operational mesoscale model. *12th Conf. Num Wea. Pred*., Amer. Meteor. Soc., Phoenix, 103-106.

Kim, D., and S.G. Benjamin, 2001: Cloud/hydrometeor initialization for the 20-km RUC using satellite and radar data. *14th Conf. on Num. Wea. Pred.*, Fort Lauderdale, FL, Amer. Meteor. Soc., J113-J115.

Kim, D., and S.G. Benjamin, 2000: An initial RUC cloud analysis assimilating GOES cloud-top data. Preprints, 9th Conf. on Aviation, Range, and Aerospace Meteorology, AMS, Orlando, 522-524.

Lynch, P. and X.-Y. Huang, 1992: Initialization of the HIRLAM model using a digital filter. *Mon. Wea. Rev.,* **120**, 1019-1034.

Pan, H.-L. and L. Mahrt, 1987: Interaction between soil hydrology and boundary-layer development. *Bound.-Layer Meteorol.,* **38**, 185-202.

Olsen, M.A., W.A. Gallus, J.L. Stanford, and J.M. Brown, 2000: An intense Midwestern cyclone: Fine-scale comparisons of model analysis with TOMS total ozone data. *J. Geophys. Res*., **105**, 20487-20495.

Pan, Z., S.G. Benjamin, J.M. Brown, and T. Smirnova. 1994. Comparative experiments with MAPS on different parameterization schemes for surface moisture flux and boundary- layer processes. *Mon. Wea. Rev*. **122**, 449-470.

Peters-Lidard, C. D., E. Blackburn, X. Liang, and E. F. Wood, 1998: The effect of soil thermal conductivity parmeterization on surface energy fluxes and temperatures, *J. Atmos. Sci*., **55**, 1209-1224.

Reisner, J., R.M. Rasmussen, and R.T. Bruintjes, 1998: Explicit forecasting of supercooled liquid water in winter storms using the MM5 mesoscale model. *Quart. J. Roy. Meteor. Soc*., **142**, 1071-1107.

Schreiner, A. J., T. J. Schmit, W. Paul Menzel, 2001: Clouds based on GOES sounder data. *J. Geophys. Res*., **106,** (D17), 20349-20363 **.**

Schwartz, B.E., and S.G. Benjamin, 2002: Verification of RUC surface forecasts at major U.S. airport hubs. *10th Conf. on Aviation, Range, and Aerospace Meteorology*, Portland, OR, Amer. Meteor. Soc., 327-330. (available in PDF from http://ruc.fsl.noaa.gov under 'RUC pubs')

Smirnova, T.G., S.G. Benjamin, and J.M. Brown, 2000: Case study verification of RUC/MAPS fog and visibility forecasts. *9th Conf. on Aviation, Range, and Aerospace Meteorology*, AMS, Orlando, 31-36.

Smirnova, T.G., J.M. Brown, S.G. Benjamin, and D. Kim, 2000: Parameterization of cold-season processes in the MAPS land-surface scheme. *J. Geophys. Res.,* **105, D3,** 4077-4086.

Smirnova, T. G., J. M. Brown, and S. G. Benjamin, 1997: Performance of different soil model configurations in simulating ground surface temperature and surface fluxes. *Mon. Wea. Rev*., **125**, 1870-1884.

Smith, T.L., and S.G. Benjamin, 2002: Visibility forecasts from the RUC20. *10th Conf. on Aviation, Range, and Aerospace Meteorology*, Portland, OR, Amer. Meteor. Soc., 150-153. (available in PDF from http://ruc.fsl.noaa.gov under 'RUC pubs')

Smolarkiewicz, P.K., 1983: A simple positive-definite advection transport algorithm. *Mon. Wea. Rev*., **111**, 479-486.

APPENDIX A. Known or suspected RUC20 biases or deficiencies as of April 2002 (per FSL)

- Some remaining light precipitation bias. Even though the RUC20 clearly has reduced the dry precipitation bias from the RUC40, some of this bias remains (Fig. 7).
- Weak diurnal cycle. Again, this problem has been considerably improved in the RUC20, but it has not disappeared. The RUC20 seems to do fairly well for daytime temperatures, but overall, does not cool quite enough at night (Fig. 8).
- Too cold at night over snow cover. The RUC20 seems to cool off at night too much over snow covered areas. FSL has developed a fix to this problem that will be tested further and, if successful, will be implemented hopefully over the next several months.

APPENDIX B. Comments from field users during RUC20 evaluation from late March to early April 2002.

Fred Mosher – SOO – Aviation Weather Center

While the time period for the RUC20 evaluation was short, and the weather was rather benign during the evaluation period, the evaluation did show the RUC20 to be a definite improvement over the current RUC2 model. The AWC evaluation focused mainly on the derived hazard fields (clouds, convection, turbulence, and visibility) rather than the traditional state of the atmosphere parameters (winds, temperature, etc.). The cloud tops and the convective cloud tops showed a major improvement, as did the visibility fields. This shows a definite improvement in the moisture distribution and the cloud physics parameterizations within the models, as well as the ability of the RUC20 to better assimilate initial time period meteorological information. We did not notice any degradation of the forecast skill for any field, and we did notice big improvements in some fields. Hence the AWC would recommend that the RUC20 model become the operational NCEP model used for short-term forecasts.

Steve Weiss – SOO – Storm Prediction Center

Our ability to assess the RUC20 has been tempered somewhat by the relatively inactive severe weather season so far this spring, however we have been able to formulate some preliminary assessments based on a small number of cases so far. I will focus on the Mar 25, Mar 29, and Apr 2 severe weather cases and attach some gif images relevant to each case. In the gif images [not shown here], the RUC40x files refer to the RUC20 output displayed on a 40 km grid. In addition, Greg Carbin has created two web pages that examine 1) a 3 hour forecast of precipitation valid at 00z Mar 18, and 2) 06z 28 Mar 00hr forecasts of 850 mb wind associated with the low level jet. These can be found at

1) http://www.spc.noaa.gov/staff/carbin/rucrvu/
2) http://www.spc.noaa.gov/staff/carbin/rucrvu2/

In Greg's first case, the RUC20 appears to overforecast the development of a precipitation along a front across the TN valley into AR, with radar showing that an elevated band of convection north of the front (and RUC20 forecast) is the primary precipitation activity at the verifying time. In his second case, he observed that the RUC20 depicts 850 mb winds that are much weaker than observed by profilers and radar VWP. (There is some question regarding a possible influence of birds and/or insects in the profiler/VAD winds, especially near the center of the 850 mb low where you might expect weaker winds.) In both cases, the RUC40 appeared to be better than the RUC20. If you have the data available, it would be good to look back at these cases. [FSL note: This case is a bird contamination flagging issue. The RUC40 does not use the Profiler Hub flags, and so it let through profiler observations that the RUC20 did not use since it honors the Profiler Hub flags.]

Our assessment focus has been primarily on short range forecasts of moisture, instability, and precipitation in support of our short range severe weather forecast mission. Overall, we have found no persistent evidence suggesting that the RUC20 should not be implemented as scheduled on April 16. The higher model resolution in the RUC20 seems to develop mesoscale features in the precipitation and vertical velocity fields that appear more realistic than the RUC40, even when viewed at identical display resolutions. In addition, our small sample indicates the forecasts of MUCAPE are better from the RUC20 than the RUC40, although aspects of low level temperature and dew point profiles from one case (Mar 29) raise interesting questions concerning the evolution of the afternoon boundary layer. Given the small number of cases we have seen, we plan to continue evaluating the RUC20 during this storm season in order to gain a better understanding of its strengths and weaknesses as it relates to convective forecasting issues. As always, we appreciate the opportunity to participate in the pre-implementation evaluation.

Mar 25...15z runs with forecasts valid at 00z and 03z
A weak surface low was forecast to move into central AR during the afternoon, and both RUC20 and RUC40 showed a similar scenario that verified well by 00z. The RUC20 predicted higher CAPE into central AR compared to the RUC40 (1000-1500 j/kg versus around 500 j/kg) and the stronger CAPE forecast also verified better. Both RUC versions predicted 3 hourly precipitation developing near the front from western TN across AR into parts of LA and east TX by 00z and continuing through 03z. Although precipitation did develop along the corridor predicted, both models were too fast in developing storms southward into east TX. The RUC20 700-500 mb mean vertical velocity and 3 hourly precipitation forecasts exhibited more detailed structures that appeared to relate better to the actual convective development when compared to the RUC40 forecasts.

Mar 29...12z runs with forecasts valid 00z
On this day, there were two severe threat areas: 1) morning elevated severe storms moving eastward from MO toward the OH valley were expected to develop southward into the warm sector over AR/TN during the afternoon, and 2) new convection was expected to develop over west/north central TX during the late afternoon or evening as moisture returned northwestward across TX in advance of a strong upper low moving toward the southern Rockies.

Both models were similar in predicting surface dew points over the lower MS valley region although the 12 hour forecast from the RUC20 was considered slightly better. Across TX both models did not transport surface moisture fast enough into southwest and central TX, with the RUC40 worse than the RUC20. This resulted in not enough instability being forecast into central and southwest TX by both models. Overall, the instability predicted over the lower MS valley region by the RUC20 was "in the ballpark", and better than that from the RUC40 (see below for more discussion of sounding profiles).

Twelve-hour forecasts of 3 hourly precipitation were similar from both models but the RUC20 showed more realistic details in structure and location when compared to observed radar images over the OH and lower TN valleys. Unlike the RUC40, the RUC20 also developed precipitation over a small part of southwest TX by 00z. Although deficient in coverage, the RUC20 forecast was more in agreement with the severe storms that had developed by that time over parts of southwest/west central TX.

We also looked closely at model forecast soundings constructed from 25 mb vertical grids, and compared the model forecasts with observed soundings at LIT, SHV, and JAN. (There was precipitation occurring at BNA by 00z, so this sounding may not be representative of the preconvective environment.) In all cases, the models were able to accurately predict the general vertical structure in the warm sector showing a warm, moist boundary layer overlaid

by an inversion based in the 800-850 mb layer, with drier conditions above the inversion before moistening again in the middle and upper levels. The forecast inversion was not as sharp as in the observed soundings, but this may be partially related to the use of 25 mb vertical grids which can smooth out some of the details between vertical levels. In all cases the RUC20 appeared to produce a boundary layer that was cooler and more moist than the observed boundary layers. The RUC40 forecast soundings were characterized by low level temperature profiles similar to observed profiles, but moisture was greater than forecast (similar to the RUC20). As a result, the RUC20 moisture/temperature errors tended to compensate for each other and forecast MUCAPE values were closer to the observed values, whereas the RUC40 MUCAPE values were much higher than observed. Here is a small table with forecast and observed MUCAPE values from two raob sites at 00z 30 Mar computed from NSHARP:

Location	RUC20	RUC40	Raob
SHV	2303	3869	2831
LIT	2708	3541	1879

(JAN observed sounding was a short run - observed MUCAPE could not be computed)

Apr 02...12z run with forecasts valid 00z
There was a slight risk of severe thunderstorms across parts of AR/west TN in the day 2 and day 1 outlooks. Moisture was forecast to return northward ahead of an advancing cold front, with an axis of instability forecast by the RUC40 and RUC20 during the afternoon. A primary question was determining whether or not thunderstorms would develop along the front during the afternoon. Both versions of the RUC indicated little in the way of precipitation by 00z, although the RUC20 showed a better defined axis of upward vertical motion in the 700-500 mb layer north of the surface front location. The lack of precipitation verified quite well, as thunderstorms failed to develop across the area. In this case, the forecast soundings were quite close to the observed sounding at LIT, including boundary layer profiles of temperature and moisture.

Tim Garner – NWS Spaceflight Meteorology Group (SMG), Johnson Space Flight Center, Houston, TX

I filled out the on-line form concerning the RUC for a forecast on 25 March for the Edwards AFB and White Sands areas. The RUC20 properly simulated that the mountains east of White Sands would block the progress of a cold front. Low level winds on either side of the Tularosa Basin (location of White Sands) were simulated quite well. Flow inside the basin during the day was quite light and variable so it was hard to ascertain how well the model performed. In general that day it did an admirable job simulating the low level winds in southern California.

I looked in more detail on the 27th when I used the 06Z and 12Z RUC20 runs as the primary tool for a landing simulation that we were working. The RUC20 appeared to be the only model (including NGM and AVN MOS) that forecasted a sea breeze in Florida. The forecast verified quite well. I had to fend off a lot of questions from some of the NASA users as to whether or not I was sure the winds would change. The RUC20 was almost spot on with the 10m winds. It did seem to overdo the precipitation in Florida later that afternoon, but I didn't stick around much after 21Z to see how well it did. This is a great improvement. I remember how poorly the RUC low level winds were over Florida when it first came out. The early RUC was so disappointing that we lost so much confidence in it that we rarely used it.

As far as precipitation forecasts go, neither Tim Oram nor I have noticed whether it has been any better or worse than the RUC40.

Pablo Santos – SOO, Miami, FL

We have been using the model operationally for almost two weeks. Weather has been quite active for us particularly during the afternoons this whole week. I used the model myself operationally for two days last week and I have gotten feedback from 2 forecasters so far. So far the model is proving to be a very good mesoscale guidance tool. It picks up the sea breeze development but not as well as the Eta 12 although we might attribute that to resolution [FSL note: Using 40km display] and the fact the we are looking at the Eta 12 in AWIPS through the D2D which gives us a lot of control over the display properties. The precipitation field forecast is

turning out to be pretty good also although we do not concentrate much on QPF but rather the when and where. In this area it seems to be hand on hand with the Eta12. Although it is to early and soon to tell given how long we have had it, you can tell data from the FSL Mesoscale data networks is going into it, and hence FAWN (Florida Agricultural Weather Network) (am I right?). It seems it produces better analysis fields to begin with that guidance we obtain from NCEP. Again, this is something I cannot conclude for certain until I get the data in AWIPS and am able to sample to grid. [FSL note: Mesonet data is only assimilated in FSL RUC20 as of this time, but is planned to be added to the NCEP RUC20 within a few months of this writing.]

The great advantage with this model is how frequently it updates. It really provides us with an excellent tool in the scale of hours when rapidly developing/weakening Florida type convection occurs. That to us is invaluable.

Chris Buonanno – SOO, Little Rock, AR

Our office has often utilized the precipitation forecasts from the RUC20. We have found these forecasts to be particularly useful during the 6-18 h time frame, to help determine areal coverage (or lack of), and quantitative precipitation amounts during convective situations. We have noted that overall locations of forecast precipitation from the RUC20 seem to be improved compared to those from the RUC40. We have also noted during several recent events that the RUC20 correctly forecasted a lack of precipitation during situations where convective inhibition limited the extent of convection.

APPENDIX D

SCREEN3 MODELING INPUT AND OUTPUT FILES

Screen3 Run

100% Load

05/07/04

12:51:43

*** SCREEN3 MODEL RUN ***
*** VERSION DATED 96043 ***

STEAG-917 ft (279.5m) Stack-100% Load, 2 Units, Steam Generator

COMPLEX TERRAIN INPUTS:

SOURCE TYPE	=	POINT
EMISSION RATE (G/S)	=	103.000
STACK HT (M)	=	279.5000
STACK DIAMETER (M)	=	11.2100
STACK VELOCITY (M/S)	=	24.9900
STACK GAS TEMP (K)	=	323.1500
AMBIENT AIR TEMP (K)	=	293.0000
RECEPTOR HEIGHT (M)	=	.0000
URBAN/RURAL OPTION	=	RURAL

THE REGULATORY (DEFAULT) MIXING HEIGHT OPTION WAS SELECTED.
THE REGULATORY (DEFAULT) ANEMOMETER HEIGHT OF 10.0 METERS WAS ENTERED.

BUOY. FLUX = 718.290 M**4/S**3; MOM. FLUX =17788.820 M**4/S**2.

FINAL STABLE PLUME HEIGHT (M) = 442.3
DISTANCE TO FINAL RISE (M) = 151.3

			VALLEY 24-HR CALCS		**SIMPLE TERRAIN 24-HR CALCS**			
TERR HT (M)	DIST (M)	MAX 24-HR CONC (UG/M**3)	CONC (UG/M**3)	PLUME HT ABOVE STK BASE (M)	CONC (UG/M**3)	PLUME HT ABOVE STK HGT (M)	SC	U10M USTK (M/S)
292.	20000.	14.71	1.961	442.3	14.71	180.5	5	1.0 3.2

05/07/04

12:51:43

*** SCREEN3 MODEL RUN ***
*** VERSION DATED 96043 ***

STEAG-917 ft (279.5m) Stack-100% Load, 2 Units, Steam Generator

SIMPLE TERRAIN INPUTS:

SOURCE TYPE	=	POINT
EMISSION RATE (G/S)	=	103.000
STACK HEIGHT (M)	=	279.5000

```
   STK INSIDE DIAM (M)    =      11.2100
   STK EXIT VELOCITY (M/S)=      24.9900
   STK GAS EXIT TEMP (K)  =     323.1500
   AMBIENT AIR TEMP (K)   =     293.0000
   RECEPTOR HEIGHT (M)    =        .0000
   URBAN/RURAL OPTION     =        RURAL
   BUILDING HEIGHT (M)    =     165.0000
   MIN HORIZ BLDG DIM (M) =      96.2000
   MAX HORIZ BLDG DIM (M) =      96.2000

THE REGULATORY (DEFAULT) MIXING HEIGHT OPTION WAS SELECTED.
THE REGULATORY (DEFAULT) ANEMOMETER HEIGHT OF 10.0 METERS WAS ENTERED.


BUOY. FLUX =  718.290 M**4/S**3;  MOM. FLUX =17788.820 M**4/S**2.

*** STABILITY CLASS  4 ONLY ***
*** ANEMOMETER HEIGHT WIND SPEED OF  10.00 M/S ONLY ***

*********************************
*** SCREEN DISCRETE DISTANCES ***
*********************************

*** TERRAIN HEIGHT OF    0. M ABOVE STACK BASE USED FOR FOLLOWING DISTANCES ***

  DIST     CONC             U10M   USTK  MIX HT   PLUME   SIGMA   SIGMA
   (M)   (UG/M**3)   STAB  (M/S)  (M/S)    (M)   HT (M)   Y (M)   Z (M)  DWASH
-------  ----------  ----  -----  -----  ------  ------  ------  ------  -----
  1000.   5.637        4    10.0   16.5  3200.0  366.45   72.51  137.16    HS
  2000.   5.610        4    10.0   16.5  3200.0  401.02  132.57  170.99    HS

*********************************
*** SCREEN DISCRETE DISTANCES ***
*********************************

*** TERRAIN HEIGHT OF   28. M ABOVE STACK BASE USED FOR FOLLOWING DISTANCES ***

  DIST     CONC             U10M   USTK  MIX HT   PLUME   SIGMA   SIGMA
   (M)   (UG/M**3)   STAB  (M/S)  (M/S)    (M)   HT (M)   Y (M)   Z (M)  DWASH
-------  ----------  ----  -----  -----  ------  ------  ------  ------  -----
  3000.   6.539        4    10.0   16.5  3200.0  372.82  187.87  177.24    HS

*********************************
*** SCREEN DISCRETE DISTANCES ***
*********************************
```

*** TERRAIN HEIGHT OF 30. M ABOVE STACK BASE USED FOR FOLLOWING DISTANCES ***

DIST (M)	CONC (UG/M**3)	STAB	U10M (M/S)	USTK (M/S)	MIX HT (M)	PLUME HT (M)	SIGMA Y (M)	SIGMA Z (M)	DWASH
4000.	5.802	4	10.0	16.5	3200.0	370.82	241.81	183.32	HS
5000.	5.235	4	10.0	16.5	3200.0	370.82	294.53	189.26	HS
6000.	4.836	4	10.0	16.5	3200.0	370.82	346.18	195.05	HS

****
*** SCREEN DISCRETE DISTANCES ***
****

*** TERRAIN HEIGHT OF 34. M ABOVE STACK BASE USED FOR FOLLOWING DISTANCES ***

DIST (M)	CONC (UG/M**3)	STAB	U10M (M/S)	USTK (M/S)	MIX HT (M)	PLUME HT (M)	SIGMA Y (M)	SIGMA Z (M)	DWASH
7000.	4.701	4	10.0	16.5	3200.0	366.82	396.93	200.72	HS

****
*** SCREEN DISCRETE DISTANCES ***
****

*** TERRAIN HEIGHT OF 60. M ABOVE STACK BASE USED FOR FOLLOWING DISTANCES ***

DIST (M)	CONC (UG/M**3)	STAB	U10M (M/S)	USTK (M/S)	MIX HT (M)	PLUME HT (M)	SIGMA Y (M)	SIGMA Z (M)	DWASH
8000.	5.512	4	10.0	16.5	3200.0	340.82	446.88	206.27	HS
9000.	5.184	4	10.0	16.5	3200.0	340.82	496.12	211.71	HS

****
*** SCREEN DISCRETE DISTANCES ***
****

*** TERRAIN HEIGHT OF 105. M ABOVE STACK BASE USED FOR FOLLOWING DISTANCES ***

DIST (M)	CONC (UG/M**3)	STAB	U10M (M/S)	USTK (M/S)	MIX HT (M)	PLUME HT (M)	SIGMA Y (M)	SIGMA Z (M)	DWASH
10000.	6.647	4	10.0	16.5	3200.0	295.82	544.72	217.04	HS

****

*** SCREEN DISCRETE DISTANCES ***
****

*** TERRAIN HEIGHT OF 152. M ABOVE STACK BASE USED FOR FOLLOWING DISTANCES ***

DIST (M)	CONC (UG/M**3)	STAB	U10M (M/S)	USTK (M/S)	MIX HT (M)	PLUME HT (M)	SIGMA Y (M)	SIGMA Z (M)	DWASH
11000.	8.070	4	10.0	16.5	3200.0	248.82	592.75	222.28	HS

****
*** SCREEN DISCRETE DISTANCES ***
****

*** TERRAIN HEIGHT OF 185. M ABOVE STACK BASE USED FOR FOLLOWING DISTANCES ***

DIST (M)	CONC (UG/M**3)	STAB	U10M (M/S)	USTK (M/S)	MIX HT (M)	PLUME HT (M)	SIGMA Y (M)	SIGMA Z (M)	DWASH
12000.	8.709	4	10.0	16.5	3200.0	215.82	640.25	227.42	HS

****
*** SCREEN DISCRETE DISTANCES ***
****

*** TERRAIN HEIGHT OF 188. M ABOVE STACK BASE USED FOR FOLLOWING DISTANCES ***

DIST (M)	CONC (UG/M**3)	STAB	U10M (M/S)	USTK (M/S)	MIX HT (M)	PLUME HT (M)	SIGMA Y (M)	SIGMA Z (M)	DWASH
13000.	8.189	4	10.0	16.5	3200.0	212.82	687.27	232.48	HS
14000.	7.640	4	10.0	16.5	3200.0	212.82	733.84	237.45	HS

****
*** SCREEN DISCRETE DISTANCES ***
****

*** TERRAIN HEIGHT OF 243. M ABOVE STACK BASE USED FOR FOLLOWING DISTANCES ***

DIST (M)	CONC (UG/M**3)	STAB	U10M (M/S)	USTK (M/S)	MIX HT (M)	PLUME HT (M)	SIGMA Y (M)	SIGMA Z (M)	DWASH
15000.	8.514	4	10.0	16.5	3200.0	157.82	779.99	242.34	HS
16000.	7.950	4	10.0	16.5	3200.0	157.82	825.76	247.17	HS

****
*** SCREEN DISCRETE DISTANCES ***
****

*** TERRAIN HEIGHT OF 213. M ABOVE STACK BASE USED FOR FOLLOWING DISTANCES ***

DIST (M)	CONC (UG/M**3)	STAB	U10M (M/S)	USTK (M/S)	MIX HT (M)	PLUME HT (M)	SIGMA Y (M)	SIGMA Z (M)	DWASH
17000.	6.866	4	10.0	16.5	3200.0	187.82	871.15	251.92	HS

****
*** SCREEN DISCRETE DISTANCES ***
****

*** TERRAIN HEIGHT OF 232. M ABOVE STACK BASE USED FOR FOLLOWING DISTANCES ***

DIST (M)	CONC (UG/M**3)	STAB	U10M (M/S)	USTK (M/S)	MIX HT (M)	PLUME HT (M)	SIGMA Y (M)	SIGMA Z (M)	DWASH
18000.	6.892	4	10.0	16.5	3200.0	168.82	916.20	251.53	HS

****
*** SCREEN DISCRETE DISTANCES ***
****

*** TERRAIN HEIGHT OF 247. M ABOVE STACK BASE USED FOR FOLLOWING DISTANCES ***

DIST (M)	CONC (UG/M**3)	STAB	U10M (M/S)	USTK (M/S)	MIX HT (M)	PLUME HT (M)	SIGMA Y (M)	SIGMA Z (M)	DWASH
19000.	6.752	4	10.0	16.5	3200.0	153.82	960.93	255.95	HS

DWASH=   MEANS NO CALC MADE (CONC = 0.0)
DWASH=NO MEANS NO BUILDING DOWNWASH USED
DWASH=HS MEANS HUBER-SNYDER DOWNWASH USED
DWASH=SS MEANS SCHULMAN-SCIRE DOWNWASH USED
DWASH=NA MEANS DOWNWASH NOT APPLICABLE, X<3*LB

****
* SUMMARY OF TERRAIN HEIGHTS ENTERED FOR *
*   SIMPLE ELEVATED TERRAIN PROCEDURE   *
****

     TERRAIN   DISTANCE RANGE (M)

HT (M)	MINIMUM	MAXIMUM
0.	1000.	--
0.	2000.	--
28.	3000.	--
30.	4000.	--
30.	5000.	--
30.	6000.	--
34.	7000.	--
60.	8000.	--
60.	9000.	--
105.	10000.	--
152.	11000.	--
185.	12000.	--
188.	13000.	--
188.	14000.	--
243.	15000.	--
243.	16000.	--
213.	17000.	--
232.	18000.	--
247.	19000.	--

****
*** REGULATORY (Default) ***
PERFORMING CAVITY CALCULATIONS
WITH ORIGINAL SCREEN CAVITY MODEL
(BRODE, 1988)
****

*** CAVITY CALCULATION - 1 ***			*** CAVITY CALCULATION - 2 ***		
CONC (UG/M**3)	=	432.6	CONC (UG/M**3)	=	432.6
CRIT WS @10M (M/S)	=	14.12	CRIT WS @10M (M/S)	=	14.12
CRIT WS @ HS (M/S)	=	27.48	CRIT WS @ HS (M/S)	=	27.48
DILUTION WS (M/S)	=	10.00	DILUTION WS (M/S)	=	10.00
CAVITY HT (M)	=	288.72	CAVITY HT (M)	=	288.72
CAVITY LENGTH (M)	=	207.63	CAVITY LENGTH (M)	=	207.63
ALONGWIND DIM (M)	=	96.20	ALONGWIND DIM (M)	=	96.20

****
END OF CAVITY CALCULATIONS
****

****

*** SUMMARY OF SCREEN MODEL RESULTS ***
****

CALCULATION PROCEDURE	MAX CONC (UG/M**3)	DIST TO MAX (M)	TERRAIN HT (M)	
SIMPLE TERRAIN	8.709	12000.	185.	
COMPLEX TERRAIN	14.71	20000.	292.	(24-HR CONC)

****
** REMEMBER TO INCLUDE BACKGROUND CONCENTRATIONS **
****

05/07/04

12:53:07

 *** SCREEN3 MODEL RUN ***
 *** VERSION DATED 96043 ***

 STEAG-917 ft (279.5m) Stack-100% Load, 1 Unit, Steam Generator

 COMPLEX TERRAIN INPUTS:
    SOURCE TYPE   =   POINT
    EMISSION RATE (G/S)   =   51.5000
    STACK HT (M)   =   279.5000
    STACK DIAMETER (M)   =   7.9200
    STACK VELOCITY (M/S)   =   24.9900
    STACK GAS TEMP (K)   =   323.1500
    AMBIENT AIR TEMP (K)   =   293.0000
    RECEPTOR HEIGHT (M)   =   .0000
    URBAN/RURAL OPTION   =   RURAL

 THE REGULATORY (DEFAULT) MIXING HEIGHT OPTION WAS SELECTED.
 THE REGULATORY (DEFAULT) ANEMOMETER HEIGHT OF 10.0 METERS WAS ENTERED.

 BUOY. FLUX = 358.541 M**4/S**3; MOM. FLUX = 8879.456 M**4/S**2.

 FINAL STABLE PLUME HEIGHT (M) = 408.6
 DISTANCE TO FINAL RISE (M)   = 151.3

                          VALLEY 24-HR CALCS   **SIMPLE TERRAIN 24-HR CALCS**
  TERR   MAX 24-HR   PLUME HT   PLUME HT
   HT   DIST   CONC   CONC   ABOVE STK   CONC   ABOVE STK   U10M USTK
  (M)   (M)   (UG/M**3)   (UG/M**3) BASE (M) (UG/M**3) HGT (M) SC   (M/S)
 ----- ------- ---------- ---------- ------   ---------- ------ -- ---- ----
  292. 20000. 11.24   1.899   408.6   11.24   95.2   6 1.0 6.2
                                                                      05/07/04
                                                                      12:53:07
  *** SCREEN3 MODEL RUN ***
  *** VERSION DATED 96043 ***

 STEAG-917 ft (279.5m) Stack-100% Load, 1 Unit, Steam Generator

 SIMPLE TERRAIN INPUTS:
    SOURCE TYPE   =   POINT
    EMISSION RATE (G/S)   =   51.5000
    STACK HEIGHT (M)   =   279.5000

```
   STK INSIDE DIAM (M)    =       7.9200
   STK EXIT VELOCITY (M/S)=      24.9900
   STK GAS EXIT TEMP (K)  =     323.1500
   AMBIENT AIR TEMP (K)   =     293.0000
   RECEPTOR HEIGHT (M)    =        .0000
   URBAN/RURAL OPTION     =        RURAL
   BUILDING HEIGHT (M)    =     165.0000
   MIN HORIZ BLDG DIM (M) =      96.2000
   MAX HORIZ BLDG DIM (M) =      96.2000

THE REGULATORY (DEFAULT) MIXING HEIGHT OPTION WAS SELECTED.
THE REGULATORY (DEFAULT) ANEMOMETER HEIGHT OF 10.0 METERS WAS ENTERED.


BUOY. FLUX =  358.541 M**4/S**3;  MOM. FLUX = 8879.456 M**4/S**2.

*** STABILITY CLASS  4 ONLY ***
*** ANEMOMETER HEIGHT WIND SPEED OF  10.00 M/S ONLY ***

*********************************
*** SCREEN DISCRETE DISTANCES ***
*********************************

*** TERRAIN HEIGHT OF    0. M ABOVE STACK BASE USED FOR FOLLOWING DISTANCES ***

  DIST     CONC             U10M   USTK  MIX HT   PLUME   SIGMA   SIGMA
   (M)   (UG/M**3)   STAB  (M/S)  (M/S)    (M)   HT (M)   Y (M)   Z (M)  DWASH
-------  ----------  ----  -----  -----  ------  ------  ------  ------  -----
  1000.    3.921        4    10.0   16.5  3200.0  348.47   70.92  136.32    HS
  2000.    4.707        4    10.0   16.5  3200.0  359.59  129.97  168.99    HS

*********************************
*** SCREEN DISCRETE DISTANCES ***
*********************************

*** TERRAIN HEIGHT OF   28. M ABOVE STACK BASE USED FOR FOLLOWING DISTANCES ***

  DIST     CONC             U10M   USTK  MIX HT   PLUME   SIGMA   SIGMA
   (M)   (UG/M**3)   STAB  (M/S)  (M/S)    (M)   HT (M)   Y (M)   Z (M)  DWASH
-------  ----------  ----  -----  -----  ------  ------  ------  ------  -----
  3000.    5.109        4    10.0   16.5  3200.0  331.39  186.05  175.31    HS

*********************************
*** SCREEN DISCRETE DISTANCES ***
*********************************
```

*** TERRAIN HEIGHT OF 30. M ABOVE STACK BASE USED FOR FOLLOWING DISTANCES ***

DIST (M)	CONC (UG/M**3)	STAB	U10M (M/S)	USTK (M/S)	MIX HT (M)	PLUME HT (M)	SIGMA Y (M)	SIGMA Z (M)	DWASH
4000.	4.390	4	10.0	16.5	3200.0	329.39	240.40	181.45	HS
5000.	3.863	4	10.0	16.5	3200.0	329.39	293.37	187.45	HS
6000.	3.490	4	10.0	16.5	3200.0	329.39	345.20	193.30	HS

****
*** SCREEN DISCRETE DISTANCES ***
****

*** TERRAIN HEIGHT OF 34. M ABOVE STACK BASE USED FOR FOLLOWING DISTANCES ***

DIST (M)	CONC (UG/M**3)	STAB	U10M (M/S)	USTK (M/S)	MIX HT (M)	PLUME HT (M)	SIGMA Y (M)	SIGMA Z (M)	DWASH
7000.	3.316	4	10.0	16.5	3200.0	325.39	396.07	199.02	HS

****
*** SCREEN DISCRETE DISTANCES ***
****

*** TERRAIN HEIGHT OF 60. M ABOVE STACK BASE USED FOR FOLLOWING DISTANCES ***

DIST (M)	CONC (UG/M**3)	STAB	U10M (M/S)	USTK (M/S)	MIX HT (M)	PLUME HT (M)	SIGMA Y (M)	SIGMA Z (M)	DWASH
8000.	3.736	4	10.0	16.5	3200.0	299.39	446.12	204.61	HS
9000.	3.462	4	10.0	16.5	3200.0	299.39	495.43	210.09	HS

****
*** SCREEN DISCRETE DISTANCES ***
****

*** TERRAIN HEIGHT OF 105. M ABOVE STACK BASE USED FOR FOLLOWING DISTANCES ***

DIST (M)	CONC (UG/M**3)	STAB	U10M (M/S)	USTK (M/S)	MIX HT (M)	PLUME HT (M)	SIGMA Y (M)	SIGMA Z (M)	DWASH
10000.	4.226	4	10.0	16.5	3200.0	254.39	544.10	215.46	HS

****

*** SCREEN DISCRETE DISTANCES ***
****

*** TERRAIN HEIGHT OF 152. M ABOVE STACK BASE USED FOR FOLLOWING DISTANCES ***

DIST (M)	CONC (UG/M**3)	STAB	U10M (M/S)	USTK (M/S)	MIX HT (M)	PLUME HT (M)	SIGMA Y (M)	SIGMA Z (M)	DWASH
11000.	4.894	4	10.0	16.5	3200.0	207.39	592.18	220.74	HS

****
*** SCREEN DISCRETE DISTANCES ***
****

*** TERRAIN HEIGHT OF 185. M ABOVE STACK BASE USED FOR FOLLOWING DISTANCES ***

DIST (M)	CONC (UG/M**3)	STAB	U10M (M/S)	USTK (M/S)	MIX HT (M)	PLUME HT (M)	SIGMA Y (M)	SIGMA Z (M)	DWASH
12000.	5.109	4	10.0	16.5	3200.0	174.39	639.72	225.92	HS

****
*** SCREEN DISCRETE DISTANCES ***
****

*** TERRAIN HEIGHT OF 188. M ABOVE STACK BASE USED FOR FOLLOWING DISTANCES ***

DIST (M)	CONC (UG/M**3)	STAB	U10M (M/S)	USTK (M/S)	MIX HT (M)	PLUME HT (M)	SIGMA Y (M)	SIGMA Z (M)	DWASH
13000.	4.761	4	10.0	16.5	3200.0	171.39	686.78	231.00	HS
14000.	4.415	4	10.0	16.5	3200.0	171.39	733.38	236.01	HS

****
*** SCREEN DISCRETE DISTANCES ***
****

*** TERRAIN HEIGHT OF 243. M ABOVE STACK BASE USED FOR FOLLOWING DISTANCES ***

DIST (M)	CONC (UG/M**3)	STAB	U10M (M/S)	USTK (M/S)	MIX HT (M)	PLUME HT (M)	SIGMA Y (M)	SIGMA Z (M)	DWASH
15000.	4.713	4	10.0	16.5	3200.0	116.39	779.56	240.93	HS
16000.	4.383	4	10.0	16.5	3200.0	116.39	825.34	245.78	HS

```
*********************************
*** SCREEN DISCRETE DISTANCES ***
*********************************

*** TERRAIN HEIGHT OF  213. M ABOVE STACK BASE USED FOR FOLLOWING DISTANCES ***

  DIST     CONC             U10M   USTK  MIX HT   PLUME   SIGMA   SIGMA
   (M)   (UG/M**3)   STAB  (M/S)  (M/S)    (M)   HT (M)   Y (M)   Z (M)  DWASH
-------  ----------  ----  -----  -----  ------  ------  ------  ------  -----
 17000.   3.844        4    10.0   16.5  3200.0  146.39  870.76  250.56    HS

*********************************
*** SCREEN DISCRETE DISTANCES ***
*********************************

*** TERRAIN HEIGHT OF  232. M ABOVE STACK BASE USED FOR FOLLOWING DISTANCES ***

  DIST     CONC             U10M   USTK  MIX HT   PLUME   SIGMA   SIGMA
   (M)   (UG/M**3)   STAB  (M/S)  (M/S)    (M)   HT (M)   Y (M)   Z (M)  DWASH
-------  ----------  ----  -----  -----  ------  ------  ------  ------  -----
 18000.   3.814        4    10.0   16.5  3200.0  127.39  915.83  250.17    HS

*********************************
*** SCREEN DISCRETE DISTANCES ***
*********************************

*** TERRAIN HEIGHT OF  247. M ABOVE STACK BASE USED FOR FOLLOWING DISTANCES ***

  DIST     CONC             U10M   USTK  MIX HT   PLUME   SIGMA   SIGMA
   (M)   (UG/M**3)   STAB  (M/S)  (M/S)    (M)   HT (M)   Y (M)   Z (M)  DWASH
-------  ----------  ----  -----  -----  ------  ------  ------  ------  -----
 19000.   3.690        4    10.0   16.5  3200.0  112.39  960.57  254.62    HS

 DWASH=   MEANS NO CALC MADE (CONC = 0.0)
 DWASH=NO MEANS NO BUILDING DOWNWASH USED
 DWASH=HS MEANS HUBER-SNYDER DOWNWASH USED
 DWASH=SS MEANS SCHULMAN-SCIRE DOWNWASH USED
 DWASH=NA MEANS DOWNWASH NOT APPLICABLE, X<3*LB

 ******************************************
 *  SUMMARY OF TERRAIN HEIGHTS ENTERED FOR  *
 *    SIMPLE ELEVATED TERRAIN PROCEDURE     *
 ******************************************

      TERRAIN        DISTANCE RANGE (M)
```

HT (M)	MINIMUM	MAXIMUM
0.	1000.	--
0.	2000.	--
28.	3000.	--
30.	4000.	--
30.	5000.	--
30.	6000.	--
34.	7000.	--
60.	8000.	--
60.	9000.	--
105.	10000.	--
152.	11000.	--
185.	12000.	--
188.	13000.	--
188.	14000.	--
243.	15000.	--
243.	16000.	--
213.	17000.	--
232.	18000.	--
247.	19000.	--

****
*** REGULATORY (Default) ***
PERFORMING CAVITY CALCULATIONS
WITH ORIGINAL SCREEN CAVITY MODEL
(BRODE, 1988)
****

*** CAVITY CALCULATION - 1 ***			*** CAVITY CALCULATION - 2 ***		
CONC (UG/M**3)	=	216.3	CONC (UG/M**3)	=	216.3
CRIT WS @10M (M/S)	=	13.82	CRIT WS @10M (M/S)	=	13.82
CRIT WS @ HS (M/S)	=	26.90	CRIT WS @ HS (M/S)	=	26.90
DILUTION WS (M/S)	=	10.00	DILUTION WS (M/S)	=	10.00
CAVITY HT (M)	=	288.72	CAVITY HT (M)	=	288.72
CAVITY LENGTH (M)	=	207.63	CAVITY LENGTH (M)	=	207.63
ALONGWIND DIM (M)	=	96.20	ALONGWIND DIM (M)	=	96.20

****
END OF CAVITY CALCULATIONS
****

****

*** SUMMARY OF SCREEN MODEL RESULTS ***
****

CALCULATION PROCEDURE	MAX CONC (UG/M**3)	DIST TO MAX (M)	TERRAIN HT (M)	
SIMPLE TERRAIN	5.109	12000.	185.	
COMPLEX TERRAIN	11.24	20000.	292.	(24-HR CONC)

****
** REMEMBER TO INCLUDE BACKGROUND CONCENTRATIONS **
****

Screen3 Run

80% Load

05/07/04

12:53:41

```
 ***  SCREEN3 MODEL RUN  ***
 *** VERSION DATED 96043 ***

 STEAG-917 ft (279.5m) Stack-80% Load, 2 Units, Steam Generator

 COMPLEX TERRAIN INPUTS:
    SOURCE TYPE            =        POINT
    EMISSION RATE (G/S)    =      82.4000
    STACK HT (M)           =     279.5000
    STACK DIAMETER (M)     =      11.2100
    STACK VELOCITY (M/S)   =      19.5000
    STACK GAS TEMP (K)     =     323.1500
    AMBIENT AIR TEMP (K)   =     293.0000
    RECEPTOR HEIGHT (M)    =        .0000
    URBAN/RURAL OPTION     =        RURAL

 THE REGULATORY (DEFAULT) MIXING HEIGHT OPTION WAS SELECTED.
 THE REGULATORY (DEFAULT) ANEMOMETER HEIGHT OF 10.0 METERS WAS ENTERED.


 BUOY. FLUX =  560.490 M**4/S**3;  MOM. FLUX =10831.380 M**4/S**2.


 FINAL STABLE PLUME HEIGHT (M) =  429.3
 DISTANCE TO FINAL RISE (M)    =  151.3

                          *VALLEY 24-HR CALCS*   **SIMPLE TERRAIN 24-HR CALCS**
  TERR         MAX 24-HR              PLUME HT              PLUME HT
   HT    DIST    CONC        CONC    ABOVE STK    CONC    ABOVE STK    U10M USTK
  (M)    (M)   (UG/M**3)   (UG/M**3)  BASE (M)  (UG/M**3)  HGT (M)  SC   (M/S)
 ----- ------- ----------  ----------  ------   ----------  ------  -- ---- ----
  292.  20000.  13.77       2.018       429.3    13.77       166.2   5  1.0  3.2
                                                                     05/07/04
                                                                     12:53:41
  ***  SCREEN3 MODEL RUN  ***
  *** VERSION DATED 96043 ***

 STEAG-917 ft (279.5m) Stack-80% Load, 2 Units, Steam Generator

 SIMPLE TERRAIN INPUTS:
    SOURCE TYPE            =        POINT
    EMISSION RATE (G/S)    =      82.4000
    STACK HEIGHT (M)       =     279.5000
```

```
   STK INSIDE DIAM (M)    =      11.2100
   STK EXIT VELOCITY (M/S)=      19.5000
   STK GAS EXIT TEMP (K)  =     323.1500
   AMBIENT AIR TEMP (K)   =     293.0000
   RECEPTOR HEIGHT (M)    =        .0000
   URBAN/RURAL OPTION     =        RURAL
   BUILDING HEIGHT (M)    =     165.0000
   MIN HORIZ BLDG DIM (M) =      96.2000
   MAX HORIZ BLDG DIM (M) =      96.2000

THE REGULATORY (DEFAULT) MIXING HEIGHT OPTION WAS SELECTED.
THE REGULATORY (DEFAULT) ANEMOMETER HEIGHT OF 10.0 METERS WAS ENTERED.


BUOY. FLUX =  560.490 M**4/S**3;  MOM. FLUX =10831.380 M**4/S**2.

*** STABILITY CLASS  4 ONLY ***
*** ANEMOMETER HEIGHT WIND SPEED OF  10.00 M/S ONLY ***

*********************************
*** SCREEN DISCRETE DISTANCES ***
*********************************

*** TERRAIN HEIGHT OF    0. M ABOVE STACK BASE USED FOR FOLLOWING DISTANCES ***

  DIST     CONC             U10M   USTK  MIX HT   PLUME   SIGMA   SIGMA
   (M)   (UG/M**3)   STAB  (M/S)  (M/S)    (M)   HT (M)   Y (M)   Z (M)  DWASH
-------  ----------  ----  -----  -----  ------  ------  ------  ------  -----
  1000.    5.863        4    10.0   16.5  3200.0  352.45   71.86  136.81    HS
  2000.    6.096        4    10.0   16.5  3200.0  377.11  131.40  170.08    HS

*********************************
*** SCREEN DISCRETE DISTANCES ***
*********************************

*** TERRAIN HEIGHT OF   28. M ABOVE STACK BASE USED FOR FOLLOWING DISTANCES ***

  DIST     CONC             U10M   USTK  MIX HT   PLUME   SIGMA   SIGMA
   (M)   (UG/M**3)   STAB  (M/S)  (M/S)    (M)   HT (M)   Y (M)   Z (M)  DWASH
-------  ----------  ----  -----  -----  ------  ------  ------  ------  -----
  3000.    6.816        4    10.0   16.5  3200.0  348.91  187.05  176.36    HS

*********************************
*** SCREEN DISCRETE DISTANCES ***
*********************************
```

*** TERRAIN HEIGHT OF 30. M ABOVE STACK BASE USED FOR FOLLOWING DISTANCES ***

DIST (M)	CONC (UG/M**3)	STAB	U10M (M/S)	USTK (M/S)	MIX HT (M)	PLUME HT (M)	SIGMA Y (M)	SIGMA Z (M)	DWASH
4000.	5.935	4	10.0	16.5	3200.0	346.91	241.17	182.48	HS
5000.	5.276	4	10.0	16.5	3200.0	346.91	294.00	188.44	HS
6000.	4.810	4	10.0	16.5	3200.0	346.91	345.74	194.26	HS

****
*** SCREEN DISCRETE DISTANCES ***
****

*** TERRAIN HEIGHT OF 34. M ABOVE STACK BASE USED FOR FOLLOWING DISTANCES ***

DIST (M)	CONC (UG/M**3)	STAB	U10M (M/S)	USTK (M/S)	MIX HT (M)	PLUME HT (M)	SIGMA Y (M)	SIGMA Z (M)	DWASH
7000.	4.612	4	10.0	16.5	3200.0	342.91	396.54	199.95	HS

****
*** SCREEN DISCRETE DISTANCES ***
****

*** TERRAIN HEIGHT OF 60. M ABOVE STACK BASE USED FOR FOLLOWING DISTANCES ***

DIST (M)	CONC (UG/M**3)	STAB	U10M (M/S)	USTK (M/S)	MIX HT (M)	PLUME HT (M)	SIGMA Y (M)	SIGMA Z (M)	DWASH
8000.	5.282	4	10.0	16.5	3200.0	316.91	446.53	205.52	HS
9000.	4.924	4	10.0	16.5	3200.0	316.91	495.81	210.97	HS

****
*** SCREEN DISCRETE DISTANCES ***
****

*** TERRAIN HEIGHT OF 105. M ABOVE STACK BASE USED FOR FOLLOWING DISTANCES ***

DIST (M)	CONC (UG/M**3)	STAB	U10M (M/S)	USTK (M/S)	MIX HT (M)	PLUME HT (M)	SIGMA Y (M)	SIGMA Z (M)	DWASH
10000.	6.133	4	10.0	16.5	3200.0	271.91	544.44	216.32	HS

****

*** SCREEN DISCRETE DISTANCES ***
****

*** TERRAIN HEIGHT OF 152. M ABOVE STACK BASE USED FOR FOLLOWING DISTANCES ***

DIST (M)	CONC (UG/M**3)	STAB	U10M (M/S)	USTK (M/S)	MIX HT (M)	PLUME HT (M)	SIGMA Y (M)	SIGMA Z (M)	DWASH
11000.	7.242	4	10.0	16.5	3200.0	224.91	592.49	221.58	HS

****
*** SCREEN DISCRETE DISTANCES ***
****

*** TERRAIN HEIGHT OF 185. M ABOVE STACK BASE USED FOR FOLLOWING DISTANCES ***

DIST (M)	CONC (UG/M**3)	STAB	U10M (M/S)	USTK (M/S)	MIX HT (M)	PLUME HT (M)	SIGMA Y (M)	SIGMA Z (M)	DWASH
12000.	7.666	4	10.0	16.5	3200.0	191.91	640.01	226.74	HS

****
*** SCREEN DISCRETE DISTANCES ***
****

*** TERRAIN HEIGHT OF 188. M ABOVE STACK BASE USED FOR FOLLOWING DISTANCES ***

DIST (M)	CONC (UG/M**3)	STAB	U10M (M/S)	USTK (M/S)	MIX HT (M)	PLUME HT (M)	SIGMA Y (M)	SIGMA Z (M)	DWASH
13000.	7.169	4	10.0	16.5	3200.0	188.91	687.05	231.81	HS
14000.	6.664	4	10.0	16.5	3200.0	188.91	733.63	236.80	HS

****
*** SCREEN DISCRETE DISTANCES ***
****

*** TERRAIN HEIGHT OF 243. M ABOVE STACK BASE USED FOR FOLLOWING DISTANCES ***

DIST (M)	CONC (UG/M**3)	STAB	U10M (M/S)	USTK (M/S)	MIX HT (M)	PLUME HT (M)	SIGMA Y (M)	SIGMA Z (M)	DWASH
15000.	7.243	4	10.0	16.5	3200.0	133.91	779.80	241.70	HS
16000.	6.747	4	10.0	16.5	3200.0	133.91	825.57	246.54	HS

****
*** SCREEN DISCRETE DISTANCES ***
****

*** TERRAIN HEIGHT OF 213. M ABOVE STACK BASE USED FOR FOLLOWING DISTANCES ***

DIST (M)	CONC (UG/M**3)	STAB	U10M (M/S)	USTK (M/S)	MIX HT (M)	PLUME HT (M)	SIGMA Y (M)	SIGMA Z (M)	DWASH
17000.	5.878	4	10.0	16.5	3200.0	163.91	870.97	251.30	HS

****
*** SCREEN DISCRETE DISTANCES ***
****

*** TERRAIN HEIGHT OF 232. M ABOVE STACK BASE USED FOR FOLLOWING DISTANCES ***

DIST (M)	CONC (UG/M**3)	STAB	U10M (M/S)	USTK (M/S)	MIX HT (M)	PLUME HT (M)	SIGMA Y (M)	SIGMA Z (M)	DWASH
18000.	5.861	4	10.0	16.5	3200.0	144.91	916.04	250.91	HS

****
*** SCREEN DISCRETE DISTANCES ***
****

*** TERRAIN HEIGHT OF 247. M ABOVE STACK BASE USED FOR FOLLOWING DISTANCES ***

DIST (M)	CONC (UG/M**3)	STAB	U10M (M/S)	USTK (M/S)	MIX HT (M)	PLUME HT (M)	SIGMA Y (M)	SIGMA Z (M)	DWASH
19000.	5.700	4	10.0	16.5	3200.0	129.91	960.77	255.35	HS

DWASH=   MEANS NO CALC MADE (CONC = 0.0)
DWASH=NO MEANS NO BUILDING DOWNWASH USED
DWASH=HS MEANS HUBER-SNYDER DOWNWASH USED
DWASH=SS MEANS SCHULMAN-SCIRE DOWNWASH USED
DWASH=NA MEANS DOWNWASH NOT APPLICABLE, X<3*LB

****
* SUMMARY OF TERRAIN HEIGHTS ENTERED FOR *
*   SIMPLE ELEVATED TERRAIN PROCEDURE   *
****

     TERRAIN   DISTANCE RANGE (M)

HT (M)	MINIMUM	MAXIMUM
0.	1000.	--
0.	2000.	--
28.	3000.	--
30.	4000.	--
30.	5000.	--
30.	6000.	--
34.	7000.	--
60.	8000.	--
60.	9000.	--
105.	10000.	--
152.	11000.	--
185.	12000.	--
188.	13000.	--
188.	14000.	--
243.	15000.	--
243.	16000.	--
213.	17000.	--
232.	18000.	--
247.	19000.	--

****
*** REGULATORY (Default) ***
PERFORMING CAVITY CALCULATIONS
WITH ORIGINAL SCREEN CAVITY MODEL
(BRODE, 1988)
****

*** CAVITY CALCULATION - 1 ***			*** CAVITY CALCULATION - 2 ***		
CONC (UG/M**3)	=	346.1	CONC (UG/M**3)	=	346.1
CRIT WS @10M (M/S)	=	11.04	CRIT WS @10M (M/S)	=	11.04
CRIT WS @ HS (M/S)	=	21.49	CRIT WS @ HS (M/S)	=	21.49
DILUTION WS (M/S)	=	10.00	DILUTION WS (M/S)	=	10.00
CAVITY HT (M)	=	288.72	CAVITY HT (M)	=	288.72
CAVITY LENGTH (M)	=	207.63	CAVITY LENGTH (M)	=	207.63
ALONGWIND DIM (M)	=	96.20	ALONGWIND DIM (M)	=	96.20

****
END OF CAVITY CALCULATIONS
****

****

*** SUMMARY OF SCREEN MODEL RESULTS ***
****

CALCULATION PROCEDURE	MAX CONC (UG/M**3)	DIST TO MAX (M)	TERRAIN HT (M)	
SIMPLE TERRAIN	7.666	12000.	185.	
COMPLEX TERRAIN	13.77	20000.	292.	(24-HR CONC)

****
** REMEMBER TO INCLUDE BACKGROUND CONCENTRATIONS **
****

05/07/04

12:54:04

*** SCREEN3 MODEL RUN ***
*** VERSION DATED 96043 ***

STEAG-917 ft (279.5m) Stack-80% Load, 1 Unit, Steam Generator

COMPLEX TERRAIN INPUTS:

SOURCE TYPE	=	POINT
EMISSION RATE (G/S)	=	41.2000
STACK HT (M)	=	279.5000
STACK DIAMETER (M)	=	7.9200
STACK VELOCITY (M/S)	=	19.5000
STACK GAS TEMP (K)	=	323.1500
AMBIENT AIR TEMP (K)	=	293.0000
RECEPTOR HEIGHT (M)	=	.0000
URBAN/RURAL OPTION	=	RURAL

THE REGULATORY (DEFAULT) MIXING HEIGHT OPTION WAS SELECTED.
THE REGULATORY (DEFAULT) ANEMOMETER HEIGHT OF 10.0 METERS WAS ENTERED.

BUOY. FLUX = 279.774 M**4/S**3; MOM. FLUX = 5406.585 M**4/S**2.

FINAL STABLE PLUME HEIGHT (M) = 398.4
DISTANCE TO FINAL RISE (M) = 151.3

			VALLEY 24-HR CALCS		**SIMPLE TERRAIN 24-HR CALCS**			
TERR HT (M)	DIST (M)	MAX 24-HR CONC (UG/M**3)	CONC (UG/M**3)	PLUME HT ABOVE STK BASE (M)	CONC (UG/M**3)	PLUME HT ABOVE STK HGT (M)	SC	U10M USTK (M/S)
292.	20000.	10.43	1.857	398.4	10.43	87.6	6	1.0 6.2

05/07/04

12:54:04

*** SCREEN3 MODEL RUN ***
*** VERSION DATED 96043 ***

STEAG-917 ft (279.5m) Stack-80% Load, 1 Unit, Steam Generator

SIMPLE TERRAIN INPUTS:

SOURCE TYPE	=	POINT
EMISSION RATE (G/S)	=	41.2000
STACK HEIGHT (M)	=	279.5000

```
   STK INSIDE DIAM (M)    =       7.9200
   STK EXIT VELOCITY (M/S)=      19.5000
   STK GAS EXIT TEMP (K)  =     323.1500
   AMBIENT AIR TEMP (K)   =     293.0000
   RECEPTOR HEIGHT (M)    =        .0000
   URBAN/RURAL OPTION     =        RURAL
   BUILDING HEIGHT (M)    =     165.0000
   MIN HORIZ BLDG DIM (M) =      96.2000
   MAX HORIZ BLDG DIM (M) =      96.2000

THE REGULATORY (DEFAULT) MIXING HEIGHT OPTION WAS SELECTED.
THE REGULATORY (DEFAULT) ANEMOMETER HEIGHT OF 10.0 METERS WAS ENTERED.


BUOY. FLUX =  279.774 M**4/S**3;  MOM. FLUX = 5406.585 M**4/S**2.

*** STABILITY CLASS  4 ONLY ***
*** ANEMOMETER HEIGHT WIND SPEED OF  10.00 M/S ONLY ***

*********************************
*** SCREEN DISCRETE DISTANCES ***
*********************************

*** TERRAIN HEIGHT OF    0. M ABOVE STACK BASE USED FOR FOLLOWING DISTANCES ***

  DIST     CONC             U10M   USTK  MIX HT   PLUME   SIGMA   SIGMA
   (M)   (UG/M**3)   STAB  (M/S)  (M/S)    (M)   HT (M)   Y (M)   Z (M)  DWASH
-------  ----------  ----  -----  -----  ------  ------  ------  ------  -----
  1000.    3.799        4    10.0   16.5  3200.0  337.98   70.50  136.10    HS
  2000.    4.575        4    10.0   16.5  3200.0  343.50  129.45  168.59    HS

*********************************
*** SCREEN DISCRETE DISTANCES ***
*********************************

*** TERRAIN HEIGHT OF   28. M ABOVE STACK BASE USED FOR FOLLOWING DISTANCES ***

  DIST     CONC             U10M   USTK  MIX HT   PLUME   SIGMA   SIGMA
   (M)   (UG/M**3)   STAB  (M/S)  (M/S)    (M)   HT (M)   Y (M)   Z (M)  DWASH
-------  ----------  ----  -----  -----  ------  ------  ------  ------  -----
  3000.    4.827        4    10.0   16.5  3200.0  315.30  185.69  174.92    HS

*********************************
*** SCREEN DISCRETE DISTANCES ***
*********************************
```

*** TERRAIN HEIGHT OF 30. M ABOVE STACK BASE USED FOR FOLLOWING DISTANCES ***

DIST (M)	CONC (UG/M**3)	STAB	U10M (M/S)	USTK (M/S)	MIX HT (M)	PLUME HT (M)	SIGMA Y (M)	SIGMA Z (M)	DWASH
4000.	4.097	4	10.0	16.5	3200.0	313.30	240.12	181.08	HS
5000.	3.570	4	10.0	16.5	3200.0	313.30	293.14	187.09	HS
6000.	3.199	4	10.0	16.5	3200.0	313.30	345.00	192.95	HS

****
*** SCREEN DISCRETE DISTANCES ***
****

*** TERRAIN HEIGHT OF 34. M ABOVE STACK BASE USED FOR FOLLOWING DISTANCES ***

DIST (M)	CONC (UG/M**3)	STAB	U10M (M/S)	USTK (M/S)	MIX HT (M)	PLUME HT (M)	SIGMA Y (M)	SIGMA Z (M)	DWASH
7000.	3.011	4	10.0	16.5	3200.0	309.30	395.90	198.68	HS

****
*** SCREEN DISCRETE DISTANCES ***
****

*** TERRAIN HEIGHT OF 60. M ABOVE STACK BASE USED FOR FOLLOWING DISTANCES ***

DIST (M)	CONC (UG/M**3)	STAB	U10M (M/S)	USTK (M/S)	MIX HT (M)	PLUME HT (M)	SIGMA Y (M)	SIGMA Z (M)	DWASH
8000.	3.339	4	10.0	16.5	3200.0	283.30	445.97	204.28	HS
9000.	3.077	4	10.0	16.5	3200.0	283.30	495.30	209.77	HS

****
*** SCREEN DISCRETE DISTANCES ***
****

*** TERRAIN HEIGHT OF 105. M ABOVE STACK BASE USED FOR FOLLOWING DISTANCES ***

DIST (M)	CONC (UG/M**3)	STAB	U10M (M/S)	USTK (M/S)	MIX HT (M)	PLUME HT (M)	SIGMA Y (M)	SIGMA Z (M)	DWASH
10000.	3.682	4	10.0	16.5	3200.0	238.30	543.97	215.15	HS

****

*** SCREEN DISCRETE DISTANCES ***
****

*** TERRAIN HEIGHT OF 152. M ABOVE STACK BASE USED FOR FOLLOWING DISTANCES ***

DIST (M)	CONC (UG/M**3)	STAB	U10M (M/S)	USTK (M/S)	MIX HT (M)	PLUME HT (M)	SIGMA Y (M)	SIGMA Z (M)	DWASH
11000.	4.184	4	10.0	16.5	3200.0	191.30	592.06	220.43	HS

****
*** SCREEN DISCRETE DISTANCES ***
****

*** TERRAIN HEIGHT OF 185. M ABOVE STACK BASE USED FOR FOLLOWING DISTANCES ***

DIST (M)	CONC (UG/M**3)	STAB	U10M (M/S)	USTK (M/S)	MIX HT (M)	PLUME HT (M)	SIGMA Y (M)	SIGMA Z (M)	DWASH
12000.	4.311	4	10.0	16.5	3200.0	158.30	639.62	225.62	HS

****
*** SCREEN DISCRETE DISTANCES ***
****

*** TERRAIN HEIGHT OF 188. M ABOVE STACK BASE USED FOR FOLLOWING DISTANCES ***

DIST (M)	CONC (UG/M**3)	STAB	U10M (M/S)	USTK (M/S)	MIX HT (M)	PLUME HT (M)	SIGMA Y (M)	SIGMA Z (M)	DWASH
13000.	4.005	4	10.0	16.5	3200.0	155.30	686.68	230.71	HS
14000.	3.706	4	10.0	16.5	3200.0	155.30	733.29	235.72	HS

****
*** SCREEN DISCRETE DISTANCES ***
****

*** TERRAIN HEIGHT OF 243. M ABOVE STACK BASE USED FOR FOLLOWING DISTANCES ***

DIST (M)	CONC (UG/M**3)	STAB	U10M (M/S)	USTK (M/S)	MIX HT (M)	PLUME HT (M)	SIGMA Y (M)	SIGMA Z (M)	DWASH
15000.	3.889	4	10.0	16.5	3200.0	100.30	779.47	240.65	HS
16000.	3.613	4	10.0	16.5	3200.0	100.30	825.26	245.51	HS

****
*** SCREEN DISCRETE DISTANCES ***
****

*** TERRAIN HEIGHT OF 213. M ABOVE STACK BASE USED FOR FOLLOWING DISTANCES ***

DIST (M)	CONC (UG/M**3)	STAB	U10M (M/S)	USTK (M/S)	MIX HT (M)	PLUME HT (M)	SIGMA Y (M)	SIGMA Z (M)	DWASH
17000.	3.189	4	10.0	16.5	3200.0	130.30	870.68	250.29	HS

****
*** SCREEN DISCRETE DISTANCES ***
****

*** TERRAIN HEIGHT OF 232. M ABOVE STACK BASE USED FOR FOLLOWING DISTANCES ***

DIST (M)	CONC (UG/M**3)	STAB	U10M (M/S)	USTK (M/S)	MIX HT (M)	PLUME HT (M)	SIGMA Y (M)	SIGMA Z (M)	DWASH
18000.	3.149	4	10.0	16.5	3200.0	111.30	915.76	249.90	HS

****
*** SCREEN DISCRETE DISTANCES ***
****

*** TERRAIN HEIGHT OF 247. M ABOVE STACK BASE USED FOR FOLLOWING DISTANCES ***

DIST (M)	CONC (UG/M**3)	STAB	U10M (M/S)	USTK (M/S)	MIX HT (M)	PLUME HT (M)	SIGMA Y (M)	SIGMA Z (M)	DWASH
19000.	3.032	4	10.0	16.5	3200.0	96.30	960.50	254.35	HS

DWASH=   MEANS NO CALC MADE (CONC = 0.0)
DWASH=NO MEANS NO BUILDING DOWNWASH USED
DWASH=HS MEANS HUBER-SNYDER DOWNWASH USED
DWASH=SS MEANS SCHULMAN-SCIRE DOWNWASH USED
DWASH=NA MEANS DOWNWASH NOT APPLICABLE, X<3*LB

****
* SUMMARY OF TERRAIN HEIGHTS ENTERED FOR *
*   SIMPLE ELEVATED TERRAIN PROCEDURE   *
****

     TERRAIN   DISTANCE RANGE (M)

HT (M)	MINIMUM	MAXIMUM
0.	1000.	--
0.	2000.	--
28.	3000.	--
30.	4000.	--
30.	5000.	--
30.	6000.	--
34.	7000.	--
60.	8000.	--
60.	9000.	--
105.	10000.	--
152.	11000.	--
185.	12000.	--
188.	13000.	--
188.	14000.	--
243.	15000.	--
243.	16000.	--
213.	17000.	--
232.	18000.	--
247.	19000.	--

****
*** REGULATORY (Default) ***
PERFORMING CAVITY CALCULATIONS
WITH ORIGINAL SCREEN CAVITY MODEL
(BRODE, 1988)
****

*** CAVITY CALCULATION - 1 ***			*** CAVITY CALCULATION - 2 ***		
CONC (UG/M**3)	=	173.0	CONC (UG/M**3)	=	173.0
CRIT WS @10M (M/S)	=	10.74	CRIT WS @10M (M/S)	=	10.74
CRIT WS @ HS (M/S)	=	20.91	CRIT WS @ HS (M/S)	=	20.91
DILUTION WS (M/S)	=	10.00	DILUTION WS (M/S)	=	10.00
CAVITY HT (M)	=	288.72	CAVITY HT (M)	=	288.72
CAVITY LENGTH (M)	=	207.63	CAVITY LENGTH (M)	=	207.63
ALONGWIND DIM (M)	=	96.20	ALONGWIND DIM (M)	=	96.20

****
END OF CAVITY CALCULATIONS
****

****

*** SUMMARY OF SCREEN MODEL RESULTS ***
****

CALCULATION PROCEDURE	MAX CONC (UG/M**3)	DIST TO MAX (M)	TERRAIN HT (M)	
SIMPLE TERRAIN	4.827	3000.	28.	
COMPLEX TERRAIN	10.43	20000.	292.	(24-HR CONC)

****
** REMEMBER TO INCLUDE BACKGROUND CONCENTRATIONS **
****

Screen3 Run

60% Load

05/07/04

12:54:26

*** SCREEN3 MODEL RUN ***
*** VERSION DATED 96043 ***

STEAG-917 ft (279.5m) Stack-60% Load, 2 Units, Steam Generator

COMPLEX TERRAIN INPUTS:

SOURCE TYPE	=	POINT
EMISSION RATE (G/S)	=	61.8000
STACK HT (M)	=	279.5000
STACK DIAMETER (M)	=	11.2100
STACK VELOCITY (M/S)	=	14.6200
STACK GAS TEMP (K)	=	323.1500
AMBIENT AIR TEMP (K)	=	293.0000
RECEPTOR HEIGHT (M)	=	.0000
URBAN/RURAL OPTION	=	RURAL

THE REGULATORY (DEFAULT) MIXING HEIGHT OPTION WAS SELECTED.
THE REGULATORY (DEFAULT) ANEMOMETER HEIGHT OF 10.0 METERS WAS ENTERED.

BUOY. FLUX = 420.224 M**4/S**3; MOM. FLUX = 6088.488 M**4/S**2.

FINAL STABLE PLUME HEIGHT (M) = 415.6
DISTANCE TO FINAL RISE (M) = 151.3

			VALLEY 24-HR CALCS		**SIMPLE TERRAIN 24-HR CALCS**			
TERR HT (M)	DIST (M)	MAX 24-HR CONC (UG/M**3)	CONC (UG/M**3)	PLUME HT ABOVE STK BASE (M)	CONC (UG/M**3)	PLUME HT ABOVE STK HGT (M)	SC	U10M USTK (M/S)
292.	20000.	12.16	1.984	415.6	12.16	100.3	6	1.0 6.2

05/07/04

12:54:26

*** SCREEN3 MODEL RUN ***
*** VERSION DATED 96043 ***

STEAG-917 ft (279.5m) Stack-60% Load, 2 Units, Steam Generator

SIMPLE TERRAIN INPUTS:

SOURCE TYPE	=	POINT
EMISSION RATE (G/S)	=	61.8000
STACK HEIGHT (M)	=	279.5000

```
   STK INSIDE DIAM (M)    =      11.2100
   STK EXIT VELOCITY (M/S)=      14.6200
   STK GAS EXIT TEMP (K)  =     323.1500
   AMBIENT AIR TEMP (K)   =     293.0000
   RECEPTOR HEIGHT (M)    =        .0000
   URBAN/RURAL OPTION     =        RURAL
   BUILDING HEIGHT (M)    =     165.0000
   MIN HORIZ BLDG DIM (M) =      96.2000
   MAX HORIZ BLDG DIM (M) =      96.2000

THE REGULATORY (DEFAULT) MIXING HEIGHT OPTION WAS SELECTED.
THE REGULATORY (DEFAULT) ANEMOMETER HEIGHT OF 10.0 METERS WAS ENTERED.


BUOY. FLUX =  420.224 M**4/S**3;  MOM. FLUX = 6088.488 M**4/S**2.

*** STABILITY CLASS  4 ONLY ***
*** ANEMOMETER HEIGHT WIND SPEED OF  10.00 M/S ONLY ***

*********************************
*** SCREEN DISCRETE DISTANCES ***
*********************************

*** TERRAIN HEIGHT OF    0. M ABOVE STACK BASE USED FOR FOLLOWING DISTANCES ***

  DIST     CONC             U10M   USTK  MIX HT   PLUME   SIGMA   SIGMA
   (M)   (UG/M**3)   STAB  (M/S)  (M/S)    (M)   HT (M)   Y (M)   Z (M)  DWASH
-------  ----------  ----  -----  -----  ------  ------  ------  ------  -----
  1000.    5.669        4    10.0   16.5  3200.0  338.48   71.22  136.48    HS
  2000.    6.088        4    10.0   16.5  3200.0  353.86  130.40  169.31    HS

*********************************
*** SCREEN DISCRETE DISTANCES ***
*********************************

*** TERRAIN HEIGHT OF   28. M ABOVE STACK BASE USED FOR FOLLOWING DISTANCES ***

  DIST     CONC             U10M   USTK  MIX HT   PLUME   SIGMA   SIGMA
   (M)   (UG/M**3)   STAB  (M/S)  (M/S)    (M)   HT (M)   Y (M)   Z (M)  DWASH
-------  ----------  ----  -----  -----  ------  ------  ------  ------  -----
  3000.    6.536        4    10.0   16.5  3200.0  325.66  186.35  175.62    HS

*********************************
*** SCREEN DISCRETE DISTANCES ***
*********************************
```

*** TERRAIN HEIGHT OF 30. M ABOVE STACK BASE USED FOR FOLLOWING DISTANCES ***

DIST (M)	CONC (UG/M**3)	STAB	U10M (M/S)	USTK (M/S)	MIX HT (M)	PLUME HT (M)	SIGMA Y (M)	SIGMA Z (M)	DWASH
4000.	5.591	4	10.0	16.5	3200.0	323.66	240.63	181.76	HS
5000.	4.901	4	10.0	16.5	3200.0	323.66	293.55	187.74	HS
6000.	4.413	4	10.0	16.5	3200.0	323.66	345.36	193.58	HS

****
*** SCREEN DISCRETE DISTANCES ***
****

*** TERRAIN HEIGHT OF 34. M ABOVE STACK BASE USED FOR FOLLOWING DISTANCES ***

DIST (M)	CONC (UG/M**3)	STAB	U10M (M/S)	USTK (M/S)	MIX HT (M)	PLUME HT (M)	SIGMA Y (M)	SIGMA Z (M)	DWASH
7000.	4.177	4	10.0	16.5	3200.0	319.66	396.21	199.29	HS

****
*** SCREEN DISCRETE DISTANCES ***
****

*** TERRAIN HEIGHT OF 60. M ABOVE STACK BASE USED FOR FOLLOWING DISTANCES ***

DIST (M)	CONC (UG/M**3)	STAB	U10M (M/S)	USTK (M/S)	MIX HT (M)	PLUME HT (M)	SIGMA Y (M)	SIGMA Z (M)	DWASH
8000.	4.674	4	10.0	16.5	3200.0	293.66	446.24	204.88	HS
9000.	4.322	4	10.0	16.5	3200.0	293.66	495.54	210.35	HS

****
*** SCREEN DISCRETE DISTANCES ***
****

*** TERRAIN HEIGHT OF 105. M ABOVE STACK BASE USED FOR FOLLOWING DISTANCES ***

DIST (M)	CONC (UG/M**3)	STAB	U10M (M/S)	USTK (M/S)	MIX HT (M)	PLUME HT (M)	SIGMA Y (M)	SIGMA Z (M)	DWASH
10000.	5.233	4	10.0	16.5	3200.0	248.66	544.20	215.72	HS

****

*** SCREEN DISCRETE DISTANCES ***
****

*** TERRAIN HEIGHT OF 152. M ABOVE STACK BASE USED FOR FOLLOWING DISTANCES ***

DIST (M)	CONC (UG/M**3)	STAB	U10M (M/S)	USTK (M/S)	MIX HT (M)	PLUME HT (M)	SIGMA Y (M)	SIGMA Z (M)	DWASH
11000.	6.014	4	10.0	16.5	3200.0	201.66	592.27	220.99	HS

****
*** SCREEN DISCRETE DISTANCES ***
****

*** TERRAIN HEIGHT OF 185. M ABOVE STACK BASE USED FOR FOLLOWING DISTANCES ***

DIST (M)	CONC (UG/M**3)	STAB	U10M (M/S)	USTK (M/S)	MIX HT (M)	PLUME HT (M)	SIGMA Y (M)	SIGMA Z (M)	DWASH
12000.	6.247	4	10.0	16.5	3200.0	168.66	639.81	226.16	HS

****
*** SCREEN DISCRETE DISTANCES ***
****

*** TERRAIN HEIGHT OF 188. M ABOVE STACK BASE USED FOR FOLLOWING DISTANCES ***

DIST (M)	CONC (UG/M**3)	STAB	U10M (M/S)	USTK (M/S)	MIX HT (M)	PLUME HT (M)	SIGMA Y (M)	SIGMA Z (M)	DWASH
13000.	5.814	4	10.0	16.5	3200.0	165.66	686.86	231.24	HS
14000.	5.387	4	10.0	16.5	3200.0	165.66	733.45	236.24	HS

****
*** SCREEN DISCRETE DISTANCES ***
****

*** TERRAIN HEIGHT OF 243. M ABOVE STACK BASE USED FOR FOLLOWING DISTANCES ***

DIST (M)	CONC (UG/M**3)	STAB	U10M (M/S)	USTK (M/S)	MIX HT (M)	PLUME HT (M)	SIGMA Y (M)	SIGMA Z (M)	DWASH
15000.	5.714	4	10.0	16.5	3200.0	110.66	779.63	241.16	HS
16000.	5.313	4	10.0	16.5	3200.0	110.66	825.41	246.01	HS

****
*** SCREEN DISCRETE DISTANCES ***
****

*** TERRAIN HEIGHT OF 213. M ABOVE STACK BASE USED FOR FOLLOWING DISTANCES ***

DIST (M)	CONC (UG/M**3)	STAB	U10M (M/S)	USTK (M/S)	MIX HT (M)	PLUME HT (M)	SIGMA Y (M)	SIGMA Z (M)	DWASH
17000.	4.670	4	10.0	16.5	3200.0	140.66	870.82	250.78	HS

****
*** SCREEN DISCRETE DISTANCES ***
****

*** TERRAIN HEIGHT OF 232. M ABOVE STACK BASE USED FOR FOLLOWING DISTANCES ***

DIST (M)	CONC (UG/M**3)	STAB	U10M (M/S)	USTK (M/S)	MIX HT (M)	PLUME HT (M)	SIGMA Y (M)	SIGMA Z (M)	DWASH
18000.	4.626	4	10.0	16.5	3200.0	121.66	915.89	250.39	HS

****
*** SCREEN DISCRETE DISTANCES ***
****

*** TERRAIN HEIGHT OF 247. M ABOVE STACK BASE USED FOR FOLLOWING DISTANCES ***

DIST (M)	CONC (UG/M**3)	STAB	U10M (M/S)	USTK (M/S)	MIX HT (M)	PLUME HT (M)	SIGMA Y (M)	SIGMA Z (M)	DWASH
19000.	4.467	4	10.0	16.5	3200.0	106.66	960.63	254.83	HS

DWASH=   MEANS NO CALC MADE (CONC = 0.0)
DWASH=NO MEANS NO BUILDING DOWNWASH USED
DWASH=HS MEANS HUBER-SNYDER DOWNWASH USED
DWASH=SS MEANS SCHULMAN-SCIRE DOWNWASH USED
DWASH=NA MEANS DOWNWASH NOT APPLICABLE, X<3*LB

****
* SUMMARY OF TERRAIN HEIGHTS ENTERED FOR *
*   SIMPLE ELEVATED TERRAIN PROCEDURE   *
****

     TERRAIN   DISTANCE RANGE (M)

HT (M)	MINIMUM	MAXIMUM
0.	1000.	--
0.	2000.	--
28.	3000.	--
30.	4000.	--
30.	5000.	--
30.	6000.	--
34.	7000.	--
60.	8000.	--
60.	9000.	--
105.	10000.	--
152.	11000.	--
185.	12000.	--
188.	13000.	--
188.	14000.	--
243.	15000.	--
243.	16000.	--
213.	17000.	--
232.	18000.	--
247.	19000.	--

****
*** REGULATORY (Default) ***
PERFORMING CAVITY CALCULATIONS
WITH ORIGINAL SCREEN CAVITY MODEL
(BRODE, 1988)
****

*** CAVITY CALCULATION - 1 ***			*** CAVITY CALCULATION - 2 ***		
CONC (UG/M**3)	=	324.5	CONC (UG/M**3)	=	324.5
CRIT WS @10M (M/S)	=	8.22	CRIT WS @10M (M/S)	=	8.22
CRIT WS @ HS (M/S)	=	16.00	CRIT WS @ HS (M/S)	=	16.00
DILUTION WS (M/S)	=	8.00	DILUTION WS (M/S)	=	8.00
CAVITY HT (M)	=	288.72	CAVITY HT (M)	=	288.72
CAVITY LENGTH (M)	=	207.63	CAVITY LENGTH (M)	=	207.63
ALONGWIND DIM (M)	=	96.20	ALONGWIND DIM (M)	=	96.20

****
END OF CAVITY CALCULATIONS
****

****

*** SUMMARY OF SCREEN MODEL RESULTS ***
****

CALCULATION PROCEDURE	MAX CONC (UG/M**3)	DIST TO MAX (M)	TERRAIN HT (M)	
SIMPLE TERRAIN	6.536	3000.	28.	
COMPLEX TERRAIN	12.16	20000.	292.	(24-HR CONC)

****
** REMEMBER TO INCLUDE BACKGROUND CONCENTRATIONS **
****

05/07/04

12:54:45

```
 ***  SCREEN3 MODEL RUN  ***
 *** VERSION DATED 96043 ***

 STEAG-917 ft (279.5m) Stack-60% Load, 1 Unit, Steam Generator

 COMPLEX TERRAIN INPUTS:
    SOURCE TYPE            =        POINT
    EMISSION RATE (G/S)    =      30.9000
    STACK HT (M)           =     279.5000
    STACK DIAMETER (M)     =       7.9200
    STACK VELOCITY (M/S)   =      14.6200
    STACK GAS TEMP (K)     =     323.1500
    AMBIENT AIR TEMP (K)   =     293.0000
    RECEPTOR HEIGHT (M)    =        .0000
    URBAN/RURAL OPTION     =        RURAL

 THE REGULATORY (DEFAULT) MIXING HEIGHT OPTION WAS SELECTED.
 THE REGULATORY (DEFAULT) ANEMOMETER HEIGHT OF 10.0 METERS WAS ENTERED.


 BUOY. FLUX =  209.759 M**4/S**3;  MOM. FLUX = 3039.125 M**4/S**2.


 FINAL STABLE PLUME HEIGHT (M) =  387.5
 DISTANCE TO FINAL RISE (M)    =  151.3

                          *VALLEY 24-HR CALCS*   **SIMPLE TERRAIN 24-HR CALCS**
  TERR         MAX 24-HR              PLUME HT              PLUME HT
   HT    DIST    CONC        CONC    ABOVE STK    CONC    ABOVE STK    U10M USTK
  (M)    (M)   (UG/M**3)   (UG/M**3)  BASE (M)  (UG/M**3)  HGT (M)  SC   (M/S)
 ----- ------- ----------  ----------  ------   ----------  ------  -- ---- ----
  292.  20000.  9.095       1.716       387.5    9.095        79.6   6  1.0  6.2
                                                                    05/07/04
                                                                    12:54:45
  ***  SCREEN3 MODEL RUN  ***
  *** VERSION DATED 96043 ***

 STEAG-917 ft (279.5m) Stack-60% Load, 1 Unit, Steam Generator

 SIMPLE TERRAIN INPUTS:
    SOURCE TYPE            =        POINT
    EMISSION RATE (G/S)    =      30.9000
    STACK HEIGHT (M)       =     279.5000
```

```
   STK INSIDE DIAM (M)    =       7.9200
   STK EXIT VELOCITY (M/S)=      14.6200
   STK GAS EXIT TEMP (K)  =     323.1500
   AMBIENT AIR TEMP (K)   =     293.0000
   RECEPTOR HEIGHT (M)    =        .0000
   URBAN/RURAL OPTION     =        RURAL
   BUILDING HEIGHT (M)    =     165.0000
   MIN HORIZ BLDG DIM (M) =      96.2000
   MAX HORIZ BLDG DIM (M) =      96.2000

THE REGULATORY (DEFAULT) MIXING HEIGHT OPTION WAS SELECTED.
THE REGULATORY (DEFAULT) ANEMOMETER HEIGHT OF 10.0 METERS WAS ENTERED.


BUOY. FLUX =  209.759 M**4/S**3;  MOM. FLUX = 3039.125 M**4/S**2.

*** STABILITY CLASS  4 ONLY ***
*** ANEMOMETER HEIGHT WIND SPEED OF  10.00 M/S ONLY ***

*********************************
*** SCREEN DISCRETE DISTANCES ***
*********************************

*** TERRAIN HEIGHT OF    0. M ABOVE STACK BASE USED FOR FOLLOWING DISTANCES ***

  DIST     CONC             U10M   USTK  MIX HT   PLUME   SIGMA   SIGMA
   (M)   (UG/M**3)   STAB  (M/S)  (M/S)    (M)   HT (M)   Y (M)   Z (M)  DWASH
-------  ----------  ----  -----  -----  ------  ------  ------  ------  -----
  1000.    3.435        4    10.0   16.5  3200.0  327.48   70.09  135.89    HS
  2000.    4.119        4    10.0   16.5  3200.0  327.86  129.01  168.25    HS

*********************************
*** SCREEN DISCRETE DISTANCES ***
*********************************

*** TERRAIN HEIGHT OF   28. M ABOVE STACK BASE USED FOR FOLLOWING DISTANCES ***

  DIST     CONC             U10M   USTK  MIX HT   PLUME   SIGMA   SIGMA
   (M)   (UG/M**3)   STAB  (M/S)  (M/S)    (M)   HT (M)   Y (M)   Z (M)  DWASH
-------  ----------  ----  -----  -----  ------  ------  ------  ------  -----
  3000.    4.228        4    10.0   16.5  3200.0  299.65  185.38  174.60    HS

*********************************
*** SCREEN DISCRETE DISTANCES ***
*********************************
```

*** TERRAIN HEIGHT OF 30. M ABOVE STACK BASE USED FOR FOLLOWING DISTANCES ***

DIST (M)	CONC (UG/M**3)	STAB	U10M (M/S)	USTK (M/S)	MIX HT (M)	PLUME HT (M)	SIGMA Y (M)	SIGMA Z (M)	DWASH
4000.	3.548	4	10.0	16.5	3200.0	297.65	239.88	180.77	HS
5000.	3.064	4	10.0	16.5	3200.0	297.65	292.94	186.78	HS
6000.	2.723	4	10.0	16.5	3200.0	297.65	344.84	192.65	HS

****
*** SCREEN DISCRETE DISTANCES ***
****

*** TERRAIN HEIGHT OF 34. M ABOVE STACK BASE USED FOR FOLLOWING DISTANCES ***

DIST (M)	CONC (UG/M**3)	STAB	U10M (M/S)	USTK (M/S)	MIX HT (M)	PLUME HT (M)	SIGMA Y (M)	SIGMA Z (M)	DWASH
7000.	2.542	4	10.0	16.5	3200.0	293.65	395.76	198.39	HS

****
*** SCREEN DISCRETE DISTANCES ***
****

*** TERRAIN HEIGHT OF 60. M ABOVE STACK BASE USED FOR FOLLOWING DISTANCES ***

DIST (M)	CONC (UG/M**3)	STAB	U10M (M/S)	USTK (M/S)	MIX HT (M)	PLUME HT (M)	SIGMA Y (M)	SIGMA Z (M)	DWASH
8000.	2.775	4	10.0	16.5	3200.0	267.65	445.84	204.00	HS
9000.	2.544	4	10.0	16.5	3200.0	267.65	495.18	209.50	HS

****
*** SCREEN DISCRETE DISTANCES ***
****

*** TERRAIN HEIGHT OF 105. M ABOVE STACK BASE USED FOR FOLLOWING DISTANCES ***

DIST (M)	CONC (UG/M**3)	STAB	U10M (M/S)	USTK (M/S)	MIX HT (M)	PLUME HT (M)	SIGMA Y (M)	SIGMA Z (M)	DWASH
10000.	2.985	4	10.0	16.5	3200.0	222.66	543.87	214.89	HS

****

*** SCREEN DISCRETE DISTANCES ***
****

*** TERRAIN HEIGHT OF 152. M ABOVE STACK BASE USED FOR FOLLOWING DISTANCES ***

DIST (M)	CONC (UG/M**3)	STAB	U10M (M/S)	USTK (M/S)	MIX HT (M)	PLUME HT (M)	SIGMA Y (M)	SIGMA Z (M)	DWASH
11000.	3.331	4	10.0	16.5	3200.0	175.66	591.97	220.17	HS

****
*** SCREEN DISCRETE DISTANCES ***
****

*** TERRAIN HEIGHT OF 185. M ABOVE STACK BASE USED FOR FOLLOWING DISTANCES ***

DIST (M)	CONC (UG/M**3)	STAB	U10M (M/S)	USTK (M/S)	MIX HT (M)	PLUME HT (M)	SIGMA Y (M)	SIGMA Z (M)	DWASH
12000.	3.389	4	10.0	16.5	3200.0	142.66	639.53	225.37	HS

****
*** SCREEN DISCRETE DISTANCES ***
****

*** TERRAIN HEIGHT OF 188. M ABOVE STACK BASE USED FOR FOLLOWING DISTANCES ***

DIST (M)	CONC (UG/M**3)	STAB	U10M (M/S)	USTK (M/S)	MIX HT (M)	PLUME HT (M)	SIGMA Y (M)	SIGMA Z (M)	DWASH
13000.	3.139	4	10.0	16.5	3200.0	139.66	686.59	230.47	HS
14000.	2.899	4	10.0	16.5	3200.0	139.66	733.21	235.48	HS

****
*** SCREEN DISCRETE DISTANCES ***
****

*** TERRAIN HEIGHT OF 243. M ABOVE STACK BASE USED FOR FOLLOWING DISTANCES ***

DIST (M)	CONC (UG/M**3)	STAB	U10M (M/S)	USTK (M/S)	MIX HT (M)	PLUME HT (M)	SIGMA Y (M)	SIGMA Z (M)	DWASH
15000.	2.994	4	10.0	16.5	3200.0	84.66	779.40	240.42	HS
16000.	2.778	4	10.0	16.5	3200.0	84.66	825.19	245.28	HS

```
*********************************
*** SCREEN DISCRETE DISTANCES ***
*********************************

*** TERRAIN HEIGHT OF  213. M ABOVE STACK BASE USED FOR FOLLOWING DISTANCES ***

  DIST     CONC             U10M   USTK  MIX HT   PLUME   SIGMA   SIGMA
   (M)   (UG/M**3)   STAB  (M/S)  (M/S)    (M)   HT (M)   Y (M)   Z (M)  DWASH
-------  ----------  ----  -----  -----  ------  ------  ------  ------  -----
 17000.   2.468        4    10.0   16.5  3200.0  114.66  870.62  250.06    HS

*********************************
*** SCREEN DISCRETE DISTANCES ***
*********************************

*** TERRAIN HEIGHT OF  232. M ABOVE STACK BASE USED FOR FOLLOWING DISTANCES ***

  DIST     CONC             U10M   USTK  MIX HT   PLUME   SIGMA   SIGMA
   (M)   (UG/M**3)   STAB  (M/S)  (M/S)    (M)   HT (M)   Y (M)   Z (M)  DWASH
-------  ----------  ----  -----  -----  ------  ------  ------  ------  -----
 18000.   2.426        4    10.0   16.5  3200.0   95.66  915.70  249.67    HS

*********************************
*** SCREEN DISCRETE DISTANCES ***
*********************************

*** TERRAIN HEIGHT OF  247. M ABOVE STACK BASE USED FOR FOLLOWING DISTANCES ***

  DIST     CONC             U10M   USTK  MIX HT   PLUME   SIGMA   SIGMA
   (M)   (UG/M**3)   STAB  (M/S)  (M/S)    (M)   HT (M)   Y (M)   Z (M)  DWASH
-------  ----------  ----  -----  -----  ------  ------  ------  ------  -----
 19000.   2.325        4    10.0   16.5  3200.0   80.66  960.45  254.13    HS

 DWASH=   MEANS NO CALC MADE (CONC = 0.0)
 DWASH=NO MEANS NO BUILDING DOWNWASH USED
 DWASH=HS MEANS HUBER-SNYDER DOWNWASH USED
 DWASH=SS MEANS SCHULMAN-SCIRE DOWNWASH USED
 DWASH=NA MEANS DOWNWASH NOT APPLICABLE, X<3*LB

 *****************************************
 *  SUMMARY OF TERRAIN HEIGHTS ENTERED FOR  *
 *    SIMPLE ELEVATED TERRAIN PROCEDURE     *
 *****************************************

      TERRAIN        DISTANCE RANGE (M)
```

HT (M)	MINIMUM	MAXIMUM
0.	1000.	--
0.	2000.	--
28.	3000.	--
30.	4000.	--
30.	5000.	--
30.	6000.	--
34.	7000.	--
60.	8000.	--
60.	9000.	--
105.	10000.	--
152.	11000.	--
185.	12000.	--
188.	13000.	--
188.	14000.	--
243.	15000.	--
243.	16000.	--
213.	17000.	--
232.	18000.	--
247.	19000.	--

****
*** REGULATORY (Default) ***
PERFORMING CAVITY CALCULATIONS
WITH ORIGINAL SCREEN CAVITY MODEL
(BRODE, 1988)
****

*** CAVITY CALCULATION - 1 ***			*** CAVITY CALCULATION - 2 ***		
CONC (UG/M**3)	=	165.2	CONC (UG/M**3)	=	165.2
CRIT WS @10M (M/S)	=	8.07	CRIT WS @10M (M/S)	=	8.07
CRIT WS @ HS (M/S)	=	15.71	CRIT WS @ HS (M/S)	=	15.71
DILUTION WS (M/S)	=	7.85	DILUTION WS (M/S)	=	7.85
CAVITY HT (M)	=	288.72	CAVITY HT (M)	=	288.72
CAVITY LENGTH (M)	=	207.63	CAVITY LENGTH (M)	=	207.63
ALONGWIND DIM (M)	=	96.20	ALONGWIND DIM (M)	=	96.20

****
END OF CAVITY CALCULATIONS
****

****

*** SUMMARY OF SCREEN MODEL RESULTS ***
****

CALCULATION PROCEDURE	MAX CONC (UG/M**3)	DIST TO MAX (M)	TERRAIN HT (M)	
SIMPLE TERRAIN	4.228	3000.	28.	
COMPLEX TERRAIN	9.095	20000.	292.	(24-HR CONC)
BLDG. CAVITY-1	165.2	208.	--	(DIST = CAVITY LENGTH)
BLDG. CAVITY-2	165.2	208.	--	(DIST = CAVITY LENGTH)

****
** REMEMBER TO INCLUDE BACKGROUND CONCENTRATIONS **
****

Screen3 Run

40% Load

05/07/04

12:55:27

*** SCREEN3 MODEL RUN ***
*** VERSION DATED 96043 ***

STEAG-917 ft (279.5m) Stack-40% Load, 2 Units, Steam Generator

COMPLEX TERRAIN INPUTS:

SOURCE TYPE	=	POINT
EMISSION RATE (G/S)	=	41.2000
STACK HT (M)	=	279.5000
STACK DIAMETER (M)	=	11.2100
STACK VELOCITY (M/S)	=	10.0000
STACK GAS TEMP (K)	=	323.1500
AMBIENT AIR TEMP (K)	=	293.0000
RECEPTOR HEIGHT (M)	=	.0000
URBAN/RURAL OPTION	=	RURAL

THE REGULATORY (DEFAULT) MIXING HEIGHT OPTION WAS SELECTED.
THE REGULATORY (DEFAULT) ANEMOMETER HEIGHT OF 10.0 METERS WAS ENTERED.

BUOY. FLUX = 287.431 M**4/S**3; MOM. FLUX = 2848.490 M**4/S**2.

FINAL STABLE PLUME HEIGHT (M) = 399.4
DISTANCE TO FINAL RISE (M) = 151.3

			VALLEY 24-HR CALCS		**SIMPLE TERRAIN 24-HR CALCS**			
TERR HT (M)	DIST (M)	MAX 24-HR CONC (UG/M**3)	CONC (UG/M**3)	PLUME HT ABOVE STK BASE (M)	CONC (UG/M**3)	PLUME HT ABOVE STK HGT (M)	SC	U10M USTK (M/S)
292.	20000.	10.27	1.818	399.4	10.27	88.4	6	1.0 6.2

05/07/04

12:55:27

*** SCREEN3 MODEL RUN ***
*** VERSION DATED 96043 ***

STEAG-917 ft (279.5m) Stack-40% Load, 2 Units, Steam Generator

SIMPLE TERRAIN INPUTS:

SOURCE TYPE	=	POINT
EMISSION RATE (G/S)	=	41.2000
STACK HEIGHT (M)	=	279.5000

```
   STK INSIDE DIAM (M)    =      11.2100
   STK EXIT VELOCITY (M/S)=      10.0000
   STK GAS EXIT TEMP (K)  =     323.1500
   AMBIENT AIR TEMP (K)   =     293.0000
   RECEPTOR HEIGHT (M)    =        .0000
   URBAN/RURAL OPTION     =        RURAL
   BUILDING HEIGHT (M)    =     165.0000
   MIN HORIZ BLDG DIM (M) =      96.2000
   MAX HORIZ BLDG DIM (M) =      96.2000

THE REGULATORY (DEFAULT) MIXING HEIGHT OPTION WAS SELECTED.
THE REGULATORY (DEFAULT) ANEMOMETER HEIGHT OF 10.0 METERS WAS ENTERED.


BUOY. FLUX =  287.431 M**4/S**3;  MOM. FLUX = 2848.490 M**4/S**2.

*** STABILITY CLASS  4 ONLY ***
*** ANEMOMETER HEIGHT WIND SPEED OF  10.00 M/S ONLY ***

*********************************
*** SCREEN DISCRETE DISTANCES ***
*********************************

*** TERRAIN HEIGHT OF    0. M ABOVE STACK BASE USED FOR FOLLOWING DISTANCES ***

  DIST     CONC             U10M   USTK  MIX HT   PLUME   SIGMA   SIGMA
   (M)   (UG/M**3)   STAB  (M/S)  (M/S)    (M)   HT (M)   Y (M)   Z (M)  DWASH
-------  ----------  ----  -----  -----  ------  ------  ------  ------  -----
  1000.    4.916        4    10.0   16.5  3200.0  323.55   70.54  136.12    HS
  2000.    5.394        4    10.0   16.5  3200.0  329.62  129.50  168.63    HS

*********************************
*** SCREEN DISCRETE DISTANCES ***
*********************************

*** TERRAIN HEIGHT OF   28. M ABOVE STACK BASE USED FOR FOLLOWING DISTANCES ***

  DIST     CONC             U10M   USTK  MIX HT   PLUME   SIGMA   SIGMA
   (M)   (UG/M**3)   STAB  (M/S)  (M/S)    (M)   HT (M)   Y (M)   Z (M)  DWASH
-------  ----------  ----  -----  -----  ------  ------  ------  ------  -----
  3000.    5.553        4    10.0   16.5  3200.0  301.42  185.72  174.96    HS

*********************************
*** SCREEN DISCRETE DISTANCES ***
*********************************
```

*** TERRAIN HEIGHT OF 30. M ABOVE STACK BASE USED FOR FOLLOWING DISTANCES ***

DIST (M)	CONC (UG/M**3)	STAB	U10M (M/S)	USTK (M/S)	MIX HT (M)	PLUME HT (M)	SIGMA Y (M)	SIGMA Z (M)	DWASH
4000.	4.666	4	10.0	16.5	3200.0	299.42	240.14	181.12	HS
5000.	4.033	4	10.0	16.5	3200.0	299.42	293.16	187.12	HS
6000.	3.587	4	10.0	16.5	3200.0	299.42	345.02	192.98	HS

****
*** SCREEN DISCRETE DISTANCES ***
****

*** TERRAIN HEIGHT OF 34. M ABOVE STACK BASE USED FOR FOLLOWING DISTANCES ***

DIST (M)	CONC (UG/M**3)	STAB	U10M (M/S)	USTK (M/S)	MIX HT (M)	PLUME HT (M)	SIGMA Y (M)	SIGMA Z (M)	DWASH
7000.	3.350	4	10.0	16.5	3200.0	295.42	395.92	198.71	HS

****
*** SCREEN DISCRETE DISTANCES ***
****

*** TERRAIN HEIGHT OF 60. M ABOVE STACK BASE USED FOR FOLLOWING DISTANCES ***

DIST (M)	CONC (UG/M**3)	STAB	U10M (M/S)	USTK (M/S)	MIX HT (M)	PLUME HT (M)	SIGMA Y (M)	SIGMA Z (M)	DWASH
8000.	3.661	4	10.0	16.5	3200.0	269.42	445.98	204.31	HS
9000.	3.358	4	10.0	16.5	3200.0	269.42	495.31	209.80	HS

****
*** SCREEN DISCRETE DISTANCES ***
****

*** TERRAIN HEIGHT OF 105. M ABOVE STACK BASE USED FOR FOLLOWING DISTANCES ***

DIST (M)	CONC (UG/M**3)	STAB	U10M (M/S)	USTK (M/S)	MIX HT (M)	PLUME HT (M)	SIGMA Y (M)	SIGMA Z (M)	DWASH
10000.	3.946	4	10.0	16.5	3200.0	224.42	543.99	215.18	HS

****

*** SCREEN DISCRETE DISTANCES ***
****

*** TERRAIN HEIGHT OF 152. M ABOVE STACK BASE USED FOR FOLLOWING DISTANCES ***

DIST (M)	CONC (UG/M**3)	STAB	U10M (M/S)	USTK (M/S)	MIX HT (M)	PLUME HT (M)	SIGMA Y (M)	SIGMA Z (M)	DWASH
11000.	4.410	4	10.0	16.5	3200.0	177.42	592.07	220.46	HS

****
*** SCREEN DISCRETE DISTANCES ***
****

*** TERRAIN HEIGHT OF 185. M ABOVE STACK BASE USED FOR FOLLOWING DISTANCES ***

DIST (M)	CONC (UG/M**3)	STAB	U10M (M/S)	USTK (M/S)	MIX HT (M)	PLUME HT (M)	SIGMA Y (M)	SIGMA Z (M)	DWASH
12000.	4.493	4	10.0	16.5	3200.0	144.42	639.63	225.65	HS

****
*** SCREEN DISCRETE DISTANCES ***
****

*** TERRAIN HEIGHT OF 188. M ABOVE STACK BASE USED FOR FOLLOWING DISTANCES ***

DIST (M)	CONC (UG/M**3)	STAB	U10M (M/S)	USTK (M/S)	MIX HT (M)	PLUME HT (M)	SIGMA Y (M)	SIGMA Z (M)	DWASH
13000.	4.162	4	10.0	16.5	3200.0	141.42	686.69	230.74	HS
14000.	3.845	4	10.0	16.5	3200.0	141.42	733.29	235.75	HS

****
*** SCREEN DISCRETE DISTANCES ***
****

*** TERRAIN HEIGHT OF 243. M ABOVE STACK BASE USED FOR FOLLOWING DISTANCES ***

DIST (M)	CONC (UG/M**3)	STAB	U10M (M/S)	USTK (M/S)	MIX HT (M)	PLUME HT (M)	SIGMA Y (M)	SIGMA Z (M)	DWASH
15000.	3.977	4	10.0	16.5	3200.0	86.42	779.48	240.68	HS
16000.	3.691	4	10.0	16.5	3200.0	86.42	825.27	245.53	HS

****
*** SCREEN DISCRETE DISTANCES ***
****

*** TERRAIN HEIGHT OF 213. M ABOVE STACK BASE USED FOR FOLLOWING DISTANCES ***

DIST (M)	CONC (UG/M**3)	STAB	U10M (M/S)	USTK (M/S)	MIX HT (M)	PLUME HT (M)	SIGMA Y (M)	SIGMA Z (M)	DWASH
17000.	3.277	4	10.0	16.5	3200.0	116.42	870.69	250.32	HS

****
*** SCREEN DISCRETE DISTANCES ***
****

*** TERRAIN HEIGHT OF 232. M ABOVE STACK BASE USED FOR FOLLOWING DISTANCES ***

DIST (M)	CONC (UG/M**3)	STAB	U10M (M/S)	USTK (M/S)	MIX HT (M)	PLUME HT (M)	SIGMA Y (M)	SIGMA Z (M)	DWASH
18000.	3.223	4	10.0	16.5	3200.0	97.42	915.77	249.92	HS

****
*** SCREEN DISCRETE DISTANCES ***
****

*** TERRAIN HEIGHT OF 247. M ABOVE STACK BASE USED FOR FOLLOWING DISTANCES ***

DIST (M)	CONC (UG/M**3)	STAB	U10M (M/S)	USTK (M/S)	MIX HT (M)	PLUME HT (M)	SIGMA Y (M)	SIGMA Z (M)	DWASH
19000.	3.090	4	10.0	16.5	3200.0	82.42	960.51	254.38	HS

DWASH=   MEANS NO CALC MADE (CONC = 0.0)
DWASH=NO MEANS NO BUILDING DOWNWASH USED
DWASH=HS MEANS HUBER-SNYDER DOWNWASH USED
DWASH=SS MEANS SCHULMAN-SCIRE DOWNWASH USED
DWASH=NA MEANS DOWNWASH NOT APPLICABLE, X<3*LB

****
* SUMMARY OF TERRAIN HEIGHTS ENTERED FOR *
*   SIMPLE ELEVATED TERRAIN PROCEDURE   *
****

     TERRAIN   DISTANCE RANGE (M)

HT (M)	MINIMUM	MAXIMUM
0.	1000.	--
0.	2000.	--
28.	3000.	--
30.	4000.	--
30.	5000.	--
30.	6000.	--
34.	7000.	--
60.	8000.	--
60.	9000.	--
105.	10000.	--
152.	11000.	--
185.	12000.	--
188.	13000.	--
188.	14000.	--
243.	15000.	--
243.	16000.	--
213.	17000.	--
232.	18000.	--
247.	19000.	--

****
*** REGULATORY (Default) ***
PERFORMING CAVITY CALCULATIONS
WITH ORIGINAL SCREEN CAVITY MODEL
(BRODE, 1988)
****

*** CAVITY CALCULATION - 1 ***			*** CAVITY CALCULATION - 2 ***		
CONC (UG/M**3)	=	314.3	CONC (UG/M**3)	=	314.3
CRIT WS @10M (M/S)	=	5.66	CRIT WS @10M (M/S)	=	5.66
CRIT WS @ HS (M/S)	=	11.01	CRIT WS @ HS (M/S)	=	11.01
DILUTION WS (M/S)	=	5.51	DILUTION WS (M/S)	=	5.51
CAVITY HT (M)	=	288.72	CAVITY HT (M)	=	288.72
CAVITY LENGTH (M)	=	207.63	CAVITY LENGTH (M)	=	207.63
ALONGWIND DIM (M)	=	96.20	ALONGWIND DIM (M)	=	96.20

****
END OF CAVITY CALCULATIONS
****

****

*** SUMMARY OF SCREEN MODEL RESULTS ***
****

CALCULATION PROCEDURE	MAX CONC (UG/M**3)	DIST TO MAX (M)	TERRAIN HT (M)	
SIMPLE TERRAIN	5.553	3000.	28.	
COMPLEX TERRAIN	10.27	20000.	292.	(24-HR CONC)

****
** REMEMBER TO INCLUDE BACKGROUND CONCENTRATIONS **
****

05/07/04

12:55:49

 *** SCREEN3 MODEL RUN ***
 *** VERSION DATED 96043 ***

 STEAG-917 ft (279.5m) Stack-40% Load, 1 Unit, Steam Generator

 COMPLEX TERRAIN INPUTS:
    SOURCE TYPE   =   POINT
    EMISSION RATE (G/S)   =   20.6000
    STACK HT (M)   =   279.5000
    STACK DIAMETER (M)   =   7.9200
    STACK VELOCITY (M/S)   =   10.0000
    STACK GAS TEMP (K)   =   323.1500
    AMBIENT AIR TEMP (K)   =   293.0000
    RECEPTOR HEIGHT (M)   =   .0000
    URBAN/RURAL OPTION   =   RURAL

 THE REGULATORY (DEFAULT) MIXING HEIGHT OPTION WAS SELECTED.
 THE REGULATORY (DEFAULT) ANEMOMETER HEIGHT OF 10.0 METERS WAS ENTERED.

 BUOY. FLUX = 143.474 M**4/S**3; MOM. FLUX = 1421.850 M**4/S**2.

 FINAL STABLE PLUME HEIGHT (M) = 374.6
 DISTANCE TO FINAL RISE (M)   = 151.3

                          VALLEY 24-HR CALCS   **SIMPLE TERRAIN 24-HR CALCS**
  TERR   MAX 24-HR   PLUME HT   PLUME HT
   HT   DIST   CONC   CONC   ABOVE STK   CONC   ABOVE STK   U10M USTK
  (M)   (M)   (UG/M**3)   (UG/M**3) BASE (M) (UG/M**3) HGT (M) SC   (M/S)
 ----- ------- ---------- ---------- ------   ---------- ------ -- ---- ----
  292. 20000. 7.172   1.450   374.6   7.172   70.1   6 1.0 6.2

05/07/04
12:55:49
 *** SCREEN3 MODEL RUN ***
 *** VERSION DATED 96043 ***

 STEAG-917 ft (279.5m) Stack-40% Load, 1 Unit, Steam Generator

 SIMPLE TERRAIN INPUTS:
    SOURCE TYPE   =   POINT
    EMISSION RATE (G/S)   =   20.6000
    STACK HEIGHT (M)   =   279.5000

```
   STK INSIDE DIAM (M)    =       7.9200
   STK EXIT VELOCITY (M/S)=      10.0000
   STK GAS EXIT TEMP (K)  =     323.1500
   AMBIENT AIR TEMP (K)   =     293.0000
   RECEPTOR HEIGHT (M)    =        .0000
   URBAN/RURAL OPTION     =        RURAL
   BUILDING HEIGHT (M)    =     165.0000
   MIN HORIZ BLDG DIM (M) =      96.2000
   MAX HORIZ BLDG DIM (M) =      96.2000

THE REGULATORY (DEFAULT) MIXING HEIGHT OPTION WAS SELECTED.
THE REGULATORY (DEFAULT) ANEMOMETER HEIGHT OF 10.0 METERS WAS ENTERED.


BUOY. FLUX =  143.474 M**4/S**3;  MOM. FLUX = 1421.850 M**4/S**2.

*** STABILITY CLASS  4 ONLY ***
*** ANEMOMETER HEIGHT WIND SPEED OF  10.00 M/S ONLY ***

*********************************
*** SCREEN DISCRETE DISTANCES ***
*********************************

*** TERRAIN HEIGHT OF    0. M ABOVE STACK BASE USED FOR FOLLOWING DISTANCES ***

  DIST     CONC             U10M   USTK  MIX HT   PLUME   SIGMA   SIGMA
   (M)   (UG/M**3)   STAB  (M/S)  (M/S)    (M)   HT (M)   Y (M)   Z (M)  DWASH
-------  ----------  ----  -----  -----  ------  ------  ------  ------  -----
  1000.   3.011        4    10.0   16.5  3200.0  311.58   69.40  135.53    HS
  2000.   3.295        4    10.0   16.5  3200.0  311.58  128.62  167.95    HS

*********************************
*** SCREEN DISCRETE DISTANCES ***
*********************************

*** TERRAIN HEIGHT OF   28. M ABOVE STACK BASE USED FOR FOLLOWING DISTANCES ***

  DIST     CONC             U10M   USTK  MIX HT   PLUME   SIGMA   SIGMA
   (M)   (UG/M**3)   STAB  (M/S)  (M/S)    (M)   HT (M)   Y (M)   Z (M)  DWASH
-------  ----------  ----  -----  -----  ------  ------  ------  ------  -----
  3000.   3.289        4    10.0   16.5  3200.0  283.38  185.11  174.31    HS

*********************************
*** SCREEN DISCRETE DISTANCES ***
*********************************
```

*** TERRAIN HEIGHT OF 30. M ABOVE STACK BASE USED FOR FOLLOWING DISTANCES ***

DIST (M)	CONC (UG/M**3)	STAB	U10M (M/S)	USTK (M/S)	MIX HT (M)	PLUME HT (M)	SIGMA Y (M)	SIGMA Z (M)	DWASH
4000.	2.728	4	10.0	16.5	3200.0	281.38	239.67	180.49	HS
5000.	2.335	4	10.0	16.5	3200.0	281.38	292.77	186.51	HS
6000.	2.059	4	10.0	16.5	3200.0	281.38	344.69	192.39	HS

****
*** SCREEN DISCRETE DISTANCES ***
****

*** TERRAIN HEIGHT OF 34. M ABOVE STACK BASE USED FOR FOLLOWING DISTANCES ***

DIST (M)	CONC (UG/M**3)	STAB	U10M (M/S)	USTK (M/S)	MIX HT (M)	PLUME HT (M)	SIGMA Y (M)	SIGMA Z (M)	DWASH
7000.	1.905	4	10.0	16.5	3200.0	277.38	395.63	198.14	HS

****
*** SCREEN DISCRETE DISTANCES ***
****

*** TERRAIN HEIGHT OF 60. M ABOVE STACK BASE USED FOR FOLLOWING DISTANCES ***

DIST (M)	CONC (UG/M**3)	STAB	U10M (M/S)	USTK (M/S)	MIX HT (M)	PLUME HT (M)	SIGMA Y (M)	SIGMA Z (M)	DWASH
8000.	2.047	4	10.0	16.5	3200.0	251.38	445.72	203.76	HS
9000.	1.867	4	10.0	16.5	3200.0	251.38	495.08	209.26	HS

****
*** SCREEN DISCRETE DISTANCES ***
****

*** TERRAIN HEIGHT OF 105. M ABOVE STACK BASE USED FOR FOLLOWING DISTANCES ***

DIST (M)	CONC (UG/M**3)	STAB	U10M (M/S)	USTK (M/S)	MIX HT (M)	PLUME HT (M)	SIGMA Y (M)	SIGMA Z (M)	DWASH
10000.	2.147	4	10.0	16.5	3200.0	206.38	543.78	214.65	HS

****

*** SCREEN DISCRETE DISTANCES ***
****

*** TERRAIN HEIGHT OF 152. M ABOVE STACK BASE USED FOR FOLLOWING DISTANCES ***

DIST (M)	CONC (UG/M**3)	STAB	U10M (M/S)	USTK (M/S)	MIX HT (M)	PLUME HT (M)	SIGMA Y (M)	SIGMA Z (M)	DWASH
11000.	2.351	4	10.0	16.5	3200.0	159.38	591.88	219.95	HS

****
*** SCREEN DISCRETE DISTANCES ***
****

*** TERRAIN HEIGHT OF 185. M ABOVE STACK BASE USED FOR FOLLOWING DISTANCES ***

DIST (M)	CONC (UG/M**3)	STAB	U10M (M/S)	USTK (M/S)	MIX HT (M)	PLUME HT (M)	SIGMA Y (M)	SIGMA Z (M)	DWASH
12000.	2.361	4	10.0	16.5	3200.0	126.38	639.45	225.14	HS

****
*** SCREEN DISCRETE DISTANCES ***
****

*** TERRAIN HEIGHT OF 188. M ABOVE STACK BASE USED FOR FOLLOWING DISTANCES ***

DIST (M)	CONC (UG/M**3)	STAB	U10M (M/S)	USTK (M/S)	MIX HT (M)	PLUME HT (M)	SIGMA Y (M)	SIGMA Z (M)	DWASH
13000.	2.180	4	10.0	16.5	3200.0	123.38	686.52	230.25	HS
14000.	2.010	4	10.0	16.5	3200.0	123.38	733.14	235.27	HS

****
*** SCREEN DISCRETE DISTANCES ***
****

*** TERRAIN HEIGHT OF 243. M ABOVE STACK BASE USED FOR FOLLOWING DISTANCES ***

DIST (M)	CONC (UG/M**3)	STAB	U10M (M/S)	USTK (M/S)	MIX HT (M)	PLUME HT (M)	SIGMA Y (M)	SIGMA Z (M)	DWASH
15000.	2.041	4	10.0	16.5	3200.0	68.38	779.33	240.21	HS
16000.	1.893	4	10.0	16.5	3200.0	68.38	825.13	245.07	HS

```
*********************************
*** SCREEN DISCRETE DISTANCES ***
*********************************

*** TERRAIN HEIGHT OF  213. M ABOVE STACK BASE USED FOR FOLLOWING DISTANCES ***

  DIST     CONC              U10M   USTK  MIX HT   PLUME   SIGMA   SIGMA
   (M)   (UG/M**3)   STAB  (M/S)  (M/S)    (M)   HT (M)   Y (M)   Z (M)  DWASH
-------  ----------  ----  -----  -----  ------  ------  ------  ------  -----
 17000.   1.693        4    10.0   16.5  3200.0   98.38  870.56  249.86    HS

*********************************
*** SCREEN DISCRETE DISTANCES ***
*********************************

*** TERRAIN HEIGHT OF  232. M ABOVE STACK BASE USED FOR FOLLOWING DISTANCES ***

  DIST     CONC              U10M   USTK  MIX HT   PLUME   SIGMA   SIGMA
   (M)   (UG/M**3)   STAB  (M/S)  (M/S)    (M)   HT (M)   Y (M)   Z (M)  DWASH
-------  ----------  ----  -----  -----  ------  ------  ------  ------  -----
 18000.   1.656        4    10.0   16.5  3200.0   79.38  915.64  249.47    HS

*********************************
*** SCREEN DISCRETE DISTANCES ***
*********************************

*** TERRAIN HEIGHT OF  247. M ABOVE STACK BASE USED FOR FOLLOWING DISTANCES ***

  DIST     CONC              U10M   USTK  MIX HT   PLUME   SIGMA   SIGMA
   (M)   (UG/M**3)   STAB  (M/S)  (M/S)    (M)   HT (M)   Y (M)   Z (M)  DWASH
-------  ----------  ----  -----  -----  ------  ------  ------  ------  -----
 19000.   1.580        4    10.0   16.5  3200.0   64.38  960.39  253.93    HS

 DWASH=   MEANS NO CALC MADE (CONC = 0.0)
 DWASH=NO MEANS NO BUILDING DOWNWASH USED
 DWASH=HS MEANS HUBER-SNYDER DOWNWASH USED
 DWASH=SS MEANS SCHULMAN-SCIRE DOWNWASH USED
 DWASH=NA MEANS DOWNWASH NOT APPLICABLE, X<3*LB

 *****************************************
 *  SUMMARY OF TERRAIN HEIGHTS ENTERED FOR  *
 *    SIMPLE ELEVATED TERRAIN PROCEDURE     *
 *****************************************

      TERRAIN        DISTANCE RANGE (M)
```

HT (M)	MINIMUM	MAXIMUM
0.	1000.	--
0.	2000.	--
28.	3000.	--
30.	4000.	--
30.	5000.	--
30.	6000.	--
34.	7000.	--
60.	8000.	--
60.	9000.	--
105.	10000.	--
152.	11000.	--
185.	12000.	--
188.	13000.	--
188.	14000.	--
243.	15000.	--
243.	16000.	--
213.	17000.	--
232.	18000.	--
247.	19000.	--

****
*** REGULATORY (Default) ***
PERFORMING CAVITY CALCULATIONS
WITH ORIGINAL SCREEN CAVITY MODEL
(BRODE, 1988)
****

*** CAVITY CALCULATION - 1 ***			*** CAVITY CALCULATION - 2 ***		
CONC (UG/M**3)	=	160.3	CONC (UG/M**3)	=	160.3
CRIT WS @10M (M/S)	=	5.55	CRIT WS @10M (M/S)	=	5.55
CRIT WS @ HS (M/S)	=	10.80	CRIT WS @ HS (M/S)	=	10.80
DILUTION WS (M/S)	=	5.40	DILUTION WS (M/S)	=	5.40
CAVITY HT (M)	=	288.72	CAVITY HT (M)	=	288.72
CAVITY LENGTH (M)	=	207.63	CAVITY LENGTH (M)	=	207.63
ALONGWIND DIM (M)	=	96.20	ALONGWIND DIM (M)	=	96.20

****
END OF CAVITY CALCULATIONS
****

****

*** SUMMARY OF SCREEN MODEL RESULTS ***
****

CALCULATION PROCEDURE	MAX CONC (UG/M**3)	DIST TO MAX (M)	TERRAIN HT (M)	
SIMPLE TERRAIN	3.295	2000.	0.	
COMPLEX TERRAIN	7.172	20000.	292.	(24-HR CONC)

****
** REMEMBER TO INCLUDE BACKGROUND CONCENTRATIONS **
****

APPENDIX E

REGIONAL HAZE ASSESSMENTS WITH CALPUFF AND FLAG: RECENT EXPERIENCES

Regional Haze Assessments with CALPUFF and FLAG: Recent Experiences

Control # 248

Prepared by Robert J. Paine and David W. Heinold

ENSR International, 2 Technology Park Drive, Westford, MA 01886

ABSTRACT

In 2001, the Federal Land Managers initiated a set of new procedures to assess the impact of proposed new sources on PSD Class I areas. These procedures, referred to as FLAG (Federal Land Managers' Air Quality Related Values Workgroup), often cause the assessment of regional haze impacts to be the most constraining issue with the new FLAG guidance. In the case of electric generation, this has the result of preventing the permitting and licensing of very well-controlled new emission sources, while older sources that have much higher emissions per megawatt are relied upon more to satisfy consumer demand. Therefore, the FLAG guidance has the unintended, but real effect of exacerbating air quality in the areas that the FLMs are trying to protect.

In technical terms, the FLAG guidance appears to be very restrictive in the following areas:

- The natural background extinction levels omit certain components, such as naturally occurring sea salt and smoke from wildfires, which have been unnaturally suppressed over the past several decades. Therefore, FLAG portrays "natural conditions" as being more pristine than they actually are.

- The perceptibility threshold of a 10% change in extinction is generally not observed in actual practice. A more likely threshold value is on the order of an 18%-20% change. Therefore, the FLAG threshold for an adverse impact from a proposed source is too stringent.

- The worst-case visibility impacts often presumed to occur during cloudy nighttime hours when there is no visibility AQRV.

- High relative humidity (RH) periods are often the most constraining, with FLAG requiring the applicant to consider RH up to 98%. However, such periods are often associated with precipitation events (which should be excluded from visibility degradation calculations because of natural obscuration to visibility), but the FLAG guidance as implemented in CALPUFF does not currently allow special handling of precipitation cases.

- The dry extinction efficiency for ammonium sulfate and ammonium nitrate should be reduced from 3.0 to 2.5, based upon a review of available data. This would reduce the impact of secondary particulates by over 15%.

- A revised f(RH) curve has been published by EPA for use in tracking progress under the Regional Haze Rule. The FLAG guidance has not yet adopted this updated curve.

- The CALPUFF default chemical transformation mechanism is the MESOPUFF-II method, which is over 20 years old. Comparisons of the model predictions versus observations show that the MESOPUFF-II method may overpredict the chemical transformation rate by at least a factor of 2. A more up-to-date method, RIVAD, is more accurate and is available as an option for running CALPUFF.

- The daily average change in visibility impact due to a proposed source can be different depending upon how one does the averaging. The FLAG procedure takes the average of 24 hourly extinction values without regard for how the hourly source impact extinction values are paired in time with the hourly natural background extinction values. The straight averaging of the extinction values tends to heavily weight the hours (often at night) with poor visibility rather than the good visibility hours, which should be given the most consideration.

The authors present several proposed changes that address the shortcomings of the FLAG procedures and result in an improved method for computing daily extinction changes to natural visibility background.

INTRODUCTION

In December 2000, the Federal Land Managers' Air Quality Related Values (AQRV) Workgroup (FLAG) issued a final Phase I Report[1]. FLAG consists primarily of representatives from the three Federal Land Managers (FLMs) that administer Federal Class I areas (U.S. Forest Service, National Park Service, Fish and Wildlife Service) supplemented with representatives from other vested groups, such as the Bureau of Land Management and the Environmental Protection Agency. The goal of FLAG is to provide consistent policies and processes in identifying and evaluating AQRVs for the review of new sources of air pollution. The FLAG Phase I Report consists of recommended procedures for FLMs to follow in the permit application process and specific guidance for the identification of AQRVs related to visibility, ozone and deposition.

The finalization of the FLAG Phase I guidelines was announced in the *Federal Register* on January 3, 2001. These guidelines have a significant effect upon one particular Air Quality Related Value, regional haze, and have significantly increased the challenge of permitting new, low-emission facilities, as reported by Paine, et al.[2].

In this paper, we present a number of issues in the following order:

1) FLAG regional haze assessment procedures are described, with particular attention to the role of relative humidity in the assessment and natural background conditions.

2) Experience with the use of the CALPUFF model in long-range transport modeling is briefly discussed, with implications for the ability of new sources to be permitted in light of the regional haze modeling constraints, and the ultimate effect upon air quality related values in PSD Class I areas.

3) Technical issues involving the regional haze analysis procedures and their resolution are then discussed at length. There are several sub-sections:

   a) determination of natural conditions,

   b) threshold for perceptibility of changes in extinction,

   c) relative humidity values used in the determination of extinction for hygroscope particles,

   d) dry extinction scattering efficiency assigned to ammonium sulfates and nitrates,

   e) the updated EPA f(RH) curve,

   f) the choice of the CALPUFF chemical mechanism method,

   g) identification of events associated with meteorological interferences, and

   h) how daily averages of the source/background extinction ratio are determined in CALPUFF and how a revised approach would eliminate weaknesses in the current approach.

FLAG REGIONAL HAZE ASSESSMENT PROCEDURES

Procedures are established in the final Phase I FLAG guidance report by which the FLM determines whether a proposed facility causes visibility impairment or contributes to a condition of pre-existing visibility impairment. The first step is to determine whether a source is to be evaluated in terms of the potential existence of a visible plume or whether it should be evaluated in terms of general haze. Plume visibility is a condition where a plume (or layered pollution) is discernable when viewed against a background sky or terrain on the background horizon. Haze is a condition where the plume becomes sufficiently well mixed that the chief contribution is a reduction in visual range, as well as a reduction in contrast and "graying" of colors. The application of CALPUFF with the FLAG procedures addresses the first of these – reduction in visual range due to increased light extinction.

FLAG provides a rule of thumb that facilities within 50 km of a protected visibility area should be evaluated according to visible plume impact and that facilities beyond 50 km should be evaluated in terms of the contribution to haze. This paper addresses the more common case in which the proposed facility is more than 50 kilometers from the nearest PSD Class I area.

FLAG adopts the Interagency Workgroup on Air Quality Models (IWAQM) Phase II recommendations[3] on how to evaluate the contribution of a facility to general haze. This involves the application of the CALPUFF[4] model to estimate maximum 24-hour average concentrations of primary and secondary particulate. The hourly modeled concentrations are then multiplied by an extinction efficiency that estimates the effect on absorption and scattering of visible light and then a relative humidity factor that simulates enlargement due to droplet formation on hygroscopic particles. The total 24-hour averaged modeled light extinction is then compared to a background extinction value to determine if the impact is significant. In making this comparison, FLAG inherently and conservatively

assumes that the peak modeled concentration at a single location is representative of a wide area surrounding the observer in the Class I area. If modeled concentrations were to be spatially averaged over a wide area through which an observer is viewing an object, the resulting average concentration would be lower.

Relative Humidity Extinction Adjustment

The relative humidity adjustment that is used to compute plume-related extinction is a major contributor to the peak predictions of regional haze impacts. Moisture plays an important role because particles that are amenable to condensation nuclei sites for water vapor will form small droplets starting at relative humidity values above 50%. These enlarged "particles" are then much more efficient at scattering light than dry particles. For values of relative humidity (RH) approaching 100%, the scattering efficiency can increase by a factor as high as 18 (at 98% RH in CALPOST) over dry conditions. Therefore, periods of high relative humidity will often lead to the worst-case regional haze impact predictions. It is also important to note that the presence of fine secondary ammonium sulfate and nitrate particles from gaseous pollutant emissions results in a source-caused extinction that has a larger extinction efficiency than natural background particles which are presumed to be predominately composed of "soils", which have a lower extinction efficiency.

Natural Background Conditions

FLAG uses the maximum 24-hour modeled concentration of primary and secondary particulate, adjusted by mean relative humidity, to estimate the extinction associated with emission sources. This value is then compared to the natural background extinction for the Class I area that is listed in Appendix 2.B of the FLAG report. As noted previously, the natural background extinction is intended to represent the state of the atmosphere in the absence of human activity, based on the 1990 NAPAP report[5]. Table 2.B-2 of that Appendix lists the presumed constituents of the natural background. For the continental United States, it corresponds to an annual PM_{10} concentration of about 5 ug/m^3 in the Eastern United States and 4 ug/m^3 in the Western United States. However, these values are a small fraction of the levels that have been characteristic of many of the Eastern Class I areas since the system of National Parks and wilderness areas was established in the early 20th century.

FLAG suggests the following criteria by which the FLM will develop recommendations: if there is no pre-existing haze concern, a single PSD source must not have impacts that exceed 5% of the natural background. If the source impacts exceed 5%, a cumulative analysis must demonstrate that the impact of all PSD sources combined does not exceed 10% of the natural background. If the pre-existing haze cumulative analysis has already established that combined PSD impacts exceed 10% of the natural background, a facility may contribute no more than 0.4% of the natural background extinction. Although commenters on the FLAG guidance suggested that these thresholds are overly protective, FLAG rejected these comments.

USE OF CALPUFF FOR LONG-RANGE TRANSPORT MODELING

For PSD permit applications, EPA recommends a steady-state plume model for distances up to 50 kilometers. For longer distances, CALPUFF is recommended. The FLMs require a PSD Class I

assessment to be conducted for all proposed sources within 100 kilometers of a PSD Class I area. For distances between 100 and 200 kilometers, some sources with very low emissions may be exempted from PSD Class I considerations. Major sources with emissions well in excess of 250 tons per year of SO_2, NO_2, and/or PM_{10} will likely be required to conduct a modeling assessment if the source is within 200 or even 300 kilometers of a PSD Class I area. As noted by Paine, et al.[2], and Walcek[6], and Moran and Pielke[7], the inability for CALPUFF to account for wind shear effects on additional plume dispersion produces a plume that is too compact, and limits the ability of CALPUFF to provide unbiased predictions beyond 200 kilometers or 12 hours of transport time. Although EPA notes that the use of puff splitting will help to alleviate this overprediction tendency, EPA has not provided any specific evidence that this is really the case. In fact, the authors' experience with the puff splitting option in CALPUFF is that it is relatively ineffective because it does not explicitly test vertical wind shear over each puff. Therefore, reliance upon puff splitting to correct the CALPUFF overprediction tendency has not been proven to be effective in our view.

Because the conservative screening CALPUFF procedures may show significant impacts from even low-emission proposed projects, most applicants will likely need to conduct a refined modeling analysis with full CALMET processing, as noted in the Wygen 2 project in Wyoming[8]. This occurs because the significant impact thresholds are only 4% of the PSD Class I increments for SO_2, NO_2, and PM_{10}, making it potentially difficult for a project to show insignificant impacts. The effort required to conduct a refined analysis is substantial.

In practice, one of the most daunting aspects of a refined PSD Class I analysis is obtaining a valid and complete background source inventory. Many state inventories are in poor condition, if they exist at all, and some states (such as New York) require the applicant to obtain verification in writing from each background source facility for every exhaust parameter input value being modeled. The effort to acquire a background emission inventory can take up to several months and significant cost to complete. Many emission inventories consist only of *actual* emissions, while the Federal Land Managers appear to want to model *allowable* emissions. The PSD regulations, however, explicitly state that actual emissions are to be considered.

Effects of FLAG on New Source Permitting

A number of CALPUFF runs were conducted by Paine, et al.[2] to determine the air quality impact of a hypothetical well-controlled coal-fired source. Their analysis indicated that the most restrictive aspect involves the regional haze analysis. Although the hypothetical project also showed significant impacts for SO_2 increment consumption, a cumulative analysis may resolve the increment consumption issue because the increment significance level is only 4% of the allowable total. However, with the regional haze cumulative impact threshold set to only 10% for all sources combined (just twice the significance level for only the proposed source), it is clear that this element of the analysis is often the controlling one. Therefore, much of the focus of this paper is on CALPUFF regional haze modeling.

Much of the attention related to the perceived degradation in air quality at several National Parks and Wilderness Areas is on large emission sources that were built prior to the implementation of New Source Performance Standards (NSPS) and the Prevention of Significant Deterioration (PSD) program

in the mid 1970s. There is concern on the part of the FLMs that emission sources that were permitted and built before this time are "beyond their control." Consequently, they focus their attention and control decisions on new PSD projects.

In many such cases, projects actually would serve to improve air quality by lowering the air pollutants emitted per unit amount of production. The new plants are also more fuel efficient, so that less energy input is required to produce a megawatt of power. In the case of electrical generation, with a fixed number of megawatt hours needed each day in the United States, the presence of new generation with its lower unit emissions will tend to continuously lower the pollutants emitted to produce the daily-required output. If new construction is denied due to unnecessarily stringent permitting conditions, then the need to run the older units with higher unit emissions will increase, resulting in an aggravation of the situation that is of concern to the FLMs. The effects of higher emissions due to lack of new sources can be further aggravated during periods of hot weather, when ozone is at its peak. In such conditions of extreme electrical demand, the lack of new base-loaded electrical generation leads not only to the maximum use of older base generation equipment, but also to the activation of many poorly controlled standby power generation units, which further stresses air quality during these most critical periods.

A comparison of typical unit emission rates between new and old units helps to illustrate this point. Figures 1**,** 2, and 3, based upon ENSR experience with numerous projects, show typical emissions of SO_2, PM_{10}, and NO_x for various types of sources relative to those from a state-of-the-art natural gas combined-cycle combustion turbine. It is evident from these figures that compared to a pre-NSPS existing coal-fired steam electric boiler, new emissions sources, even coal-fired, have much lower emissions.

The next section discusses why the FLAG guidance is very conservative in its handling of regional haze impacts from new, clean emission sources, and presents suggestions to correct some technical deficiencies in the guidance.

Figure 1
Combustion Source Emissions of SO_2
Relative to State of the Art, Natural Gas fired
Combined Cycle Power Plant

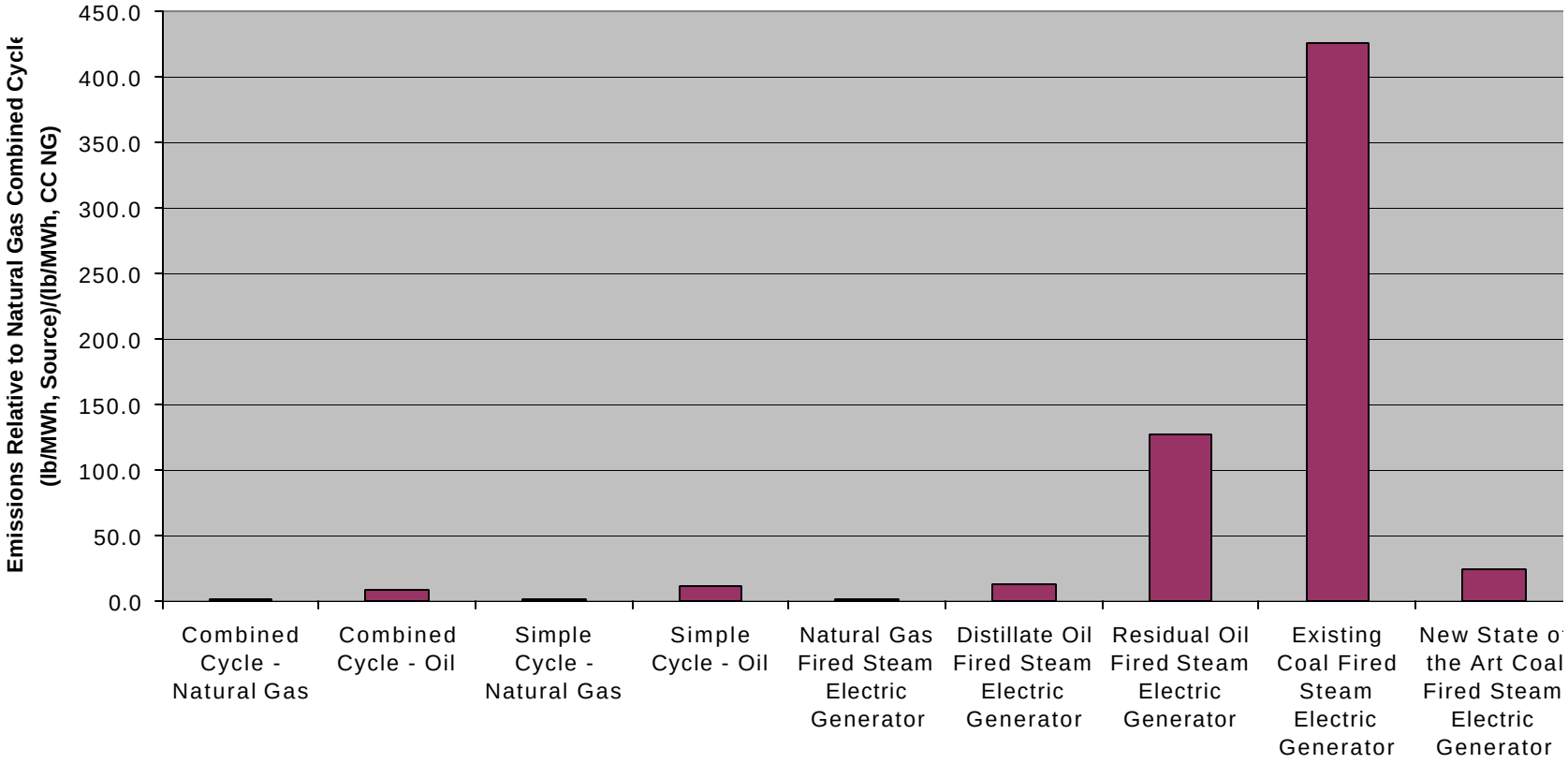

Figure 2
Combustion Source Emissions of NOx
Relative to State of the Art, Natural Gas fired
Combined Cycle Power Plant

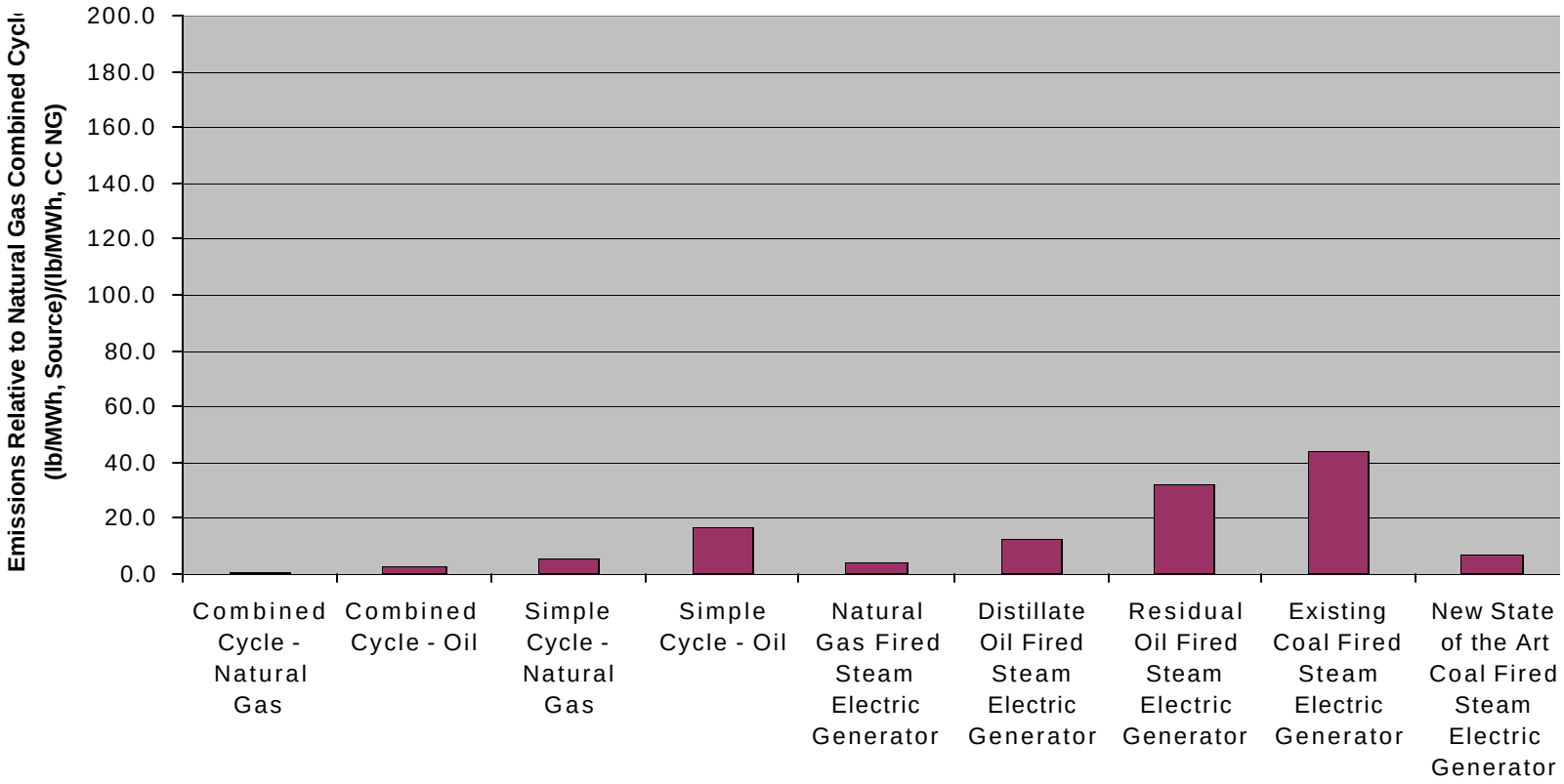

Figure 3
Combustion Source Emissions of PM-10
Relative to State of the Art, Natural Gas fired
Combined Cycle Power Plant

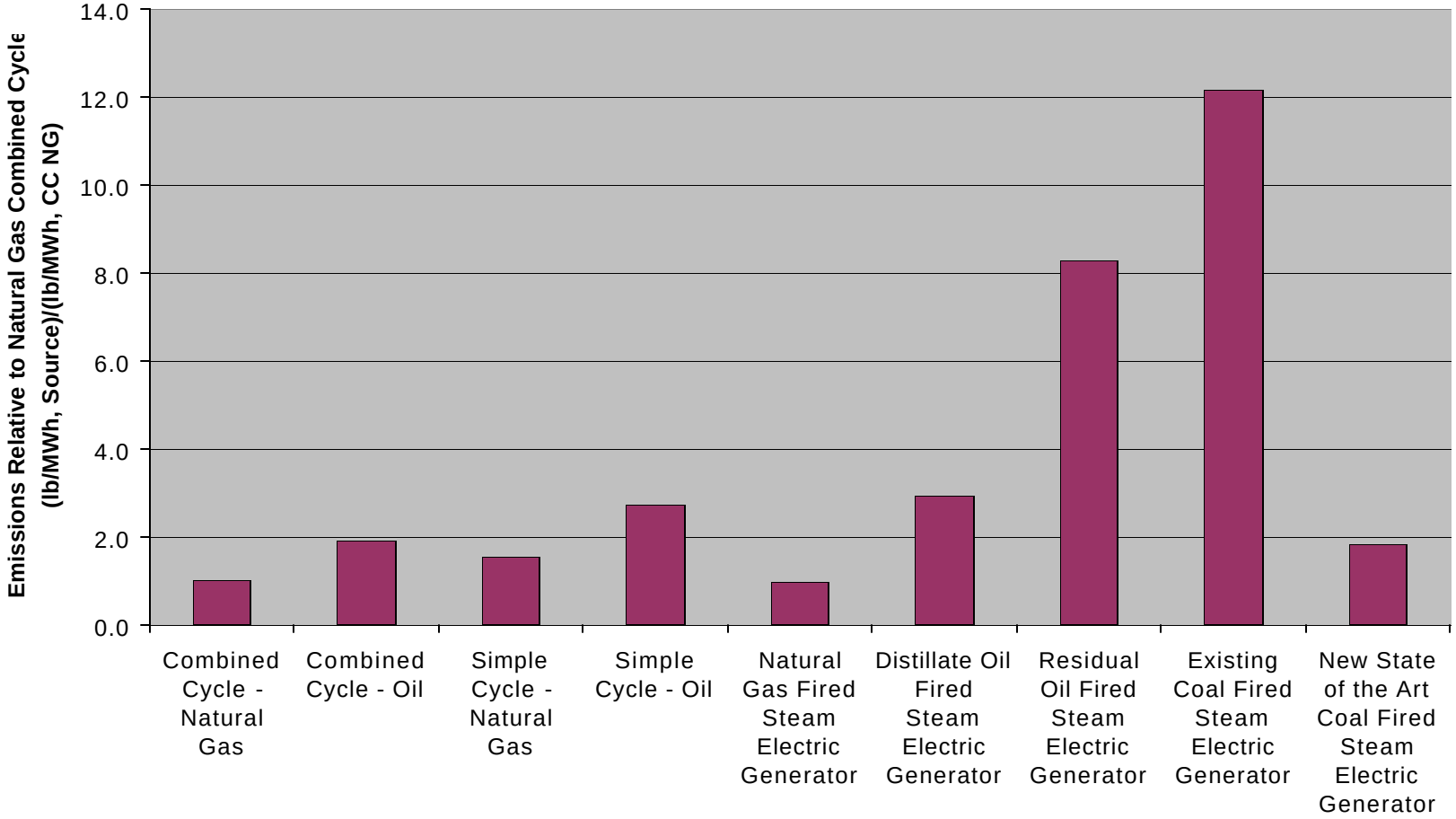

TECHNICAL ISSUES INVOLVING THE REGIONAL HAZE ANALYSIS PROCEDURES AND THEIR RESOLUTION

The tendency for CALPUFF modeling results of regional haze impacts to dominate the permitting process for new sources with the implementation of FLAG guidance has resulted in increased scrutiny of the shortcomings of the FLAG guidance and the modeling procedures involved. Paine, et al.[2] described several technical problems with the way the prescribed system is set up to analyze regional haze impacts. This paper updates this discussion and offers specific enhancements to CALPUFF to help eliminate the shortcomings.

1) Depiction of Background Visual Range

Inclusion of Naturally Occurring Salt Particles

In the Draft Guidance for Estimating Natural Visibility Conditions Under the Regional Haze Program[9], there is a discussion in Section 1.11 regarding the preliminary estimates of natural conditions. This discussion notes that the NAPAP report[5] from which the estimates are derived "provides annual average estimates of natural concentrations of these six main components of PM for eastern and western regions of the country." These estimates were used to estimate natural background under the FLAG guidance. The six components referred to in the quotation are sulfate, nitrate, organic carbon, elemental carbon, and crustal materials. The category of naturally occurring salt particles is not included in the list. Furthermore, since the estimates in the NAPAP report are averages over the entire eastern and western parts of the country, they do not include the influence of sea salt at coastal and near-coastal locations.

Because Class I areas, especially those on or near ocean coastlines or near numerous salt flats in the western United States, might have significant contributions from naturally occurring sea salt aerosols, the lack of their inclusion may significantly underestimate the natural background light extinction. This discussion presents and documents example estimates of the average contributions of sea salt aerosols to light extinction in coastal and near-coastal Class I areas in the Southeast United States. The same procedure can be used for any PSD Class I area, but the largest effect will be realized for PSD Class I areas near the oceans and the salt flats in the West.

Paine, et al.[10] provide a detailed explanation as to how to incorporate the effects of naturally occurring salt particles into the background visual range calculation. Basically, salt aerosol concentrations can be estimated from sodium and chloride concentrations measured at IMPROVE[11] network monitoring sites, based on the assumption that all of the sodium and chloride are present in naturally occurring salt. The IMPROVE database includes reported $PM_{2.5}$ concentrations of elemental sodium, ionic chloride and elemental chlorine. Seasonal averages of the reported values of sodium and chloride were calculated by Paine, et al.[10]. The chlorine data were not used, because chlorine is volatilized from the filter during sampling[12].

Information regarding the dry light extinction efficiency for sea salt particles was not found in the technical literature. However, the dry light extinction efficiency is generally related to the size distribution of the particles at low relative humidity, although other factors such as refractive index also play a part.

Gartrell, et al.[13] have shown that the typical particle size distributions for soil and for sea salt are very similar. The dry light extinction efficiency, for fine soil is commonly accepted to be around 1 m^2/g (Malm, et al.[14]). Therefore, 1 m^2/g was used as the dry particle light extinction efficiency for sea salt in these analyses.

The hygroscopic nature of salt particles is well established (Tang[15], Tang and Munkelwitz[16], Tang, et al.[17], Ansari and Pandis[18]). Both pure salts (e.g., NaCl) and mixed salts (e.g., KCl-NaCl) have been shown to exhibit substantial particle growth as a function of relative humidity. Sea salt particles often contain organic materials in internal mixtures, and these mixed salt-organic particles have been shown to be hygroscopic, as well (Ming and Russell[19]). Furthermore, the hygroscopic properties of salt particles are generally similar to those of ammonium sulfate and ammonium nitrate (the hygroscopic species represented by f(RH) values in Table 2.A-1 of the FLAG Phase I Report[1]). For example, the deliquescence humidity (at 25° C) is 75.7% for NaCl, compared to 79.5% for ammonium sulfate (Tang[15]).

Specific values of f(RH) for sea salt have been determined through field measurements, as reported by Paine, et al[10]. Their Table 3 shows that the sea salt f(RH) values match those from CALPOST reasonably well, especially between 60% and 90% RH. Therefore, within reasonable uncertainty bounds, the CALPOST f(RH) values in FLAG Table 2.A-1 can be used to model the growth of sea salt particles.

Recent field studies have found that sodium measured in coastal areas is often in the form of sodium nitrate rather than sodium chloride, probably due to reactions with nitric acid[20]**.** The Aerosol Inorganics Model, available at http://mae.ucdavis.edu/~wexler/aim/aim.htm, indicates that sodium nitrate deliquesces at a slightly lower relative humidity than sodium chloride, but the water uptake by sodium chloride is greater than for sodium nitrate. However, for natural conditions, which is what FLAG is designed to address, there would likely be much lower levels of nitric acid than are currently present, and the chloride would likely not be displaced by nitrate.

The FLAG guidance provides f(RH) values for use with seasonal and annual average concentrations of ammonium sulfate and ammonium nitrate (FLAG[1]). Table 2.B-1 of the guidance document lists these values for individual Class I areas along with estimates of the extinction coefficient for natural conditions. The values in Table 2.B-1, along with a dry light extinction efficiency of 1 m^2/g, were applied by Paine, et al.[10] to the estimates of seasonal and annual average sea salt aerosol concentrations to estimate sea salt aerosol contributions to light extinction; see Table 1.

In their review of the data analysis protocols developed for IMPROVE for assessing compliance under EPA's Regional Haze Rule, Lowenthal and Kumar[21] note that the methods for reconstructing light extinction from particulate measurements is overly simplified. These simplifications can lead to biases in the apportionment of light extinction to sources, and therefore to a misallocation of resources for emissions reductions. They specifically note that concentrations of sodium and chlorine are available at all IMPROVE sites, so "there is no reason why they should not be included in reconstructed mass." The authors concur that this is just one example of oversights in the FLAG procedures that have caused a flawed system to be implemented for the permitting of new, clean emission sources.

Table 1. Estimated seasonal and annual average light extinction under natural conditions with aged salt aerosol contributions.

Site	Season	Light Extinction Coefficient Without Sea Salt[a] (Mm^{-1})	Aged Sea Salt Contribution to Light Extinction Coefficient (Mm^{-1})		Light Extinction Coefficient With Aged Sea Salt Contribution (Mm^{-1})	
			Lower Limit	Upper Limit	Lower Limit	Upper Limit
Cape Romain NWR	Winter	21.1	3.6	5.6	24.7	26.7
	Spring	21.4	5.6	9.1	27.0	30.5
	Summer	22.0	4.9	7.9	26.9	29.9
	Fall	21.5	3.3	5.3	24.8	26.8
	Annual	21.5	4.3	6.9	25.8	28.4
Okefenokee NWR	Winter	21.3	2.3	3.6	23.6	24.9
	Spring	21.5	3.5	5.6	25.0	27.1
	Summer	22.0	3.5	5.5	25.5	27.5
	Fall	21.7	2.9	4.4	24.6	26.1
	Annual	21.7	3.0	4.7	24.7	26.4

[a] From FLAG[1], Table 2.B-1

Inclusion of Wildfire Smoke Emissions

Throughout history, except for the past few decades, fire has been used to clear land, change plant and tree species, sterilize land, maintain certain types of habitat, among other purposes. Native Americans[22] used fire as a technique to maintain certain pieces of land or to improve habitats. Although early settlers often used fire in the same way as the Native Americans, major fires on public domain land were largely ignored and were often viewed as an opportunity to open forestland for grazing.

Whether lightning-caused or started by native peoples, wildfires were once common occurrences throughout the grasslands and forests of the Colorado Plateau, the location of many PSD Class I areas. Prior to white settlement, fires likely burned through the Plateau's extensive piñon-juniper woodlands every 10–30 years, through the region's ponderosa pine communities every 2–10 years, and through mixed-conifer forests every 5–25 years.

Especially large fires raged in North America during the 1800's and early 1900's. The public was becoming slowly aware of fire's potential for life-threatening danger. Federal involvement in trying to control forest fires began in the late 1890's with the hiring of General Land Office rangers during the fire season. When the management of the forest reserves (now called national forests) was transferred to the new Forest Service in 1905, the agency took on the responsibility of creating professional standards for firefighting, including having more rangers and hiring local people to help put out fires.

Since the beginning of the 20th century, fire suppression has resulted in a buildup of vegetative "fuels" and catastrophic wildfires. Recent estimates of background visual range, such as NAPAP[5] may have underestimated the role of managed fire on regional haze. Various government agencies are now planning to increase prescribed burning to reduce the threat of dangerous wildfires. The increased presence of the atmospheric loading of particulate due to burning needs to be included in background visual range estimates attributed to "natural conditions". While this adjustment is not further discussed in this paper, it is yet another factor that makes the present estimates of natural background visual range excessively high. In addition, natural biogenic emissions of volatile organic compounds need to be included in the estimates of natural conditions.

It is especially important that the role of soot from wildfires be incorporated into natural background visibility estimates. Since FLAG was initiated in early 2001, the Federal Land Managers have focused their attention on increasing the extinction efficiency assumptions for new, clean emission sources, looking at soot and secondary organic aerosol speciation. Soot (or elemental carbon) is particularly important because it has an extinction efficiency that is 10 times more potent than non-carbon "soils". However, the FLMs have ignored similar issues with natural background, especially that from wildfires which under natural conditions would be much more widespread and would contribute much more soot to the atmosphere.

EPA's "Guidance for Estimating Natural Visibility Conditions Under the Regional Haze Program"[23] acknowledges that wildfires are a contributor to natural visibility conditions, but the data used in estimates of natural conditions were taken during a period of artificial fire suppression. The report notes that "data should be available for EPA and States to develop improved estimates of the contribution of fire emissions to natural visibility conditions in mandatory Federal Class I areas over time." The authors caution that the impact due to natural fire levels is underestimated from recent data, and that the assessment of natural conditions should take this into account.

2) Threshold for Perceptible Visibility Changes

FLAG establishes a 5 percent change to natural background light extinction as a threshold at which a facility's impact on haze is considered insignificant. FLAG's "one-size fits all" approach in applying the 5 percent of background extinction threshold for visibility impairment does not meet the requirements of visibility regulations, which indicate that the determination of adverse impact should be made on a case-by-case basis.

There are two inherent problems with this criterion: 1) it does not reflect the observers' experiences pertinent to a particular Class I area, and 2) the level is probably well below detection for any observer at any Class I area. The 5 percent criterion is based on the supposition about the change in extinction that is detectable. Regional haze regulations assume that this threshold is 1 deciview. The deciview ($d\nu$) is defined as:

$$d\nu = 10 \ln(b_{ext}/10)$$

where b_{ext} represents the extinction coefficient and units are Mm^{-1}.

The 5 percent of background threshold roughly corresponds to 0.5 deciview and 10 percent of background corresponds to 1 deciview. Thus, the 5 percent threshold represents a policy decision by FLMs that no single PSD source use up more than half of the "visibility increment" of 1 deciview. This means that a source that marginally exceeds the threshold would not be detectable even there were no other sources of man-made pollution on the planet. A recent paper[24] by Ron Henry entitled "Just-Noticeable Differences in Atmospheric Haze" concludes that even the 1 deciview change that forms the basis of a detectable change is, in fact, not detectable. Henry finds that while haze decreases visual range and reduces contrast, the most important and sensitive parameter to observers is the decreased colorfulness of viewed objects. Based on experimental data, he shows that a 1 deciview change is never noticeable and that the deciview level that can be detected varies over a wide range of about 2 to 10, depending on the distance to the object with respect to the visual range (referred to as optical thickness) and the colorfulness of the object of interest.

Based on these results, an adjustment to the significance criterion should be considered. Figure 2 in Henry's paper indicates that a change of 2 deciviews represents a "just noticeable change" for any combination of object colorfulness and distance. According to equation listed above, this corresponds to an 18 percent change in background extinction rather than the 10 percent now used. Applying the FLAG argument that a single source should use only about half of the detectable change results in a screening threshold of about 9 percent instead of 5 percent. Because this threshold corresponds to a very bright object (a colorfulness scale of 75, where 100 is bright red and 0 is gray), it is possible that few, if any, natural objects match this colorfulness level. For a refined assessment on a site-by site basis, it also might be possible to account for the colorfulness of the objects being viewed in establishing appropriate detection thresholds.

3) Use of Relative Humidity in CALPOST

Measurements of relative humidity are most uncertain at high values. RH is not measured directly but generally computed from simultaneous measurements of temperature and dew point. RH, in turn, can be very sensitive to small changes in dew point and temperature. For instance, at 60 degrees Fahrenheit (°F), a 1°F dew point depression (i.e., 59°F) corresponds to 96 percent RH, 2°F depression to 93 percent RH and 3°F depression to 90 percent RH. Present-day automated measurements by the National Weather Service measure dew point with optical techniques to determine the temperature at which condensation takes place on a chilled mirror. Even with these automated techniques, measurement problems have been noted. For example, dew point measurements sometimes "stick" near freezing and higher than actual dew points are measured when mirrors become coated with dust or aerosol.

Currently, the relative humidity at the nearest surface station is used to adjust the natural background visual range (or extinction) due to the sensitivity of hygroscopic particulate to humidity. In areas where such surface stations are quite distant from the PSD Class I areas under consideration, the use of relative humidity from MM5 data may be preferable because of the good spatial coverage of the MM5 data. The CALPOST user should also be careful about using airport sites that experience higher relative humidity values due to their typical location in valleys (with more cooling at night than high elevation areas).

The current guidance for Estimating Natural Visibility Conditions Under the Regional Haze Rule uses a 95% cap for RH visibility effects by hygroscopic particles. In addition, a 90 % RH cutoff has been established in the transmissometer data reduction and validation procedures[12]. In this protocol document, it is stated that "when the RH is above 90 percent at one end of the path, small random temperature or absolute humidity fluctuations along the path can lead to condensation of water vapor, causing meteorological interferences." Correspondingly, an RH cap of between 90 and 95% should be implemented in CALPOST.

4) Characterization of Background Visual Range During Periods of Meteorological Interferences

The natural background assumed by FLAG ignores natural obscuration during fog, precipitation, and cloud nighttime periods. This is a major omission that has led to unnecessarily conservative estimates of proposed project impacts ever since FLAG was implemented in early 2001. Recently, the assistant secretary of the Department of the Interior, Mr. Craig Manson, in a letter dated January 10, 2003 regarding the Roundup Power Plant permit application in Wyoming, has carefully considered evidence that peak predicted impacts due to a proposed source occur during periods of natural obscuration. This concept should be made a permanent feature of the FLAG process. A proposed method for doing this is described below is the discussion of daily average calculations of extinction change.

Surface meteorological stations (or site-specific measurements in the applicable PSD Class I area, as used by Pearson et al.[25]) can be used to determine whether there is any fog or precipitation. For hours with detected precipitation, Pearson and Nall used the measured background visual range as a replacement for the FLAG natural background. While this method may work for areas with such measurements, there are many PSD Class I areas with no such measurements, and others with such a large extent (e.g., Shenandoah National Park) that only one measurement might not always be representative of the entire area. Instead, the authors recommend that the presence of precipitation be used as an indicator that visibility degradation is not important. It is a common experience that periods of meteorological interferences such as precipitation and fog have significantly degraded background visibility such that the regional haze influence of a distant plume is generally imperceptible.

Likewise, during periods at night when there is a cloud ceiling (coverage more than 50%), the only source of light (the moon, stars, and planets) are effectively hidden from view, and there is no visual resource to protect.

The notion that periods of meteorological interferences need special handling is generally in line with the points made by Dr. Warren White[26] in his comments on the Air & Waste Management Association's Critical Review of Visibility issues last year.

Dr. White explained in his review that the Regional Haze Rule overlooks other plausible ways to assess visibility degradation. For example as Dr. White notes, in California, the procedures for assessing visibility impacts have reasonable alternatives:

- Daytime visibility only is assessed (in this paper, we propose that nighttime visibility during periods of an observed cloud ceiling be assigned a background visual range of zero).

- Periods of elevated humidity are discarded from further review. White notes that IMPROVE optical measurements at relative humidities greater than 90% are withheld from summary calculations since they are deemed to be subject to "weather interferences". However, the FLAG guidance requires relative humidities as high as 98% to be included in regional haze calculations.

- Visibility is characterized in terms of visual range, rather than particle extinction.

The authors generally agree with Dr. White and note that many of the changes proposed in this paper are consistent with his recommendations.

5) Dry Extinction Efficiency for Sulfates and Nitrates

Lowenthal and Kumar[21] note that the "consensus" value reported by Watson[26] for the dry scattering efficiencies of ammonium sulfate and nitrate is 3 m^2/g. However, Lowenthal and Kumar found from a closer examination of field study data and comparison of the reconstructed light extinction to actual IMPROVE extinction measurements that a revised value of 2.5 m^2/g provides a better fit to these various databases. The current use of 3 m^2/g as the dry extinction scattering efficiency would tend to overstate the role of ammonium sulfates and nitrates in visibility impacts. This revision can be implemented in CALPOST manually until future code changes incorporate this more accurate extinction efficiency value.

6) Revised f(RH) Curve

EPA, in its September 2003 *Guidance for Tracking Progress Under the Regional Haze Rule*[27], has published a revised (smoothed) set of f(RH) values that determine the relationship between light scattering efficiency of hygroscopic particles and relative humidity. These values are lower than the original FLAG f(RH) values for relative humidity in the important range of 85 to 95%. To avoid inconsistencies in the treatment of regional haze applications, the FLAG procedures should adopt the EPA published f(RH) values.

7) Choice of the CALPUFF Chemical Mechanism Method

Morris[28] discusses shortcomings in the default CALPUFF chemical transformation method referred to as the MESOPUFF-II procedure. This method dates back to 1983 and is based upon regression equations using 144 box model simulations of a 1982 photochemical mechanism. The aqueous-phase sulfate formation in the MESOPUFF-II algorithm is solely based upon surface relative humidity, while Morris notes that this rate of formation is often limited by available oxidants, especially in rural areas. Furthermore, the lack of temperature effects in the MESOPUFF-II mechanism and a 50ºF minimum temperature used in the development of the MESOPUFF-II method will tend to overstate sulfate and nitrate formation in cold conditions.

Morris concludes that the MESOPUFF-II mechanism:

- Overstates the daytime gas-phase sulfate and nitrate formation rates by a factor of 2-3 on average,
- Understates the sulfate formation when clouds and oxidants are present by up to 100%
- Has no sensitivity to NO_x and temperature, and
- Is too sensitive to ozone and relative humidity.

Moore shows very good comparisons between the RIVAD predictions and full-science models. Therefore, this alternative mechanism should be seriously considered for predictions of secondary sulfate and nitrate formation in CALPUFF applications for regional haze predictions.

8) Daily Averages of the Source/Background Extinction Ratio

Paine, et al.[2] discussed the effects of the FLAG guidance in permitting a well-controlled hypothetical emissions source in the Midwest. FLAG and IWAQM require the computation of hourly light extinction because the source-related extinction is a function of the hourly particulate concentration, and both the source-related and background extinction are functions of the hourly relative humidity. Humidity affects only the fraction of particulate that is hygroscopic. Because source-related particulate (beyond 50 km) is primarily hygroscopic whereas the currently estimated "natural background" particulate is mostly non-hygroscopic, high humidity has a greater effect on source-related extinction than on natural background extinction.

In the FLAG approach, the daily average source-related and background extinction values are computed separately as the arithmetic means of the computed hourly extinction values. The ratio of these mean values is computed daily and the largest of the daily ratios are used to evaluate the significance of a source's contribution to haze. The FLAG method is not a valid measure of the average visibility impairment for a number of reasons:

a) A few hours with very high humidity tend to dominate the source-related and background-related averages, thus dominating the daily ratio. The high relative humidity periods often occur during cloudy nighttime hours or precipitation periods, when natural visibility conditions are impaired. In the daily averaging, the hours of the highest visual range (lowest extinction) are weighted the least.

b) The standard CALPOST method computes the daily average extinction associated with a source and adds this daily average extinction to the average background extinction to estimate the change in total daily average extinction. Because this method uses daily averages, it does not directly relate to the visual experience of a visitor, which varies from hour to hour, according to variations in the modeled concentration and humidity. There may also be certain times during the day that visibility is naturally obscured, although it may not be obscured for the whole 24-hour period. Therefore, days with some hours of obscuration due to meteorological interferences need to be processed in a different manner than days with no interferences, but those days should not necessarily be discarded from the analysis.

The authors propose a modified hour-by-hour analysis that would compute the hourly ratio of the total (modeled source-caused+ background) extinction to the background extinction. (The hourly information is available within the CALPOST code and the authors have enhanced CALPOST to provide this information.) Each hourly ratio would then represent the change in extinction due to the source impact that a visitor would experience for that hour. The measure of the average visibility degradation experienced over the day would then be computed by taking the mean of the 24 hourly extinction ratios. A geometric mean is most appropriate as an unbiased statistical measure for taking the mean of ratios. In a day without meteorological interferences, the geometric mean of 24 hourly ratios would be taken directly to determine the daily change in extinction.

For hours where natural obstructions to visibility occur, the corresponding extinction ratio would be set to 1, indicating that the source has a negligible effect upon visibility that is already degraded, due to meteorological interferences. There are two types of meteorological conditions that would be considered as contributing to natural obscuration:

a) Precipitation and fog: Hours when recorded weather observations at a representative meteorological station (or radar records) indicate that precipitation or fog is occurring. For a case where there is a question of whether a specific model receptor within the Class I areas is affected, the presence of precipitation and/or fog over the area can be confirmed by reviewing archived weather surface and radar maps covering the Class I areas. Other confirmation methods include a review of hourly transmissometer or nephalometer data, as used by Pearson et al.[25].

b) Cloudy nights: After the time of civil twilight and before civil dawn, the only natural sources of illumination (and objects of viewing) are the moon, planets, and stars. When the sky is mostly cloudy or overcast (i.e., there is a ceiling reported), the visitor would not consider visibility to be an Air Quality Related Value. This method still counts periods near sunrise and sunset, which are some favorite viewing times for visitors to our national parks.

Once the extinction change ratios for these hours are corrected to 1.0, the resultant daily geometric mean would be computed, providing a more realistic evaluation of days with potentially significant impacts. In this case, a daily ratio less than 1.05 would indicate no significant visual impact for a single source (with the current FLAG threshold of a 5% change), and a daily ratio less than 1.10 would indicate no significant visual impact for a cumulative source inventory.

The example provided below shows how the refinement would be implemented. An enhanced CALPOST program available to the authors offers the capability of obtaining the hourly extinction changes due to source impacts. These can be placed in a spreadsheet, as shown in Table 2 and in Figure 4. The table shows the hourly background and source-caused extinction ("Bext(BKG)" and "Bext(SRC)"). The column labeled "Interf.?" indicates whether a case of natural obscuration is present (if 1). If so, the column labeled "Hourly extinction ratio w/Interferences" is set to 1.0, while the working column labeled "Hourly extinction ratio" does not set the ratio of these values to 1.0. It can be seen that the CALPOST calculation results in a daily extinction change exceeding 20% using the current techniques, which is considerably influenced by the cloudy nighttime hours. In this example application,

the use of the geometric mean of the hourly values results in an extinction change of about 17% without considering interferences, and less than 10% with consideration of interferences.

It is evident from Table 2 that different methods to average the results of the same CALPUFF model predictions can result in quite different answers. The use of the geometric mean of the hourly extinction ratios is, in our view, more compatible with the hourly visual experience of a person in a Class I area, especially during periods of meteorological interferences.

Another benefit that results from the adoption of the proposed ratio method is that a substitute visual range during periods of meteorological interferences is not required. In addition, days with meteorological interferences are still considered, but the hours of naturally degraded visual range are treated appropriately.

Table 2. Working Spreadsheet for Regional Haze Refinement Calculation

Hour of the Day	Bext(BKG)	Bext(Src)	Interf.?	Hourly Extinction Ratio	Hourly Extinction Ratio w/interferences
1	26.0	7.0	1	1.27	1.00
2	24.8	5.0	1	1.20	1.00
3	24.8	5.0	1	1.20	1.00
4	32.1	12.0	1	1.37	1.00
5	32.1	12.0	1	1.37	1.00
6	32.1	12.0	1	1.37	1.00
7	32.1	12.0	0	1.37	1.37
8	32.1	12.0	0	1.37	1.37
9	24.8	10.0	0	1.40	1.40
10	20.8	6.0	0	1.29	1.29
11	20.3	4.0	0	1.20	1.20
12	19.9	3.0	0	1.15	1.15
13	19.6	2.0	0	1.10	1.10
14	19.5	1.1	0	1.06	1.06
15	19.5	1.0	0	1.05	1.05
16	19.5	0.8	0	1.04	1.04
17	19.5	0.8	0	1.04	1.04
18	19.6	0.9	0	1.04	1.04
19	19.6	0.9	0	1.04	1.04
20	20.5	1.7	0	1.08	1.08
21	20.0	1.2	0	1.06	1.06
22	20.3	1.3	0	1.07	1.07
23	20.8	1.5	0	1.07	1.07
24	21.9	1.5	0	1.07	1.07
Average	**23.4**	**4.8**			
	CALPOST:	**20.39%**		**1.172**	**1.098**

Figure 4. Display of Hourly Extinction Ratio with and without Considering Interferences

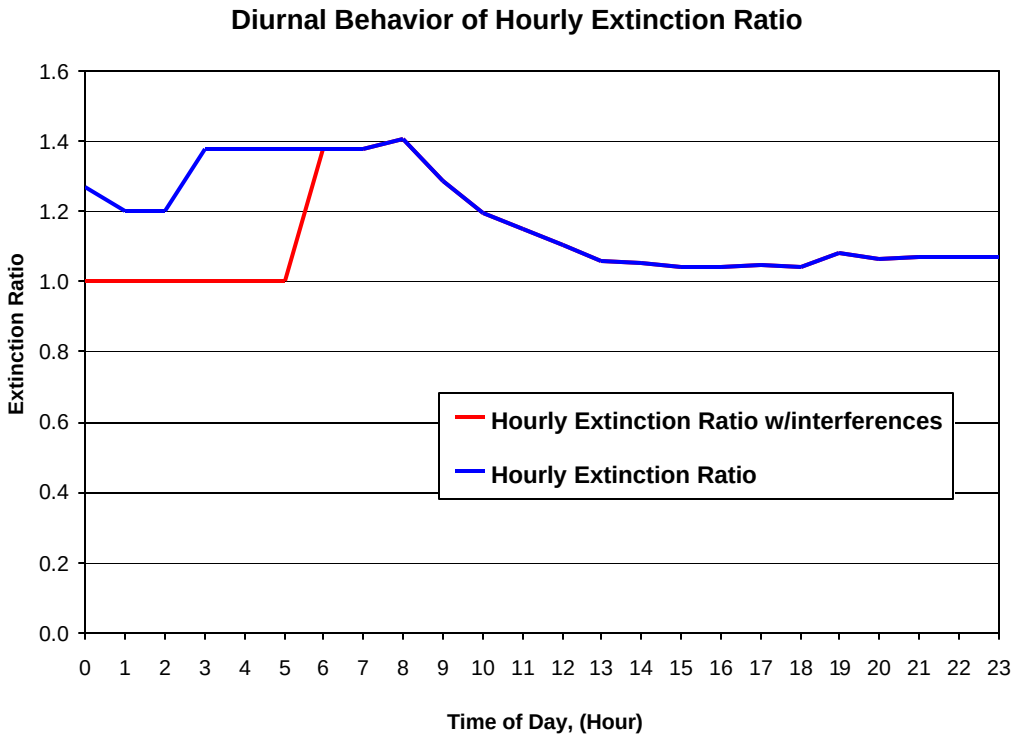

CONCLUSIONS

The adoption of the FLAG guidance and its implementation with CALPUFF has important implications for the ability for most proposed new or modified emission sources to be permitted in the United States. The FLAG restrictions on new source permitting are aggravating air quality. There are several features of the CALPUFF modeling system and the application of the FLAG procedures that add considerable and unwarranted conservatism to the results. Besides the known limitations of CALPUFF to account for plume spreading associated with nocturnal wind shear, these features and suggested correction approaches include the following items:

- Omission of certain components of naturally occurring particulates, such as natural salt particles and wildfire emissions, which have considerable soot content, is important. To correct this deficiency, use IMPROVE data to determine the natural salt content of the atmosphere and change the natural background extinction. FLAG should also account for wildfire emissions in future updates to the natural background extinction.

- How sensitive the CALPUFF results are to relative humidity and how to deal with unrepresentative RH input data should be accounted for. In this case, the user could adopt the RH values from an MM5 database or scrutinize the station database for unrepresentative stations that should be omitted from the analysis. In addition, the maximum RH value to be used for the f(RH) calculation should be in the range of 90-95%.

- The choice of the percent change in extinction that is just noticeable is too stringent. A significance level of a 9% change, and a cumulative acceptable level of an 18% change should be adopted.

- How cloudy nighttime conditions and precipitation/fog events can inappropriately influence the visibility assessments and should be properly accounted for. Precipitation events can be verified with radar reports. The CALPUFF user can assume that specific hours with meteorological interferences have a negligible visibility change due to a source emission impact.

- The dry extinction scattering efficiency for ammonium sulfates and nitrates should be revised from 3 m^2/g to 2.5 m^2/g. This change can be done immediately with a manual process until CALPOST has been revised to accommodate this refinement.

- The latest EPA-published f(RH) curves should be adopted for the FLAG procedures as well.

- Use of an alternative method such as the RIVAD chemical mechanism for computing formation rates of sulfates and nitrates should be considered. The current MESOPUFF-II method can often overpredict these rates by at least a factor of 2.

- How the daily averages of the ratio of the source-caused to background light extinction are calculated should be re-examined. A *geometric mean of hourly ratios* of the altered and "natural" extinction should be calculated, accounting for meteorological interference hours by assuming no discernible visibility degradation.

The authors' experience with permitting under the FLAG process to date has been that the FLMs seem to be reluctant to accept refinements to FLAG. It is interesting that a National Park Service reviewer of this paper states that FLAG is a "screening tool designed to sort out extremely small proposed sources which warrant no further analysis; it is therefore designed to be conservative". The authors hope that the refinements described in this paper are welcomed by the FLMs to provide a way to get beyond the acknowledged screening process that the FLAG procedures are.

REFERENCES

1. Federal Land Managers. *Federal Land Managers' Air Quality Related Values Workgroup (FLAG) Phase I Report*. http://www2.nature.nps.gov/ard/flagfree/index.htm (accessed January 2001)

2. Paine, R.J., J.A. Connors, and D.W. Heinold. FLAG Aftermath: Effects of the Federal Land Managers' Modeling Guidance on CALPUFF Applications for New Source Permitting. Paper #42534, presented at the 95th Annual Conference and Exhibition of the Air & Waste Management Association, Baltimore, MD (2002)

3. Interagency Workgroup on Air Quality Modeling. *Interagency Workgroup On Air Quality Modeling (IWAQM) Phase 2 Summary Report and Recommendations for Modeling Long Range Transport Impacts*. EPA-454/R-98-019. (December, 1998)

4. Dispersion Model (Version 5.4). http://www.epa.gov/scram001 (under 7th Modeling Conference link to Earth Tech web site). (accessed December 2000)

5. National Acid Precipitation Assessment Program. *Acidic Deposition: State of Science and Technology, Report 24, Visibility: Existing and Historical Conditions – Causes and Effects.* (1990)

6. Walcek, C.J. Lagrangian vs. Eulerian Dispersion Modeling: Effects of Wind Shear on Pollution Dispersion. Paper 8.7, presented at the 12th Joint Conference on Applications of Air Pollution Meteorology with the Air & Waste Management Association. American Meteorological Society, Boston, MA (2002)

7. Moran, M.D. and R.A. Pielke. Delayed Shear Enhancement in Mesoscale Atmospheric Dispersion. Paper 3.1 in proceedings of the Eighth Joint Conference on Applications of Air Pollution Meteorology with A&WA. American Meteorological Society, Boston, MA. (1994)

8. Carl, F. and B. Petermann. WYGEN 2 – A Case Study on Resolving BACT and Visibility Impact Issues for New Coal Plant Development within the Current Regulatory Regime. Paper C2e, presented at the 6th Electric Utilities Environmental Conference, Tucson, AZ. (January 27-30, 2003)

9. U.S. Environmental Protection Agency. *Draft Guidance for Estimating Natural Visibility Conditions Under the Regional Haze Rule*, Office of Air Quality Planning and Standards, Research Triangle Park, NC, September 27. Available at http://www.epa.gov/ttn/amtic/visinfo.html (accessed March 2002)

10. Paine, R.J., S.L. Heisler, and D.W. Heinold. Regional Haze Assessments with CALPUFF: Application of Refined Procedures. Presented at the Air & Waste Management Association's 96th Annual Conference and Exhibition, San Diego, CA. (June, 2003)

11. IMPROVE. Data downloaded from http://vista.cira.colostate.edu/improve/Data/IMPROVE/improve_date.htm. (accessed January, 2002)

12. IMPROVE . IMPROVE Standard Operating Procedure 351, Data Processing and Validation, p. A-58, October. Available at http://vista.cira.colostate.edu/improve/Publications/SOPs/ucdsop.asp (1997)

13. Gartrell, G. Jr., Heisler, S.L. and Friedlander, S.K. "Relating Particulate Properties to Sources : The Results of the California Aerosol Characterization Experiment," in *The Character and Origins of Smog Aerosols, A Digest of Results from the California Aerosol Characterization Experiment* (ACHEX) (G. M. Hidy, Ed.), John Wiler & Sons, New York. (1980)

14. Malm, W.C., Day, Derek, E. and Kreidenweis, S.M. Light Scattering Characteristics of Aerosols as a Function of Relative humidity: Part I - A Comparison of Measured Scattering and Aerosol

Concentrations Using the Theoretical Models; *J. Air & Waste Manage. Assoc*. 50, 686-700. (2000)

15. Tang, I.N. "Deliquescence Properties and Particle Size Change of Hygroscopic Aerosols;" in *Generation of Aerosols* (K. Willeke, Ed.); Chap. 7 Ann Arbor Science, Ann Arbor, MI. (1980)

16. Tang, I.N. and Munkelwitz, H.R. Composition and Temperature Dependence of the Deliquescent Properties of Hygroscopic Aerosols; *Atmospheric Environment*, *27A*, 467-473. (1993)

17. Tang, I.N., Tridico, A.C. and Fung, K.H. Thermodynamic and Optical Properties of Sea Salt Aerosols; *Journal of Geophysical Research*, 102, 23,269-23,275. (1997)

18. Ansari, A.S. and Pandis, S.N. Prediction of Multicomponent Inorganic Atmospheric Aerosol Behavior; *Atmospheric Environment, 33*, 745-757. (1999)

19. Ming, Y. and Russell, L.M. Predicted Hygroscopic Growth of Sea Salt Aerosol; *Journal of Geophysical Research, 106*, 28, 259-28,274. (2001)

20. Arnold, J.R., W.T. Luke amd T.B. Watson, Nitrate Aersol Partitioning in the 2003 Bay Regional Atmopsheric Chemistry Experiment : Aloft and Surface Comparisons, 2003 Fall Meeting of the American Geophysical Union, San Francisco. (December, 2003)

21. Lowenthal, D.H. and N. Kumar. $PM_{2.5}$ Mass and Light Extinction Reconstruction in IMPROVE. *J. Air & Waste Manage. Assoc., 53*:1109-1120. (2003)

22. Williams, G.W. References on the American Indian Use of Fire in Ecosystems. http://fs.jorge.com/archives/Reference/Biblio_IndianUseofFire.htm. (accessed February 2002)

23. United States Environmental Protection Agency. Guidance for Estimating Natural Visibility Conditions Under the Regional Haze Program. EPA-454/B-03-005. Office of Air Quality Planning and Standards, Research Triangle Park, NC. (2003)

24. Henry, R. C. Just-Noticeable Differences in Atmospheric Haze. *Journal of the Air and Waste Management Association.* Vol. 52, pp1238-1243. (2002)

25. Pearson, R. L., J. Nall, S. Sands, D. Caniparoli, and M. Bennett. 2003. Estimation of Natural Background Light Extinction for Use in Determining New Source Impact on Class I Air Quality Related Values. Paper #69926, presented at the 96th Annual Conference and Exhibition of the Air & Waste Management Association, San Diego, CA. (2003)

26. Chow, J.C., J.D. Bachmann, S.S.G. Wierman, C.V. Mathai, W.C. Malm, W.H. White, P.K. Mueller, N. Kumar, and J.G. Watson. Visibility: Science and Regulation. *J. Air & Waste Manage. Assoc. 52: 973-999.* (2002)

27. United States Environmental Protection Agency. Guidance for Tracking Progress Under the Regional Haze Program. EPA-454/B-03-004. Office of Air Quality Planning and Standards, Research Triangle Park, NC. (2003)

28. Morris, R. Evaluation of the Sulfate and Nitrate Formation Mechanism in the CALPUFF Modeling System. Presented at the AWMA Specialty Conference – Guideline on Air Quality Models: The Path Forward. (October, 2003)

KEYWORDS

PSD Class I

Visibility assessment

CALPUFF

FLAG

Federal Land Manager

Regional haze

APPENDIX F

CONTRIBUTION OF SALT PARTICLES TO NATURAL BACKGROUND LIGHT EXTINCTION AT PSD CLASS I AREAS

APPENDIX F

Contribution of Salt Particles to Natural Background

Light Extinction at PSD Class I Areas

Steven Heisler and Robert Paine, ENSR Corporation

Guidance for estimating natural background light extinction at federal Class I areas issued by the Federal Land Managers' Air Quality Related Values Workgroup (FLAG 2000) does not include estimates of contributions of naturally occurring salt aerosols. In their review of the data analysis protocols developed for IMPROVE for assessing compliance under EPA's Regional Haze Rule, Lowenthal and Kumar (2003) note that the methods for reconstructing light extinction from particulate measurements are overly simplified. They specifically note that concentrations of sodium and chlorine are available at all IMPROVE sites, so "there is no reason why they should not be included in reconstructed mass."

Because Class I areas on or near ocean coastlines or near salt flats or salt lakes in the West might have significant contributions from naturally occurring salt aerosols, the lack of their inclusion may significantly underestimate the natural background light extinction.

The contribution to light extinction by a specific aerosol component is typically expressed as:

$$E = k\, f(RH)\, [component] \quad (1)$$

where:

- E = contribution to light extinction by the specific component (Mm^{-1})
- k = light extinction efficiency of the component at low relative humidity (also called the "dry" light extinction efficiency) (m^2/g)
- $f(RH)$ = an empirical function describing the increase in light extinction due to the growth of particles of a hygroscopic component as the relative humidity (RH) increases
- [component] = atmospheric concentration of component ($\mu g/m^3$)

The following steps were used as an example to estimate the salt aerosol contributions using Equation 1:

1. Annual and seasonal average salt aerosol concentrations ([Salt]) at one coastal and one near-coastal Class I area in the Southeast were estimated using data collected by the Interagency Monitoring for the Protection of Visual Environments (IMPROVE) program.

2. The technical literature was reviewed to estimate the dry light extinction efficiency (k) and the variation of light extinction by salt aerosols [f(RH)] with relative humidity.
3. Equation 1 was applied to the annual and seasonal average salt aerosol concentrations to estimate annual average contributions to estimate contributions to light extinction.

Salt Aerosol Concentrations

Salt aerosol concentrations were estimated from sodium and chloride concentrations measured at IMPROVE network monitoring sites, based on the assumption that all of the sodium and chloride are present in naturally occurring salt. Data for Cape Romain National Wildlife Refuge (NWR), on the coast of South Carolina, and for Okefenokee NWR, near the coast of Georgia, were used. Measurements at Cape Romain NWR began in early-September 1994, and measurements at Okefenokee NWR begain in late-September 1991. Data through the end of February 2000 were available from the IMPROVE Web site (IMPROVE 2002).

The IMPROVE database includes reported $PM_{2.5}$ concentrations of elemental sodium, ionic chloride and elemental chlorine. Seasonal averages of the reported values of sodium and chloride were calculated. The chlorine data were not used, because chlorine is volatilized from the filter during sampling (IMPROVE 1997). The definitions of the seasons followed the definitions used by IMPROVE: winter is December, January and February; Spring is March, April and May; summer is June, July and August; and fall is September, October and November. Concentrations below the reported method detection limit (MDL) were set to one-half the MDL prior to calculating the average values. As shown below, a substantial number of values were available for each season, so no substitutions for missing data were made. The annual average concentrations were calculated as the averages of the four seasonal average concentrations. This averaging of the seasonal averages avoided biases introduced by uneven distributions of available data among seasons.

The average concentrations are presented in Table 1, along with the ratio of average sodium to average chloride. The ratio of sodium to chloride in seawater is about 0.56 (Gartrell et al., 1980), while the ratios in the table all exceed 2.0. As described by Tang et al. (1997), this chloride deficiency can be caused by reactions with sulfuric or nitric acid that liberate gaseous hydrogen chloride and increase concentrations of sulfate or nitrate in the sea salt particles. Chloride deficits in sea salt particles may also be caused by reactions with gaseous nitrogen dioxide or by oxidation of dissolved sulfur dioxide by ozone.

Gartrell et al. (1980) used the percentage of sodium in sea salt to estimate the atmospheric concentration of sea salt prior to chloride loss. They then assumed that the lost chloride was replaced by sulfate (one sulfate ion for two chloride ions) to estimate the sea salt concentration after chloride loss. This approach leads to a higher mass

concentration of salt aerosol than would be present if the chloride were not displaced, because the formula weight of sulfate is larger than the atomic weight of chlorine. To allow for the possibility that this process occurs under natural conditions, this same approach was used to estimate salt aerosol concentrations from the average sodium concentrations in Table 1. The following equation was used for the calculation:

$$[Salt] = [Na] / 0.306 + -(1.79\,[Na] - [Cl]) + 1.35\,(1.79\,[Na] - [Cl^-]) \quad (2)$$

where:

[Salt] = Salt aerosol concentration ($\mu g/m^3$)

[Na] = Sodium concentration ($\mu g/m^3$)

0.306 = Mass fraction of sodium in sea salt (Gartrell et al., 1980)

1.35 = Formula weight of sulfate (96) divided by two times the formula weight of chloride (35.5)

1.79 = Mass ratio of chloride to sodium in sea salt

$[Cl^-]$ = Chloride concentration ($\mu g/m^3$)

The first term in Equation 2 represents the salt aerosol concentration without chloride displacement, the second term represents the chloride concentration that is displaced, and the last term accounts for the mass concentration of sulfate that displaced the chloride.

Because chloride displacement by other substances may not occur under natural conditions, when concentrations of acidic gases and particulate constituents would be lower, a lower-limit estimate for the salt aerosol concentration was calculated by using only the first term in Equation 2.

Table 1

Seasonal and Annual Average Sodium, Chloride and Chlorine Concentrations

Site	Season	Sodium		Chloride		Sodium/ Chloride
		Concentration ($\mu g/m^3$)	Number	Concentration ($\mu g/m^3$)	Number	
Cape Romain NWR	Winter	0.380	140	0.173	128	2.20
	Spring	0.518	118	0.142	106	3.65
	Summer	0.388	120	0.134	107	2.90
	Fall	0.308	140	0.104	130	2.96
	Annual	0.398		0.138		2.88
Okefenokee NWR	Winter	0.215	220	0.084	187	2.56
	Spring	0.316	207	0.111	170	2.85
	Summer	0.271	189	0.091	158	2.98
	Fall	0.243	195	0.117	165	2.08
	Annual	0.261		0.101		2.58
Values are based on IMPROVE monitoring data.						

The resulting estimates of the seasonal and annual average salt aerosol concentrations are listed in Table 2. The lower and upper limits of the estimated annual average concentrations are about 1.3 $\mu g/m^3$ and 1.5 $\mu g/m^3$, respectively, at Cape Romain NWR, and about 0.9 and 1.0 $\mu g/m^3$, respectively, at Okefenokee NWR. For comparison, the estimated annual average natural concentration in the East of hygroscopic $PM_{2.5}$ constituents proposed in US EPA Draft Guidance for Estimating Natural Visibility Conditions Under the Regional Haze Rule (US EPA 2001) is 0.33 $\mu g/m^3$, which is about a third or less of the salt aerosol mass concentration estimates.

Table 2
Seasonal and Annual Average Estimates of Salt Aerosol Concentrations

Site	Season	Lower Limit[a] ($\mu g/m^3$)	Upper Limit[b] ($\mu g/m^3$)
Cape Romain NWR	Winter	1.242	1.419
	Spring	1.692	1.968
	Summer	1.269	1.464
	Fall	1.006	1.163
	Annual	1.302	1.502
Okefenokee NWR	Winter	0.703	0.808
	Spring	1.032	1.192
	Summer	0.887	1.024
	Fall	0.795	0.905
	Annual	0.854	0.981

[a] Lower limit assumes no replacement with chloride by other substances.
[b] Upper limit assumes chloride replacement by sulfate.

Salt Aerosol Light Extinction Efficiency

Information regarding the dry light extinction efficiency for salt particles was not found in the technical literature. However, the dry light extinction efficiency is generally related to the size distribution of the particles at low relative humidity, although other factors such as refractive index also play a part. Gartrell, et al. (1980) have shown that the typical particle size distributions for soil and for sea salt are very similar. The dry light extinction efficiency, for fine soil is commonly accepted to be around 1 m^2/g (Malm, et al., 2000). Therefore, 1 m^2/g was used as the dry particle light extinction efficiency for salt aerosol in these analyses.

The hygroscopic nature of salt particles is well established (Tang, 1980; Tang and Munkelwitz, 1993; Tang, et al., 1997; Ansari and Pandis, 1999). Both pure salts (e.g., NaCl) and mixed salts (e.g., KCl-NaCl) have been shown to exhibit substantial particle growth as a function of relative humidity. Airborne salt particles often contain organic

materials in internal mixtures, and these mixed salt-organic particles have been shown to be hygroscopic, as well (Ming and Russell, 2001). Furthermore, the hygroscopic properties of salt particles are generally similar to those of ammonium sulfate and ammonium nitrate (the hygroscopic species represented by f(RH) values in Table 2.A-1 of the FLAG (2000) Phase I Report). For example, the deliquescence humidity (at 25° C) is 75.7% for NaCl, compared to 79.5% for ammonium sulfate (Tang, 1980).

Specific values of f(RH) for sea salt have been determined through field measurements. Gasso, et al. (1998) conducted aircraft-based measurements of the aerosol over the east subtropical Atlantic Ocean, near the Canary Islands. Their measurements were conducted in June and July of 1997 as part of the Aerosol Characterization Experiment 2 (ACE2). They used a humidygraph, consisting of two nephelometers attached to the same inlet probe. One nephelometer measures ambient light scattering, and the inlet to the other nephelometer is heated to provide a measure of scattering by dry particles. This dual sampling approach measures two points on the scattering versus RH curve, in order to obtain an estimate of the dependence of aerosol light scattering on RH.

The ACE2 measurements obtained data in three classes of ambient conditions: polluted, dust, and marine. The marine days (no pollution or dust as determined by back trajectory modeling) represented light scattering by sea salt particles.

The marine days data yielded the following f(RH) function:

$$f(RH) = (1 - RH/100)^{-?} \qquad (3)$$

where:

? = 0.6276 +/- 0.1159

When this equation is applied to RH, it yields numerical values of f(RH) as shown in Table 3. Also shown, for comparison, are the CALPOST f(RH) values from FLAG Table 2.A-1.

It is evident from Table 3 that the salt aerosol f(RH) values match those from CALPOST reasonably well, especially between 60% and 90% RH. Therefore, within reasonable uncertainty bounds, the CALPOST f(RH) values in FLAG Table 2.A-1 can be used to model the growth of salt particles.

Table 3
F(RH) For Sea Salt Particles and for the CALPOST Hygroscopic Species (Ammonium Sulfate And Ammonium Nitrate)

RH (%)	f(RH) - Sea Salt	f(RH) - CALPOST
5	1.0	1.0
10	1.1	1.0
15	1.1	1.0
20	1.2	1.0
25	1.2	1.0
30	1.3	1.0
35	1.3	1.0
40	1.4	1.1
45	1.5	1.2
50	1.5	1.2
55	1.7	1.3
60	1.8	1.4
65	1.9	1.7
70	2.1	1.9
75	2.4	2.2
80	2.7	2.7
85	3.3	3.4
90	4.2	4.7
95	6.6	9.8

Contributions of Salt Aerosols to Light Extinction

The FLAG guidance provides f(RH) values for use with seasonal and annual average concentrations of ammonium sulfate and ammonium nitrate (FLAG 2000). Table 2.B-1 of the guidance document lists these values for individual Class I areas along with estimates of the extinction coefficient for natural conditions. The values in Table 2.B-1, along with a dry light extinction efficiency of 1 m^2/g, were applied to the estimates of seasonal and annual average sea salt aerosol concentrations to estimate sea salt aerosol contributions to light extinction.

Estimated seasonal and annual average salt aerosol contributions to the light extinction coefficient are listed in Table 4, and the estimated total seasonal and annual average light extinction coefficients without and with the salt aerosol contributions are listed in Table 5. As seen in Table 4, including the salt aerosol contribution increases the estimated natural background light extinction coefficient significantly. The lower and upper bounds for the percentage increase in the annual average estimated

Table 4
Estimated Seasonal and Annual Average Salt Aerosol Contributions to Light Extinction

Site	Season	f(RH)[a]	Concentration ($\mu g/m^3$)		Light Extinction Coefficient[b] (Mm^{-1})	
			Lower Limit	Upper Limit	Lower Limit	Upper Limit
Cape Romain NWR	Winter	2.9	1.24	1.42	3.6	4.1
	Spring	3.3	1.69	1.978	5.6	6.5
	Summer	3.9	1.27	1.46	4.9	5.7
	Fall	3.3	1.01	1.16	3.3	3.8
	Annual	3.3	1.30	1.50	4.3	5.0
Okefenokee NWR	Winter	3.2	0.70	0.81	2.3	2.6
	Spring	3.4	1.03	1.19	3.5	4.0
	Summer	3.9	0.89	1.02	3.5	3.5
	Fall	3.6	0.80	0.91	2.9	3.3
	Annual	3.5	0.85	0.98	3.0	3.4

[a] From FLAG (2000), Table 2.B-1
[b] Based on 1 m^2/g dry light extinction efficiency

Table 5
Estimated Seasonal and Annual Average Light Extinction Under Natural Conditions with Salt Aerosol Contributions

Site	Season	Light Extinction Coefficient Without Salt[a] (Mm^{-1})	Salt Contribution to Light Extinction Coefficient (Mm^{-1})		Light Extinction Coefficient With Salt Contribution (Mm^{-1})	
			Lower Limit	Upper Limit	Lower Limit	Upper Limit
Cape Romain NWR	Winter	21.1	3.6	4.1	24.7	25.2
	Spring	21.4	5.6	6.5	27.0	27.9
	Summer	22.0	4.9	5.7	26.9	27.7
	Fall	21.5	3.3	3.8	24.8	25.3
	Annual	21.5	4.3	5.0	25.8	26.5
Okefenokee NWR	Winter	21.3	2.3	2.6	23.6	23.6
	Spring	21.5	3.5	4.0	25.0	25.5
	Summer	22.0	3.5	3.5	25.5	25.5
	Fall	21.7	2.9	3.3	24.6	25.0
	Annual	21.7	3.0	3.4	24.7	25.1

[a] From FLAG (2000), Table 2.B-1

light extinction coefficient are 20 and 23 percent, respectively, at Cape Romain NWR. The lower and upper bounds for the percentage increase in the annual average light extinction coefficient at Okefonekee NWR are 14 and 16 percent, respectively.

References

Ansari, A.S. and Pandis, S.N. (1999) Prediction of Multicomponent Inorganic Atmospheric Aerosol Behavior; Atmospheric Environment, *33*, 745-757.

FLAG (2000) Federal Land Managers' Air Quality Related Values Workgroup (FLAG) Phase I Report, U.S. Forest Service – Air Quality Program, National Park Service – Air Resources Division, and U.S. Fish And Wildlife Service – Air Quality Branch, December.

IMPROVE (1997) IMPROVE Standard Operating Procedure 351, Data Processing and Validation, p. A-58, October. Available at http://vista.cira.colostate.edu/improve/Publications/SOPs/ucdsop.asp

IMPROVE (2002) Data downloaded from http://vista.cira.colostate.edu/improve/Data/IMPROVE/improve_data.htm, January.

Gartrell, G. Jr., Heisler, S.L. and Friedlander, S.K. (1980) "Relating Particulate Properties to Sources : The Results of the California Aerosol Characterization Experiment," in *The Character and Origins of Smog Aerosols, A Digest of Results from the California Aerosol Characterization Experiment (ACHEX***)** (G. M. Hidy, Ed.), John Wiler & Sons, New York.

Gasso, S., Hegg, D.A., Covert,D.S. Noone, K., Ostrom, E., Schmid, B, Russell, P. B., Livingston, J.M., Exposito, J.F., Durkee, P.A. and Jonsson, H. (1998) Optical and Hygroscopic Aerosol Properties in the East Subtropical Atlantic; 5th International Global Atmospheric Chemistry (IGAC) Scientific Conference, Seattle, August 1998.

Lowenthal, D.H. and N. Kumar. (2003) $PM_{2.5}$ Mass and Light Extinction Reconstruction in IMPROVE. *J. Air & Waste Manage. Assoc., 53*:1109-1120.

Malm, W.C., Day, Derek, E. and Kreidenweis, S.M. (2000) Light Scattering Characteristics of Aerosols as a Function of Relative humidity: Part I - A Comparison of Measured Scattering and Aerosol Concentrations Using the Theoretical Models; J. Air & Waste Manage. Assoc. 50, 686-700.

Ming, Y. and Russell, L.M. (2001) Predicted Hygroscopic Growth of Sea Salt Aerosol; Journal of Geophysical Research 106, 28, 259-28,274.

Tang, I.N. (1980) “Deliquescence Properties and Particle Size Change of Hygroscopic Aerosols;” in Generation of Aerosols (K. Willeke, Ed.); Chap. 7 Ann Arbor Science, Ann Arbor, MI.

Tang, I.N. and Munkelwitz, H.R. (1993) Composition and Temperature Dependence of the Deliquescent Properties of Hygroscopic Aerosols; Atmospheric Environment 27A, 467-473.

Tang, I.N., Tridico, A.C. and Fung, K.H. (1997) Thermodynamic and Optical Properties of Sea Salt Aerosols; Journal of Geophysical Research, *102*, 23,269-23,275.

U.S. Environmental Protection Agency (2001) Draft Guidance for Estimating Natural Visibility Conditions Under the Regional Haze Rule, Office of Air Quality Planning and Standards, Research Triangle Park, NC, September 27. Available at http://www.epa.gov/ttn/amtic/visinfo.html

APPENDIX G

COMPARISON OF CALMET (RUC) WINDS VERSUS SELECTED AIRPORT WINDS

Comparison of CALMET (RUC) Winds vs. Selected Airport Winds

This Appendix includes box plots comparing wind direction and wind speed from the CALMET output versus airport data at four locations as described in the modeling protocol document. Due to the high weighting of the RUC (Step 1) data versus the airport data, the CALMET output basically represents the RUC input data. However, CALMET grid points relatively close to the selected airports were used to provide a meaningful comparison.

The comparisons at the four airports (Farmington, NM; MOAB, UT; Flagstaff, AZ; and Santa Fe, NM) are provided in the order of those locations in this appendix. Plots of wind speed and wind direction comparisons are provided in pairs, for each of three years (2001-2003).

For the wind speed comparisons, the wind speed range is divided into four parts (up to 4 knots, 5-6 knots, 7-9 knots, and at least 10 knots). For each wind speed "bin", all hours with nonmissing data for the airport had the ratio of the CALMET wind speed at 10 meters and the 10-m airport measurement computed. A range of the various ratios computed for each wind speed bin is displayed in the accompanying box plot. The box is constructed so that the bounds of the box represent the 10% and 90% ranked values, with 25%, 50%, and 75% values plotted within the box.

For wind direction comparisons, the wind direction range is divided into four quadrants. The difference of the two wind directions is plotted on the y-axis in a box plot similar to the one for wind speeds.

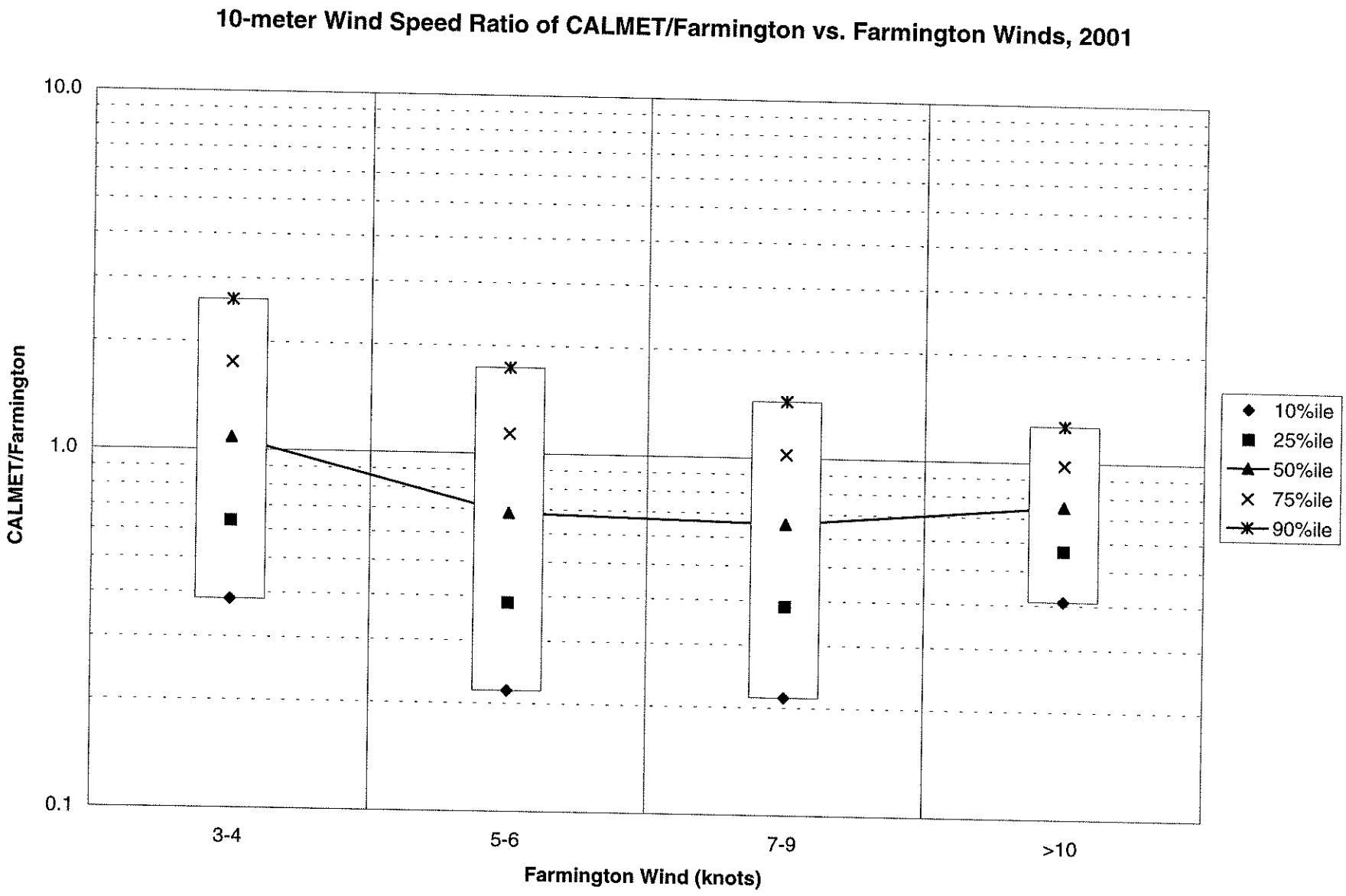
10-meter Wind Speed Ratio of CALMET/Farmington vs. Farmington Winds, 2001
10.0
1.0
0.1
CALMET/Farmington
3-4
5-6
7-9
>10
Farmington Wind (knots)
10%ile
25%ile
50%ile
75%ile
90%ile

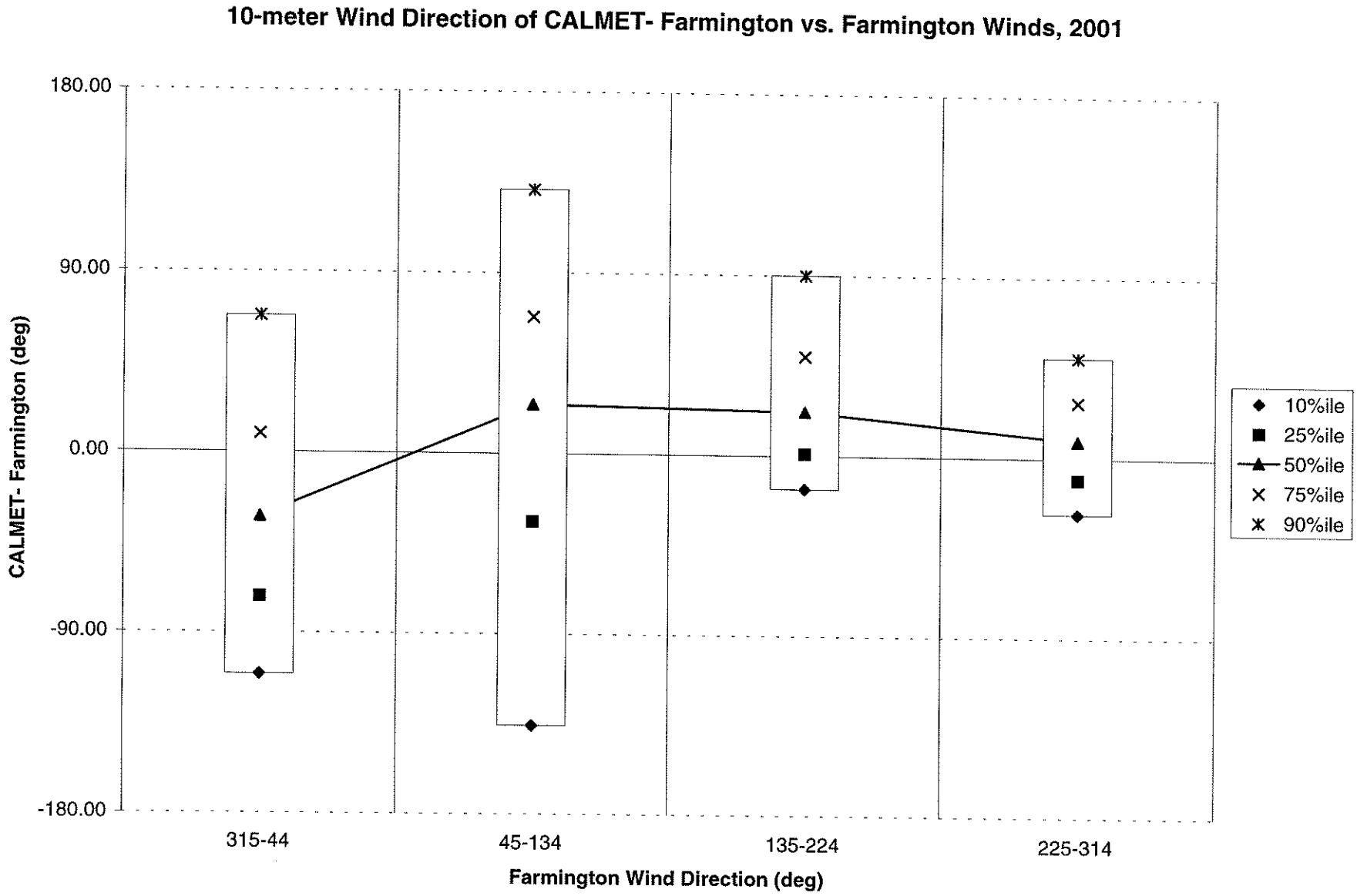
10-meter Wind Direction of CALMET- Farmington vs. Farmington Winds, 2001
180.00
90.00
0.00
-90.00
-180.00
CALMET- Farmington (deg)
315-44
45-134
135-224
225-314
Farmington Wind Direction (deg)
10%ile
25%ile
50%ile
75%ile
90%ile

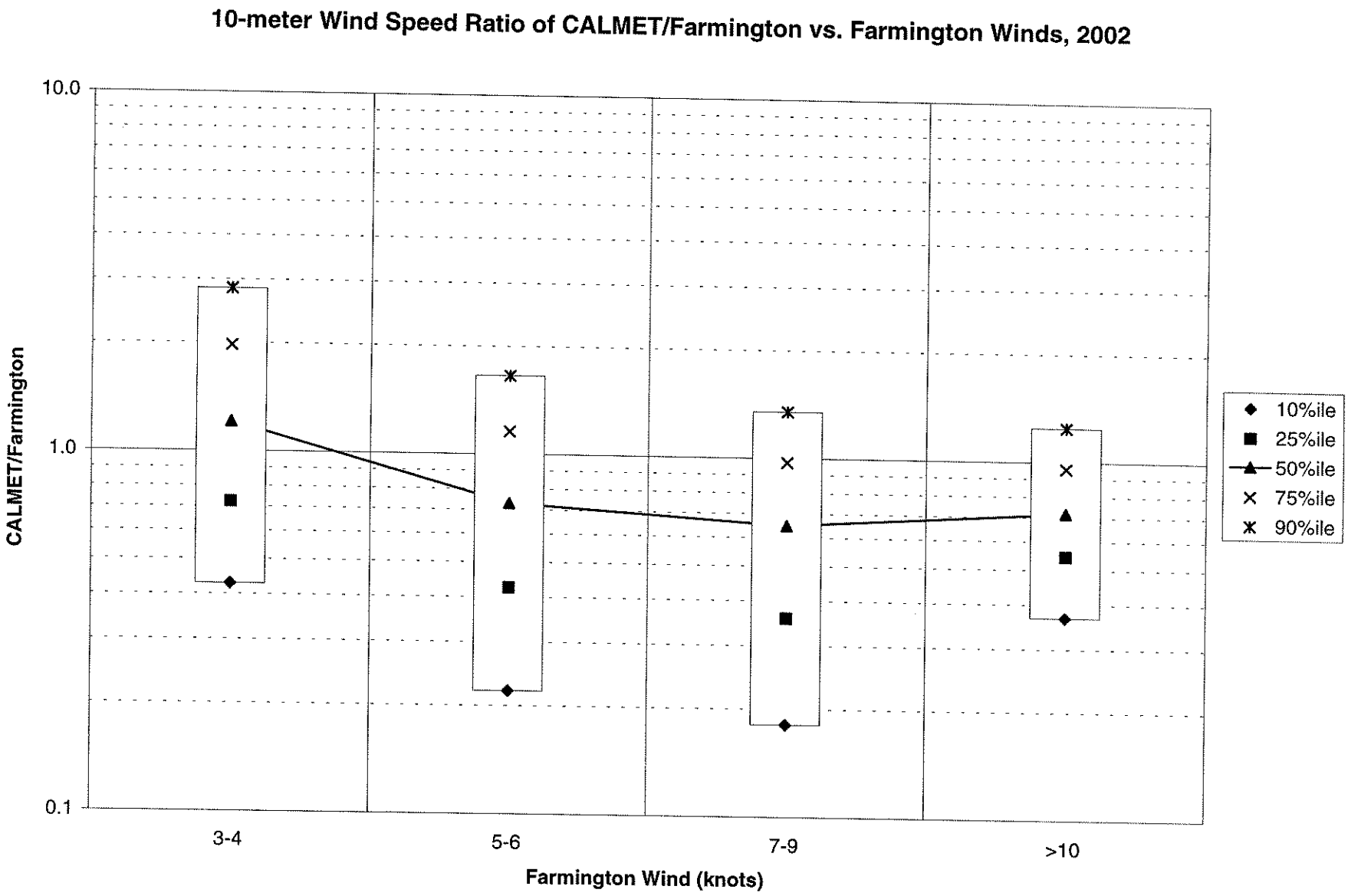
10-meter Wind Speed Ratio of CALMET/Farmington vs. Farmington Winds, 2002
10.0
1.0
0.1
CALMET/Farmington
3-4
5-6
7-9
>10
Farmington Wind (knots)
10%ile
25%ile
50%ile
75%ile
90%ile

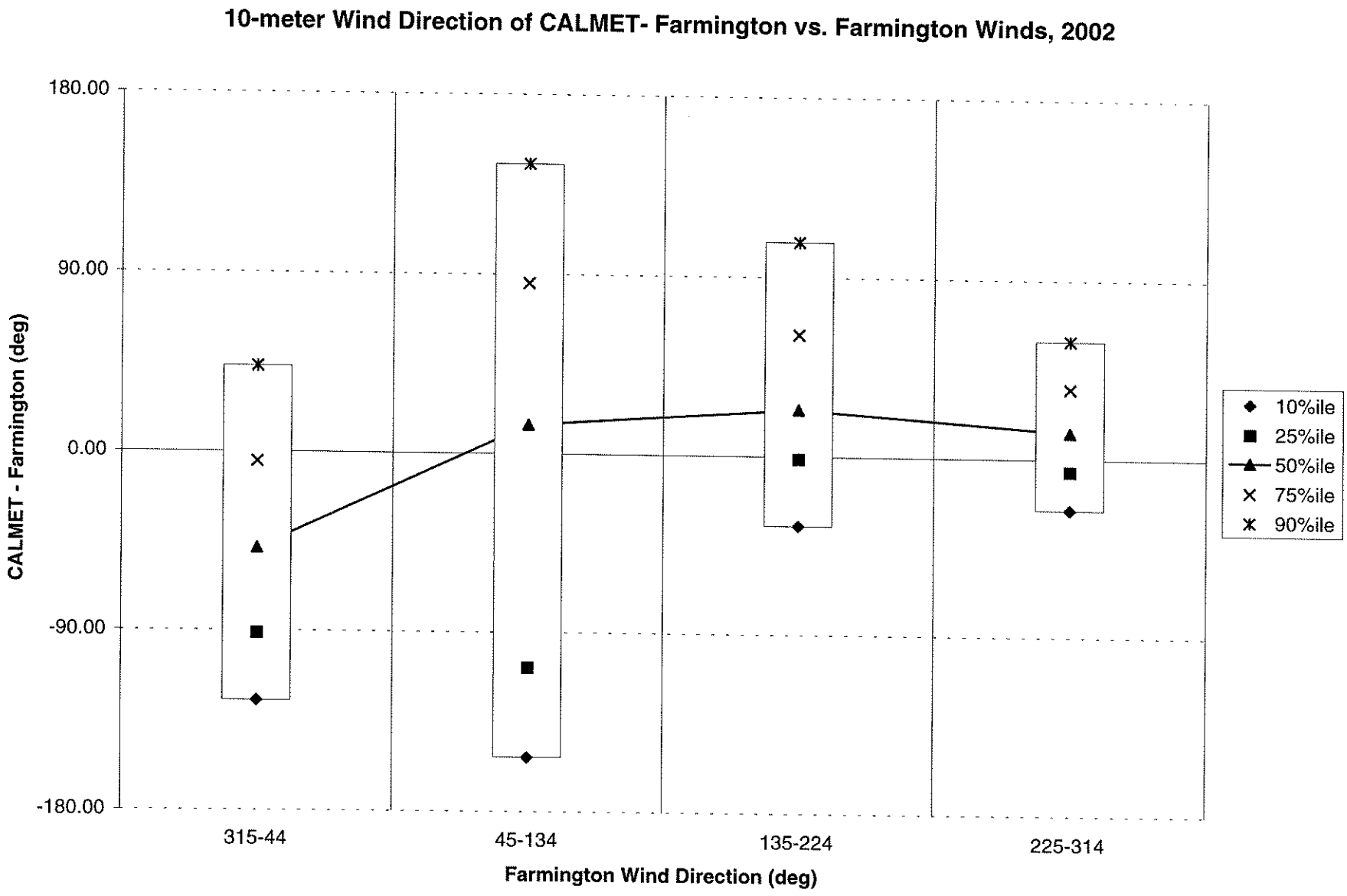
10-meter Wind Direction of CALMET- Farmington vs. Farmington Winds, 2002
180.00
90.00
0.00
-90.00
-180.00
CALMET - Farmington (deg)
315-44
45-134
135-224
225-314
Farmington Wind Direction (deg)
10%ile
25%ile
50%ile
75%ile
90%ile

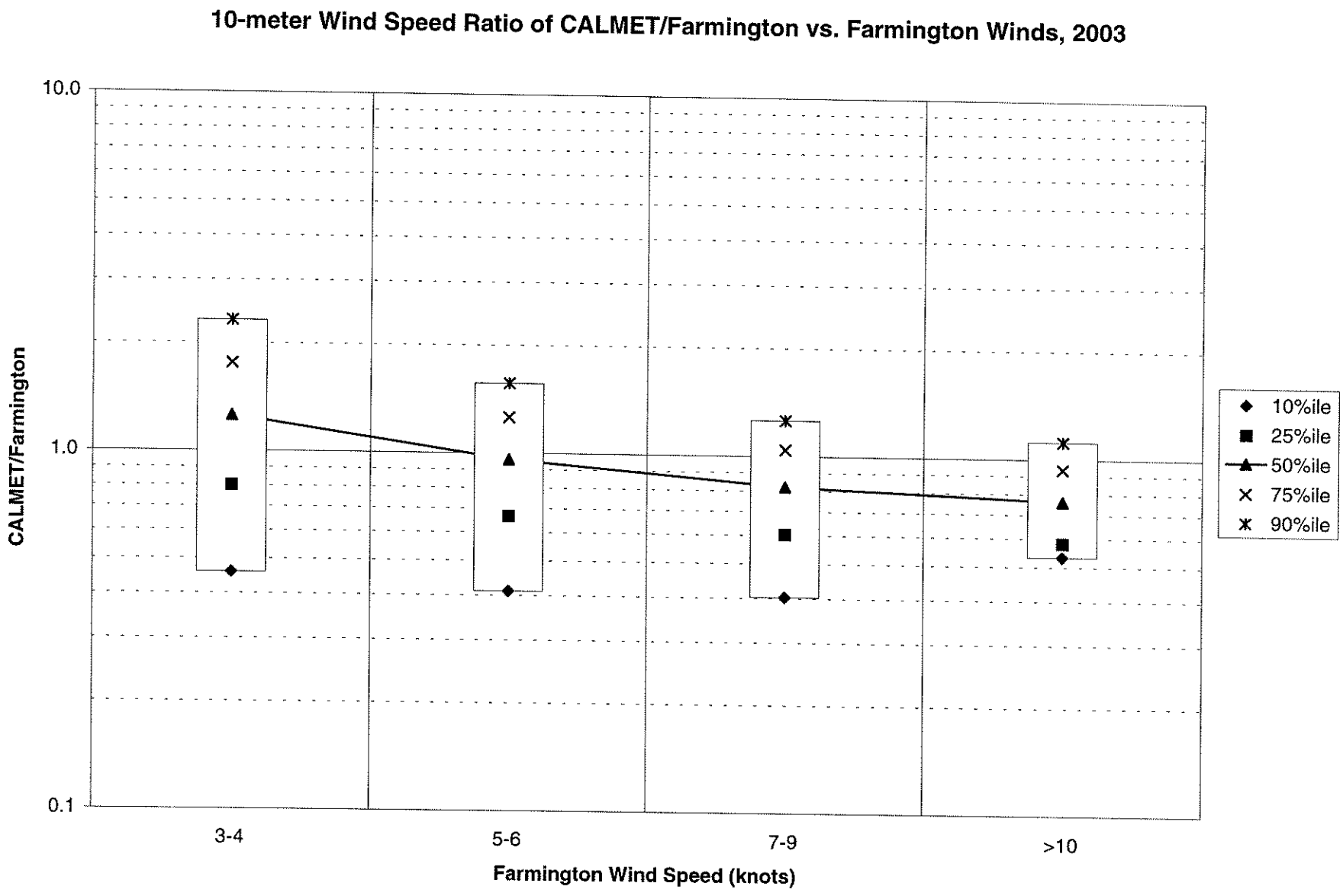
10-meter Wind Speed Ratio of CALMET/Farmington vs. Farmington Winds, 2003
10.0
1.0
0.1
CALMET/Farmington
3-4
5-6
7-9
>10
Farmington Wind Speed (knots)
10%ile
25%ile
50%ile
75%ile
90%ile

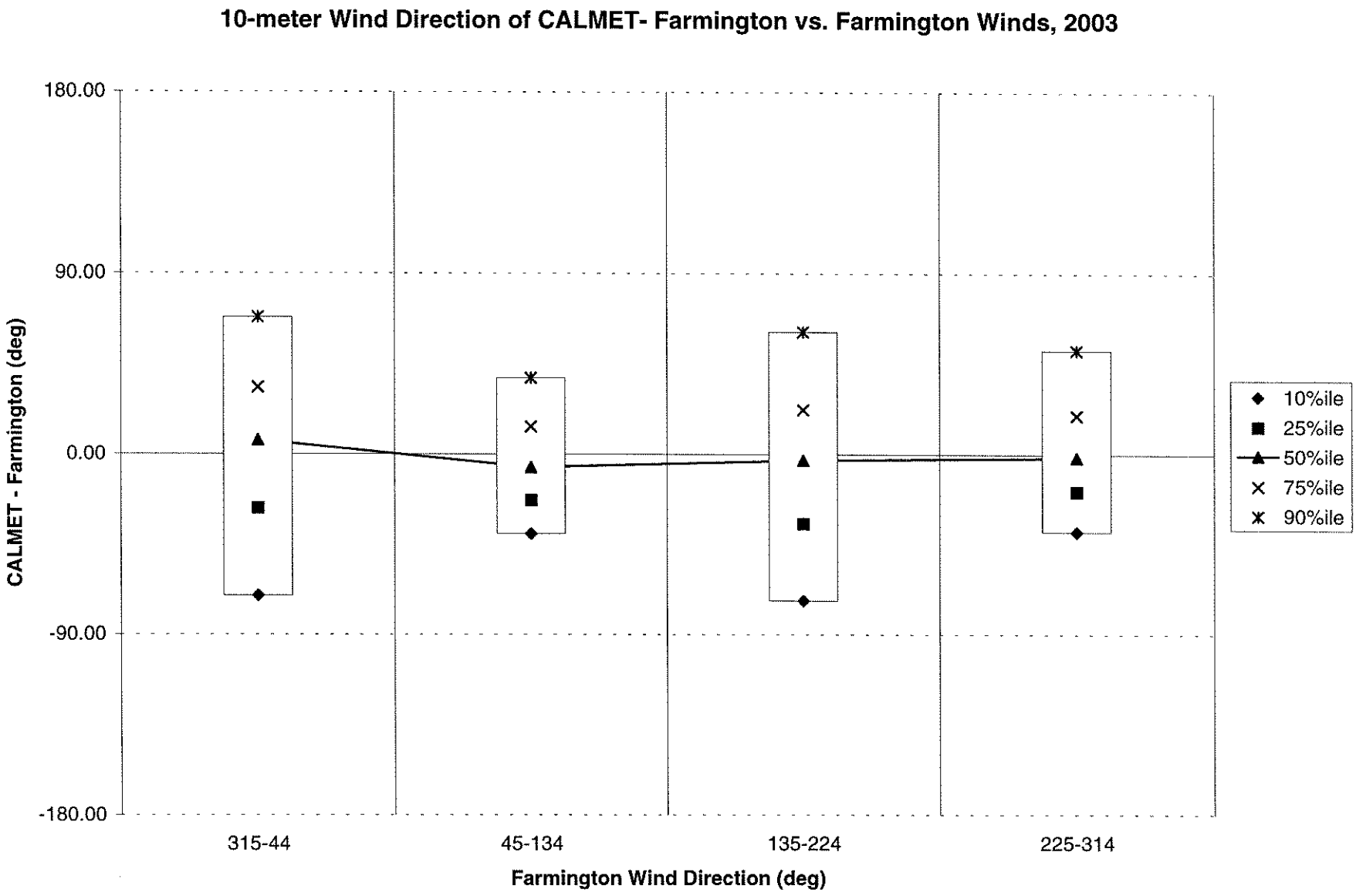
10-meter Wind Direction of CALMET- Farmington vs. Farmington Winds, 2003
180.00
90.00
0.00
-90.00
-180.00
CALMET - Farmington (deg)
315-44
45-134
135-224
225-314
Farmington Wind Direction (deg)
10%ile
25%ile
50%ile
75%ile
90%ile

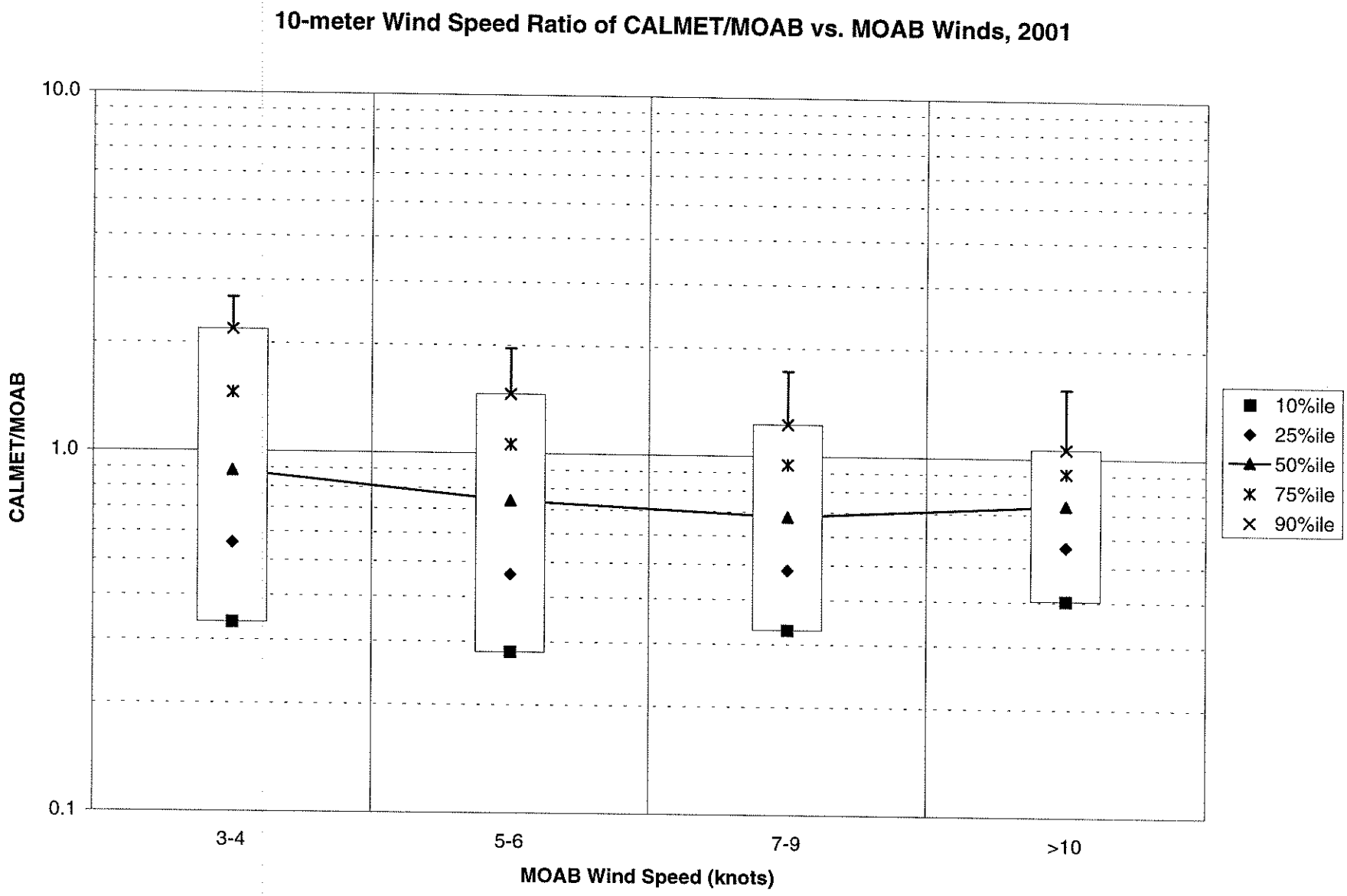
10-meter Wind Speed Ratio of CALMET/MOAB vs. MOAB Winds, 2001
10.0
1.0
0.1
CALMET/MOAB
3-4
5-6
7-9
>10
MOAB Wind Speed (knots)
10%ile
25%ile
50%ile
75%ile
90%ile

10-meter Wind Direction of CALMET- MOAB vs. MOAB Winds, 2001

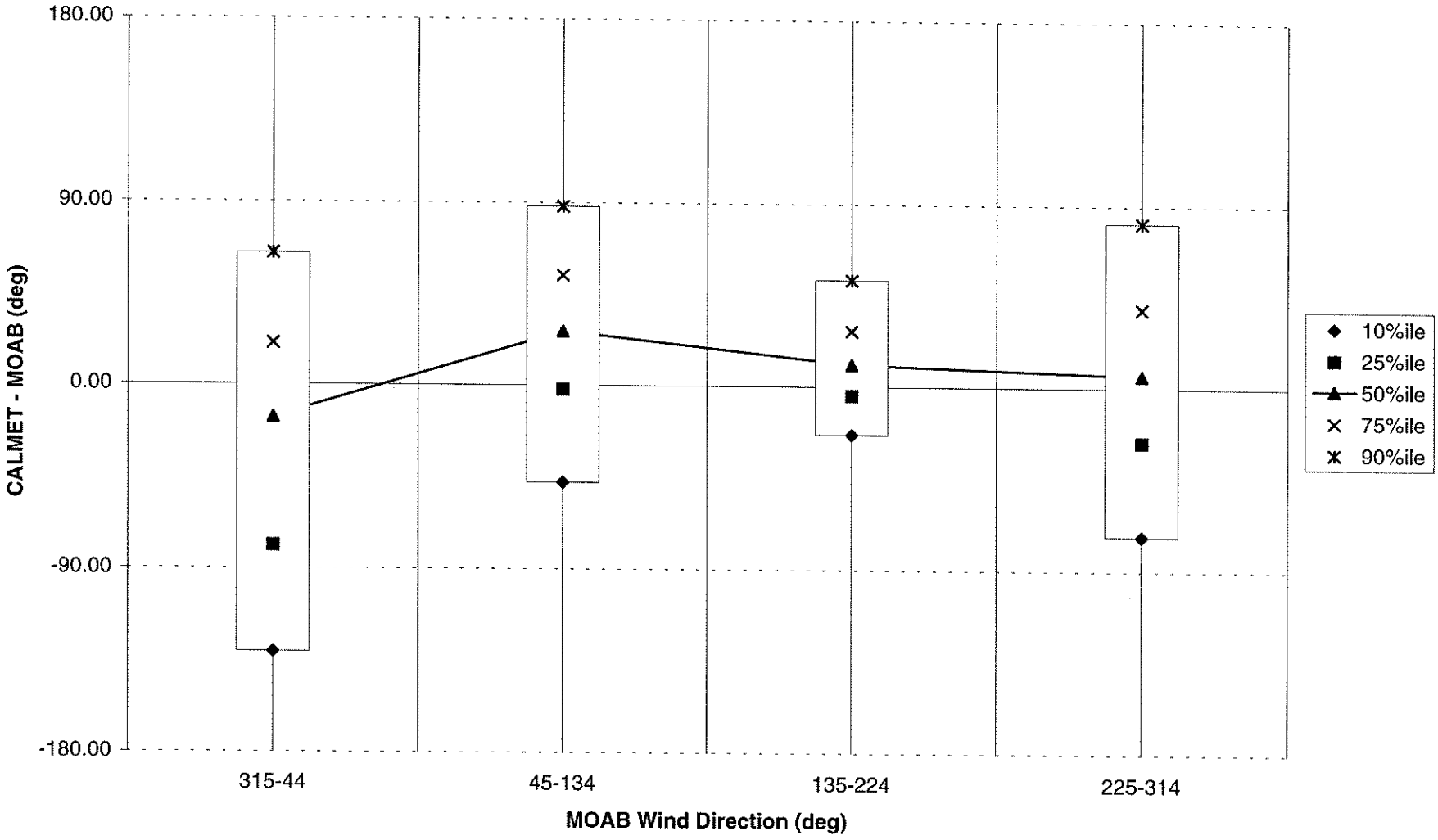

10-meter Wind Speed Ratio of CALMET/MOAB vs. MOAB Winds, 2002

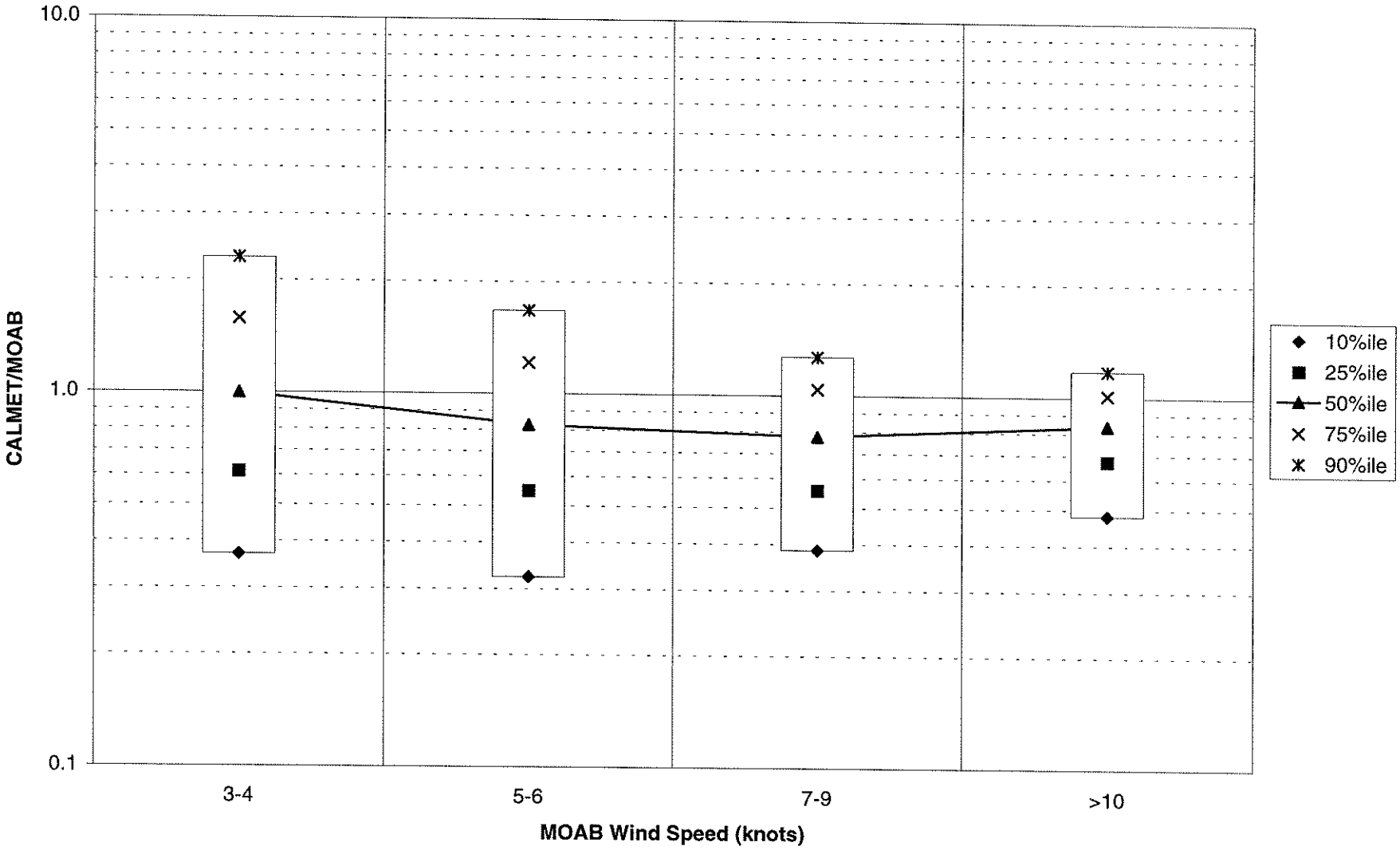

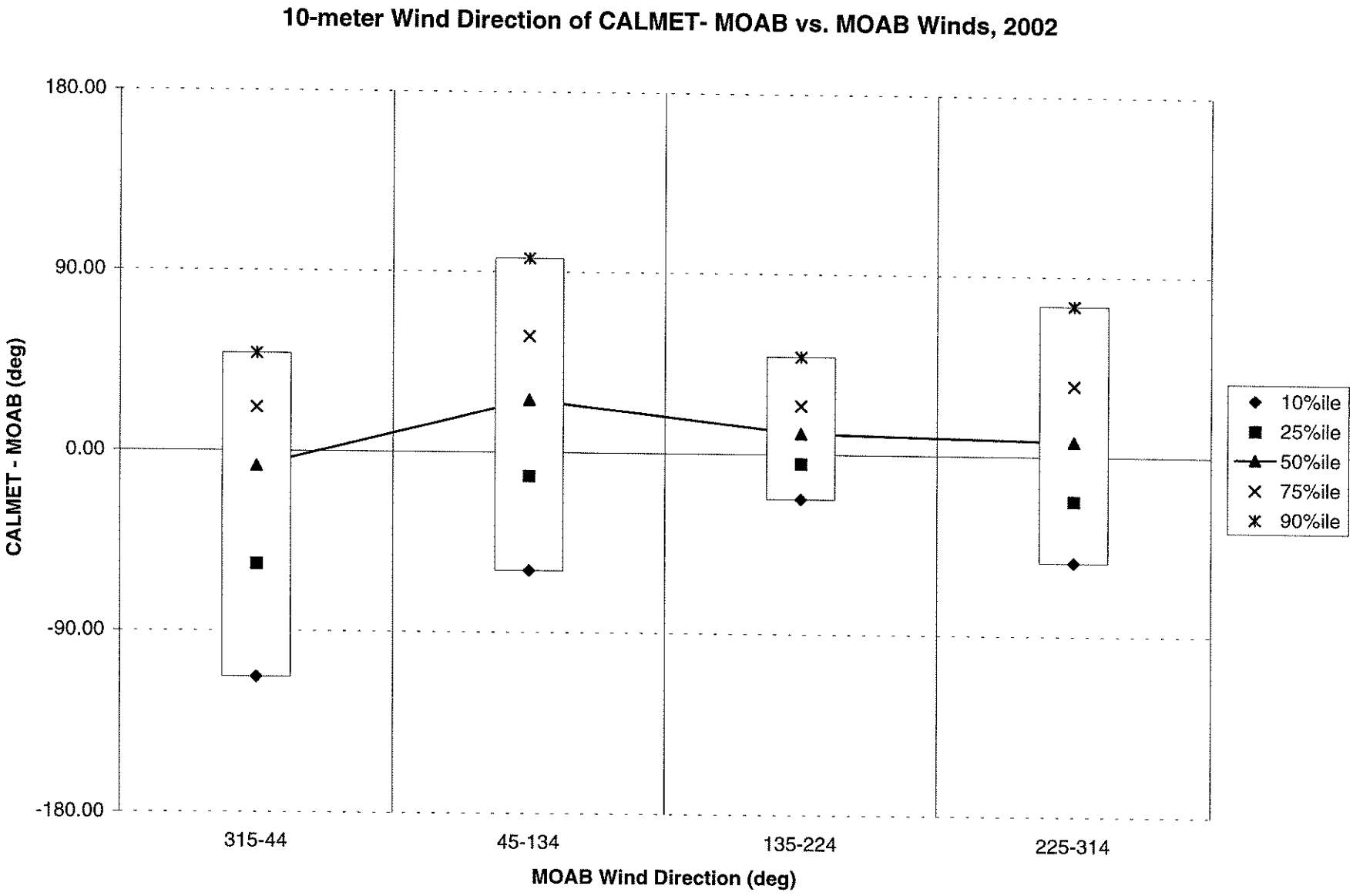
10-meter Wind Direction of CALMET- MOAB vs. MOAB Winds, 2002
180.00
90.00
0.00
-90.00
-180.00
CALMET - MOAB (deg)
315-44
45-134
135-224
225-314
MOAB Wind Direction (deg)
10%ile
25%ile
50%ile
75%ile
90%ile

10-meter Wind Speed Ratio of CALMET/MOAB vs. MOAB Winds, 2003

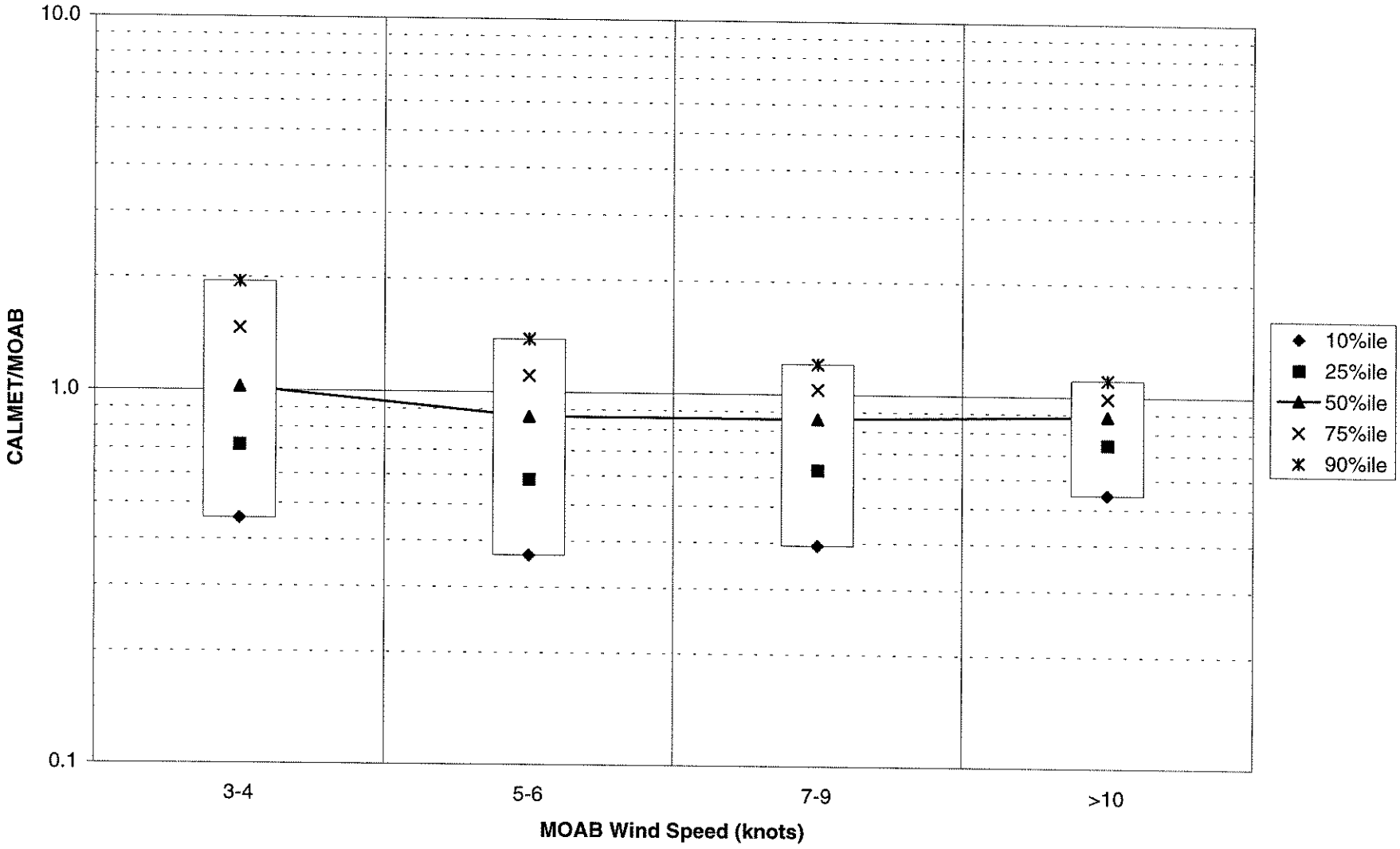

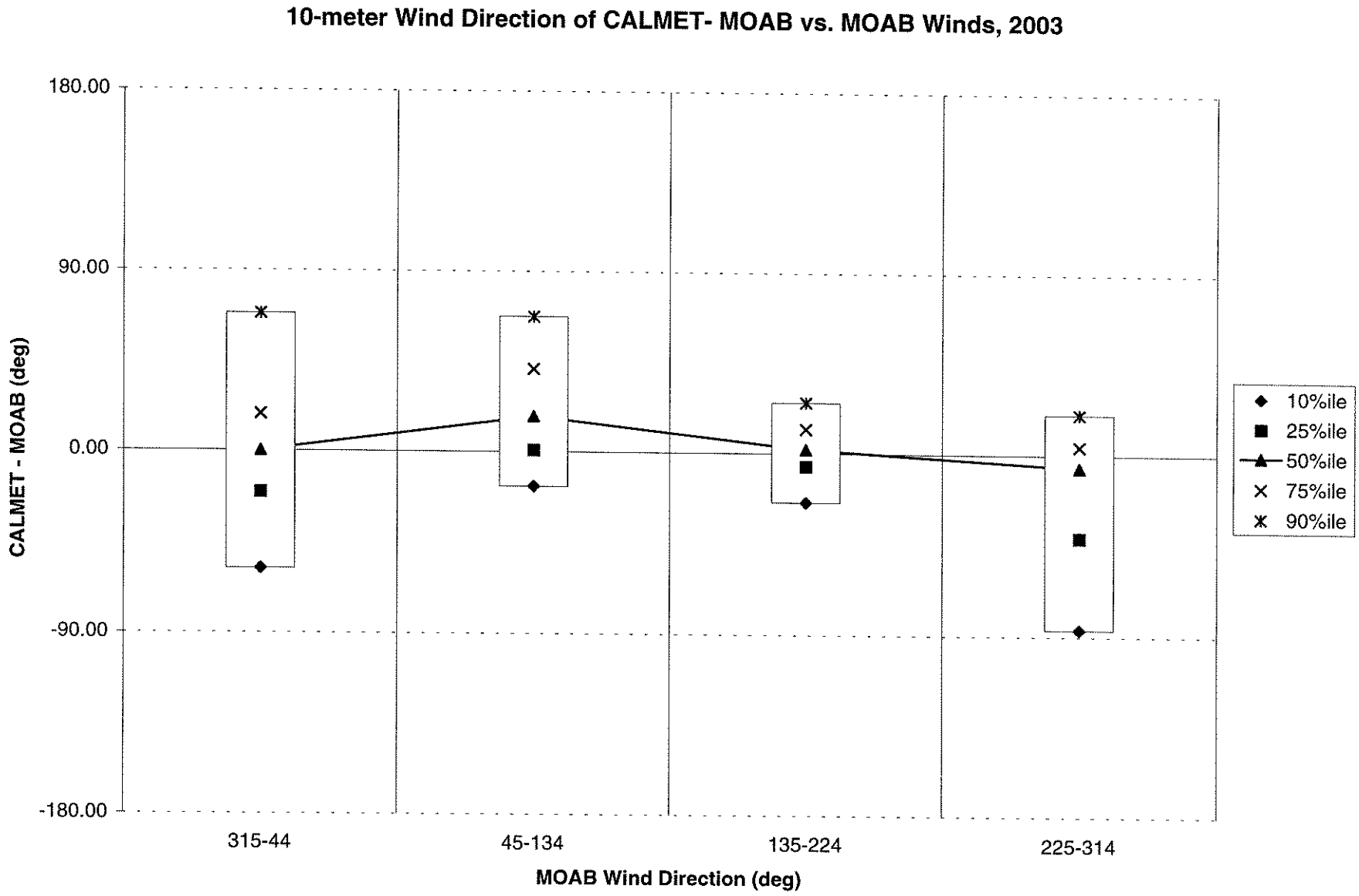
10-meter Wind Direction of CALMET- MOAB vs. MOAB Winds, 2003
180.00
90.00
0.00
-90.00
-180.00
CALMET - MOAB (deg)
315-44
45-134
135-224
225-314
MOAB Wind Direction (deg)
10%ile
25%ile
50%ile
75%ile
90%ile

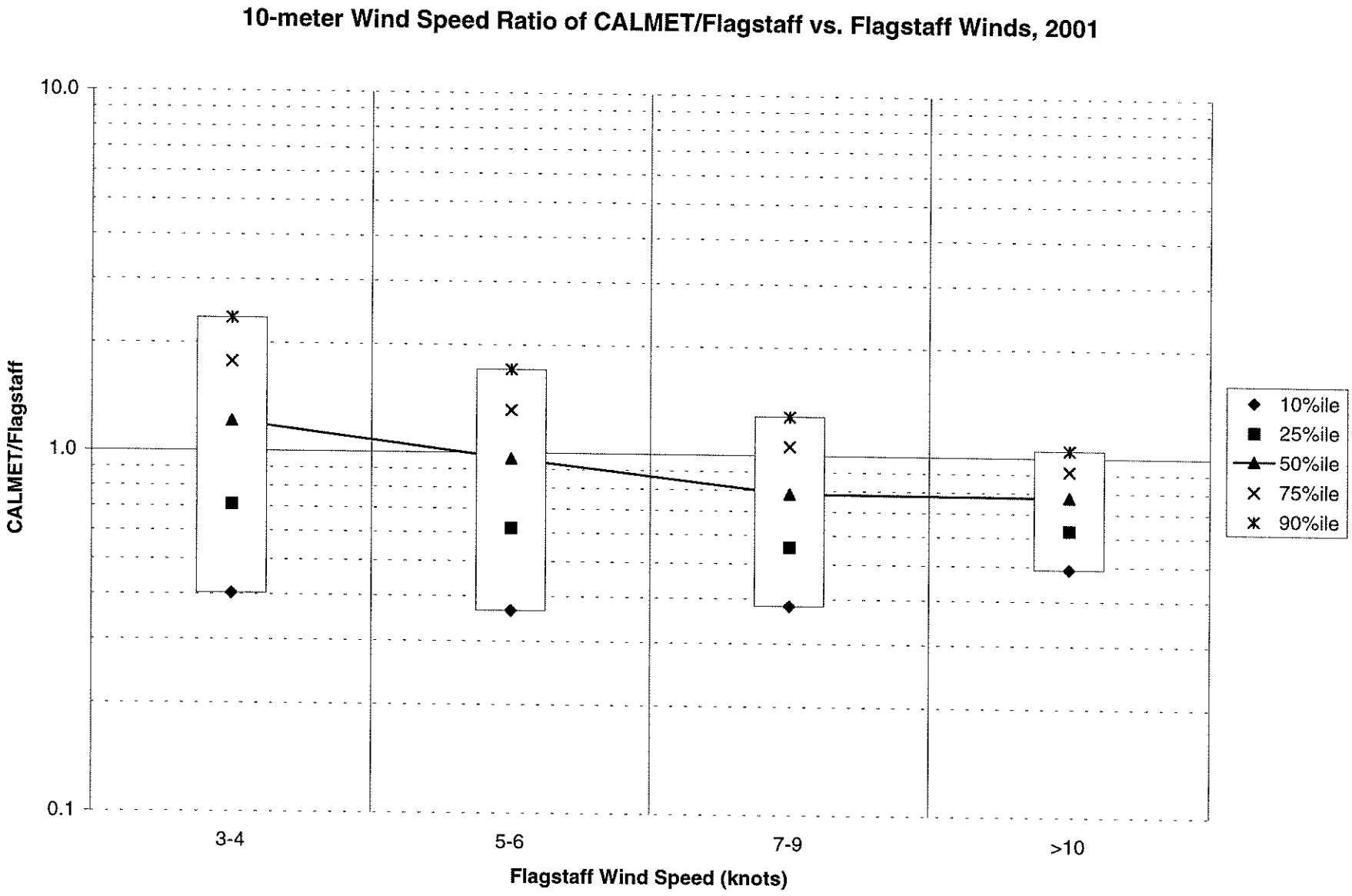
10-meter Wind Speed Ratio of CALMET/Flagstaff vs. Flagstaff Winds, 2001
10.0
1.0
0.1
CALMET/Flagstaff
3-4
5-6
7-9
>10
Flagstaff Wind Speed (knots)
10%ile
25%ile
50%ile
75%ile
90%ile

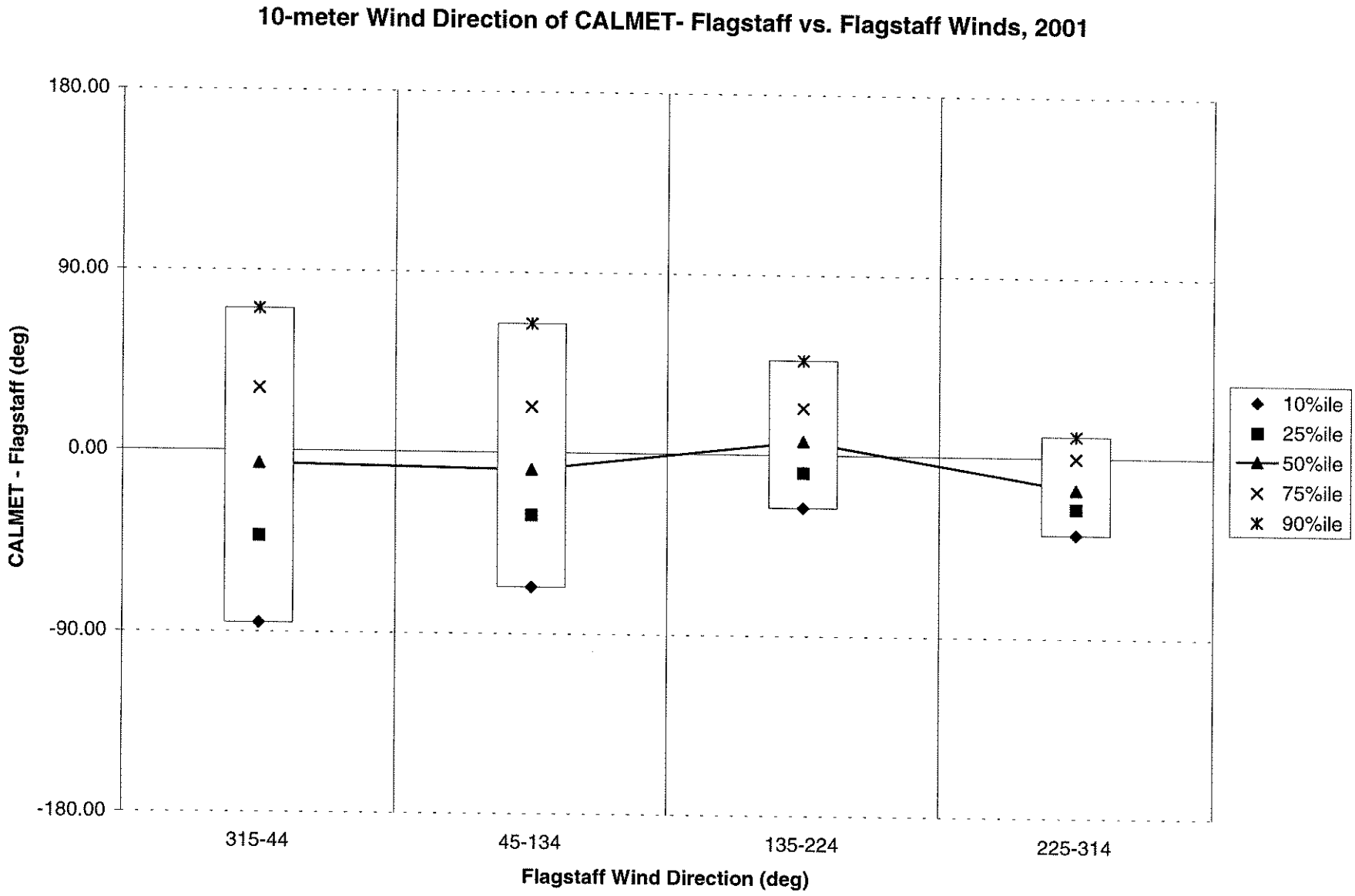
10-meter Wind Direction of CALMET- Flagstaff vs. Flagstaff Winds, 2001
180.00
90.00
0.00
-90.00
-180.00
CALMET - Flagstaff (deg)
315-44
45-134
135-224
225-314
Flagstaff Wind Direction (deg)
10%ile
25%ile
50%ile
75%ile
90%ile

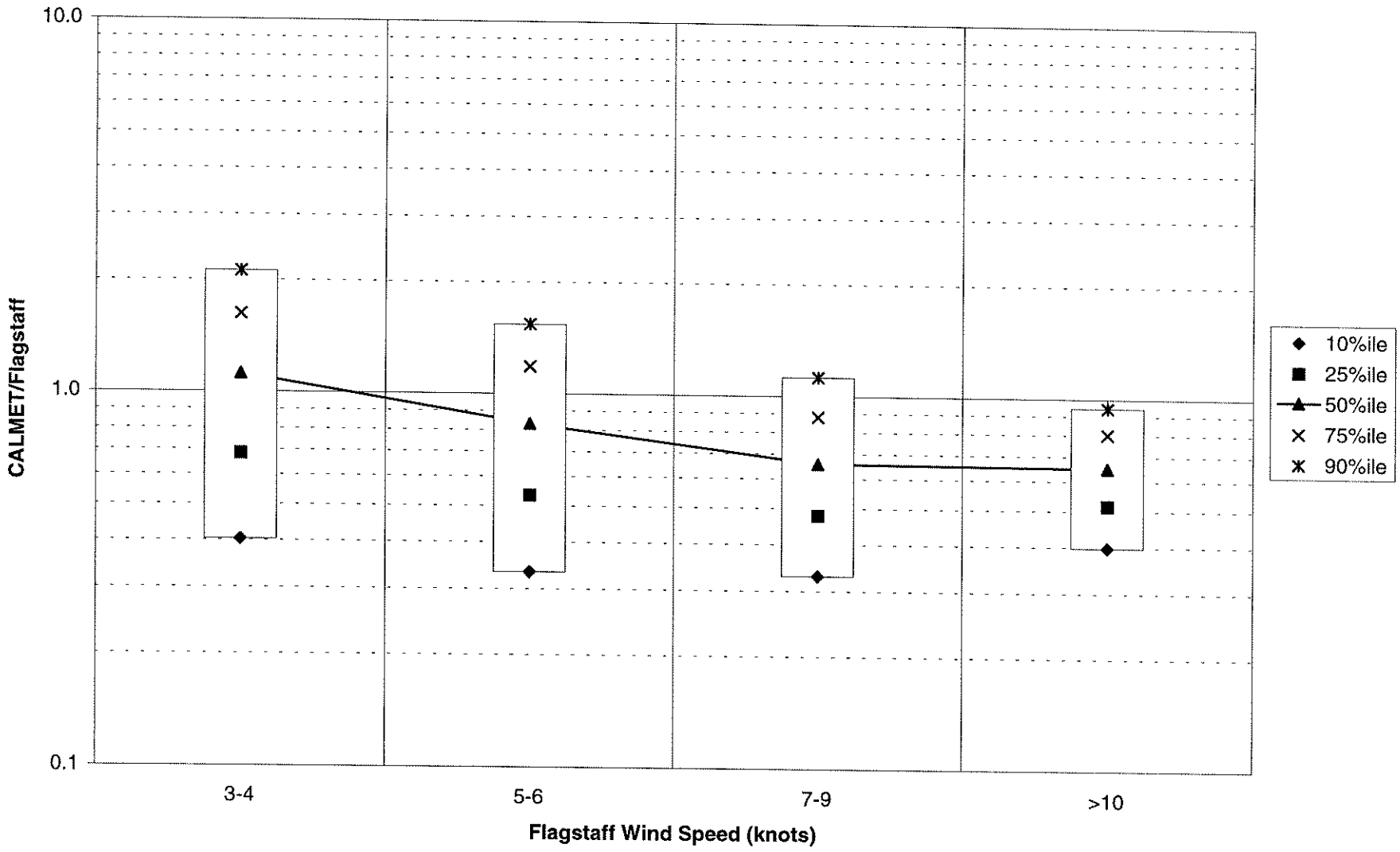
10-meter Wind Speed Ratio of CALMET/Flagstaff vs. Flagstaff Winds, 2002
10.0
1.0
0.1
CALMET/Flagstaff
3-4
5-6
7-9
>10
Flagstaff Wind Speed (knots)
10%ile
25%ile
50%ile
75%ile
90%ile

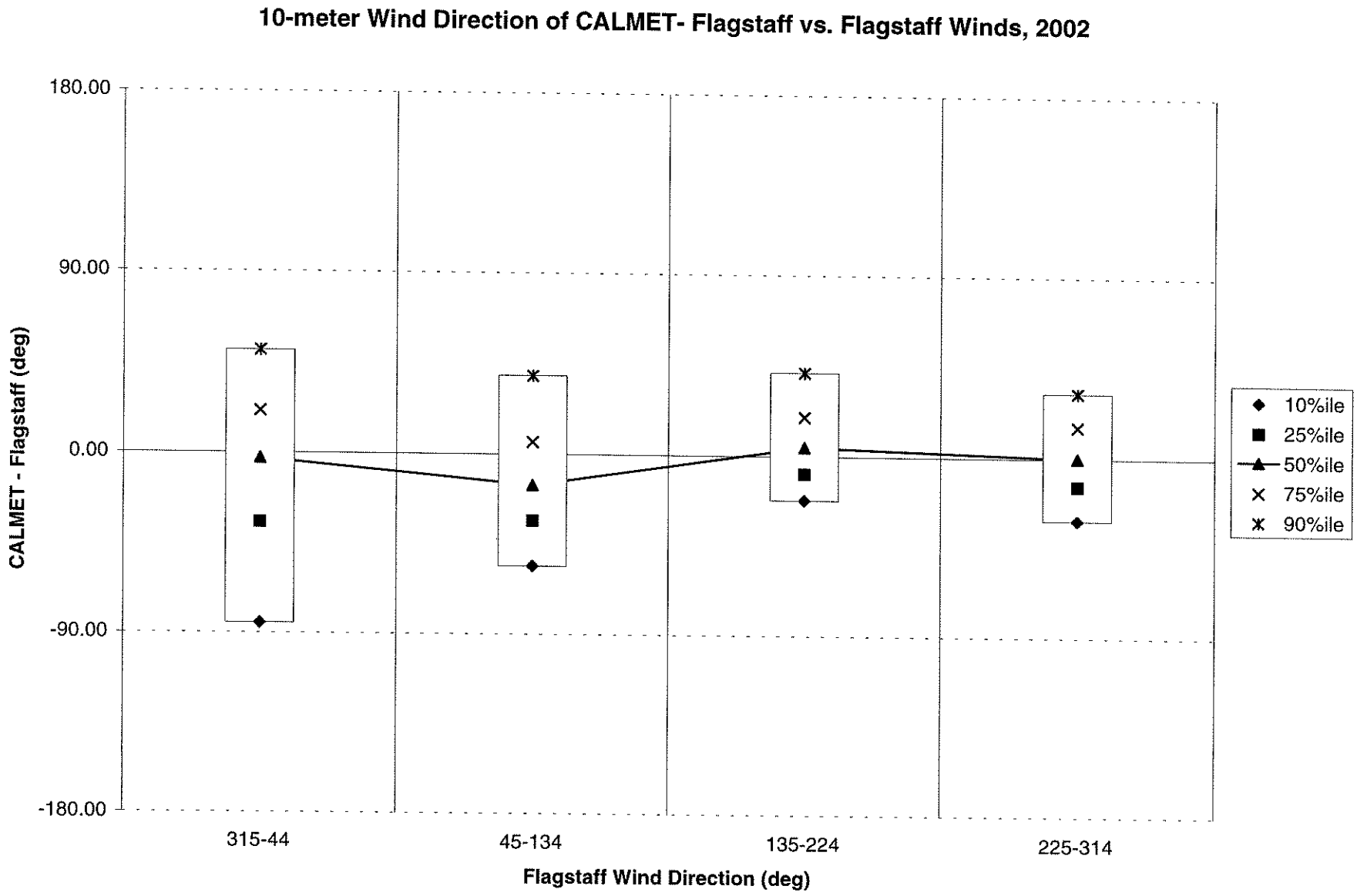
10-meter Wind Direction of CALMET- Flagstaff vs. Flagstaff Winds, 2002
180.00
90.00
0.00
-90.00
-180.00
CALMET - Flagstaff (deg)
315-44
45-134
135-224
225-314
Flagstaff Wind Direction (deg)
10%ile
25%ile
50%ile
75%ile
90%ile

10-meter Wind Speed Ratio of CALMET/Flagstaff vs. Flagstaff Winds, 2003

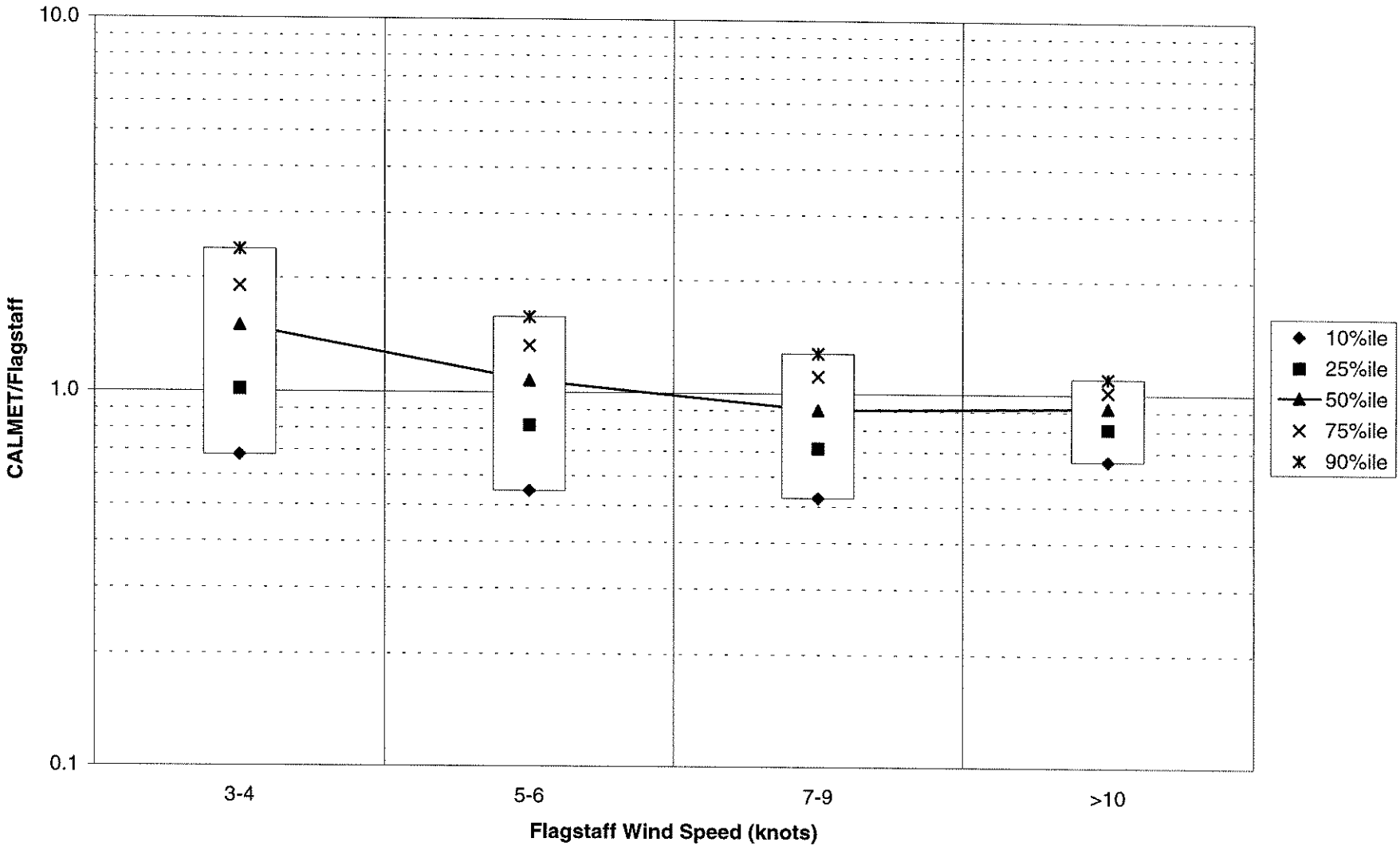

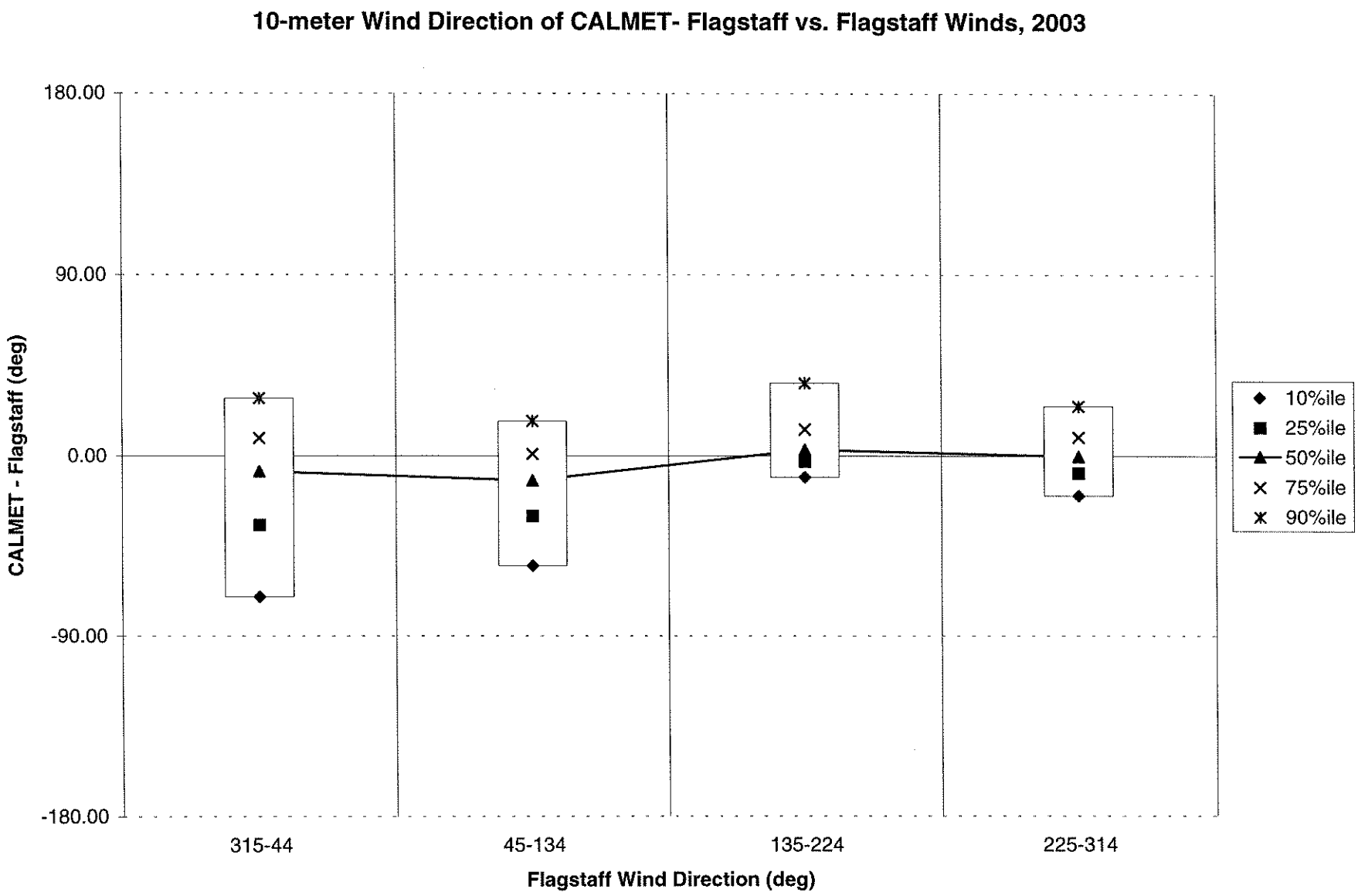
10-meter Wind Direction of CALMET- Flagstaff vs. Flagstaff Winds, 2003
180.00
90.00
0.00
-90.00
-180.00
CALMET - Flagstaff (deg)
315-44
45-134
135-224
225-314
Flagstaff Wind Direction (deg)
10%ile
25%ile
50%ile
75%ile
90%ile

10-meter Wind Speed Ratio of CALMET/Santa Fe vs. Santa Fe Winds, 2001

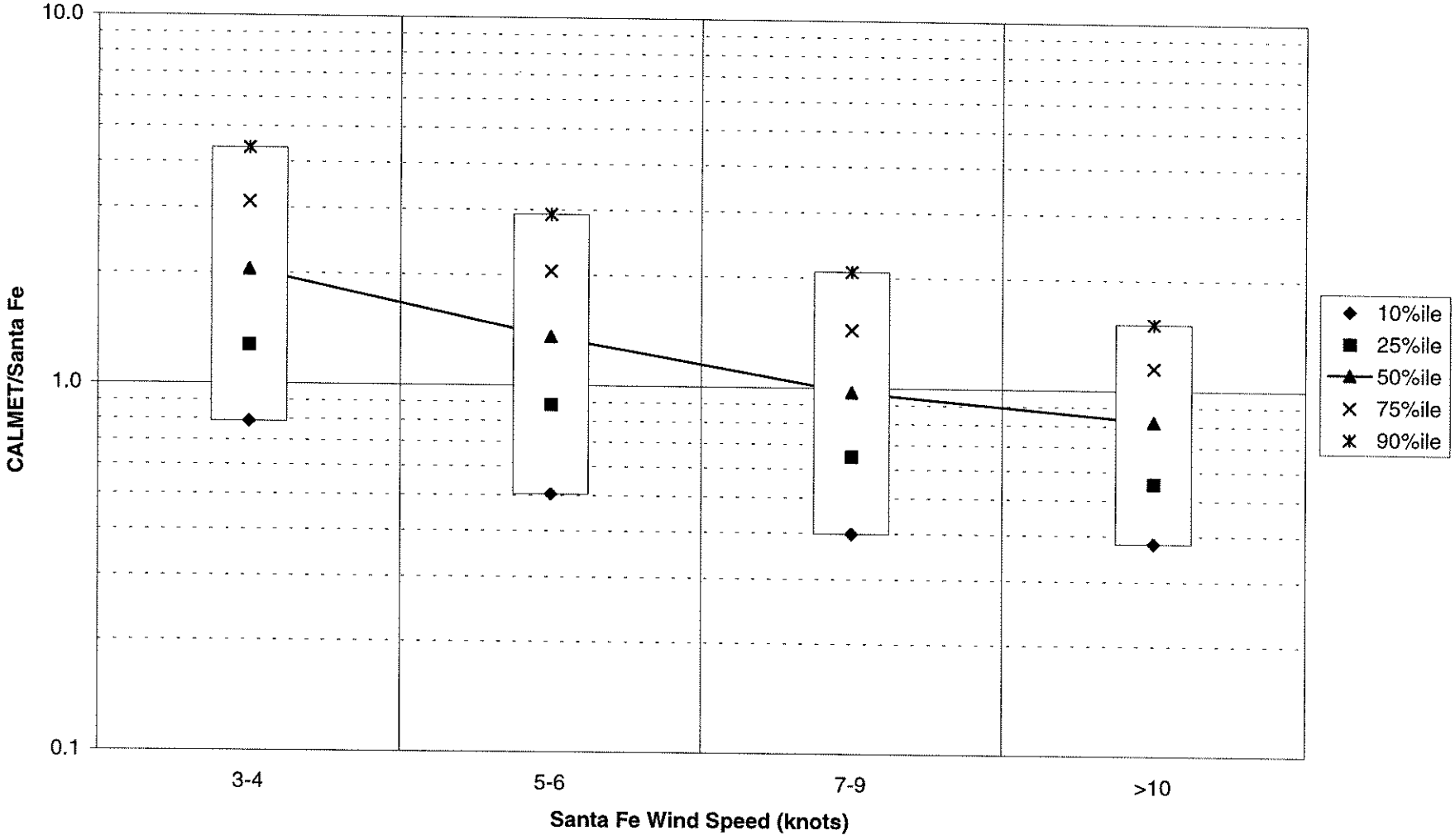

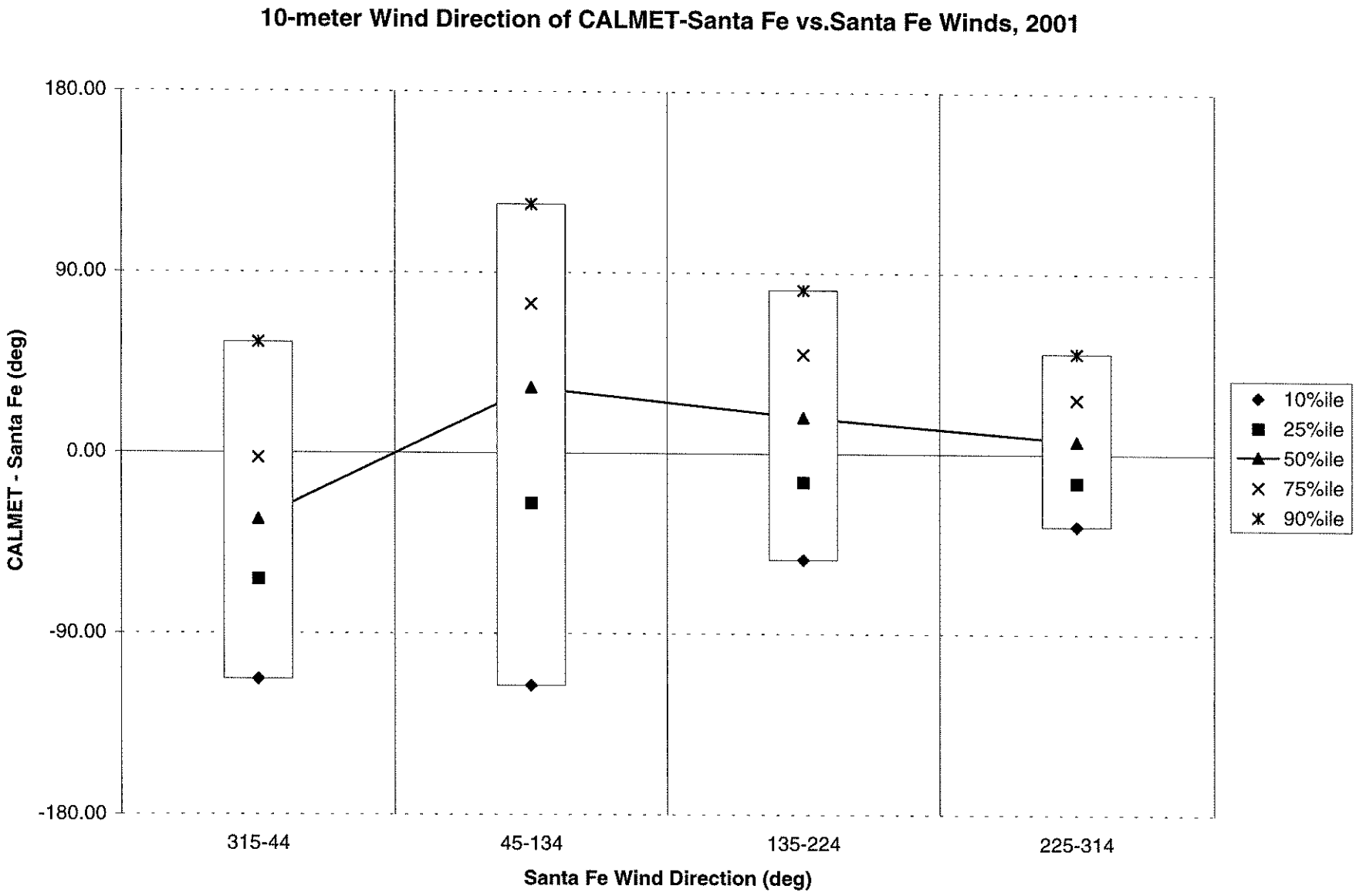
10-meter Wind Direction of CALMET-Santa Fe vs.Santa Fe Winds, 2001
180.00
90.00
0.00
-90.00
-180.00
CALMET - Santa Fe (deg)
315-44
45-134
135-224
225-314
Santa Fe Wind Direction (deg)
10%ile
25%ile
50%ile
75%ile
90%ile

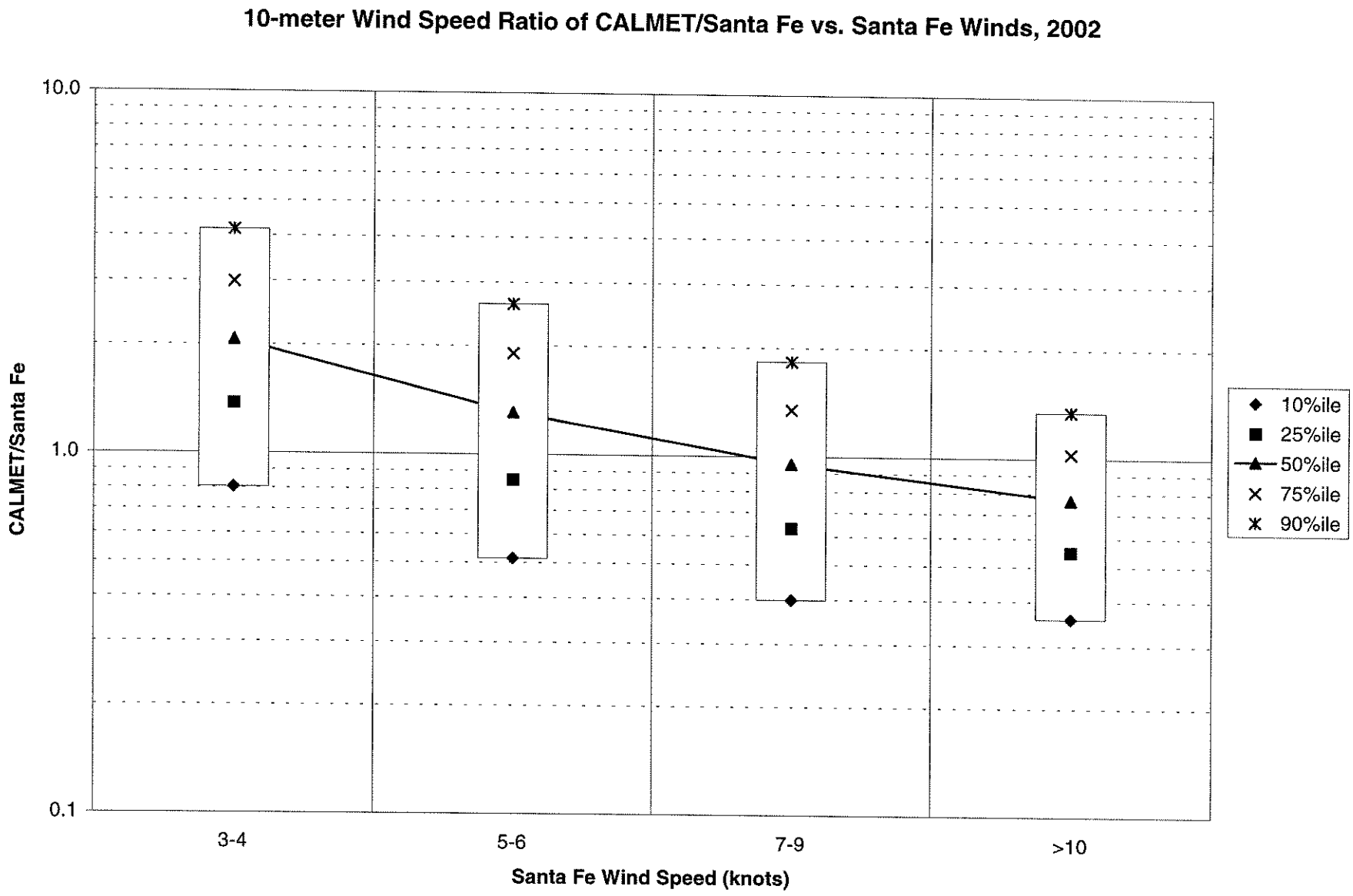
10-meter Wind Speed Ratio of CALMET/Santa Fe vs. Santa Fe Winds, 2002
10.0
1.0
0.1
CALMET/Santa Fe
3-4
5-6
7-9
>10
Santa Fe Wind Speed (knots)
10%ile
25%ile
50%ile
75%ile
90%ile

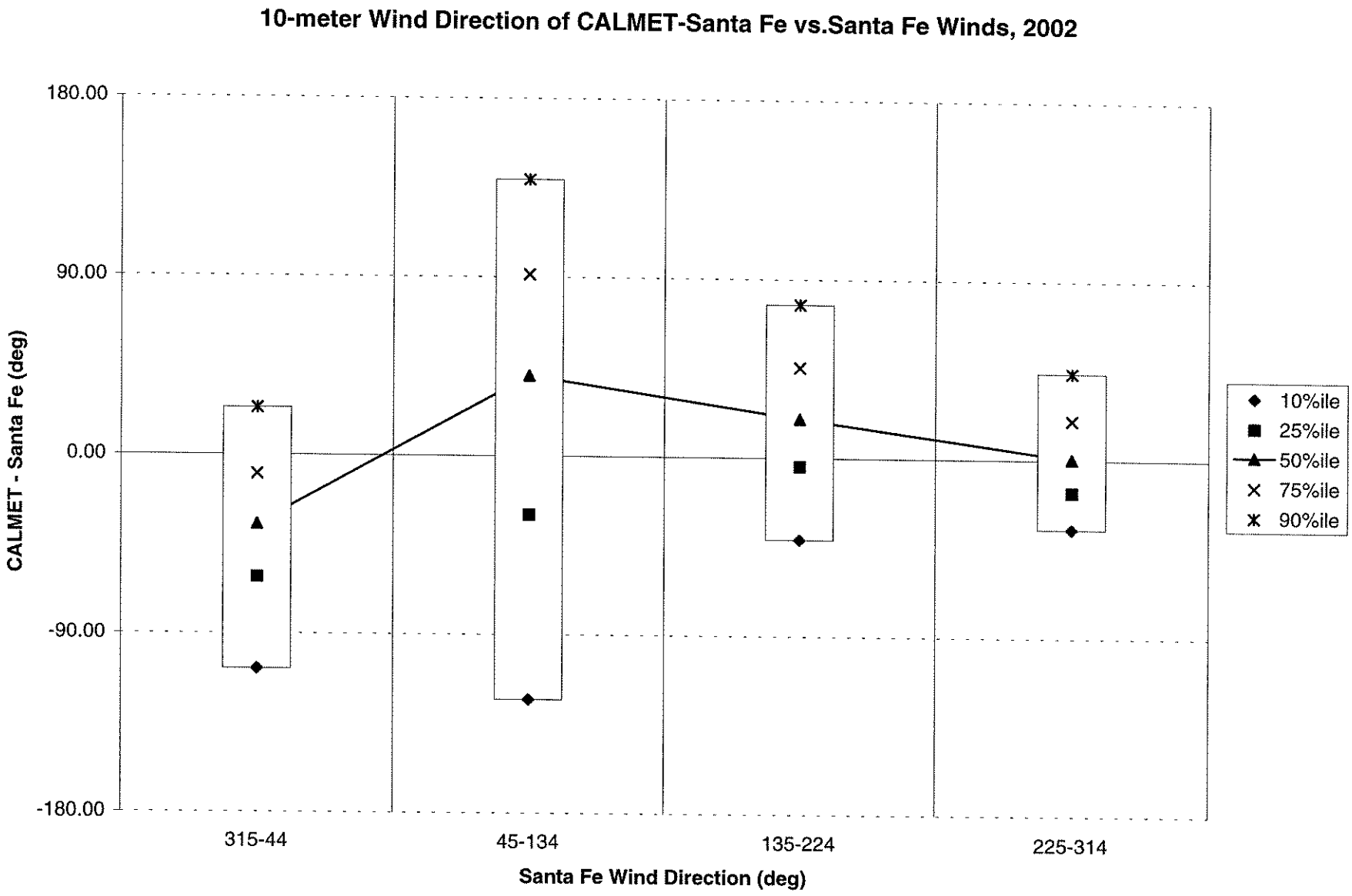
10-meter Wind Direction of CALMET-Santa Fe vs.Santa Fe Winds, 2002
180.00
90.00
0.00
-90.00
-180.00
CALMET - Santa Fe (deg)
315-44
45-134
135-224
225-314
Santa Fe Wind Direction (deg)
10%ile
25%ile
50%ile
75%ile
90%ile

10-meter Wind Speed Ratio of CALMET/Santa Fe vs. Santa Fe Winds, 2003

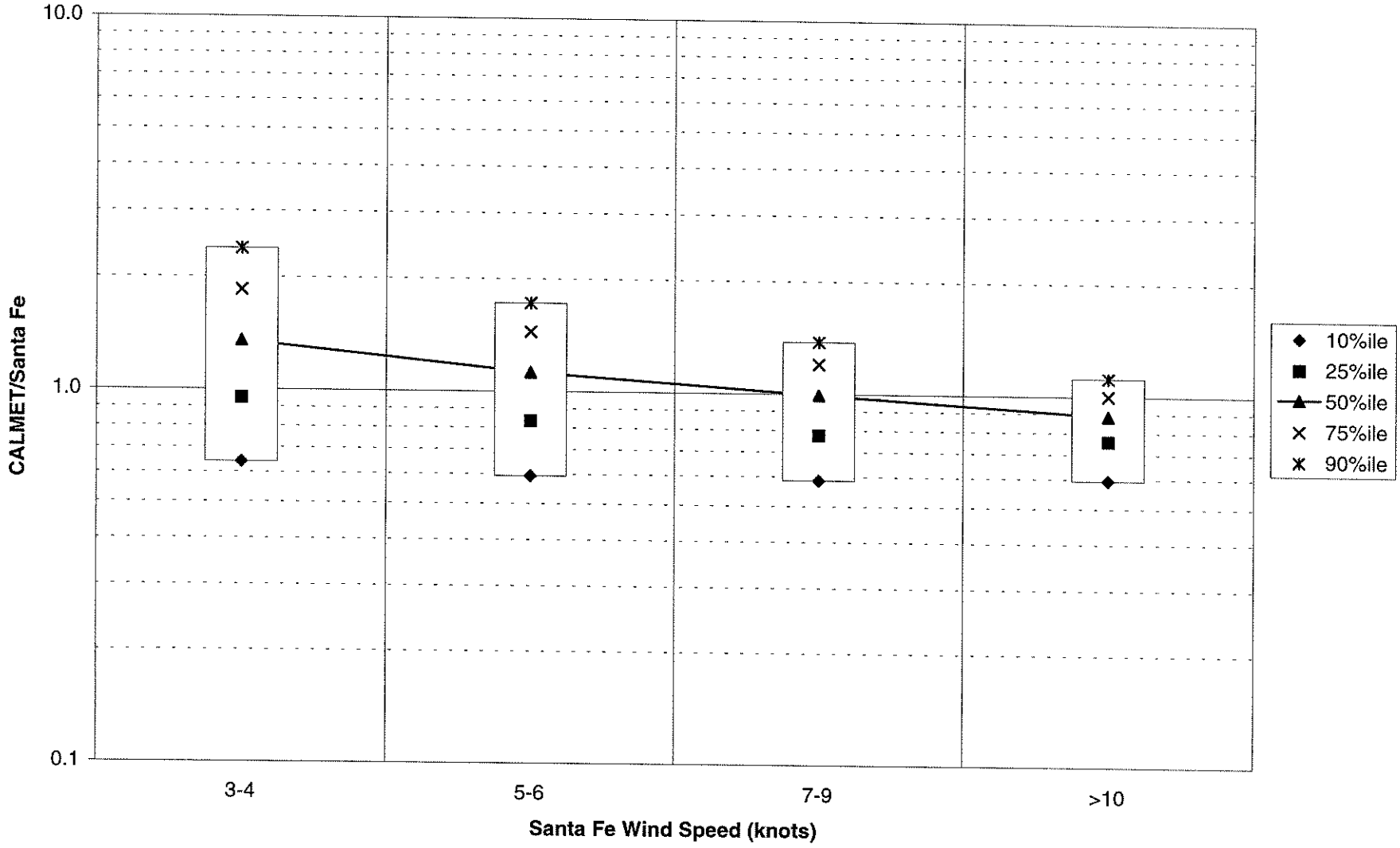

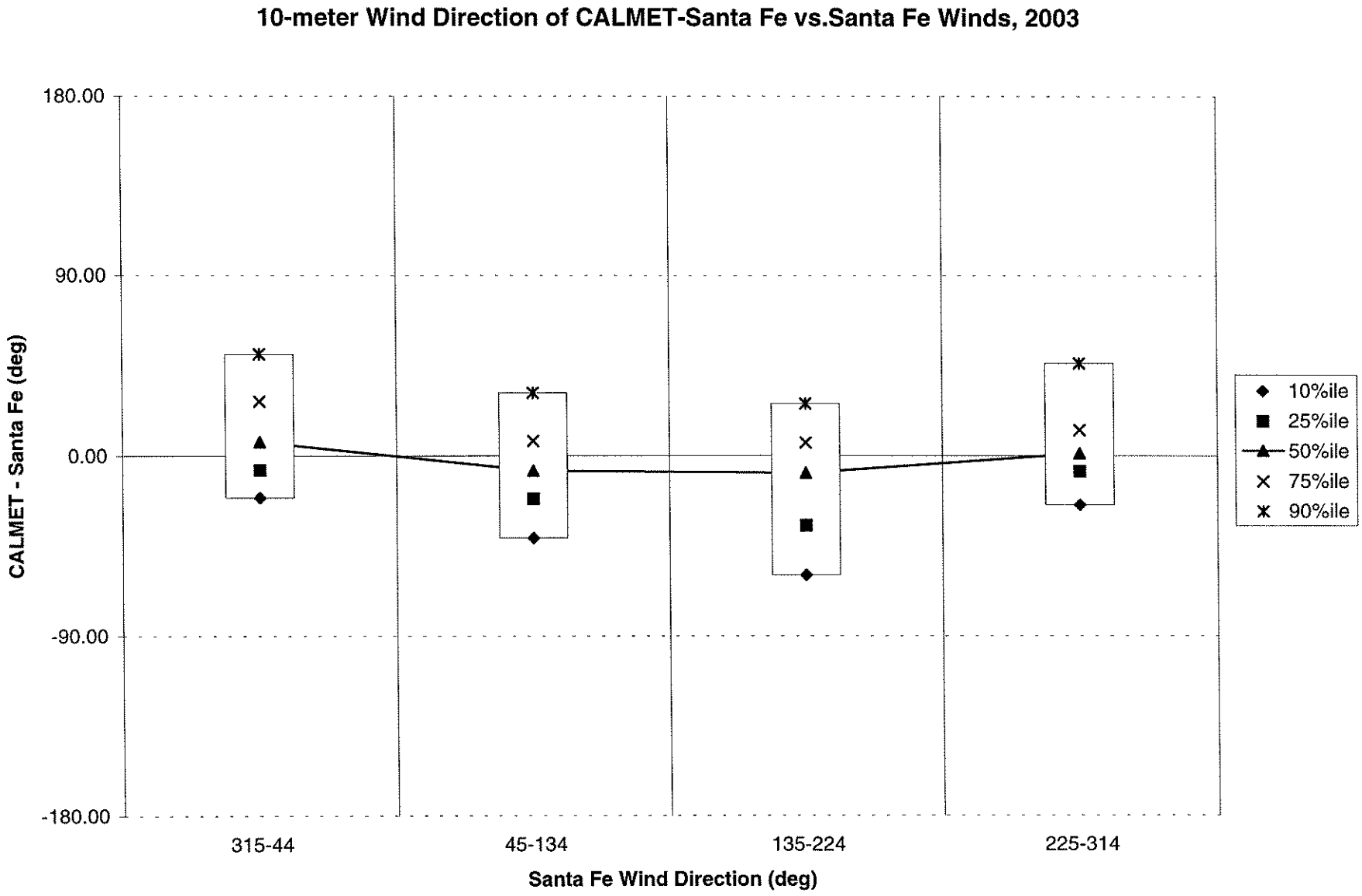
10-meter Wind Direction of CALMET-Santa Fe vs.Santa Fe Winds, 2003
180.00
90.00
0.00
-90.00
-180.00
CALMET - Santa Fe (deg)
315-44
45-134
135-224
225-314
Santa Fe Wind Direction (deg)
10%ile
25%ile
50%ile
75%ile
90%ile

APPENDIX H

SCREENING DOCUMENTATION FOR ANALYSIS OF ACID NEUTRALIZING CAPACITY OF LAKES

Screening Methodology for Calculating ANC Change to High Elevation Lakes

USDA Forest Service Rocky Mountain Region
January, 2000

Introduction

The purpose of this screening methodology is provide a simplistic step-by-step process that can be used in New Source Review and NEPA(National Environmental Policy Act) processes to predict air pollution caused changes to the chemistry of sensitive lakes. Like other air quality related value screening methodologies this relatively conservative approach can be used to determine if a proposed source or group of sources either do not have the potential to impact to impact wilderness lakes or if it is appropriate to conduct a more complex but less conservative analysis.

This screening methodology uses a very simplistic set of equations to estimate how additions of sulfate and/or nitrate deposition from air pollution sources may cause a change in lake acid neutralizing capacity (ANC) from a monitored baseline. The methodology uses the following assumptions:

* The generation of acid neutralizing capacity in the watershed catchment to be analyzed is constant over time.

* All atmospheric deposition of sulfates and nitrates into the catchment enters the lake and neutralizes an equivalent amount of acid neutralizing capacity.

* The monitored baseline acid neutralizing capacity of the lake represents baseline acid neutralizing capacity of all of the water in the catchment.

These assumptions are meant to be conservative and, as such, do not incorporate aquatic ecosystem biogeochemistry. However, the methodology is appropriate to produce a relatively low cost screening level estimate of potential change in acid neutralizing capacity caused by a single pollution source or group of sources.

This approach is based on previous research papers by Fox, 1983 and Clayton, 1998, with changes suggested by Jim Clayton (personal communication) and John Turk (personal communication). In complex situations or where the screening results exceed Forest Service Limits of Acceptable Change (thresholds of concern) , a more sophisticated model such as the Model of Acidification of Groundwater in Catchments (MAGIC) should be run (Sullivan, 1995).

In order to assist in the use of this screening methodology the Forest Service will provide new source applicants or those persons conducting NEPA analysis with the following:

(1) A list of lakes for which potential change in acid neutralizing capacity should be calculated in the wilderness areas of concern, along with map coordinates for those lakes. In most cases, only one or two lakes per wilderness will be identified for analysis.

(2) Baseline lake acid neutralizing capacity as determined by monitored chemistry at the lakes of concern. Baseline acid neutralizing capacity values will usually be for the most sensitive (10% lowest) acid neutralizing capacity values from the lake so that predicted lake chemistry changes will consider sensitive (low acid neutralizing capacity) conditions that may occur on an episodic or seasonal basis.

(3) Estimates of watershed catchment size.

(4) Estimates of the average annual precipitation amounts for the catchment area.

For each analysis, the screening methodology will usually be applied twice:

* first to predict any change in acid neutralizing capacity from the proposed new source or proposed action by itself and,

* second to predict any change in acid neutralizing capacity from the cumulative total of all emissions sources that are included in the cumulative impact analysis (where applicable).

Process

Step 1: Computation of Deposition Flux from Annual N and S Emissions

The purpose of the following conversions is to produce outputs in both kg/ha/yr for reporting deposition (to evaluate aquatic and terrestrial effects) and in eq/m^2/yr to evaluate lake ANC change. Various models produce outputs in different formats. The following instructions will provide model outputs in the correct format to proceed with Step 2.

A.) **CALPUFF model output**: includes S from SO_2 and SO_4; and N from NO_2, HNO_3, and NO_3. Use the recommendations in IWAQM-Phase 2 (p 30-31) for calculation of N and S deposition in kg/ha/yr from the CALPUFF or CALPUFF-Screen modeling outputs. Ds will be the sum of all sulfur species and Dn will be the sum of all nitrogen species

OR

B) **ISCST or other approved model outputs**: some models may report all S outputs as SO_2 and all N outputs as NO_2. In this case, use the calculation below to estimate total (wet plus dry) deposition of S from SO_2 and N from NO_2.

$$Ds \text{ or } Dn = (X)(Vd)(R)(DEP)(Fc)$$

where: Ds = sulfur deposition flux (kg/ha/yr)
Dn = nitrogen deposition flux (kg/ha/yr)
X = pollutant concentration (ug/m^3)
Vd = deposition velocity of 0.005 m/sec for SO_2 or 0.05 m/sec for HNO_3 (ref. IWAQM Phase1)
R = Ratio of molecular weights of elements to convert from SO_2 to S and NO_2 to N (14/46 = .3 for NO_2; 32/64 = .5 for SO_2)

Molecular weight of H=1, N=14, O=16, S=32.
DEP = total deposition to dry deposition ratio (assume this equals 2.0 unless there is other info)
Fc = units conversion of ug/m^3 x m/sec to kg/ha/yr (315.4)

Step 2: Computation of Alkalinity Change from Annual Deposition Flux
This calculation provides an estimate of total equivalents of acid deposition over a year that either fall directly into the lake, or are deposited in the catchment that flows into the lake. This screening model assumes that all the equivalents of acidity eventually reach the lake, where they titrate the alkalinity.

Equation: % ANC change = [Hdep/ANC(o)] x 100
where:

ANC(o) = baseline ANC for entire lake catchment in eq = W x P x (1-Et) x A x (10,000m^2/ha) x (eq/10^6 ueq) x (10^3 liters/m^3)
A = baseline lake sample alkalinity in ueq/l
Hdep = acid deposition in eq = [H(s) + H(n)] x W x 10,000m^2/ha
Hs = sulfur deposition in eq/m^2/yr = Ds (kg/ha/yr) x (ha/10,000m^2) x (1000g/kg) x (eq/16g S)
Hn = nitrogen deposition in eq/m^2/yr = Dn (kg/ha/yr) x ha/10,000m^2) x (1000g/kg) x (eq/14g N)
W = watershed area in ha
P = average annual precipitation in meters
Et = fraction of the annual precipitation lost to evaporation and transpiration (assume Et = .33 unless better info available)
Ds = sulfur deposition in kg/ha/yr from all sulfur species
Dn = nitrogen deposition in kg/ha/yr from all nitrogen species

Example

Wilderness Name: Sangre de Cristo Wilderness
Lake Name : Lower Stout Lake
Lake Location: UTM coordinates 4,245,150 N and 422,300 E

Input Data:

A (baseline ANC)	= 165 ueq/l
Ds (sulfur deposition)	= 0.023 kg/ha/yr
Dn (nitrogen deposition)	= 0.112 kg/ha/yr
W (watershed area)	= 16 hectares
P (precipitation)	= 1.1 meters

Intermediate Values:

ANC(o)	= 19,457 eq
Hs	= 0.000144 eq/m^2
Hn	= 0.0008 eq/m^2
H(dep)	= 151.04 eq

% ANC change = [151.04/19,457)] x 100
= 0.78% change in Lower Stout Lake ANC projected from source specific sulfur and nitrogen deposition

References

Clayton, James. Alkalinity Generation in Snowmelt and Rain Runoff During Short Distance Flow Over Rock. Research Paper RMRS-RP-12. Ogden, UT; U.S. Department of Agriculture, Rocky Mountain Research Station. 1998.

Clayton, James. Research Soil Scientist and Watershed Team Leader of the Aquatics/Watershed Research Work Unit, USDA Forest Service- Rocky Mountain Research Station. Personal communication, August 1999.

Fox, Doug. "A Suggested Methodology for an Acid Deposition Screening Technique Applicable Within 200 km of Isolated Sources" Preliminary Draft, 1983.

Sullivan, T.J. and B.J. Cosby. Testing, Improvement and Confirmation of a Watershed Model of Acid-Base Chemistry. Water, Air and Soil Pollution 85:2607-2612. 1995.

Turk, John. Water Dipper Inc., formerly USGS Biogeochemistry Research Scientist. Personal communication, August-September 1999.

U.S. EPA Interagency Workgroup on Air Quality Modeling (IWAQM) Phase 2 Summary Report and Recommendations for Modeling Long Range Transport Impacts. EPA-454/R-98-019. December 1998

U.S. EPA Interagency Workgroup on Air Quality Modeling (IWAQM) Phase 1 Report: Interim Recommendations for Modeling Long Range Transport and Impacts on Regional Visibility. EPA-454/R-93-015. April 1993.